

THERMO-HYGROSCOPIC ENVELOPE TO SUPPORT ALTERNATIVE COOLING SYSTEMS:
SPECULATIVE FEASIBILITY STUDY IN A SMALL OFFICE BUILDING

A Thesis
Presented to
The Academic Faculty

By

Marionyt Tyrone Marshall

In Partial Fulfillment
Of the Requirements for the Degree
Master of Science in Architecture

Georgia Institute of Technology
December 2014

THERMO-HYGROSCOPIC ENVELOPE TO SUPPORT ALTERNATIVE COOLING SYSTEMS:
SPECULATIVE FEASIBILITY STUDY IN A SMALL OFFICE BUILDING

Approved by:

Dr. Godfried Augenbroe, Advisor
School of Architecture
Georgia Institute of Technology

Dr. Jason Brown, Advisor
School of Architecture
Georgia Institute of Technology

Dr. John Haymaker, Advisor
School of Architecture
Georgia Institute of Technology

Dr. Jeannette Yen, Advisor
School of Biology
Georgia Institute of Technology

Date Approved August 22, 2014

ACKNOWLEDGEMENTS

I express the deepest appreciation to the thesis advisors and readers from the School of Architecture and the School of Biology. The team dedication exceeded all expectations and provided support for an invaluable learning experience and journey.

TABLE OF CONTENTS

ACKNOWLEDGEMENTS	iii
LIST OF TABLES	viii
LIST OF FIGURES	x
NOMENCLATURE	xiv
SUMMARY	xv
CHAPTER 1: INTRODUCTION	1
1.1 Introduction and Expectations	2
1.1.1 Indoor Air Quality, Ozone Depletion, and Global Warming Potential	2
1.1.2 Population Growth and Energy Consumption	5
1.1.3 Building Water and Energy Consumption	11
1.1.4 Adaptive Hygroscopic Building Envelope	12
CHAPTER 2: PROCESS	13
2.1 Research, Prototype Models, and Building Modeling Simulation	13
2.1.1 Thesis Process Map	13
2.1.2 Driving Forces for Alternative Air Conditioning Systems	13
2.1.3 An Alternative Strategy	15
2.1.4 The Prototype	15
2.1.5 Building Design and Energy Nexus	15
CHAPTER 3: ORIGINS	21
3.1 Origins of Hygroscopic Systems in HVAC	21
3.1.1 Dewponds 10,000 B.C. to 2,000 B.C.	22
3.1.1.1 Dewpond Construction	23
3.1.1.2 Dewpond Thermodynamics	23
3.1.1.3 Dewpond Constraints	23
3.1.1.4 Dewpond Performance Criteria	23
3.1.2 Air Wells	24
3.1.2.1 Air Well Thermodynamics	25
3.1.2.2 Air Well Failures	25

3.1.2.3	Air Well Simulation	26
3.1.2.4	Air Well Performance Criteria	26
3.1.3	Early Solar Vapor Compression Cycle System with Solar Regeneration	27
3.2	Historical Uses	29
3.2.1	Vapor Compression System with Solar Regeneration	29
3.2.2	Modern Consideration of Liquid Desiccants	30
3.2.3	Modern Modified Open Absorption Liquid Desiccant System	30
3.2.4	Modern Liquid Desiccant Heat Exchanger	31
3.3	Shared Convergence Early and Modern Hygroscopic Systems Research	31
CHAPTER 4: PAST RESEARCH		33
4.1	Biological Inspired Design Analogues	33
4.1.1	Leaf Cutting Ant Harnesses Wind	34
4.1.1.1	Nest Seasonal Adaptation	34
4.1.1.2	Nest Structure	35
4.1.1.3	Nest Cultivation	35
4.1.1.4	Nest Thermal Convection	35
4.1.1.5	Nest Induced Convection	36
4.1.1.6	Nest Tunnel Workings	36
4.1.1.7	Nest Tunnel Torrents	37
4.1.1.8	Nest Carbon Dioxide	37
4.1.1.9	Leaf-Cutting Ant Nest Performance	38
4.1.2	Great Plains Prairie Dog Harnesses Wind	48
4.1.2.1	Burrow Specificity	48
4.1.2.2	Burrow Structure	48
4.1.2.3	Burrow Configuration	49
4.1.2.4	Burrow Physics	49
4.1.2.5	Burrow Air Movement	49
4.1.2.6	Burrow Mounds	50
4.1.2.7	Burrow Humidity	50
4.1.2.8	Burrow Exergy	50
4.2	Models for Decoupling Dehumidification from Air Conditioning	61
4.2.1	Liquid Desiccant Mass Transfer Physics	61

4.2.1.1	Mass Transfer Water Vapor from Liquid Desiccant to Ambient Air	62
4.2.1.2	Mass Transfer Water Vapor From Ambient Air to Liquid Desiccant	64
4.2.2	Solar Absorption Unit Characteristics	66
4.2.2.1	Absorption Solar Unit System Process	67
4.2.2.2	Absorbent Performance	67
4.2.3	Liquid Desiccant Solar Absorption Diurnal System	71
4.2.3.1	Absorption Solar Unit Day Function	71
4.2.3.2	Absorption Solar Unit Day System	71
4.2.3.3	Absorption Solar Unit Night Function	72
4.2.3.4	Absorption Solar Unit Night System	72
4.2.4	Liquid Desiccant Solar Absorption System Absorber and Regenerator	79
4.2.4.1	The Absorber	79
4.2.4.2	The Regenerator	79
4.2.5	Different Methods for Water Extraction from Humid Air	79
4.2.5.1	Vapor Absorption	80
4.2.5.2	Vapor Compression	82
4.2.5.3	Adsorption	83
4.2.5.4	Absorption	84
4.3	Issues Present in Current Models	85
CHAPTER 5: PROGRAM AND SYSTEM		96
5.1	Architectural Program	96
5.2	Project Specifics	96
5.3	Cross Laminated Timber Panel Exterior Wall, Interior Wall, Floor, Ceiling, and Roof Construction	97
5.4	Reversible Hygroscopic Envelope Wall Operation	98
5.5	Desiccant Characteristics	98
5.6	Hygroscopic Building Envelope	100
CHAPTER 6: DATA		102
6.1	Site Specific Data for Atlanta, Georgia Near Auburn Ave and Jackson Street	102
6.2	Cross-laminated Timber	102
6.3	Fire Protection Performance of Cross-Laminated Timber Panel	102
6.4	Lower Embodied Energy of Cross Laminated Timber Panel	103

6.5	Phenolic Resin Wood Panels Exterior Rain Screen Panels	104
CHAPTER 7: DAYLIGHTING		105
7.1	Daylighting	105
7.2	Proto Model Assumptions	105
7.3	Metrics for Simulation Work	105
7.3.1	2.5 H Guideline Daylight Calculation	106
7.3.2	15/30 Guideline for Daylighting Calculation	108
7.4	High Performance Building Design Strategy	111
7.4.1	Daylight Optimized Building Footprint and Climate Responsive Window to Wall Area Ratio	111
7.4.2	Daylighting Optimized Fenestration Design	112
7.4.3	Daylight Redirection Devices, Solar Shading Devices, and Exterior Overhand Louver	112
7.4.4	Daylight Responsive Electric Lighting Controls and Optimized Interior Design	112
7.5	Proto Model Basis and Simulation	113
7.5.1	Daylighting Simulation Proto Model Iteration 1	114
CHAPTER 8: SYSTEM		133
8.1	Direct Expansion Vapor Compression Refrigeration Air Conditioning System	133
8.2	Thermo-hygroscopic Solar Liquid Desiccant Air Conditioning System	136
CHAPTER 9: SYNTHESIS		146
9.1	Historical Implications	146
9.2	Biological Inspiration Implications	146
9.3	Implications for Energy Reductions, Consumption, and Cost	148
9.3.1	Proto Model System for Stacking Humidity and Temperature Control	150
9.4	Building Systems Including Decoupled Mechanical and Fabrication Implications	150
9.4.1	Systems Packages	150
9.4.2	Interior Packages	151
9.5	Potential mechanical assembly testing issues	151
9.6	Conclusion	151
REFERENCES		153

LIST OF TABLES

1.2	Air Conditioning Refrigerants and Ozone Depletion Risk	4
1.3	Air Conditioning Refrigerants and Global Warming Potential	4
1.4	Commercial Building Types 2003 Percent Floor Space and Energy Consumption	7
3.1	Dewpond Performance Criteria	24
3.2	Air well Performance Criteria	26
3.3	Dewpond and Air well Comparison	27
4.1	Leaf-Cutting Ant Nest Performance Criteria	38
4.2	Great Plains Prairie Dog Burrow Performance Criteria	51
4.3	Prairie Dog Burrow and Leaf-Cutting Ant Nest Comparison	51
5.1	Desiccant Characteristics, Portion Of Data Derived from [22]	99
5.2	Calcium Chloride and Calcium Nitrate Concentration Performance, Data Derived from [22]	100
5.3	Best Neutral Salt Mixtures for Hygroscopic Brine Solution	100
6.1	CLT and Phenolic Resin Wood Rainscreen Wall Thermal and Physical Properties	103
6.2	CLT and Phenolic Resin Wood Rainscreen Wall Thermal and Physical Properties	103
6.3	CLT and Phenolic Resin Wood Rainscreen Wall Thermal and Physical Properties	104
7.1	Proto Model Average Daylight Factor Calculations, See section 7.1 for equation	106
7.2	Proto Model 2.5 H Daylight Guideline Calculations	106
7.3	Proto Model 15/30 Guideline Daylight Factor Calculations	108
7.4	Proto Model Assumptions for Desired Daylighting Simulation	109
7.5	Proto Model Detail Interior Assumptions for Desired Daylighting Simulation	109
7.6	Daylighting Illuminance Calculations for Atlanta 33.63° N Latitude	109
7.7	Daylighting Illuminance Calculations for Atlanta 33.63° N Latitude	110
7.8	Daylighting Illuminance Calculations for Atlanta 33.63° N Latitude	110
7.9	Daylighting Preferred Illuminance Values for Atlanta 33.63° N Latitude	110
7.10	Daylight Window to Wall Ratio Percentages for Proto Model	111
7.11	Proto Model Daylighting and Visual lighting Glass	112
7.12	Proto Model Simulation Surface Properties	113
8.1	Thermo-hygroscopic Model Data and Conditions for Summer Heat Load	143
8.2	Heat and Solar Gain Transmission from People, Lights, Equipment, Walls, Windows, and Roof	143
8.3	Calculation of Amount of Cooling Needed for Prototype Model	144
8.4	Heating Load on Cooling Equipment, Tons of Cooling Required Calculation	144

8.5	Psychrometric Data for Plot of Table 8.1, 8.2, 8.3, and 8.4	145
9.1	Thermo-hygroscopic Envelope and Dewponds	147
9.2	Thermo-hygroscopic Envelope and Air wells	147
9.3	Thermo-hygroscopic Envelope and Leaf-Cutting Ant Nest	148
9.4	Thermo-hygroscopic Envelope and Prairie Dog Burrow	148
9.5	Conventional Air Conditioning Equipment Systems and Leaf-Cutting Ant Nest	149
9.6	Conventional Air Conditioning Equipment Systems and Prairie Dog Burrow	149

LIST OF FIGURES

1.1	Thesis Statement Process Diagram	1
1.2	Air Conditioning Refrigerants and Global Warming Potential in Percent	5
1.3	World Energy Consumption and Population	6
1.4	Commercial Buildings Energy and Consumption By End Use	8
1.5	Parallel Coordinates Plot of 2003 Commercial Building Types Percent Floor and Energy Consumption	9
1.6	2010 Commercial Buildings Energy End-Use Carbon Dioxide Emissions Percent Totals	10
1.7	Parallel Coordinates Plot of 2010 Commercial Buildings Energy End-Use Carbon Dioxide Emissions	11
2.1	Project Hierarchical Process Map	14
2.2	Project Hierarchical Process Map	17
2.3	Project Hierarchical Process Map	18
2.4	Project Hierarchical Process Map	19
2.5	Project Hierarchical Process Map	20
3.1	Timeline of Early Hygroscopic Research	21
3.2	Timeline of Modern Hygroscopic Research	28
4.1	Leaf Cutting Ant Climatic Diagram	33
4.2	Leaf Cutting Ant Biological Analogue Hierarchical Key Map	39
4.3	Leaf Cutting Ant Biological Analogue Nest Seasonal Adaptation Hierarchical Map	40
4.4	Leaf Cutting Ant Biological Analogue Nest Structure Hierarchical Map	41
4.5	Leaf Cutting Ant Biological Analogue Nest Cultivation Hierarchical Map	42
4.6	Leaf Cutting Ant Biological Analogue Nest Thermal Convection Hierarchical Map	43
4.7	Leaf Cutting Ant Biological Analogue Nest Induced Convection Hierarchical Map	44
4.8	Leaf Cutting Ant Biological Analogue Nest Tunnel Workings Hierarchical Map	45
4.9	Leaf Cutting Ant Biological Analogue Nest Tunnel Torrents Hierarchical Map	46
4.10	Leaf Cutting Ant Biological Analogue Nest Carbon Dioxide Hierarchical Map	47
4.11	Prairie Dog Biological Analogue Hierarchical Key Map	52
4.12	Prairie Dog Burrow Specificity Hierarchical Map	53
4.13	Prairie Dog Burrow Structure Hierarchical Map	54
4.14	Prairie Dog Burrow Configuration Hierarchical Map	55
4.15	Prairie Dog Burrow Physics Hierarchical Map	56
4.16	Prairie Dog Burrow Air Movement Hierarchical Map	57

4.17	Prairie Dog Burrow Mounds Hierarchical Map	58
4.18	Prairie Dog Burrow Humidity Hierarchical Map	59
4.19	Prairie Dog Burrow Exergy Hierarchical Map	60
4.20	Liquid Desiccant Mass Transfer Physics Hierarchical Key Map	61
4.21	Liquid Desiccant to Ambient Air Mass Transfer Physics Hierarchical Map	63
4.22	Liquid Desiccant to Ambient Air Mass Transfer Physics Diagram	64
4.23	Ambient Air to Liquid Desiccant Mass Transfer Physics Hierarchical Map	65
4.24	Ambient Air to Liquid Desiccant Mass Transfer Physics Diagram	66
4.25	Absorption Solar Unit Hierarchical Key Map	68
4.26	Absorption Solar Unit System Process Hierarchical Map	69
4.27	Absorption Solar Unit Energy Characteristics Hierarchical Map	70
4.28	Absorption Solar Unit Diurnal Hierarchical Key Map	74
4.29	Absorption Solar Unit Day Function Hierarchical Map	75
4.30	Absorption Solar Unit Day System Hierarchical Map	76
4.31	Absorption Solar Unit Night Function Hierarchical Map	77
4.32	Absorption Solar Unit Night System Hierarchical Map	78
4.33	Models for Liquid Desiccant Air Conditioning Hierarchical Key Map	80
4.34	Vapor Absorption Hierarchical Map	86
4.35	Vapor Absorption Hierarchical Map	87
4.36	Vapor Absorption Hierarchical Map	88
4.37	Vapor Compression Hierarchical Map	89
4.38	Vapor Compression Hierarchical Map	90
4.39	Vapor Compression Hierarchical Map	91
4.40	Adsorption Hierarchical Map	92
4.41	Adsorption Hierarchical Map	93
4.42	Absorption Hierarchical Map	94
4.43	Absorption Hierarchical Map	95
5.1	Proto Model Primary Workspace Floor Plan Sketch	97
7.1	Section 2.5H Guideline for Daylighting of Proto Model	107
7.2	Section 2.5H Guideline for Daylighting of Proto Model	107
7.3	Floor Plan of 15/30 Guideline for Daylighting of Proto Model	108
7.4	Daylighting for Atlanta Summer Noon Overcast Sky Plan View in VELUX	114
7.5	Daylighting for Atlanta Spring Noon Overcast Sky Plan View in VELUX	115

7.6	Daylighting for Atlanta Winter Noon Overcast Sky Plan View in VELUX	115
7.7	Daylighting for Atlanta Summer Noon Overcast Sky Iso Contour Plan View in VELUX	116
7.8	Daylighting for Atlanta Spring Noon Overcast Sky Iso Contour Plan View in VELUX	116
7.9	Daylighting for Atlanta Winter Noon Overcast Sky Iso Contour Plan View in VELUX	117
7.10	Daylighting for Atlanta Summer Noon Overcast Sky False Color Plan View in VELUX	117
7.11	Daylighting for Atlanta Spring Noon Overcast Sky False Color Plan View in VELUX	118
7.12	Daylighting for Atlanta Winter Noon Overcast Sky False Color Plan View in VELUX	118
7.13	Daylighting for Atlanta Summer Noon Overcast Sky North South Section View in VELUX	119
7.14	Daylighting for Atlanta Spring Noon Overcast Sky North South Section View in VELUX	119
7.15	Daylighting for Atlanta Winter Noon Overcast Sky North South Section View in VELUX	120
7.16	Daylighting for Atlanta Summer Noon Overcast Sky Iso Contour North South Section View in VELUX	120
7.17	Daylighting for Atlanta Spring Noon Overcast Sky Iso Contour North South Section View in VELUX	121
7.18	Daylighting for Atlanta Winter Noon Overcast Sky Iso Contour North South Section View in VELUX	121
7.19	Daylighting for Atlanta Summer Noon Overcast Sky False Color North South Section View in VELUX	122
7.20	Daylighting for Atlanta Spring Noon Overcast Sky False Color North South Section View in VELUX	122
7.21	Daylighting for Atlanta Winter Noon Overcast Sky False Color North South Section View in VELUX	123
7.22	Daylighting for Atlanta Summer Noon Overcast Sky East West Section View in VELUX	123
7.23	Daylighting for Atlanta Spring Noon Overcast Sky East West Section View in VELUX	124
7.24	Daylighting for Atlanta Winter Noon Overcast Sky East West Section View in VELUX	124
7.25	Daylighting for Atlanta Summer Noon Overcast Sky Iso Contour East West Section View in VELUX	125
7.26	Daylighting for Atlanta Spring Noon Overcast Sky Iso Contour East West Section View in VELUX	125
7.27	Daylighting for Atlanta Winter Noon Overcast Sky Iso Contour East West Section View in VELUX	126
7.28	Daylighting for Atlanta Summer Noon Overcast Sky False Color East West Section View in VELUX	126
7.29	Daylighting for Atlanta Spring Noon Overcast Sky False Color East West Section View in VELUX	127
7.30	Daylighting for Atlanta Winter Noon Overcast Sky False Color East West Section View in VELUX	127
7.31	Daylighting for Atlanta Summer Noon Overcast Sky Perspective View in VELUX	128

7.32	Daylighting for Atlanta Spring Noon Overcast Sky Perspective View in VELUX	128
7.33	Daylighting for Atlanta Winter Noon Overcast Sky Perspective View in VELUX	129
7.34	Daylighting for Atlanta Summer Noon Overcast Sky Iso Contour Perspective View in VELUX . . .	129
7.35	Daylighting for Atlanta Spring Noon Overcast Sky Iso Contour Perspective View in VELUX . . .	130
7.36	Daylighting for Atlanta Winter Noon Overcast Sky Iso Contour Perspective View in VELUX . . .	130
7.37	Daylighting for Atlanta Summer Noon Overcast Sky False Color Perspective View in VELUX . . .	131
7.38	Daylighting for Atlanta Spring Noon Overcast Sky False Color Perspective View in VELUX	131
7.39	Daylighting for Atlanta Winter Noon Overcast Sky False Color Perspective View in VELUX . . .	132
8.1	Direct Expansion Vapor Compression Refrigeration System Sketch, Derived from[30]	134
8.2	Building Air Conditioning Process Sketch, Derived from [30]	135
8.3	Direct Expansion Vapor Compression Refrigeration Process Psychrometric Chart	135
8.4	Plan Sketch of South Thermal-hygroscopic Envelope Design Option A	136
8.5	Plan Sketch of North and South Thermal-hygroscopic Envelope Design Option B	137
8.6	Section Sketch of South Thermal-hygroscopic Envelope Design Option A	137
8.7	Section Sketch of North and South Thermal-hygroscopic Envelope Design Option B	137
8.8	Section Sketch of East and West Thermal-hygroscopic Envelope Design Option	137
8.9	Solar Liquid Desiccant Air Conditioning Building Envelope System Sketch	140
8.10	Solar Liquid Desiccant Air Conditioning Building Envelope System Sketch Detail	141
8.11	Air Conditioning Dehumidification Process in Psychrometric Chart for Thesis Liquid Desiccant System	142
8.12	Solar Liquid Desiccant Air Conditioning Building Envelope Multi-Level Section Sketch	142
8.13	Psychrometric Chart for Plot of Tables 8.1, 8.2, 8.3, and 8.4 Calculations	144

NOMENCLATURE

COP	Coefficient of performance (COP) refers to amount of heating or cooling a system usually a heat pump provides in comparison to the amount of electrical energy it requires for that heating or cooling function. Coefficient of performance greater than 1 provides energy efficiency versus when it is less than 1. The ratio is the amount of heating or cooling divided by the amount of energy required to provide that function. 11
Exergy	Exergy measures the quantity of the most useful work to be done by a system interacting within its environment where temperature and pressure are constant. 24
Hygroscopic Brine Solution	A hygroscopic brine solution is a liquid desiccant salt and water mixture in varying concentrations to lower or raise surface vapor pressure of the solution compared to vapor pressure of a passing stream of humid air. 99
Hygroscopic Salt	A hygroscopic salt refers to a specific chemical composition of desiccants such as calcium chloride. 15
Proto Model	refers to prototype model consisting of characteristics for design, energy modeling, and system specifications 105

SUMMARY

The thesis explores the technical feasibility of an alternative method of decoupling air-conditioning systems function within the context of ecological issues. The system is a variant of dedicated outdoor air systems to separate dehumidification and cooling in air conditioning equipment. The project specifically investigates locating these components within the building envelope. Placement in the envelope moves the systems closer to fresh air and offers architectural expression for components that are normally out of sight.

Designers, engineers, building science, mechanical, structural, biologist, and architectural engineers ideally as agents offer beneficial improvement to the system. The reduction in size of components into the building envelope offers risk. The thesis design space uses historical works, biological analogues, and past work to ground the technical understanding of the topic. Specific use of biological inspired design realizes translation from other systems to improve the alternative decoupled air conditioning system.

The thesis develops prototype models for lighting analysis and for sensible and latent heat calculations. Psychrometric charts serve as tools to understand the thermodynamic air-conditioning process in conventional direct expansion vapor compression and solar liquid desiccant air conditioning systems. Data, models, and sketches provide tools for improvements to the 'thick' building envelope. Finally, the diagrams translate into functional decompositions for modifications to improve the system. The thesis probes the constraints in the areas of cost, fabrication, and technology that may not yet exist for selective improvement rather than a barrier to development of the thesis.

CHAPTER 1: INTRODUCTION

The thesis research focuses on inspired design of a system of equipment that is theoretical, experimental, and may not yet be commercially available now. Figure 1.1 is a process map diagram to unpack the strategy for the work in this thesis. The goal is to understand how a solar liquid desiccant building envelope conditions fresh air with low-grade thermal energy. The thesis investigates the technical feasibility of an alternative method of decoupling air-conditioning systems function ecologically within the context of rising population growth, environmental concerns, and energy consumption.

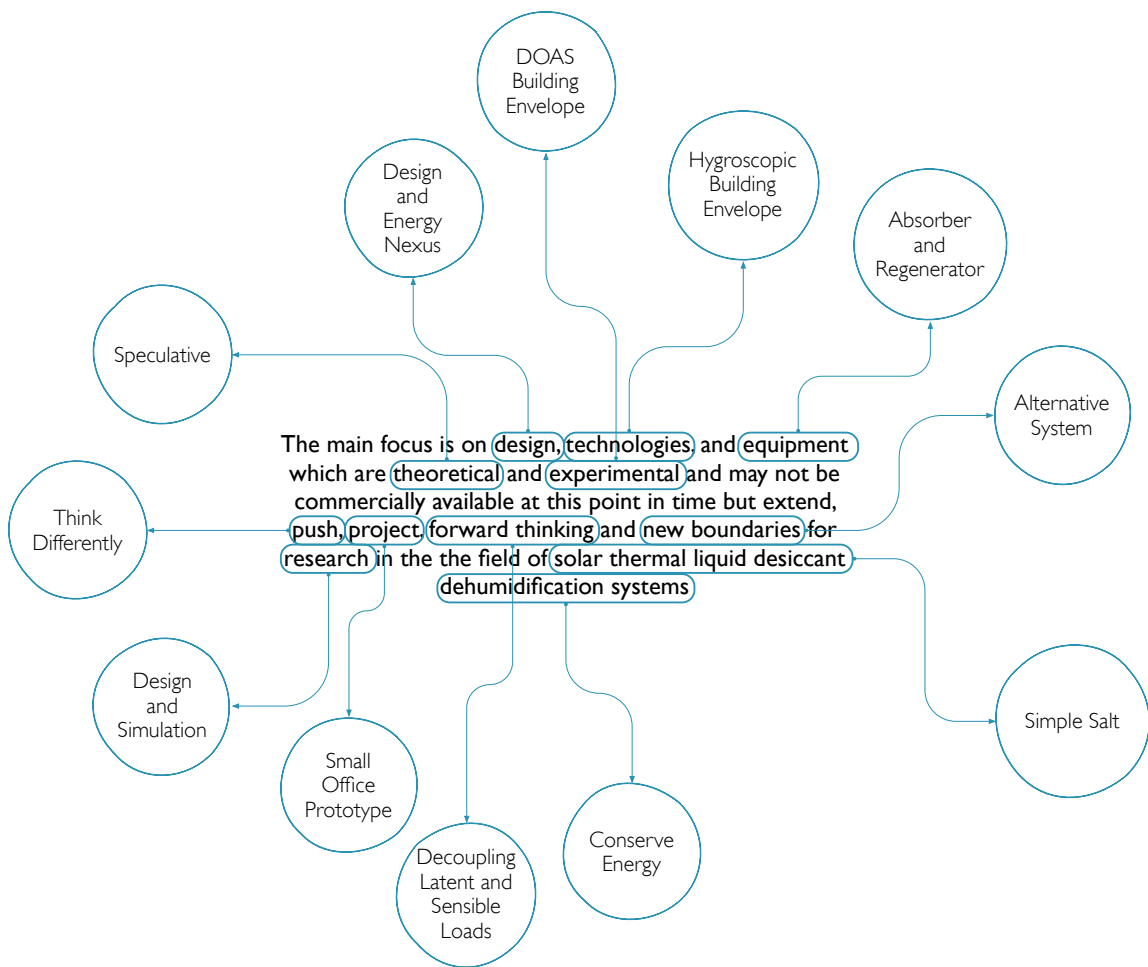


Figure 1.1. Thesis Statement Process Diagram

1.1 Introduction and Expectations

The use of seemingly disparate diagrams and comparative data represents models leading to the unexpected. Technically, the proposition for decoupling air conditioning systems from dehumidification and cooling is not impossible, nor is it a new idea. As new systems, these undergo rapid configuration and experimentation. There are improvements to the design for air conditioning equipment. The movement of air conditioning equipment from the building roof or mechanical space to the building envelope is uncertain and risky. It requires consideration for different solutions in the earliest points of building design and simulation.

The thesis covers many issues and maps them to understand the varying overlaps and points of intersection. It may suggest components and technology not yet available, tested, and fabricated, however these are only intermediary issues. The system separates moisture removal from cooling of fresh air for indoor air conditioning. Currently, dedicated outdoor systems provide decoupling of cooling from dehumidification. The systems offer little opportunity for architectural integration or expression. The systems are located 'out of sight' from occupants. The speculative feasibility is not without issues of risky structural, thermal, cost, and energy issues. The thesis discusses a system that can incorporate agents in design, building science, mechanical engineering, structural, and architectural to improve integration, offer aesthetic response, and play a larger role in the expression of buildings in their specific environment.

1.1.1 Indoor Air Quality, Ozone Depletion, and Global Warming Potential

How can changes in air-conditioning improve comfort in indoor spaces? A number of variables affect indoor environment quality such as temperature, humidity, ventilation, and air pollutants. The design of the building envelope and air conditioning system greatly affects these factors. The performance of the envelope and the air conditioning system affects energy consumption. The growth of microbial fungus in response to poor ventilation and moisture control directly affects occupant health. More ventilation including fan and pumps, and lower chiller water temperatures to cool and dehumidify is one method to remove moisture from fresh air.

Demand and adoption rates for air conditioning are rising all over the world. Indoor air quality issues increase at the same time[1]. Conventional air conditioning systems maintain comfortable indoor environments. These systems minimize the growth of microbial fungus, mildew, musty odors in HVAC condensate pan, and moist

air in duct work[2]. Typical air loading to conditioned spaces is about 15-20 ft.³/min. per person mixture with fresh air[2]. Fresh air has much more moisture content than the sensible heat load within a conditioned space[2]. Conventional air-conditioning equipment efficiently removes sensible loads with thin coils and high supply air velocities[2]. The equipment cools air temperatures below 7°C and consumes energy to improve latent thermal energy removal efficiency [2]. Conventional air conditioning systems based on vapor compression cycles maintain temperature in ductwork above dew point to prevent moisture, mold, and mildew.

Refrigerant manufacture and charging in commercial and residential air conditioning equipment is flammable, toxic, contributes to greenhouse gases, and depletes the ozone layer. The current list of chemicals that are in use, in process of phasing out of use in new equipment but still present in existing air conditioning equipment is chlorofluorocarbons (CFCs) for R-11 and R-12, hydro-chlorofluorocarbons (HCFCs) for R-22 and R123, and hydro-fluorocarbons (HFCs) for 134a and 410A. The chemical compound in these refrigerants is largely carbon, chlorine, and fluorine. The United States prohibits importation of these compounds. However, there is no restriction to the use of refrigerants in new equipment built before January 2020 for any HCFC compounds[3]. The U.S. Environmental Protection Agency HCFC phase-out schedule places limits on the production of hydro-chlorofluorocarbons[3]. The restriction on refrigerants does not apply to vapor compression refrigeration systems. These systems continue in operation and maintenance with the potential for improper handling and release into the environment. Table 1.2 shows the commonly used compounds with refrigerant signifier in relation to its ozone depletion risk. The table shows CFC-11 (R-11) as having an ozone depletion risk (ODP) of one. An ODP of one signifies high damaging risk while values less than one indicates less risk. A single chlorine atom has the potential to destroy 100,000 ozone molecules. HFCs are now widely accepted as replacement for CFCs, and HCFCs because it poses no harm to the ozone layer; but this is a temporary solution as the compound is a high contributor to the emission of greenhouse gases that adversely affects climate change and global warming potential. Table 1.3 shows the commonly used refrigerants and their global warming potential. The global warming potential index identifies compounds that inhibit the escape of infrared radiation from the earth's atmosphere. Carbon dioxide is a reference marker for comparing other compounds, as its GWP is one. Figure 1.2 is shown to understand the magnitude when compared with carbon dioxide which is a single line pointing from the center of the pie chart to exactly zero degrees north.

Table 1.2. Air Conditioning Refrigerants and Ozone Depletion Risk

Refrigerant	Ozone Depletion Potential
CFC-11	1
CFC-12	1
HCFC-22	0.055
HCFC-123	0.02
HFC-134a	0
HFC-410A	0

Table 1.3. Air Conditioning Refrigerants and Global Warming Potential

Refrigerant	Global Warming Potential
CO ₂	1.00
CFC-11	5,000.00
CFC-12	8,500.00
HCFC-22	1,700.00
HCFC-123	80.00
HFC-134a	1,300.00
HFC-410A	1,890.00

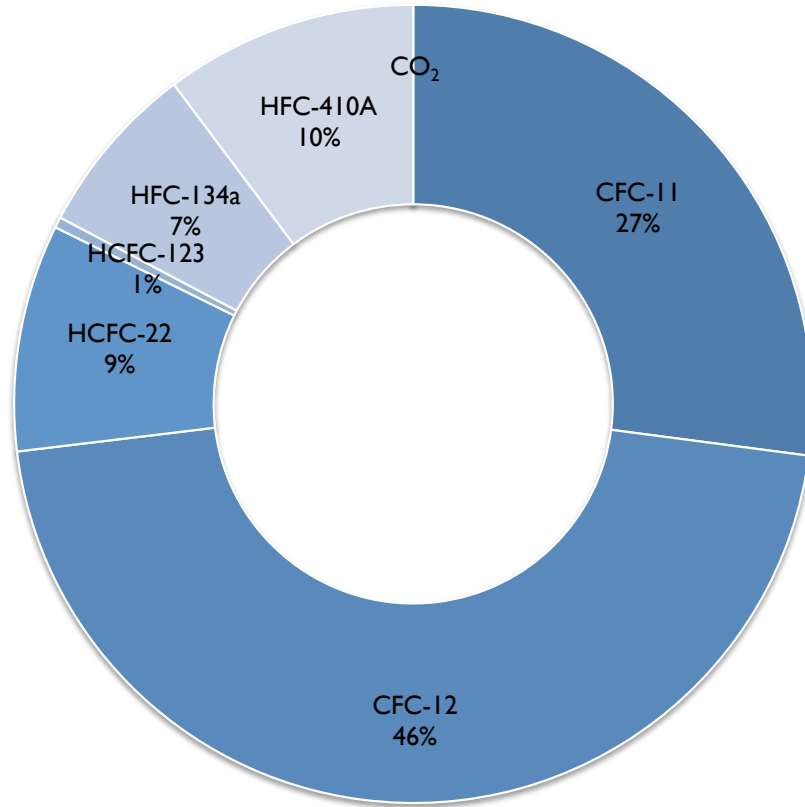


Figure 1.2. Air Conditioning Refrigerants and Global Warming Potential in Percent

1.1.2 Population Growth and Energy Consumption

Figure 1.3 shows current population areas, population growth, and energy consumption worldwide[4]. Asia represents an area with the largest population, population growth, and energy consumption. It also happens to be an area with large-scale urban development as demographics and policies within nations move their people from rural area to urban centers. The eastern coast of China is hot and humid with significant annual precipitation[5]. Cooling and dehumidifying requires removing sensible and latent or total thermal energy while cooling requires removing only sensible thermal energy. Conventional vapor compression refrigerant based air conditioning systems are most prevalent in rapidly and highly urbanizing country of China[6]. The 1997 Kyoto Protocol to the United Nations Framework Convention on Climate Change is an international environmental treaty that commits industrialized countries to stabilize greenhouse gas emissions[7]. Most of Asia including China, India, the Middle East, Central America, and South America do not have any binding targets for greenhouse gas emissions reductions. In terms of greenhouse gases, the Kyoto agreement has less cooperation worldwide and

even less to restrictions on the use of HCFCs and HFCs. There is unrestricted use of ozone depletion and global warming potential refrigerants for new and existing air conditioning equipment.

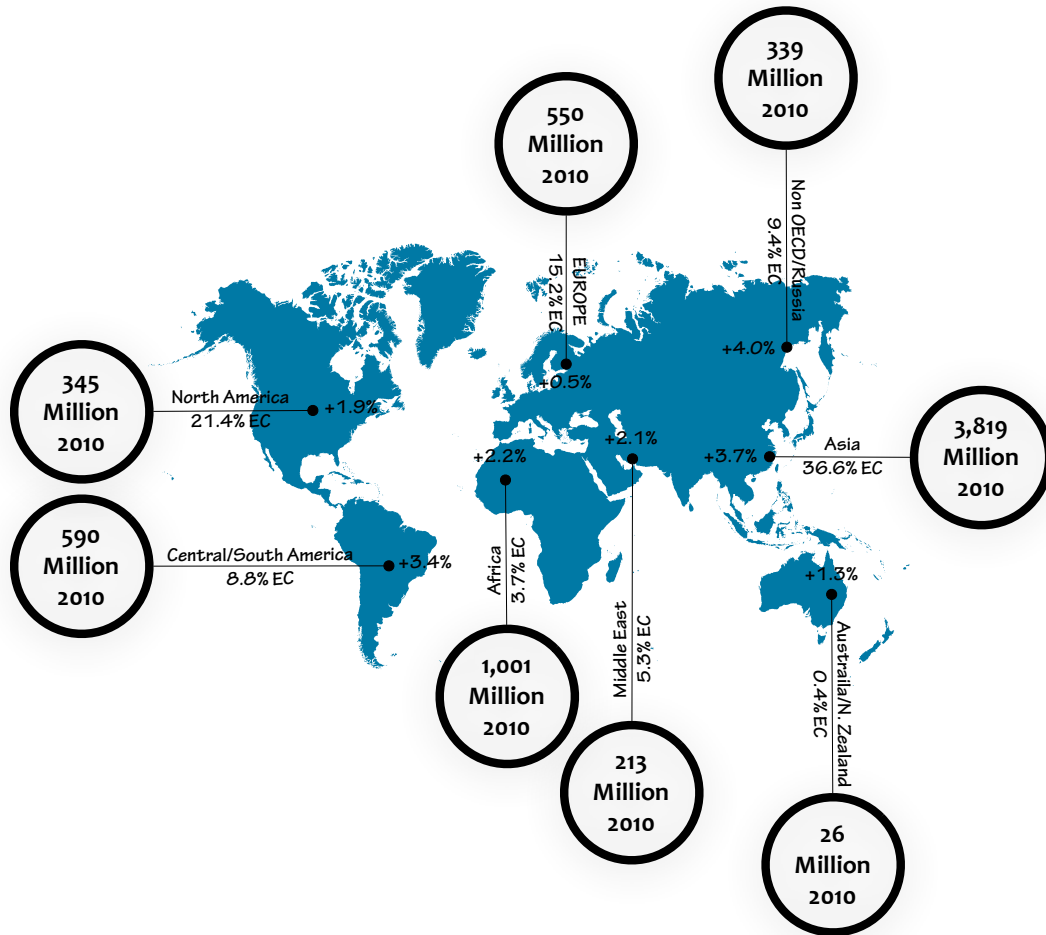


Figure 1.3. World Energy Consumption and Population

Table 1.4. Commercial Building Types 2003 Percent Floor Space and Energy Consumption

Commercial Building Type	Total Floorspace	Total Buildings	Primary Energy Consumption
Office	17%	17%	19%
Mercantile	16%	14%	18%
Retail	6%	9%	5%
Enclosed & Strip Malls	10%	4%	13%
Education	14%	8%	11%
Warehouse and Storage	14%	12%	7%
Lodging	7%	3%	7%
Service	6%	13%	4%
Public Assembly	5%	6%	5%
Religious Worship	5%	8%	2%
Health Care	4%	3%	8%
Inpatient	3%	0%	6%
Outpatient	2%	2%	2%
Food Sales	2%	5%	5%
Food Service	2%	6%	6%
Public Order and Safety	2%	1%	2%
Other	2%	2%	4%
Vacant	4%	4%	1%

Commercial office buildings data shows a relationship between floor space, building number, and primary energy consumption[4]. Table 1.4 shows office buildings account for the largest aggregation of floor space, number of buildings, and primary energy consumption[4]. Figure 1.5 shows a parallel coordinates plot of the data. Most commercial building types have lower primary energy consumption when compared with commercial office space. For total buildings, most of the commercial building types trend less than 10% and 17% for commercial buildings. The parallel coordinates plot shows overall trends in this data for most commercial building as flat or rising trend of floor space compared to primary energy use. The trend for office commercial buildings is flat for total floor space and total buildings while primary energy consumption is higher by a percent difference of just over 11 percent.

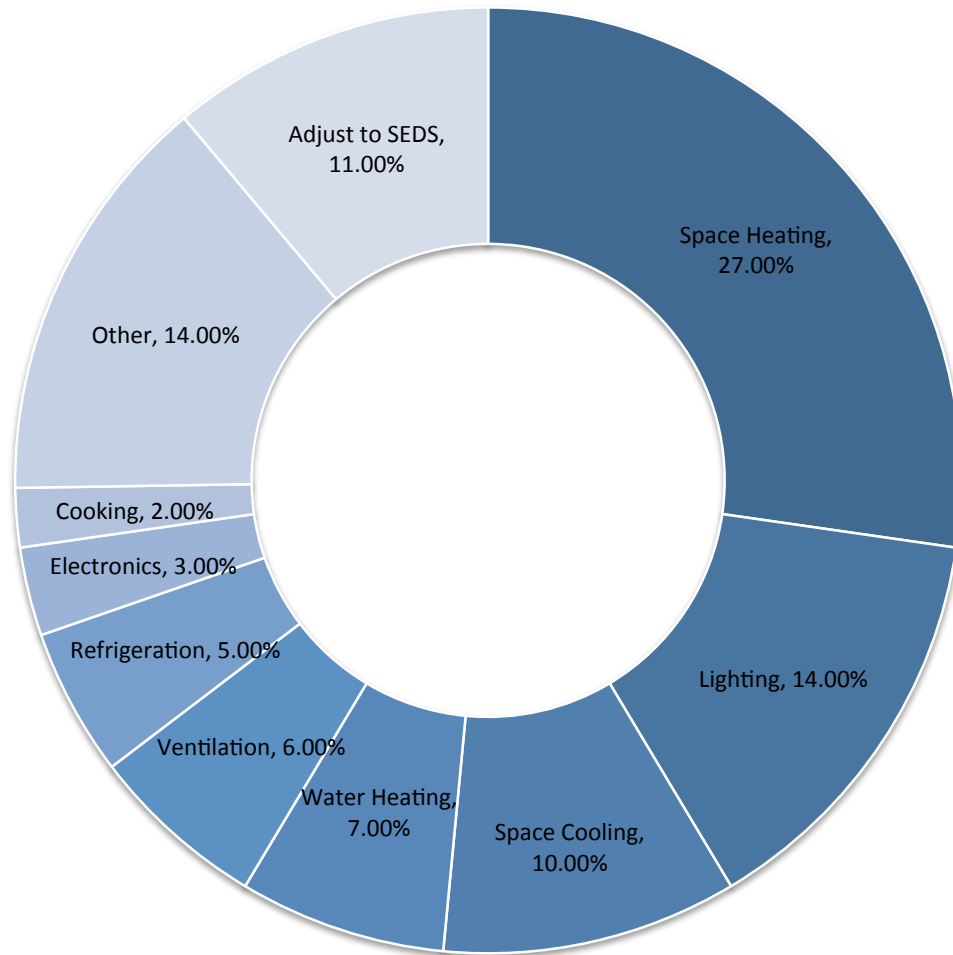


Figure 1.4. Commercial Buildings Energy and Consumption By End Use

Figure 1.4 shows percentage of energy and consumption by end use for commercial buildings[4]. The largest end use of energy consumption for commercial buildings is space heating, lighting, space cooling, other, and SEDS. The 'other' category refers to energy consumption from service station equipment, ATMs, telecommunication equipment, medical equipment, pumps, emergency electric generators, combined heat and power in commercial buildings, and manufacturing performed in commercial buildings which are not directly addressed in the topic relating to space conditioning and occupant comfort[4]. The 'SEDS' category refers to 'Adjustment to SEDS' or the manner in that the Energy Information Agency, the original providers of the data, use to relieve discrepancies between data sources. The data allows for classification for energy attributed to commercial building sector but not directly related to specific end-uses[4]. The largest areas that affect space conditioning are space heating, lighting, and space cooling. In terms of air conditioning systems for cooling and dehumidification, space cooling and lighting are two areas to lower energy consumption. The reduction of lighting requirements directly

contributes to sensible loads. Generous wall and window ratios transmit solar heat gain for the mechanical system to remove.

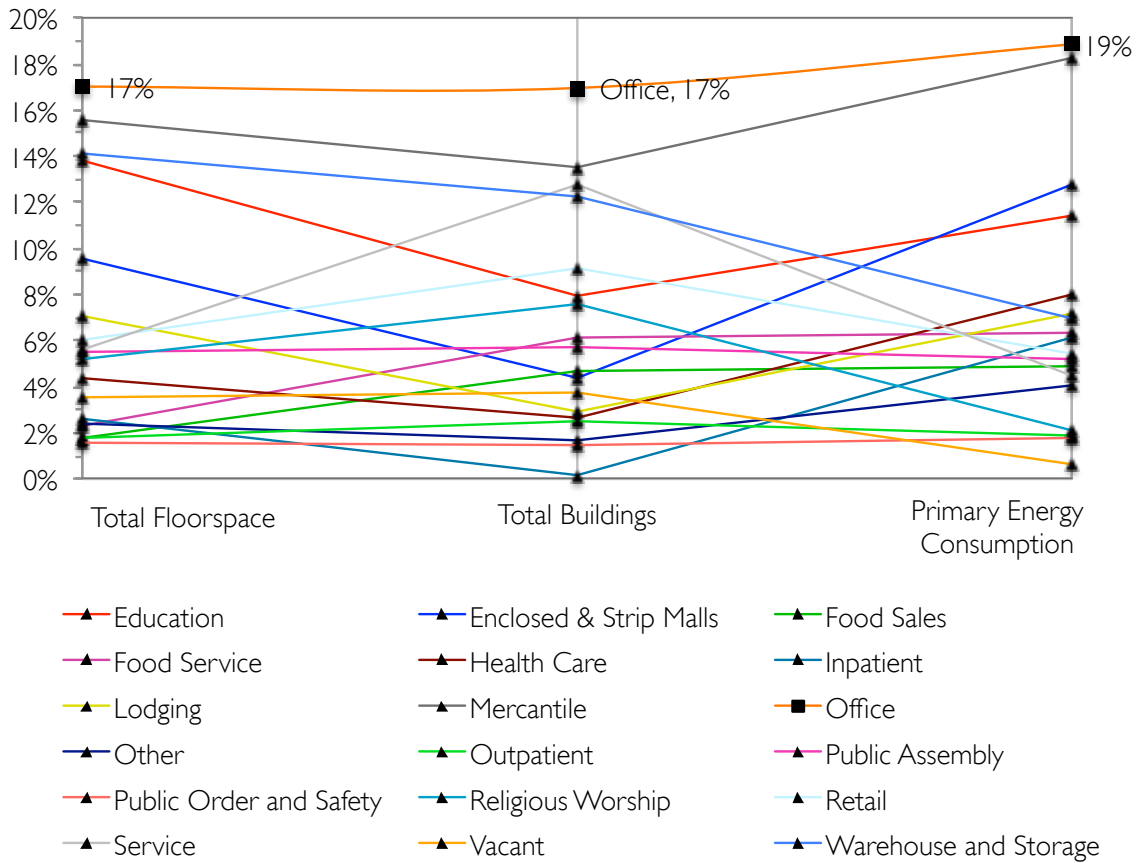


Figure 1.5. Parallel Coordinates Plot of 2003 Commercial Building Types Percent Floor and Energy Consumption

In 2010, the data for commercial buildings energy end-use carbon dioxide emissions is shown in Figure 1.6[4]. Figure 1.6 shows the breakdown in terms of greenhouse gas emissions for dominant end-use contributors such as lighting, space heating, and space cooling. These end-uses comprise the majority of carbon dioxide emissions by slightly more than 50% than all other end-uses. Space cooling varies from space heating by a percent difference of 6%. Figure 1.7 shows the data in terms of millions of metric tons of carbon dioxide emissions from the same commercial building end-uses from previous discussion. The trend in the data shows that lighting and space cooling are the dominant and intensive energy end-uses for electricity. Commercial buildings types such as mercantile, education, lodging, and office may have long hours of occupation during a day and up to 24 hours

per day[4]. In other data for commercial buildings, the energy intensity has remained relatively constant between 1980 and 2010 while the primary energy consumption per square foot has increased by eight percent[4]. For alternative air conditioning systems, it is imperative that these systems make use of as much renewable energy as possible to reduce the emissions from carbon dioxide.

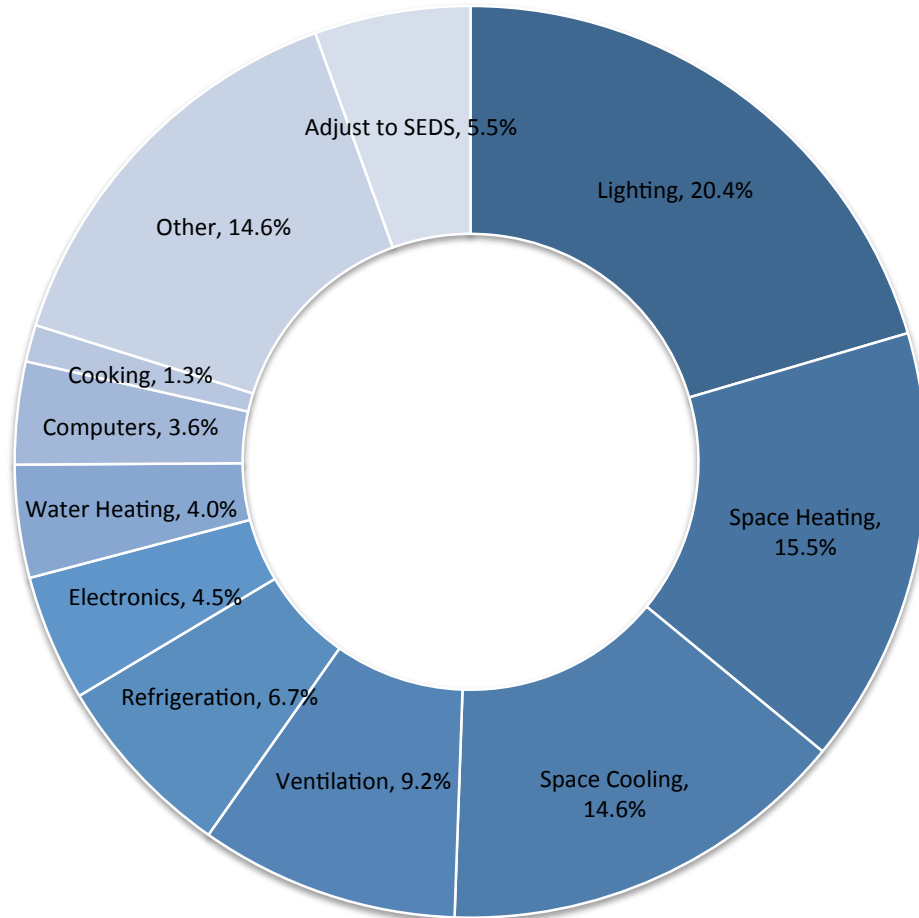


Figure I.6. 2010 Commercial Buildings Energy End-Use Carbon Dioxide Emissions Percent Totals

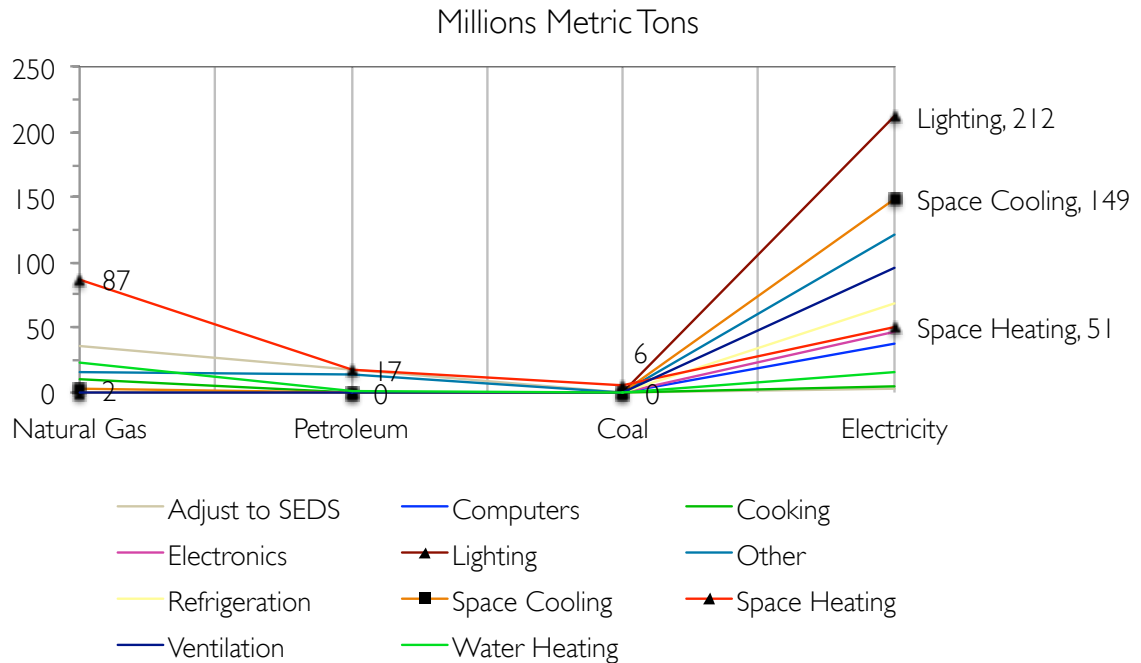


Figure 1.7. Parallel Coordinates Plot of 2010 Commercial Buildings Energy End-Use Carbon Dioxide Emissions

1.1.3 Building Water and Energy Consumption

Conventional air conditioning systems cool air below the dew-point temperature to condense moisture vapor out of the air and remove latent thermal energy[1]. Although not always the case, these systems can consume electrical energy in a second pass to reheat the same air stream after cooling such that the air temperature reaches a point that is a comfortable for occupants before delivery to the intended spaced for conditioning[1]. The chilled water system cools water lower than fresh air for larger temperature difference requiring more electrical energy. In single system heat exchanger, the process for dehumidification for latent heat and sensible heat removal occurs in the system unit and at the same time[1]. The systems run longer reach these lower chiller water[8]. The system operates in an overcooling state. An air-conditioning system with three to four EER signifies the COP is less than or slightly more than one. EER of this magnitude implies that the system removes heat to provide cooling at higher electrical energy consumption per hour.

1.1.4 Adaptive Hygroscopic Building Envelope

The building envelope can connect and directly dehumidify fresh air driving energy expenditure to its lowest level. The components that describe the separation of latent load removal and sensible heat remove within the building envelope are theoretical, experimental, and risky. Liquid solutions can scavenge water vapor from air including pollutants and separately lower air temperature. These systems have similar strategies the design of conventional systems in that they are operate at a distance from the building envelope. A different approach is to relocate these components to the building envelope at the nearest point of contact with fresh air. The process for how this may take place follows in a detailed look at strategies for scavenging moisture vapor from outside air. A more general approach is to describe the organization of a thermo-hygroscopic building envelope as a biomimetic skin where components for dehumidifying air and harvesting energy and water are located within the building facade[5]. This article discusses the design and structure of a prototype model for the commercial office building typology. A prototype provides a test platform for the building envelope decoupling strategy of dehumidification and smaller air conditioning system for cooling. The system for dehumidification is biologically inspired and makes use of a benign liquid desiccant salt solution. A site location will allow for the design of a prototype model for a small commercial office space of about 1000 square foot. Methods for modular deployment of a prototype commercial office model imply stacking strategies for building envelope and air conditioning system including issues for future work.

CHAPTER 2: PROCESS

2.1 Research, Prototype Models, and Building Modeling Simulation

2.1.1 *Thesis Process Map*

The process for this thesis starts as a collection of text and line work that maps array of interconnected ideas. The process map shown in Figure 2.1 organizes the work in a dense and compact radial flow of information. The multi-point logic map uses its own spatial syntax of datum points that have the capacity for ease of arrangement for further elaboration. The syntax of the diagram uses arrows to connect to the next idea logic point. The dotted circular line shows the direction of progression using a 'dot' for the start and an 'arrow' for the end of the progression. The process map breaks down the thesis exploration of a thermo-hygroscopic building envelope.

2.1.2 *Driving Forces for Alternative Air Conditioning Systems*

The previous chapter discusses the manner in which indoor spaces are conditioned. Figure 2.2 is an enlargement of the process diagram that focuses on the components that organize the first two chapters of this thesis. Population growth and energy consumption, production and air-conditioning refrigerants influence the production of greenhouse gases and deterioration of the ozone layer drive exploration for alternative dehumidification and cooling air-conditioning equipment in commercial office buildings. An integrated building envelope that decouples cooling, dehumidification, lower energy consumption, and preserves daylighting could influence the design expression of building in hot and humid climates.

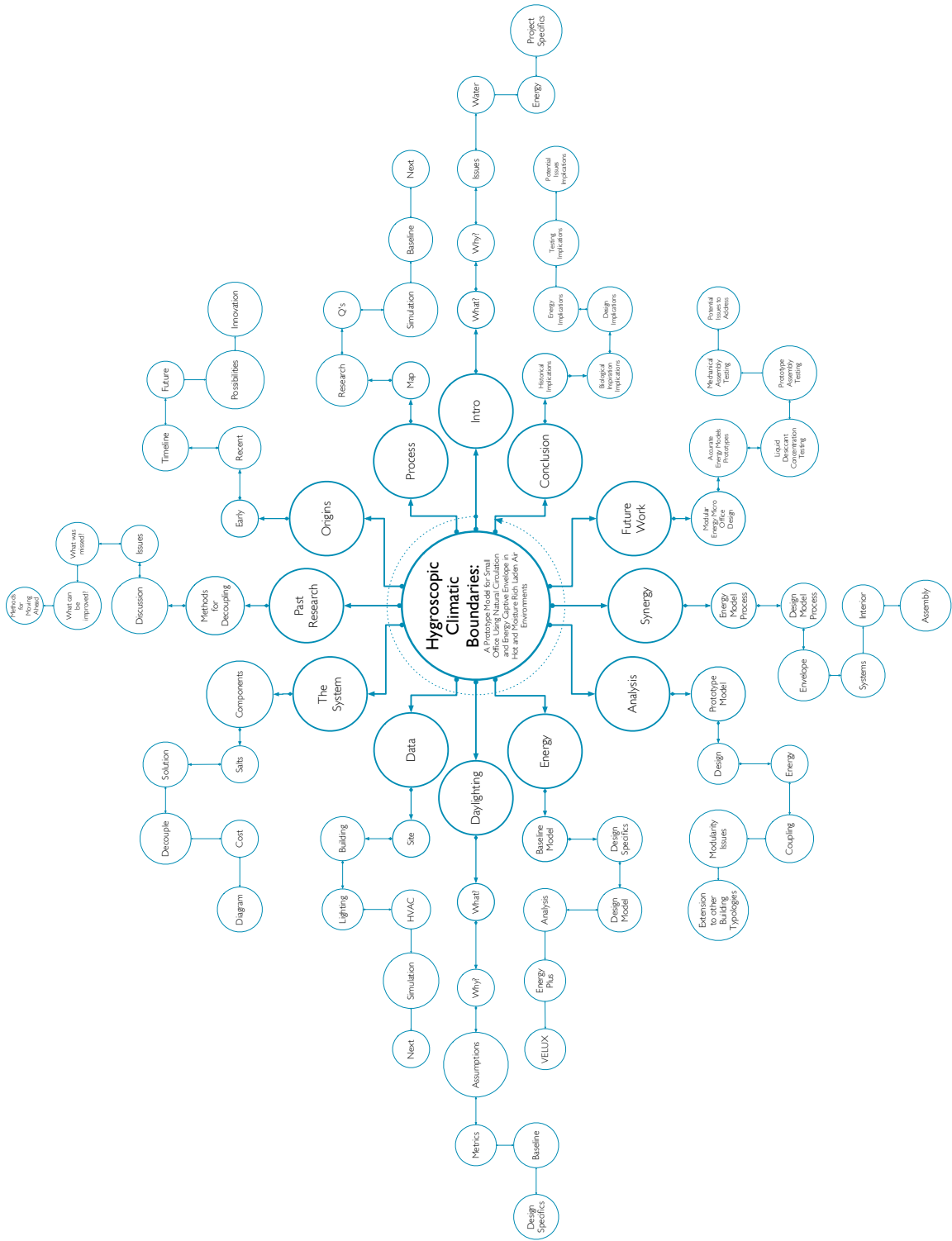


Figure 2.1. Project Hierarchical Process Map

2.1.3 An Alternative Strategy

Figure 2.3 shows an enlargement of subsequent topics for discussion later in the paper that focus on the origins of developments that scavenge moisture from outside air in various ways. It is necessary to understand that the idea is not a new one and has progressively been in use in various forms throughout human development. The issue that presents itself to modern civilization is in the context of anthropogenic impact on the environment in a very small amount of time. Anthropogenic impact on the environment is a term that signifies environmental effects caused by human activity around the world. The detailed discussion of anthropogenic activities is outside the scope of this thesis. Certain refrigerants in production and use for air conditioning are toxic and negatively affect the environment in terms of depletion of the ozone layer and contribute to global warming potential. The detailed discussion of refrigerants and conventional air conditioning equipment is outside the scope of this thesis. The thesis focuses on an alternative strategy for space conditioning in the service of occupant comfort that have benign impact on the environment by avoiding the use of toxic compounds that contribute to global warming potential and depletion of the ozone layer. A discussion of early hygroscopic climatic boundaries may suggest new potentialities for further development towards less energy consumptive and environmentally benign strategies for space conditioning in hot and humid climates. The thesis discusses the components of the system, the types of Hygroscopic Salt and mixtures for consideration of their benign impact on humans and the environment, and the costs associated with decoupling air conditioning systems from dehumidification and cooling.

2.1.4 The Prototype

Figure 2.4 shows an enlargement of topics that consider the prototype commercial office-building model in terms of data, daylighting, and energy. The thesis focuses on site description, building components, lighting, air-conditioning system components, and simulation issues. The simulation of the prototype model in terms of design and daylighting for reduction in energy consumption follows with metrics and design specifications for the project. The models reserves detail simulation for future work.

2.1.5 Building Design and Energy Nexus

Figure 2.5 shows the topics for discussion of the prototype model in the thesis, the potential synergy that come with coupling concepts of design and energy model and future work. The analysis portion discusses the

potential for the prototype model in terms of design and energy as a representation of modular building energy performance and unit using concepts of decoupling dehumidification and cooling. The prototype model presents a process for coupling design and energy modeling strategies at the intersection of building envelope, daylighting, and air conditioning systems in a small prototype office model. A conclusion covers the impacts of historical developments, energy and design strategies, and simulation assessment issues for improvements in future work.

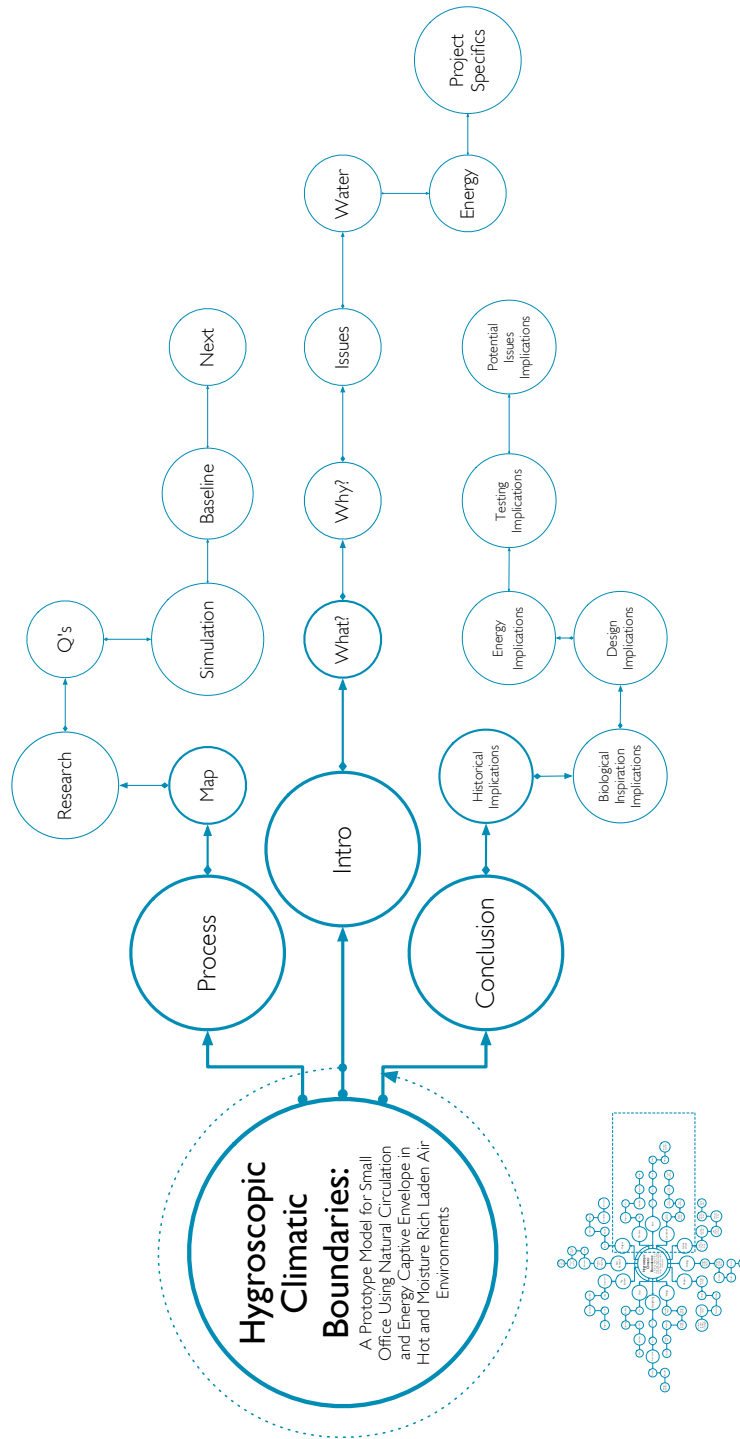


Figure 2.2. Project Hierarchical Process Map

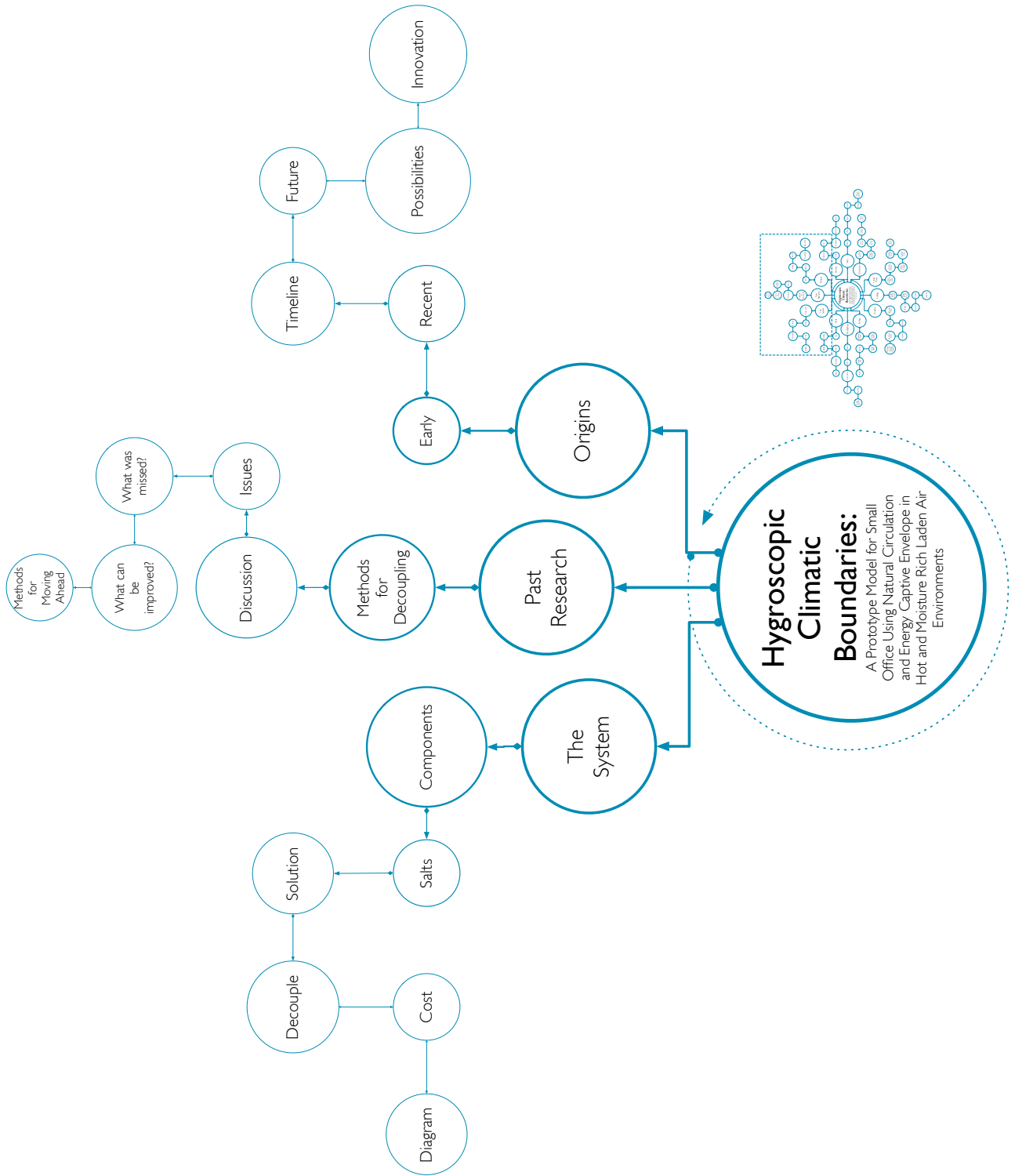


Figure 2.3. Project Hierarchical Process Map

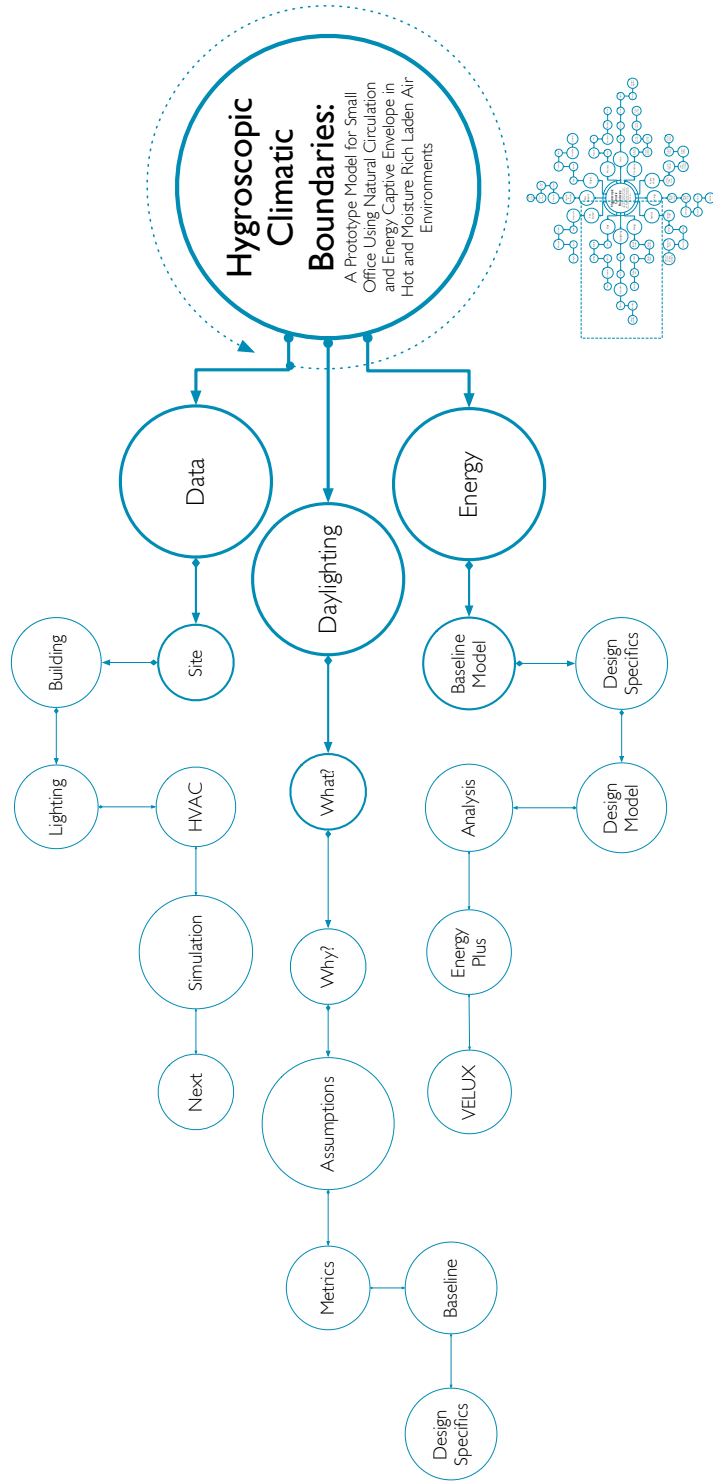


Figure 2.4. Project Hierarchical Process Map

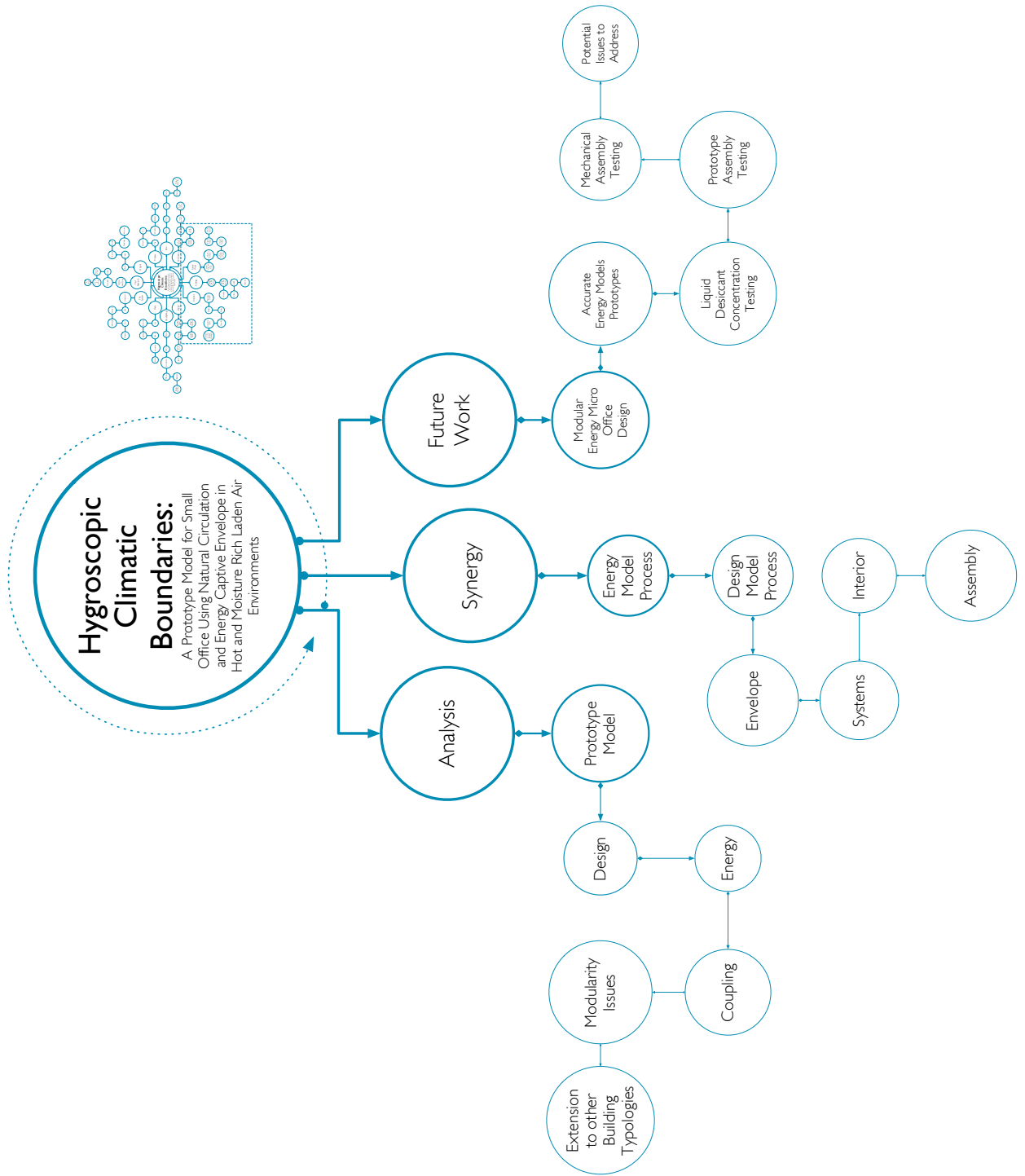


Figure 2.5. Project Hierarchical Process Map

CHAPTER 3: ORIGINS

3.1 Origins of Hygroscopic Systems in HVAC

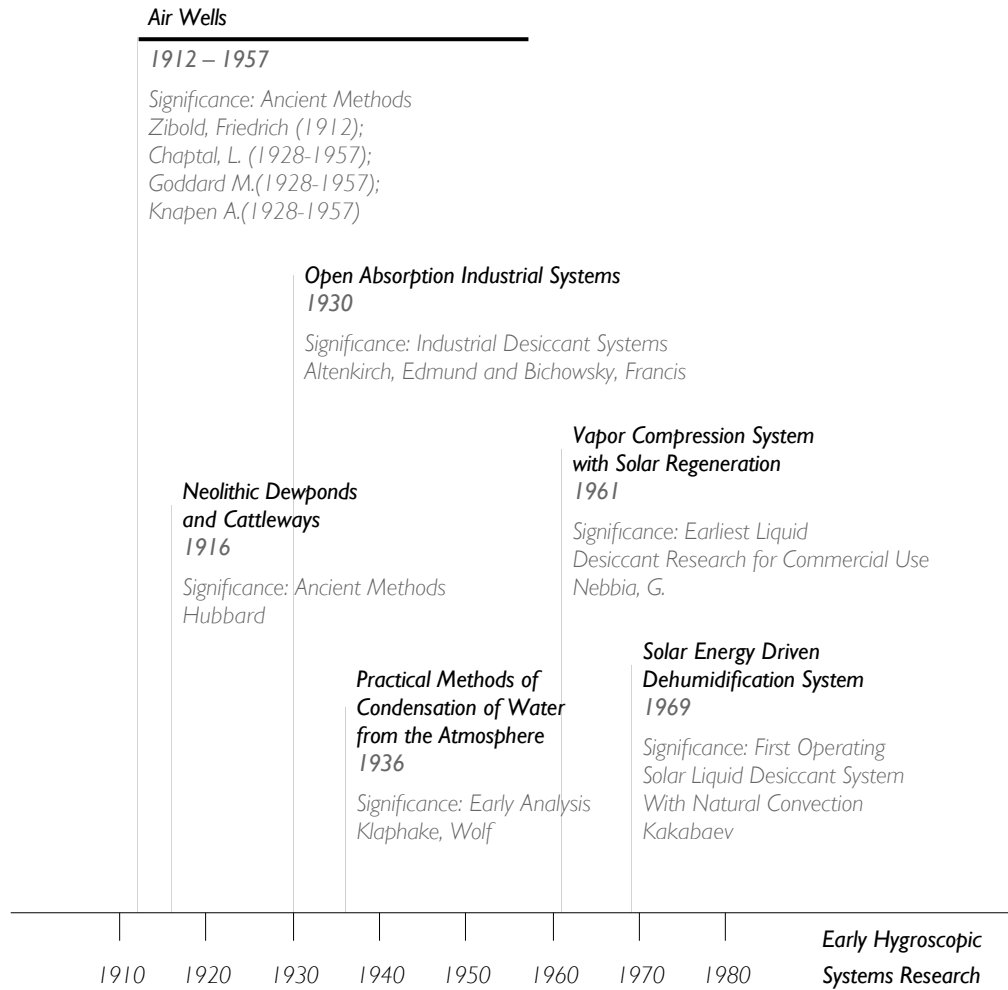


Figure 3.1. Timeline of Early Hygroscopic Research

Figure 3.1 shows a timeline of research and development for early hygroscopic systems research for this thesis. It is not a conclusive timeline of every invention or research document concerning desiccant systems for water generation or dehumidification. The timeline aids understanding of common traits such as the use of hygroscopic materials to absorb and condense moisture vapor from ambient air. The use of hygroscopic and insulation materials is instrumental in the functioning of certain devices. These common convergences may transfer to a building envelope based liquid desiccant system with absorbent surfaces and insulating surfaces.

3.1.1 Dewponds 10,000 B.C. to 2,000 B.C.

The earliest strain of works that deal with the use of hygroscopic materials that interact with moist ambient air begins in one of the remote periods of human development. Humans gather in small groupings as cattle herdsman in what is now modern England, their only natural danger to survival is the wolf. Herdsmen maintain their cattle in the uplands away from the wolves. From ancient remains, earthworks, and cattle tracks, the authors A. Hubbard and G. Hubbard piece together the methods for how these early people survived their condition. The higher elevations in this part of the world did not have generous streams or springs as source for fresh water. Areas such as the Poundbury Camp site near the city of Dorchester present Neolithic humans with an interesting method for keeping their cattle safe and ensuring their survival[9]. Poundbury camp features a containment area with a forward vertical wall embankment as an artificial hillside and platform and open country to the forward end[9]. Neolithic humans devise methods for building containment platforms for their cattle at the base of the highlands where the transition from hillside slopes downward and connects with the lower plains[9]. The containment plains are twenty feet above the adjacent plains and about twenty feet wide[9]. Moving their cattle amongst these platforms produces cattle tracks or paths that over many centuries the cattle developed generational memory. At various points, the cattle need fresh water. Neolithic humans need temporary shelter at these various stopping points for a number of developments such as watch areas, and in some cases more permanent shelter structures. The guard, temporary, and permanent shelters locations are in close proximity to the cattle platforms to provide ample spaces for watching over their precious herds. Fresh water generation to sustain cattle affords Neolithic humans survival.

Neolithic humans develop larger dewponds nearer the end of the period around 2000 BC. The basic construction of the dewpond is a round artificial depression in the ground with a neighboring embankment. Remaining ancient ponds still function today in their capacity to hold water in typically dry soil. The dry soil or clay in this case performs as the hygroscopic material. The Hubbards insist that the development of dewponds enables Neolithic human habitation of large tracts of land that in any other sense is desolate[9]. The dewponds may have provided over a thousand sheep with daily water requirements from one single dewpond[9]. Dewponds use a hygroscopic process cycle to provide a continuing filling of the ponds with water each morning.

3.1.1.1 Dewpond Construction

Modern construction of dewponds of these ancient earth works is to hollow out the earth with a larger radius than required for the final pond[9]. A coating of dry straw covers the hollow depression[9]. A layer of puddled clay lays covers over the straw. Next, a layer of stones covers over puddled clay[9]. The observation of the earth works show that the ponds fill with water in the absence of rainfall and larger depression ponds fill more rapidly.

3.1.1.2 Dewpond Thermodynamics

The stone layer absorbs heat. The stones transfer heat from radiation from the sky to the puddled clay by conduction. The straw is an insulating material in the dewpond construction. The straw layer isolates the puddled clay from subsurface ground and creates a stable temperature difference boundary. As long as the dry bulb ambient air temperature is higher than the subsurface ground, temperature there is always the potential for moisture to condense on the outer clay surface.

3.1.1.3 Dewpond Constraints

Dewpond thermodynamic performance is highly dependent upon the stable dry straw insulation layer. The insulation layer must not become moist or wet as this lowers the insulation resistance between the puddled clay and subsurface ground. Conduction of heat from the subsurface ground to the puddled clay will interrupt the performance of the condenser surface.

3.1.1.4 Dewpond Performance Criteria

Table 3.1 shows performance criteria assessment for the dewpond research. The analysis relates the mechanism, function, constraints, and characteristics for the land structure. Performance characteristics such as geometry, materials, orientation, Exergy, and regeneration afford improvements for transfer to dehumidification applications.

Table 3.1. Dewpond Performance Criteria

Performance Criteria	Dewponds
Condensing Mechanism	Contact with Ambient Air
Regenerative Function	Regeneration
Regeneration Mechanism	Drying
Condensing Constraints	Long Time
Condensing Surface	Large and Thin Clay Layer
Regeneration Shape	Depression
Regeneration Orientation	Horizontal
Condensing Material	Solid Desiccant (Clay)
Water Desorption	Decoupled clay surface from ground
Water Generation Mechanism	Stable Dry Straw Insulation Layer
Exergy	Water Harvesting Includes Opportunity to Use Dry Air

3.1.2 Air Wells

In the earth 20th century, F.I. Zibold reinvents the dew condenser based on the work of ancient Greeks in Theodosia, a city on the Crimean peninsula in Ukraine in 700 B.C. Dew condensers condense water from moisture laden ambient air. Zibold assumes that in the absence of nearby sources of water and the discovery of ancient piping and water channels in numerous mounds that these were ancient dew condensers[10]. Unfortunately, there is little support for the use of dew condensers within these mounds to support his assumptions. Archaeological excavations reveal that the mounds were burial tombs of the ancient Greeks or Scythes from around 500 to 400 B.C[10].

Zibold's condenser is a huge cone with the top cut off. The cone structure made from stacked sea-beach pebbles[10]. The cone and funnel mound mounts a concrete base in the shape of a bowl[10]. In 1912, meteorologist Jacob Mironovitch Nikitas remarks that the condenser when functioning yields 300 to 360 liters per day[10]. Unfortunately, Zibold's condenser did stop functioning. The cone of sea-beach pebbles no longer stands and all that remains of the work is the concrete bowl foundation[10]. No documents or records confirm the yield or cause of the condensers failure. From 1928 to 1957, experimental massive aerial built works by

French hydrologist L. Chaptal, M. Goddard, and Belgian engineer A. Knapen[10] arose in the South of France. These constructions made yields of several liters of water a day.

3.1.2.1 *Air Well Thermodynamics*

In 1996, the researchers Nikolayev et al investigated Zibold's original manuscripts, documents, and construction remains to understand the cause for the failure of the dew condenser[10]. The operation of the dew condenser relies on radiation surface and ground temperature differences. The cold night sky is an immense surface that receives heat via radiation from a warm surface. The warm surface is able to cool from the heat loss. The amount of cooling capacity for the radiating surface lowers when thermally connected to the ground. The cooling capacity of the radiating surface improves when it and the ground is thermally isolated from each other. A thermally isolated radiating surface prevents conduction of heat from ground during the nighttime cycle. In this situation, the radiating surface will radiate most heat to the night sky surface with a smaller amount to convective heat air currents.

3.1.2.2 *Air Well Failures*

The air wells from 1928-1957 in the South of France did not yield much water because of their failure from thermal contact with the ground through their thick and massive concrete shells and foundations[10]. Zibold's condenser made from pebbles had weak contact with other pebbles but was essentially in thermal contact with concrete bowl foundation connected to the ground[10]. The earliest dew condenser that Zibold constructed is essentially a thin radiating surface for heat to the ambient sky surface with very little penetration of humid air into the structure for condensing moisture.

Nikolayev et al show that Zibold's porous structure can be represented by having a large surface (S_c) for heat exchange because of the inherent construction technique of using pebbles to create interior surface areas. The interior surface area (S_i) created from the pebbles presents a much larger surface than the actual exterior radiating surface of the condenser [10]. The heat exchange porous surface (S_c) linearly changes with wind speed. The higher wind speeds create a larger (S_c)[10]. Analysis of (S_c) and (S_i) is shown in a ratio where (S_c)/(S_i) for Zibold's dew condenser is much closer to two in the presence of strong wind speeds such as 10 m/s[10]. Zibold's condenser is a massive condenser because (S_c) is greater than (S_i)[10]. An ideal condenser is

a ratio where (S_c) is equal to (S_i) which is similar to a thin double-sided plane where condensation occurs on both sides of the thin plane[10].

3.1.2.3 Air Well Simulation

Numerical simulation by Nikolayev et al, shows that for September 4, 1992 in Feodosia, Zibold's condenser may in fact yield up to 221 liters of water per day[10]. Zibold's condenser would generate 100 to 200 liters of water per day if there were similar shell surface area and interior surface area, and decoupling between condensing surfaces and ground. The massive constructions create thermal lag response to day heating and night cooling[10]. The structures could not cool down to low enough temperature during the night for dew formation. The ratio between the surface for condensation and the surface for radiation is too large. The air wells could not become cooler than ground temperature and essentially continued radiating heat to the cooler night sky surface.

3.1.2.4 Air Well Performance Criteria

Table 3.2 shows performance criteria assessment for air wells and analysis by Nikolayev et al that improves the engineering of the structures. Ground decoupling and thin double-sided surface geometry improve the performance of the air wells. Table 3.3 shows dewponds and air wells performance criteria for side-by-side comparison. Both structures have many common characteristics related to their performance. The two structures have many similarities but small number of differing characteristics that influence their water generating capacity. Dewponds work because of their insulation layer and air wells work better with low thermal lag construction.

Table 3.2. Air well Performance Criteria

Performance Criteria	Air wells
Condensing Mechanism	Contact with Ambient Air
Regenerative Function	Regeneration
Regeneration Mechanism	Drying
Condensing Constraints	Long Time
Condensing Surface Area	Large and Thin Double-Sided Condensing Plane
Regeneration Shape	Depression
Orientation	Horizontal
Condensing Material	Porous Desiccant (Stone and Air Voids)
Water Desorption	Decoupled condensing structure from ground
Water Generation Mechanism	Low thermal lag response
Exergy	Water Harvesting Includes Opportunity to Use Dry Air

Table 3.3. Dewpond and Air well Comparison

Performance Criteria	Dewponds	Comparison	Air wells
Condensing Mechanism	Contact with Ambient Air	Same	Contact with Ambient Air
Regenerative Function	Regeneration	Same	Regeneration
Regeneration Mechanism	Drying	Same	Drying
Condensing Constraints	Long Time	Same	Long Time
Condensing Surface	Large Surface Area	Same	Large Surface Area
Regeneration Shape	Depression	Same	Depression
Regeneration Orientation	Horizontal	Same	Horizontal
Condensing Material	Solid Desiccant	Different	Porous Desiccant
Water Desorption	Decoupled from ground	Same	Decoupled from ground
Water Generation Mechanism	Stable Insulation Layer	Different	Low thermal lag response
Exergy	Water Harvesting/Dry Air	Same	Water Harvesting/Dry Air

3.1.3 Early Solar Vapor Compression Cycle System with Solar Regeneration

In Sounion, Greece in 1961, Nebbia produces a thesis for the earliest form of a solar liquid desiccant air conditioning system. Nebbia describes the basis for the unit as an evaporator coil, condenser coil, and ambient air blown by a fan[11]. The simple components have a different construction and strategy for use but it is essentially works to condense moisture from ambient air in a similar process as dewponds, and air wells condensers. Instead of connection to subsurface ground, Nebbia's work uses a cooling coil as the temperature sink where air from an inlet flows over the cooling coil. The cool air leaves the unit with less moisture at the same dry-bulb temperature[11]. The process removes latent heat with constant air temperature. The energy consumption equals about 600 kcal/kg condensed water[11]. Nebbia estimates the system removes up to five units of heat for each unit of energy consumed[11]. The system separates 120 kcal/kg of water. He notes that the system can use solar energy for the absorption refrigeration process. Nebbia understood the process of mixing moist air with solid desiccants such as silica gel and liquid desiccants as the system absorbent. Industrial applications in this time use solid and liquid desiccants to lower moisture in storage warehouses[11]. The transformation of these systems for commercial use had not yet been feasible.

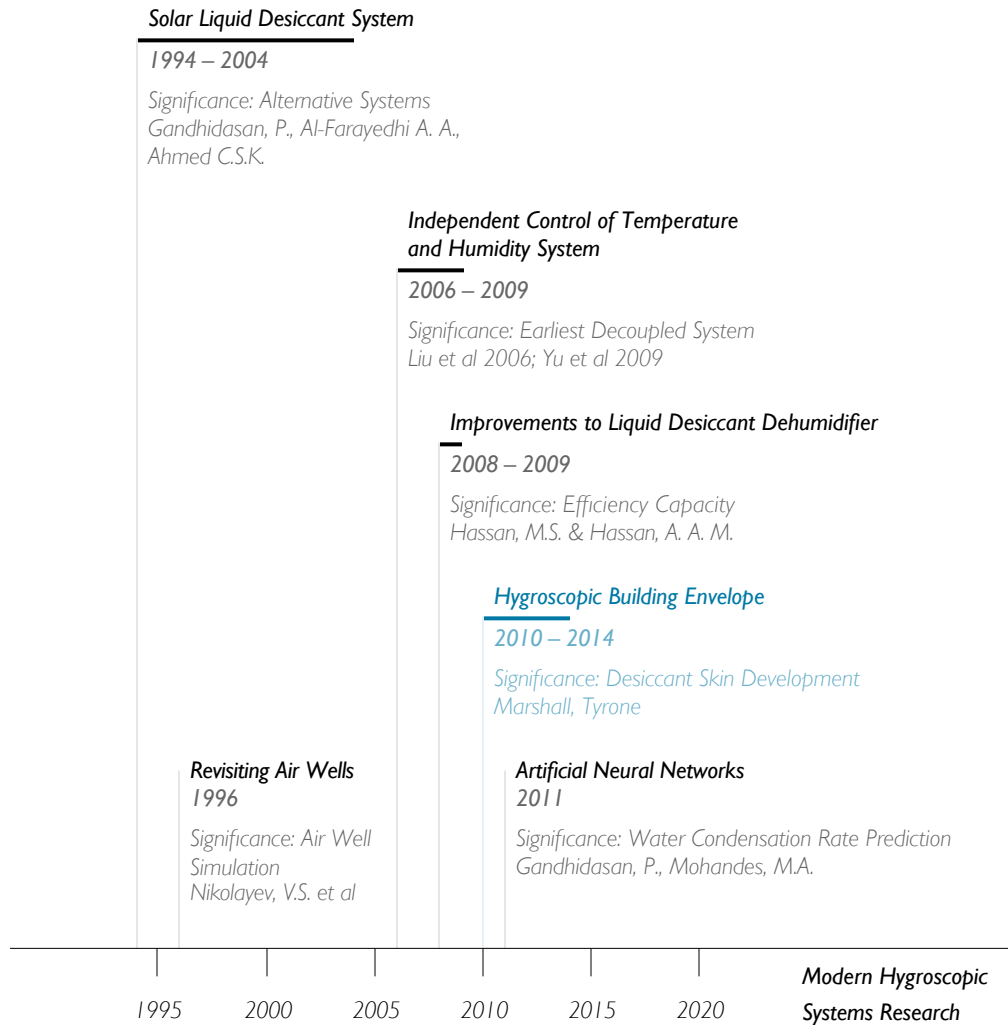


Figure 3.2. Timeline of Modern Hygroscopic Research

Figure 3.2 shows the timeline for modern hygroscopic research for this thesis. The timeline aggregates some of the current research in the area of liquid desiccant air conditioning systems. The modern hygroscopic systems research is work that concerned with liquid desiccant performance, critical analysis of past work, and continuous development of next generation systems.

3.2 Historical Uses

Open absorption liquid desiccant systems in industrial and agricultural industries closely resemble liquid desiccant systems for use in commercial indoor dehumidification[5]. Use of liquid desiccant systems has application in textile mills, post harvests, and low temperature crop drying in stores[6]. Edmund Atenkirch and Francis Bichowsky's early work in industrial liquid desiccant systems is responsible for the longevity of these industrial systems[5]. Other application of industrial use of liquid desiccant systems is in the deep-frying and precise humidity control, ice rinks, and supermarket refrigeration and frozen aisles[8]. The inappropriateness in the past for conversion to commercial use is in response to moisture carryover and corrosion issues. Lithium chloride corrodes metal when in contact with oxygen. Corrosion affects components downstream of the absorber. Moisture carryover can corrode ducts and coils. Carryover of toxic liquid desiccants may cause potential health concerns[8]. The adaptation of these systems for commercial office buildings is not feasible due to high cost of liquid desiccant such as lithium chloride. Currently, advanced liquid desiccant and dedicated outdoor air systems cost 65 percent more than dedicated outdoor systems using conventional vapor-compression technology[8].

3.2.1 *Vapor Compression System with Solar Regeneration*

Vapor compression system with solar regeneration cool fresh air to below the dew point temperature and absorb water using a solid absorbent or a hygroscopic solution. Solid and liquid absorbents absorb water when cool and evaporate water when heated. Vapor compression systems with solar regeneration make use of a liquid desiccant, absorber, and regenerator[8]. A strong concentrated liquid desiccant flows into an absorber and downward using gravity in a thin flow to present a large surface for absorption[8]. Packed beds of desiccant granules or other enhanced mass transfer surface improve the absorption process. Usually ambient outside air passes through an absorber in the opposite direction to the liquid desiccant flows. Crossing paths transfer moisture and heat from the fresh air stream into the thin liquid desiccant flow[8]. During the moisture transfer, the liquid desiccant becomes cooler and more diluted. The less concentrated liquid desiccant leaves the absorber chamber and flows into the regenerator[8]. The regenerator makes use of solar energy to heat the cool and weak desiccant solution. Heating the desiccant solution increases the vapor pressure of the water[8]. A second chamber of counter-flowing air stream allows for a spray of this heated weak desiccant to release moisture to a scavenging air stream[8]. The second chamber is where the liquid desiccant regenerates through the rise in concentration due to moisture scavenging by second air stream that could be exhaust air. A heat pump system

instead of a heat exchanger can increase the quality of heat transfer cooling the liquid desiccant[8]. The return feed of the regenerator passes through a cooling tower or chiller to remove more heat from the regenerator[8]. The liquid desiccant is hot and concentrated after regeneration. The process restarts with the liquid desiccant leaving the regenerator and flowing downward over the absorber surface in contact with fresh air.

Vapor compression systems with solar regeneration exhaust either condensate or condensate mixed with air to ambient. The opportunity to harvest condensate or moist air is mostly lost. Dewponds and air wells generate water but miss the opportunity to harvest low moisture content air. The attractiveness of liquid desiccant air conditioning systems provides a direct path from fresh air to indoor air[12]. Locating dehumidification components in the building envelope close to fresh air offers improvement in the dehumidification process with less energy losses.

3.2.2 Modern Consideration of Liquid Desiccants

Liquid desiccants have flexibility to store and release moisture vapor when applying and removing regeneration heat. The solution reaches equilibrium once the differential between the amounts of moisture vapor evaporating and condensing reaches zero. Liquid desiccant regeneration requires temperature of 122 °F (50 °C) to 140 °C(60 °C)[2]. Low-grade thermal energy such as waste heat, photovoltaic, and geothermal qualify as liquid desiccant regeneration heat sources.

3.2.3 Modern Modified Open Absorption Liquid Desiccant System

Gandhidasan proposes a modern modified open absorption liquid desiccant system based on simple absorber and solar regenerator. The system uses liquid desiccant to absorb water vapor from contact with fresh air[13]. Gandhidasan's absorber places a single glass plane over absorber for the solar regenerator[13]. A thin free falling layer of liquid creates a small temperature gradient[13]. The absorber uses calcium chloride as the liquid desiccant. After moisture absorption, the dry warm air cools by sensible or evaporative cooling. Another process heats the diluted liquid desiccant to remove the newly absorbed moisture vapor[13]. Gandhidasan's simple system is not useful in hot and humid climates as the liquid desiccant heating temperature is too low for evaporation[13]. There is little allowance for mass transfer of moisture to occur in hot and humid climates using Gandhidasan's design. For the system to work in hot and humid climates, liquid desiccant regeneration require

sufficient heating to increase its surface vapor pressure above ambient air vapor pressure[14]. The simple system is most useful as an alternative to vapor compression systems as it uses a liquid desiccant to store energy in chemical form rather than as thermal energy.

3.2.4 Modern Liquid Desiccant Heat Exchanger

The majority of systems in development for advanced liquid desiccant air conditioning systems use a dense array of parallel plates for liquid desiccant spray mechanism. The liquid desiccant spray allows a thin constant falling film flow to create a large surface for moisture absorption from counter-flow of passing air stream[2]. Lithium bromide as liquid desiccant improves performance in these systems. Hybrid liquid desiccant systems reach high efficiency when combined with vapor compression chillers[6]. The chiller operates with high efficiency from higher evaporator operating temperature and heating of absorber air in a multi pass system[6]. In the first pass, air flows through an absorber in contact with hot concentrated liquid desiccant. The higher surface vapor pressure of the liquid desiccant absorbs moisture from the air. The dry air in this pass undergoes independent handling of latent load and is useful for space conditioning by undergoing a separate independent handling of sensible loads[6]. In a second pass, a separate stream cools dry airflows over warm and weak concentrated liquid desiccant. The second pass of air absorbs most of the moisture vapor from the cool dilute liquid desiccant. Multiple absorbers and regenerator can transfer weak and strong desiccant back and forth with multiple fresh air intakes including storage capacity for strong desiccant. The use of liquid desiccant systems with combined heat and power system generate and store strong desiccant using excess waste heat on off-peak hours for additional cooling capacity during peak demand hours[8].

3.3 Shared Convergence Early and Modern Hygroscopic Systems Research

These various strategies seem to have divergent uses. On the first hand, there are methods for water generation from air and on the second hand; there are methods for dehumidification of air. Both methods use similar condensing mechanism that contacts fresh air and absorbs moisture vapor. Water generation from and dehumidification of fresh air is essentially the same process. Fresh air as a dynamic layer for mass transfer of water vapor serves no benefit other than water generation. Fresh air that enters a thin double-sided structure, as improved by Nikolayev et al, leaves the structure through its own inertia providing a volume for mass transfer of water vapor that serves no other benefit. Dehumidifying fresh air offers dry air for air conditioning indoor

spaces and water harvesting.

There is a common convergence between dewponds, air wells, and solar liquid desiccant air conditioning systems. Surfaces perform as an absorber and evaporator at the lowest level of common traits. The movement of moisture vapor from air to a surface through condensation is commonplace. The dewponds and air wells are remarkably passive structures in their performance of water condensation from ambient air. The early and modern solar liquid desiccant systems have the potential to use of low-grade waste energy to offset energy requirements for a distinct third element or regenerator.

CHAPTER 4: PAST RESEARCH

4.1 Biological Inspired Design Analogues

Biological analogues offer useful models of biologically inspired design for their adaptation and deployment of low-energy and resource economy[15]. Biological inspired design analogues offer unique methods of innovative adaptations for airflow movement in nature. Biological adaptations resemble human technological design in function but differ in energy expenditure. Air conditioning systems rely on high-energy intensive functions that require high-grade energy to provide indoor air comfort. Biological analogues offer strategies that use low-grade energy expenditures for airflow regulation, temperature, and humidity control.

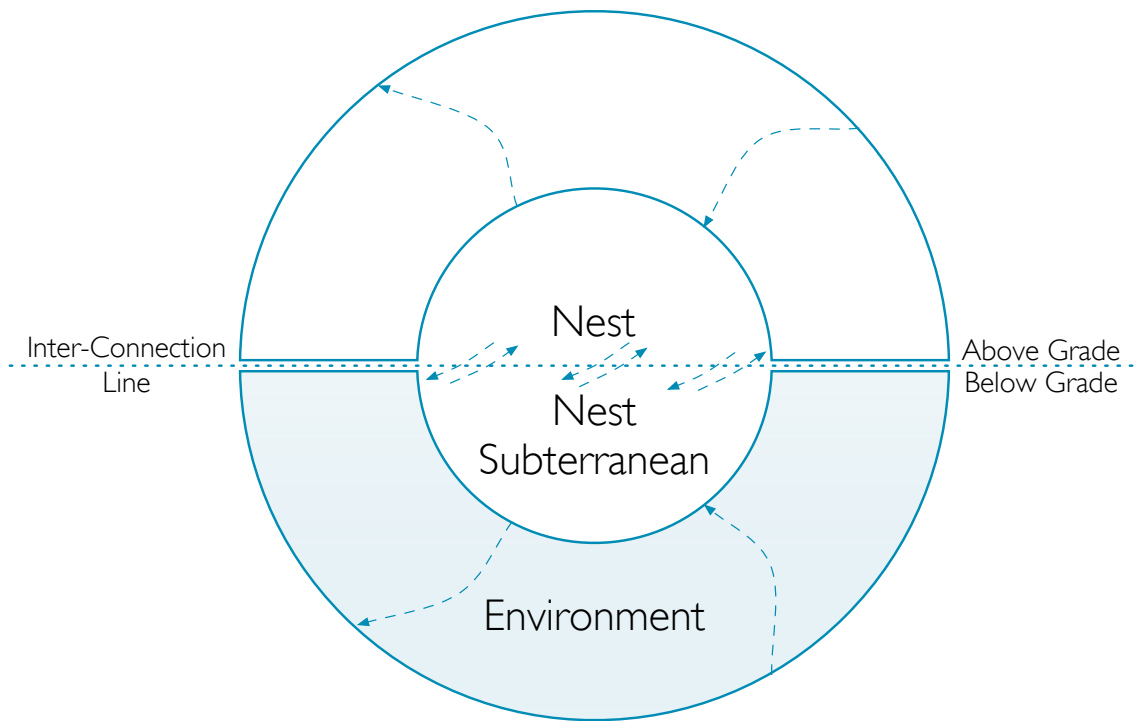


Figure 4.1. Leaf Cutting Ant Climatic Diagram

Biological analogues sometimes layer components by varying scale and thickness to develop hard materials. The abalone shell uses layering, scale, and geometrical alignment of calcium carbonate, aragonite, and a polymer mortar to produce a biologically hard material[15]. The benefit of studying abalone shells offer improvements

to manufacturing of new composites that are stronger, flexible, and less energy intensive to fabricate. Biological analogues for airflow control, temperature and humidity control make use of their immediate environment to create an associative, connective, and functional physical habitat. The leaf-cutting ant (*Atta vollenweideri*) harnesses the wind through adaptations to nest architecture. The Great Plains prairie dog harnesses the wind through its tunnel architecture. The architectural characteristics of leaf cutting ant nest and Great Plains prairie dog tunnel may offer adaptations for passive airflow control of temperature, humidity, and ventilation.

4.1.1 Leaf Cutting Ant Harnesses Wind

The nest structure of the leaf-cutting ant consists of an upper and lower area of inter-connective relationships. Figure 4.1 shows graphic depiction of the relationship between leaf cutting ant above ground nest, below ground nest, and environment. The inter-connective line modulates the exchange of temperature, humidity, and gas exchange within the nest structure. The nest structure functions similarly to a building envelope in that it provides protection from predators and climatic conditions yet provide dynamic relationship between inflow of air, gases, and outflow of air [16]. The nest adaptation for passive nest ventilation uses wind induced air flow [17]. Figure 4.2 shows a hierarchical key map of the layering of adaptations that allow the leaf cutting ant mound to achieve passive nest ventilation. Figure 4.2 allows for a complete spatial integration of the key components. The key components consist of the following adaptations the leaf-cutting ant deploys: nest seasonal adaptation, nest structure, nest cultivation, nest thermal convection, nest induced convection, nest tunnel workings, nest tunnel torrents, and nest carbon dioxide controls. Deployment of key components of the nest hierarchical structure allows highly inter-connective strategy to achieve multiple low energy functions and resource economy.

4.1.1.1 Nest Seasonal Adaptation

Figure 4.3 shows the seasonal adaptation characteristics for leaf cutting ant nest. The leaf cutting ant workers locate their nest structure to influence wind-induced ventilation. In warm and humid seasons, the leaf cutting ant workers show a behavior to open large number of nest entrances solely for wind-induced ventilation [17]. In autumn, the leaf cutting ant workers close up to 90 percent of their nest entrances to reduce wind induced nest ventilation [17].

4.1.1.2 Nest Structure

Figure 4.4 shows structural characteristics of the leaf cutting ant nest. The leaf cutting ant mounds require the excavation of 15 m^3 for mature nests in clay soils[17]. The scale of the leaf cutting ant nest is a large-scale structure that can host upwards of 5 million inhabitants[17]. The structures can reach and exceed heights of six meters[17]. In some species of these ants, the nest area for these excavations extend over 220 m^2 including the network of foraging tunnels and fungus chambers[16]. The nest below grade network consists of large horizontal primary branching tunnels, small mostly vertical or downward sloping secondary branching tunnels, and smaller short tunnel connections to fungus chambers[16]. The nest tunnels branch out in a radial pattern from the nest center[16]. The below grade depth of these nests can extend downward to seven meters[16]. The fungus chambers are located typically one meter below grade.

4.1.1.3 Nest Cultivation

Figure 4.5 shows characteristics of the nest fungus cultivation. The leaf-cutting ant may have upwards of almost eight thousand fungus chambers[16]. The leaf cutting ants cultivate large numbers of fungus chambers deep within the nest using plant fragments[16]. The growth of fungus provides food for leaf cutting ant larvae and for the worker ants[16]. The leaf cutting ants locate the fungus in chambers where the average temperature is 74°C and high humidity[16].

4.1.1.4 Nest Thermal Convection

Figure 4.6 shows the characteristics of leaf cutting ant nest thermal convection. Most work to understand passive nest ventilation uses propane tracer gas, carbons dioxide, and oxygen for concentration detection in nest excavation, cement castings of nest tunnels, and fungus chambers[16]. Concentrations for these gases show inflow and outflow of carbon dioxide and oxygen into the low placed openings at the mound interface with the ground and out of the higher locations for nest mound openings[16]. While wind energy induction provides airflow movement through the center of the mound to the upper portions of the mound, airflow does not influence deeper regions of the mound below grade and near the fungus chambers[16]. The deeper below grade areas of the mound have lower concentrations of oxygen and higher concentrations of carbon dioxide[16]. These lower and deeper areas rely mostly on diffusion airflows from leaf cutting ant worker and

fungus respiration, nest chamber air, nest tunnel air, and soil mass[16]. The combination of upper nest induced wind air flow and lower nest diffusive air flows maintain nest temperatures below 30 °C as temperatures above 30 °C damage fungus growth[17].

4.1.1.5 Nest Induced Convection

Figure 4.7 shows the characteristics for leaf cutting ant induced convection. The leaf cutting ant workers adapt their nest design by connecting ambient air to their nest interior with tunnels and tunnel openings at different vertical locations[16]. The direction of air movement under these configurations is always to pull air into the lower elevation openings and push air out of the higher elevation openings[17]. Airflows into the nest mound by low pressure created at the mound top are due to general principles in wind velocities over ground surface. Wind speeds over ground surfaces show a rising velocity with rising elevation. The changes in wind speed are from higher laminar airflow resistances at lower elevations. Outward air flows under high internal nest pressures at the top with a pressure drop[16]. The leaf cutting ant worker modifies the openings with torrent features. The torrent adaptations improve induced wind airflow. The leaf-cutting nest feature a large number of inflow and outflow tunnels. Most nest openings are not foraging tunnels; in fact, most traffic is through a small number of available openings such as eighteen out of one hundred and sixty-nine tunnels[17].

4.1.1.6 Nest Tunnel Workings

Figure 4.8 show characteristics for leaf cutting ant nest tunnel workings. The negative pressure flow firstly pulls air into the mound towards the center: The leaf cutting ant workers construct high mound openings to face parallel with wind direction to create negative wind pressure[17]. Low periphery mound openings face upwind to pull airflow into nest mound[17]. The airflow inflow and outflow works by negative pressure from openings near the top of the mound. The leaf cutting ant larvae and fungus chambers located at shallow depths below ground benefit from the inflow and outflow of induced airflow mass into the nest. Small inflow of oxygen feeds the brood and fungus chambers in combination with diffusive airflow from soil mass. The more deeply located fungus chambers benefit from dynamic exchanges of small amounts of oxygen inflow with leeching of oxygen from soil mass against respiration of carbon dioxide from leaf cutting ants, fungus, and soil mass.

4.1.1.7 Nest Tunnel Torrents

Figure 4.9 shows the leaf cutting ants mound location and shape adaptation to harness energy from passing wind over nest openings to drive shallow and above ground nest ventilation[16]. The ants raise mound heights to influence airflow movement passing overhead[16]. The nest openings feature torrent structures that resemble articulated collars. The articulated collars create low pressure at the mound openings. The lower periphery mound openings create higher wind pressures from upwind alignment. The mound shape and mound opening adaptations use Bernoulli's law to influence airflow mass into and out of the leaf cutting ant nest[17].

4.1.1.8 Nest Carbon Dioxide

Figure 4.10 shows the characteristics of nest carbon dioxide adaptation. The leaf cutting ant workers (*Atta vollenweideri*) have high tolerance of carbon dioxide concentrations and low oxygen concentrations. Portions of the nest below grade surpass depths of seven meters[16]. The ratio of carbon dioxide concentration has a linear relationship to soil depth. At lower depths, carbon dioxide concentration rises towards hypercapnia levels[16]. The symbiotic relationship between the leaf cutting ants and fungus generates additional carbon dioxide within the nest and in the fungus chambers. Main tunnel shafts and fungus chambers do not connect. The fungus chambers attach to small short tunnels that connect to small mostly vertical secondary tunnels. These fungus chambers do not benefit from nest inflow and outflow air movement. Instead, the subterranean fungus chambers participate in a diffusive exchange of carbon dioxide and oxygen with the surrounding soil mass[16]. High levels of carbon dioxide do not benefit the growth of nest fungus. The leaf cutting ants mitigate high carbon dioxide and low oxygen fungus response by relocating the fungus to more shallow areas. The dynamics of gas exchange within the lower regions of the nest is through diffusion. The nest and below grade soil functions balance oxygen and carbon dioxide storage capacity[16]. The surrounding soil mass in the deeper levels of the nest leeches oxygen to the air mass in the deep regions of the nest. The surrounding soil mass provides additional carbon dioxide storage capacity. Inflows of air into the nest add more oxygen to the nest above and below grade areas. The leaf cutting ants and fungus remove oxygen from inflows and add carbon dioxide to the nest air mass from respiration. The equilibrium balance within the deeper nest below grade areas moves towards the levels of carbon dioxide and oxygen present in the soil mass. The nest and soil mass work in a symbiotic relationship to maintain the equilibrium of carbon dioxide and oxygen in response to nest air inflows, nest air outflows, and leaf cutting ant and fungus respiration exchanges.

4.1.1.9 Leaf-Cutting Ant Nest Performance

Table 4.1 shows performance criteria for leaf-cutting ant nest wind-induced ventilation. The nest habitation relies on the manipulation of nest openings and subtle gas exchange in the upper and lower areas. The interconnected dependency on interactions to direct airflow and tune torrent definition offer transferable characteristics for wind-induced apertures such as an articulated ventilation flap for buildings.

Table 4.1. Leaf-Cutting Ant Nest Performance Criteria

Performance Criteria	Leaf-Cutting Ant Nest
Seasonal Adaptation	Orientation for wind-induced Ventilation
Seasonal Adaptation Mechanism	Ants Open and Close Nest Entrances
Structure	Parallel Connecting Tunnels
Humidity Control	Nest Cultivation of Fungus
Thermal Convection	Natural Convective Upper Nest /Diffusive Lower Nest
Airflow Movement	Natural Convective Upper Nest /Diffusive Lower Nest
Airflow Mechanism	Offset Inlet and Outlet Air Nest Openings
Airflow Performance Adaptation	Pressure Drop
Airflow Penetrations	Large Number
Airflow Adaptation	Torrent Definition Improve Induced Wind Airflow
Directional Adaptation	Mound openings oriented parallel to wind direction
Exergy Adaptation	Wind Harvesting

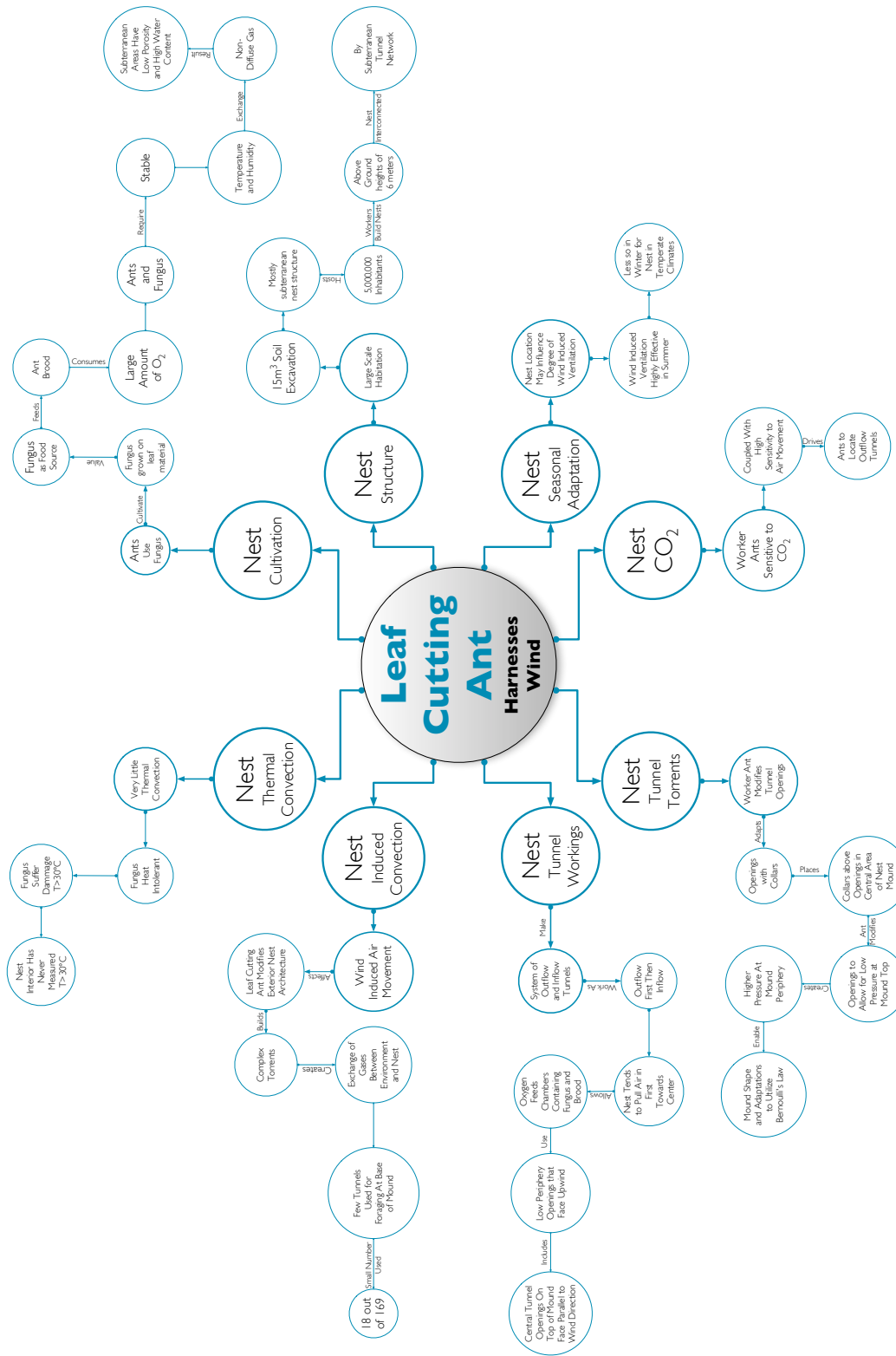
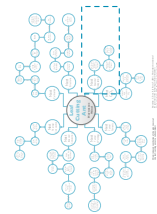
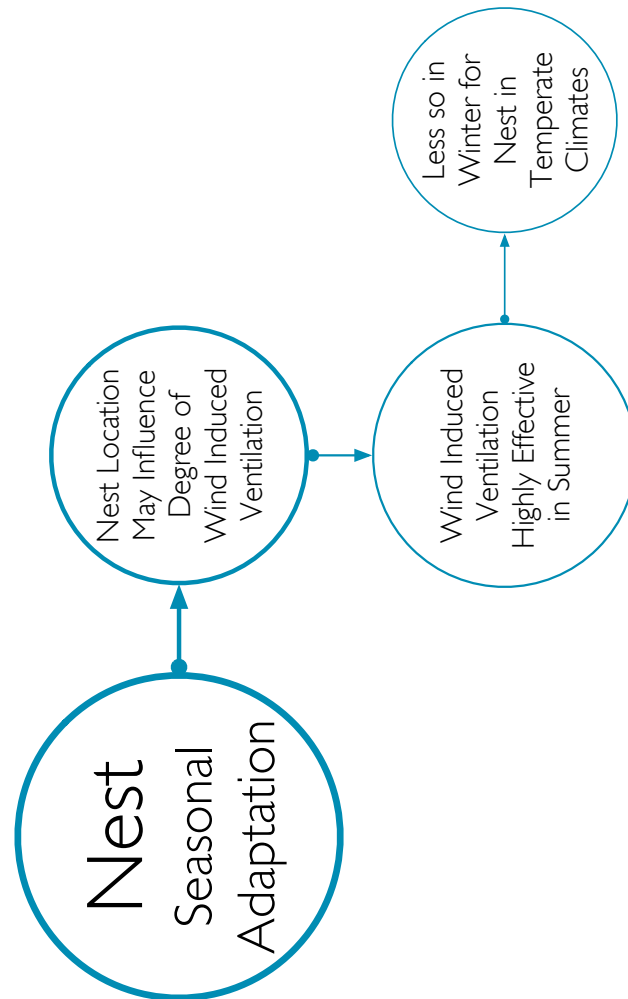


Figure 4.2. Leaf Cutting Ant Biological Analogue Hierarchical Key Map

Kleineidam, C., Ernst, R., & Rocas, F. (2001). Wind-induced ventilation of the giant nests of the leaf-cutting ant *Atta vollenweideri*. *Naturwissenschaften*, 88(7), 301-305. <http://dx.doi.org/10.1007/s001140100235>

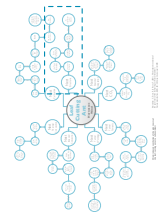
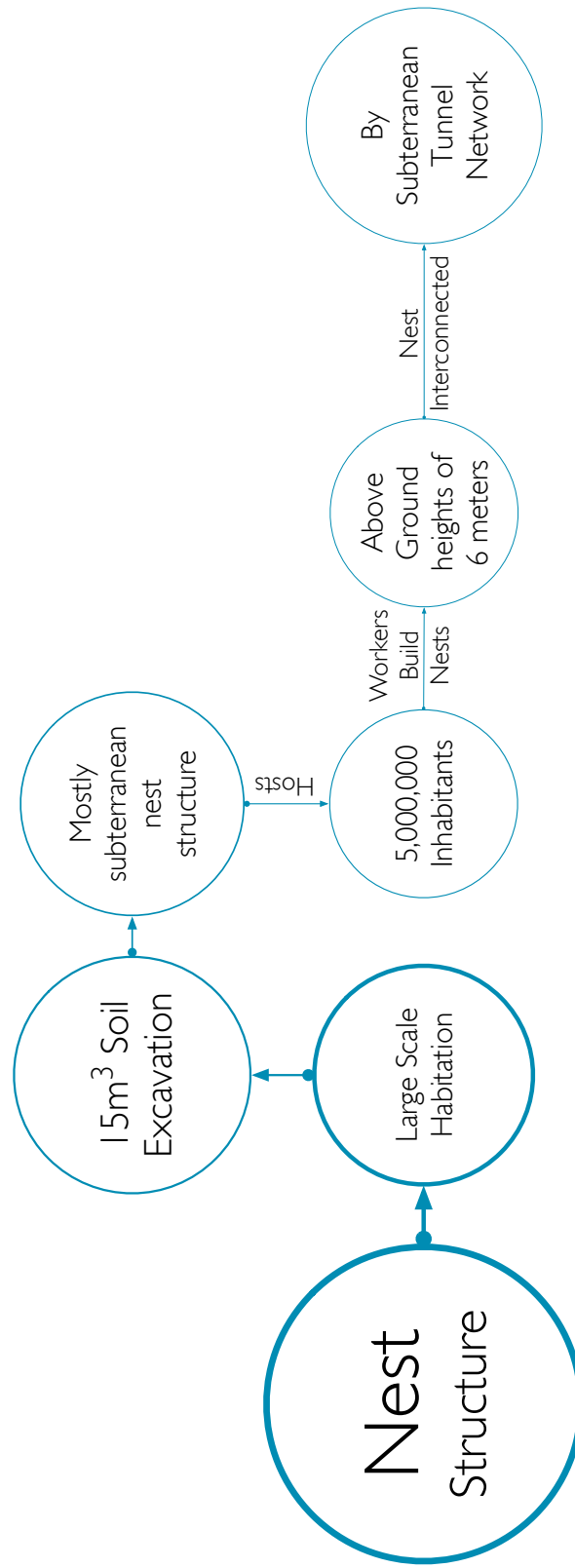
Wind-induced ventilation of the giant nests of the leaf-cutting ant *Atta vollenweideri*



Wind-induced ventilation of the giant nests of the leaf-cutting ant *atta vollenweideri*

Kleineidam, C., Ernst, R., & Roces, F. (2001). Wind-induced ventilation of the giant nests of the leaf-cutting ant *Atta vollenweideri*. *Naturwissenschaften*, 88(7), 301-305. <http://dx.doi.org/10.1007/s001140100235>

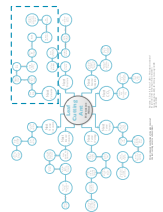
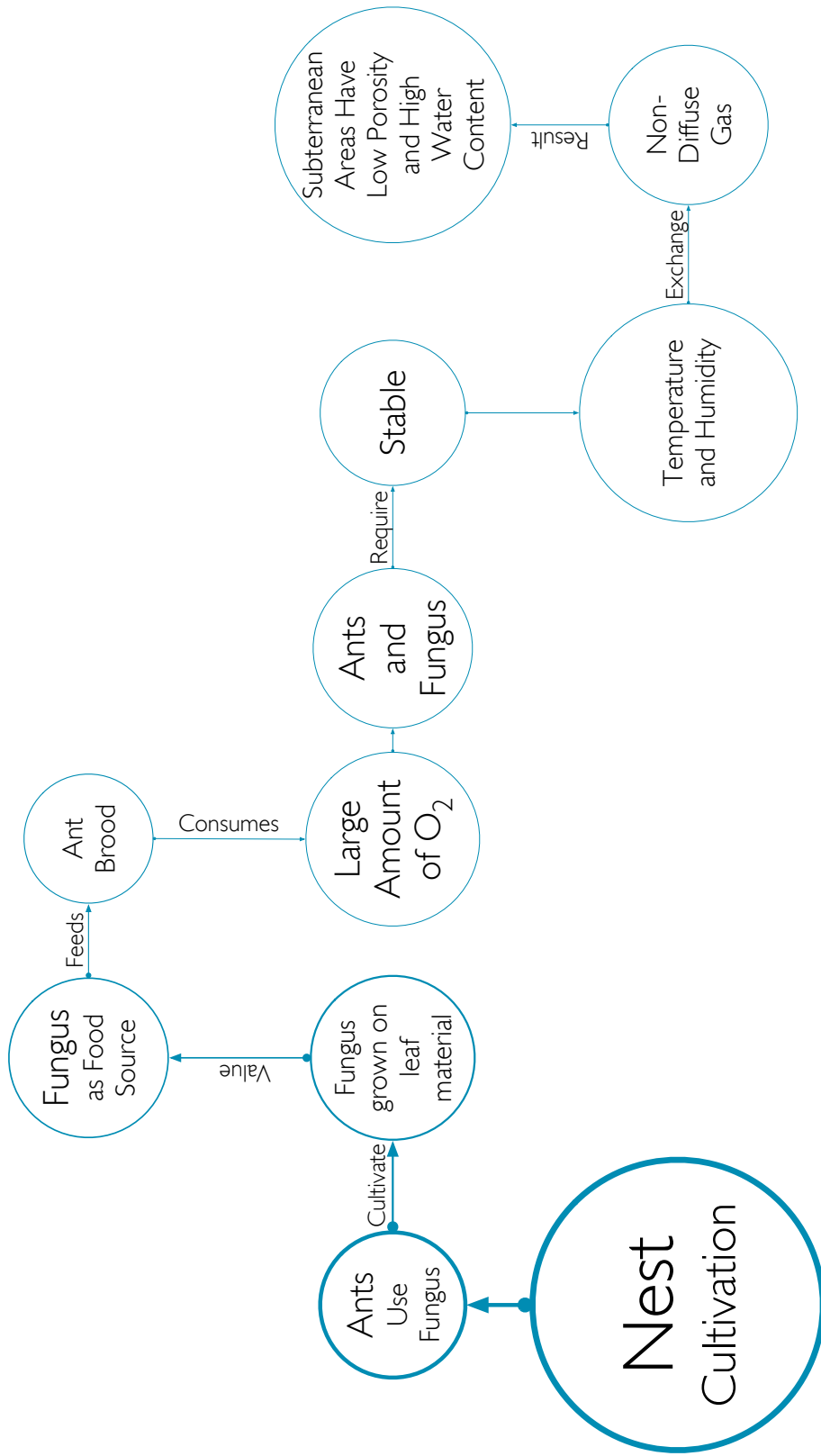
Figure 4.3. Leaf Cutting Ant Biological Analogue Nest Seasonal Adaptation Hierarchical Map



Wind-induced ventilation of the giant nests of the leaf-cutting ant *atta vollenweideri*

Kleineidam, C., Ernst, R., & Roces, F. (2001). Wind-induced ventilation of the giant nests of the leaf-cutting ant *Atta vollenweideri*. *Naturwissenschaften*, 88(7), 301-305. <http://dx.doi.org/10.1007/s001140100235>

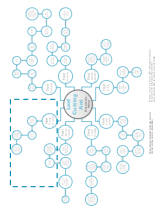
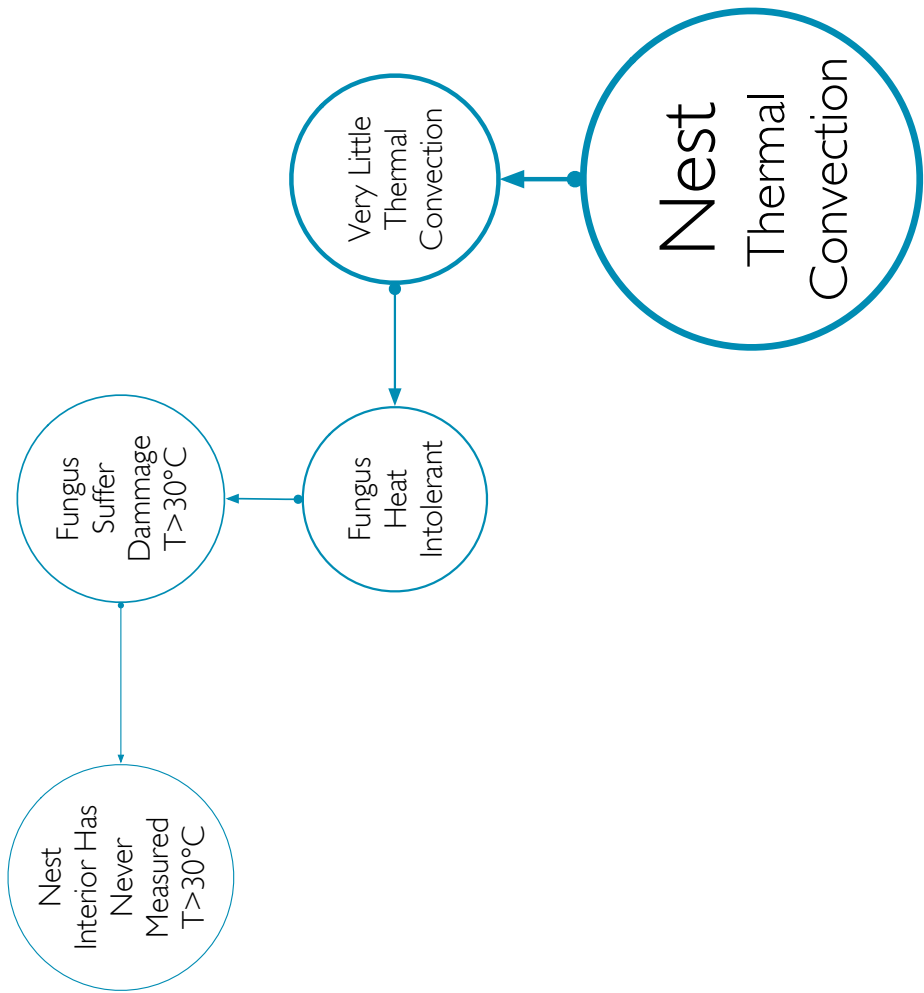
Figure 4.4. Leaf Cutting Ant Biological Analogue Nest Structure Hierarchical Map



Wind-induced ventilation of the giant nests of the leaf-cutting ant *atta volleneideri*

Kleineidam, C., Ernst, R., & Roces, F. (2001). Wind-induced ventilation of the giant nests of the leaf-cutting ant *Atta volleneideri*. *Naturwissenschaften*, 88(7), 301-305. <http://dx.doi.org/10.1007/s001140100235>

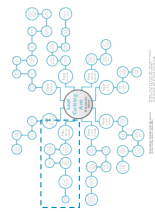
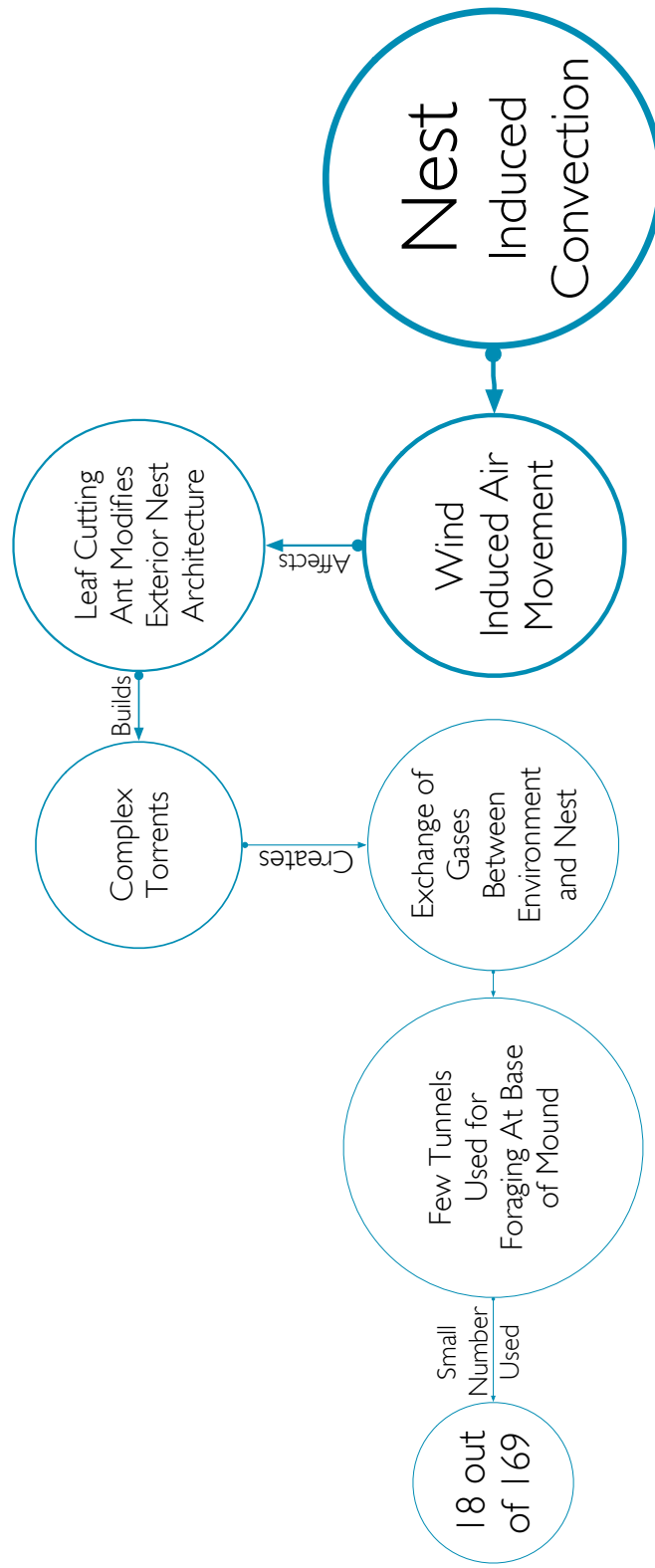
Figure 4.5. Leaf Cutting Ant Biological Analogue Nest Cultivation Hierarchical Map



Wind-induced ventilation of the giant nests of the leaf-cutting ant *atta vollenweideri*

Kleineidam, C., Ernst, R., & Roces, F. (2001). Wind-induced ventilation of the giant nests of the leaf-cutting ant *Atta vollenweideri*. *Naturwissenschaften*, 88(7), 301-305. <http://dx.doi.org/10.1007/s001140100235>

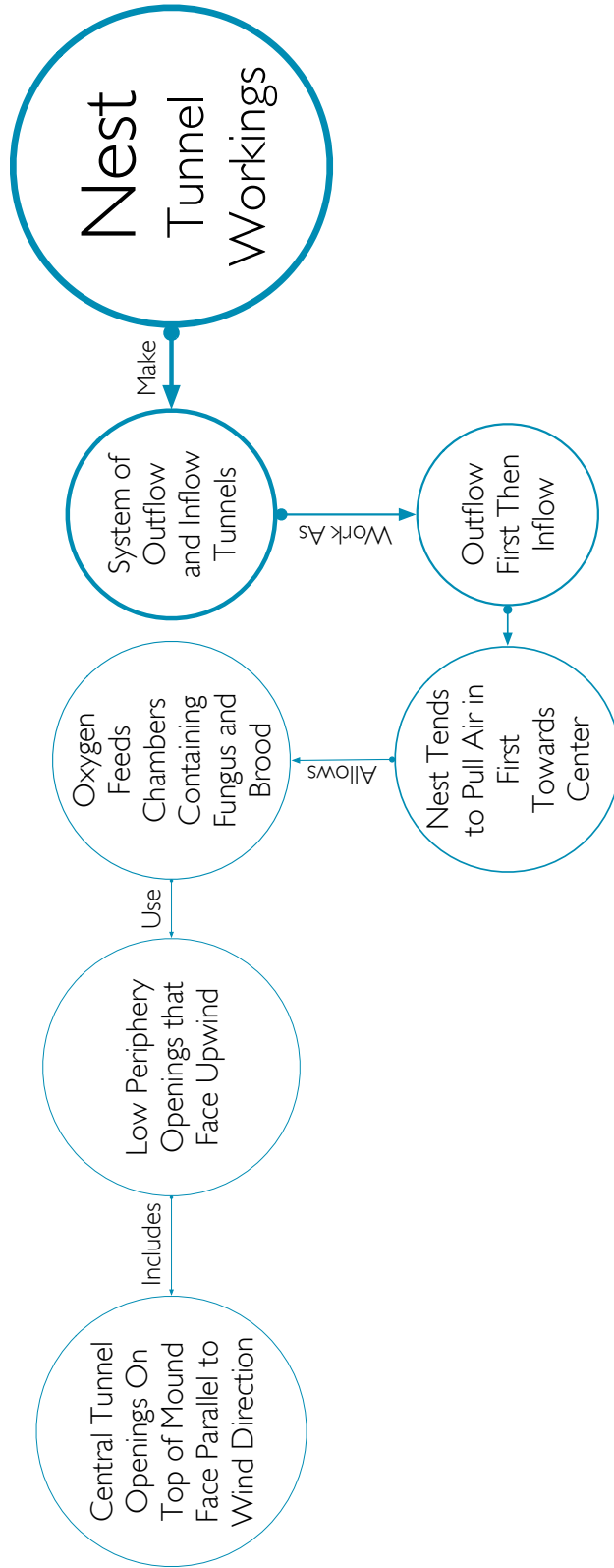
Figure 4.6. Leaf Cutting Ant Biological Analogue Nest Thermal Convection Hierarchical Map



Wind-induced ventilation of the giant nests of the leaf-cutting ant *atta vollenweideri*

Kleineidam, C., Ernst, R., & Roces, F. (2001). Wind-induced ventilation of the giant nests of the leaf-cutting ant *Atta vollenweideri*. *Naturwissenschaften*, 88(7), 301-305. <http://dx.doi.org/10.1007/s001140100235>

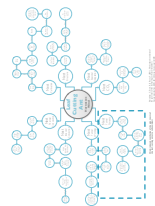
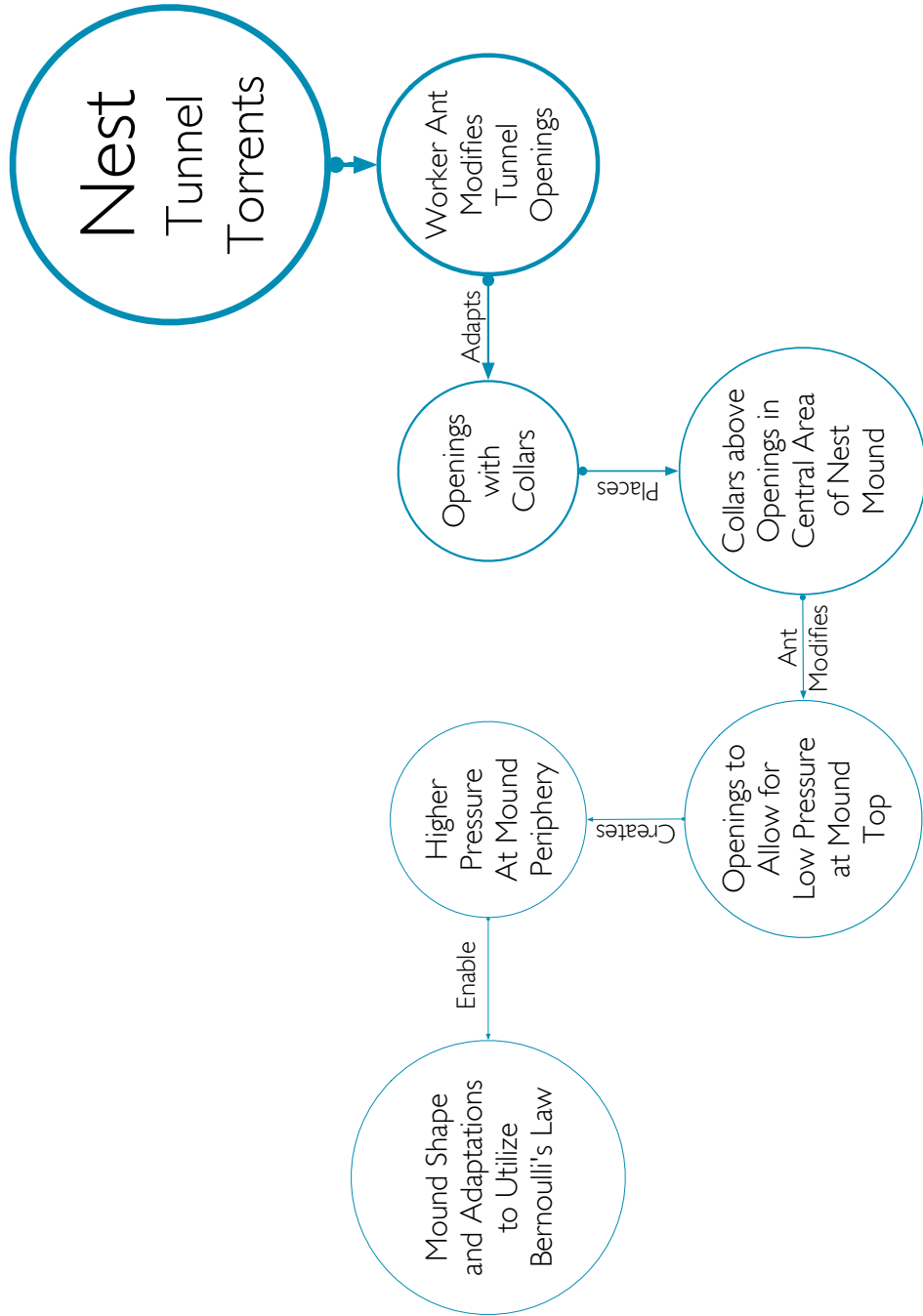
Figure 4.7. Leaf Cutting Ant Biological Analogue Nest Induced Convection Hierarchical Map



Wind-induced ventilation of the giant nests of the leaf-cutting ant *atta vollenweideri*

Kleineidam, C., Ernst, R., & Roces, F. (2001). Wind-induced ventilation of the giant nests of the leaf-cutting ant *Atta vollenweideri*. *Naturwissenschaften*, 88(7), 301-305. <http://dx.doi.org/10.1007/s001140100235>

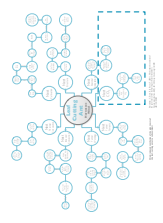
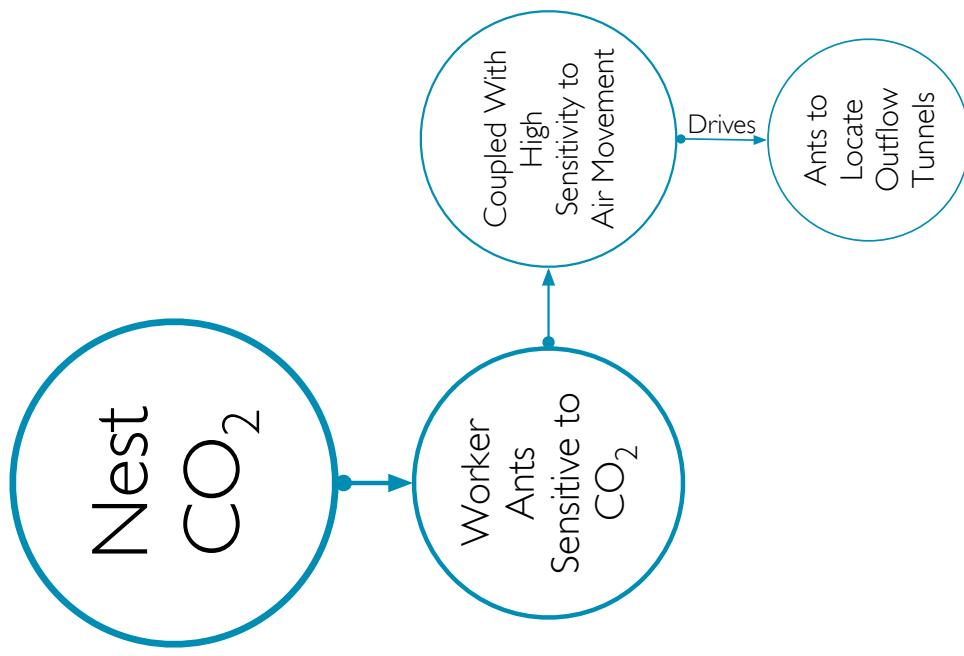
Figure 4.8. Leaf Cutting Ant Biological Analogue Nest Tunnel Workings Hierarchical Map



Wind-induced ventilation of the giant nests of the leaf-cutting ant *atta vollenweideri*

Kleineidam, C., Ernst, R., & Roces, F. (2001). Wind-induced ventilation of the giant nests of the leaf-cutting ant *Atta vollenweideri*. *Naturwissenschaften*, 88(7), 301-305. <http://dx.doi.org/10.1007/s001140100235>

Figure 4.9. Leaf Cutting Ant Biological Analogue Nest Tunnel Torrents Hierarchical Map



Wind-induced ventilation of the giant nests of the leaf-cutting ant *atta vollenweideri*

Kleineidam, C., Ernst, R., & Roces, F. (2001). Wind-induced ventilation of the giant nests of the leaf-cutting ant *Atta vollenweideri*. *Naturwissenschaften*, 88(7), 301-305. <http://dx.doi.org/10.1007/s001140100235>

Figure 4.10. Leaf Cutting Ant Biological Analogue Nest Carbon Dioxide Hierarchical Map

4.1.2 Great Plains Prairie Dog Harnesses Wind

The Great Plains prairie dog burrows harness wind energy through the development of changes in laminar flow along ground surface. Figure 4.11 shows a hierarchical key map of characteristics that contribute to its unique adaptation for harnessing wind energy. The key components from Figure 4.11 show relationship between burrow configuration, air movement, humidity control, and exergy. The Great Plains prairie dog burrow adaptations allow the small animal to survive in long below grade tunnels for long periods with adequate air mass exchange.

4.1.2.1 Burrow Specificity

Figure 4.12 shows burrow specificity adaptation. The Great Plains prairie dog strategically places raised mounds to develop wind driven velocity gradients[18]. The Great Plains is an arid climate with very little vegetation and wind swept[18]. The use of raised mounds creates low-pressure regions above ground similarly to the leaf cutting ant nest openings at the top of the mound. The adaptation of raised surface mounds in a climate with undeterred airflows over ground surfaces improves induced wind airflow into prairie dog burrows.

4.1.2.2 Burrow Structure

Figure 4.13 shows the Great Plains prairie dog burrow structure adaptation to harness wind energy. The burrows structure is typically ten to thirty meters long below ground[18]. Side passages branch off from the main burrow tunnel and they provide humid areas for storage of plant material[18]. The burrow depth is similar to the depths of leaf cutter ant workers placement of fungus chambers and larvae within nest structure below ground. The burrows feature usually two with some having three raised mounds above ground surface[18]. The burrows are essentially shallow tunnels with a shallow entry mound and steep exit mound[18]. The prairie dog excavates the long shallow burrows starting with the entry mound and clears sequentially towards the exit mound. The sequence of construction allows for strategic buildup of a larger rim for the exit mound. The larger exit rim mound is vertically taller than the shallow entry rim mound. The pressure drop across the two differential height mounds is one of the primary adaptations to harness wind energy.

4.1.2.3 *Burrow Configuration*

Figure 4.14 shows burrow configuration adaptation. The spatial configuration of the mound allows for diffusive gas exchange. The prairie dog burrows are long enough below grade to create inadequate dimension for airflow movement to penetrate them entirely[18]. The use of openings at either end is the primary adaptation for wind-induced ventilation[18]. Test models of prairie dog burrows show that only one mound opening is sufficient for wind-induced ventilation[18]. The prairie dog uses the taller rim exit mound as a lookout from other predators and as an anti-flooding device[18]. The Great Plains prairie dog burrow is adapted specifically for wind-induced ventilation using height differential between entry and exit mounds. The spatial configuration of entry and exit mounds allow for adequate diffusive gas exchange throughout the burrow.

4.1.2.4 *Burrow Physics*

Figure 4.15 shows the physical adaptation for wind-induced ventilation in prairie dog burrows. The specificity of the Great Plains features unidirectional bulk airflow masses that generate negative pressure from small height differentials over ground obstructions[18]. Height differentials between entry and exit mounds pull air into the burrow using Bernoulli principle[18]. The use of pressure differentials to drive wind-induced ventilation in prairie dog burrows is similar to leaf cutting ant worker nest. The differences in configuration and structure between the burrows and the nest respond to their environment.

4.1.2.5 *Burrow Air Movement*

Figure 4.16 shows burrow air movement characteristics. Max Kleiber metabolic rates and Adolf Frick's diffusion equations aids in understanding the length of burrow to sustain oxygen consumption of small animal with adequate gas exchange[18]. The maximum length of the prairie dog's burrow calculates to less than four centimeters using the typical burrow cross section and length[18]. The length is inadequate for gas diffusion within the burrow as primary contribution to airflow movement. The calculated length is two orders of magnitude shorter than the black tailed prairie dog length that is much less, than the actual burrow lengths[18]. The dissimilar shape mounds create low volume of air exchange throughout the burrow. The air exchange rate for complete replacement with fresh air requires ten hours at a speed of about 0.0013 mph[18]. The black tailed prairie dog adapts the burrow tunnel for unique airflow movements using pressure differentials to sustain adequate gas

exchange with ambient air and burrow air.

4.1.2.6 *Burrow Mounds*

Figure 4.17 shows the adaptations for black tailed prairie dog burrow mounds. The burrows are typically one to two and a half meters in depth[18]. The burrows feature shape characteristics for the entry and exit mounds. The shape characteristic of steep and sharp mound rim at burrow exit improves performance over round shallow rim mound at the burrow entry[18]. Both mounds types feature a rim that flares outward at the top of the mound to improve airflow pressure drop between the two openings[18].

4.1.2.7 *Burrow Humidity*

Figure 4.18 shows the adaptation for humidity control in Great Plains prairie dog burrow mounds. The Great Plains has scarce water resources. The humidity level within the subterranean burrows is much higher than it is above ground dry air by two to five times. The high humidity levels promote less water loss when the animals seek shelter within the burrows[18]. The prairie dog burrow adaptation provides a high humidity environment to conserve water loss[18]. The side tunnel passageways provide plant storage, high water vapor content, and gas diffusion between burrow air mass and soil mass.

4.1.2.8 *Burrow Exergy*

Figure 4.19 shows the burrow adaptation for exergy. Exergy drives adaptation of biological analogues towards low-energy interaction with their environments. The Great Plains presents the prairie dog with a renewable energy resource for wind harvesting. Wind harvesting provides the prairie dog with a survivable below grade shelter from predators and environment. The configuration of the burrow provides the prairie dog with adequate gas exchange and humidity control. The burrow provides an environment for the prairie dog to experience minimal water loss. Wind driven airflow across the ground exergy improves by prairie dog entry and exit mound differential height and collar structures to make useful work in ventilating the burrow.

Table 4.1 shows performance criteria for the prairie dog burrow adaptation for wind-induced ventilation. Similarly,

to the leaf-cutting ant, the prairie dog orients their inlet and outlet mounds to direction parallel to wind flow with articulation characteristics. The offset inlet and outlet mound openings have similarities to offset ventilation. The small number of openings resembles strategies for minimizing openings in buildings. Table 4.3 compares the prairie dog and leaf-cutting ant criteria. Insect and animal share similar performance mechanisms in orientation of mound and nest openings where they orient them parallel to wind flow over the ground surface. Both use branching parallel connections to main tunnel or burrow. Torrent articulation behavior is another shared performance characteristic that improves wind harvesting in their specific environments.

Table 4.2. Great Plains Prairie Dog Burrow Performance Criteria

Performance Criteria	Great Plains Prairie Dog Burrow
Seasonal Adaptation	Orientation for wind-induced Ventilation
Seasonal Adaptation Mechanism	No specific Adaptation
Structure	Parallel Connecting Tunnels
Humidity Control	Side Passages Balance Humidity
Thermal Convection	Induced Wind Airflow
Airflow Movement	Induced Wind Airflow
Airflow Mechanism	Offset Raised Shallow Inlet and Steep Outlet Burrow Mounds
Airflow Performance Adaptation	Pressure Drop
Airflow Penetrations	Small Number
Airflow Adaptation	Torrent Definition Improve Induced Wind Airflow
Directional Adaptation	Mound openings oriented parallel to wind direction
Exergy Adaptation	Wind Harvesting

Table 4.3. Prairie Dog Borrow and Leaf-Cutting Ant Nest Comparison

Performance Criteria	Great Plains Prairie Dog Burrow	Comparison	Leaf-Cutting Ant Mound
Seasonal Adaptation	Wind Orientated	Same	Wind Orientated
Adaptation Mechanism	No specific Adaptation	Different	Open/Close Nest Openings
Structure	Parallel Connecting Tunnels	Same	Parallel Connecting Tunnels
Humidity Control	Side Passages Balance Humidity	Different	Nest Cultivation of Fungus
Thermal Convection	Induced Wind Airflow	Different	Convective/Diffusive
Airflow Movement	Induced Wind Airflow	Different	Convective/Diffusive
Airflow Mechanism	Offset Inlet and Outlet	Similar	Offset Inlet and Outlet
Airflow Adaptation	Pressure Drop	Same	Pressure Drop
Airflow Penetrations	Small Number	Different	Large Number
Airflow Adaptation	Torrent Articulation	Similar	Torrent Articulation
Directional Adaptation	Openings Parallel to Wind	Same	Openings Parallel to Wind
Exergy Adaptation	Wind Harvesting	Same	Wind Harvesting

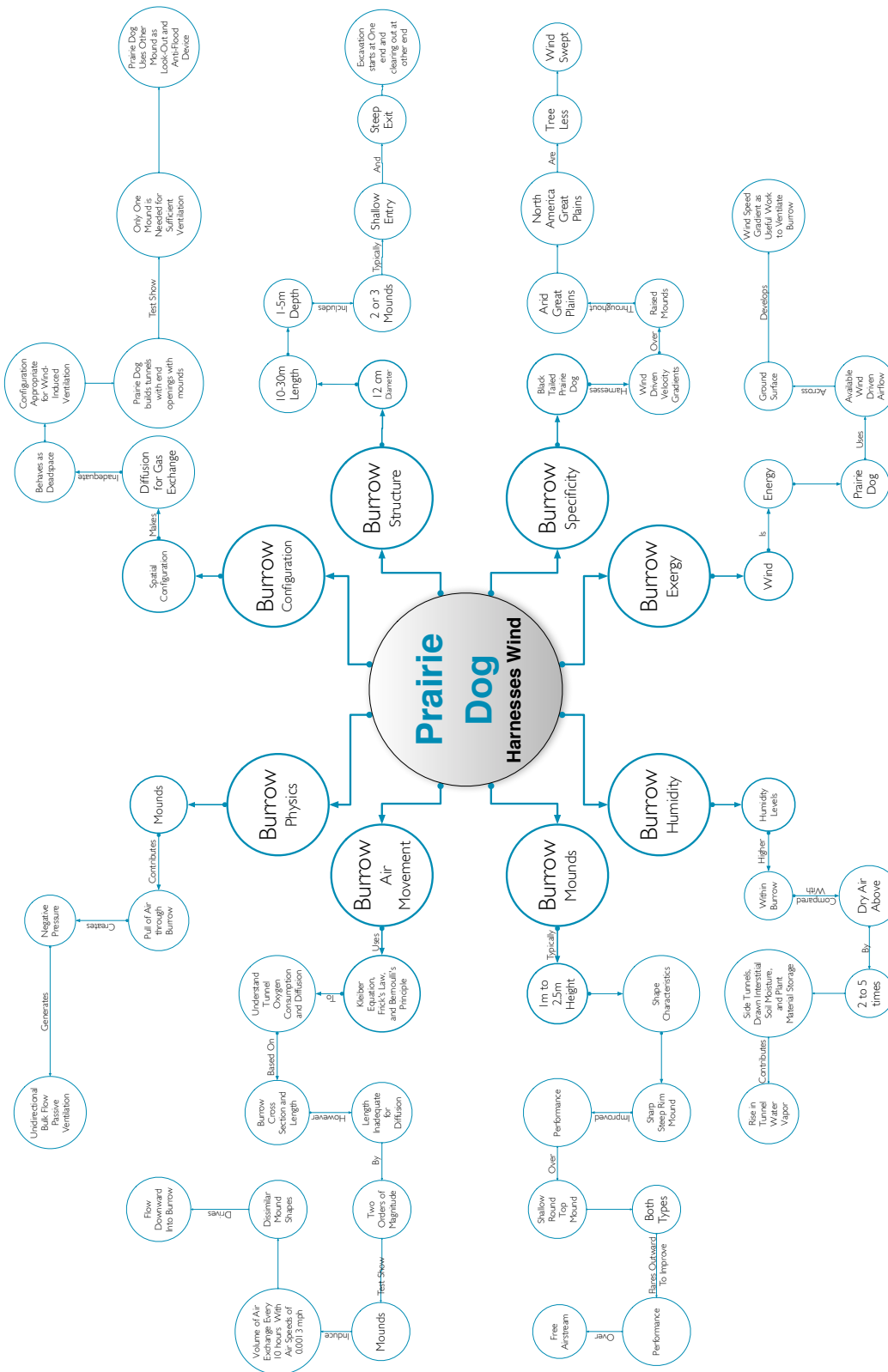


Figure 4.11. Prairie Dog Biological Analogue Hierarchical Key Map

Vogel, S., Ellington, Charles P., J., & Kilgore, Delbert L., J. (1973). Wind-induced ventilation of the burrow of the prairie-dog, *Cynomys ludovicianus*. *Journal of Comparative Physiology*, 85(1), 1-14. <http://dx.doi.org/10.1007/BF00694136>

Wind-induced ventilation of the burrow of the prairie-dog, *Cynomys ludovicianus*

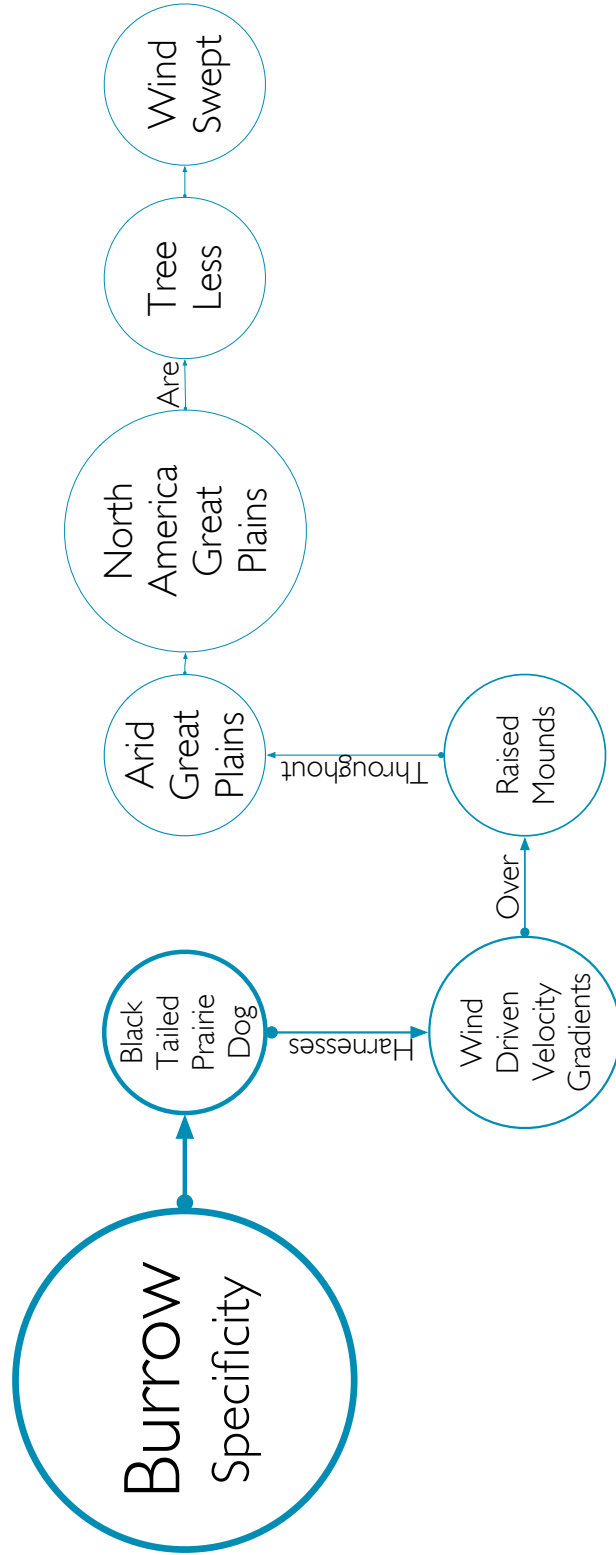
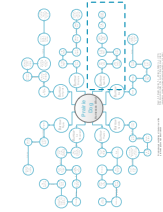


Figure 4.12. Prairie Dog Burrow Specificity Hierarchical Map



Wind-induced ventilation of the burrow of the prairie-dog

Vogel, S., Ellington, Charles P., J., & Kilgore, Delbert L., J. (1973). Wind-induced ventilation of the burrow of the prairie-dog *Cynomys ludovicianus*. *Journal of comparative physiology*, 85(1), 1-14. <http://dx.doi.org/10.1007/BF00694136>

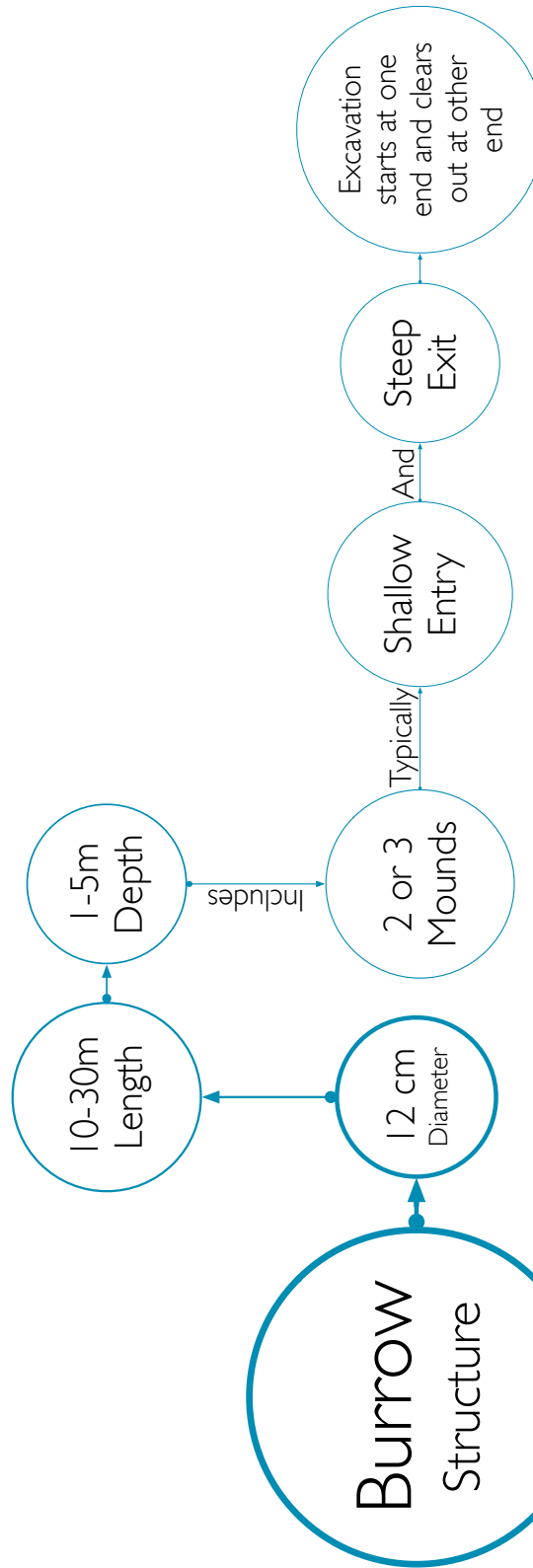
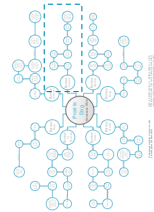
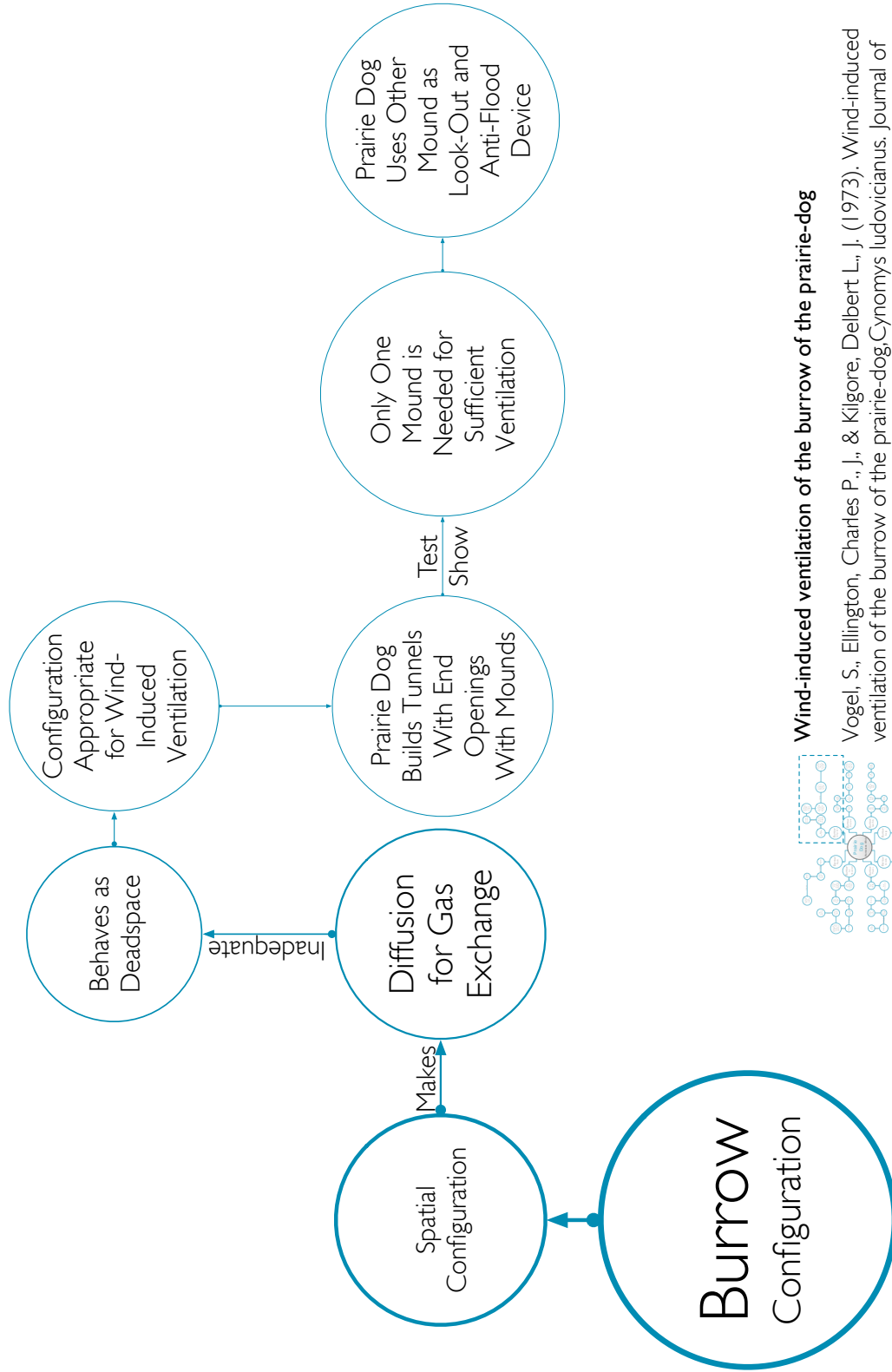


Figure 4.13. Prairie Dog Burrow Structure Hierarchical Map

Wind-induced ventilation of the burrow of the prairie-dog



Vogel, S., Ellington, Charles P., J., & Kilgore, Delbert L., J. (1973). Wind-induced ventilation of the burrow of the prairie-dog *Cynomys ludovicianus*. *Journal of comparative physiology*, 85(1), 1-14. <http://dx.doi.org/10.1007/BF00694136>



Wind-induced ventilation of the burrow of the prairie-dog
 Vogel, S., Ellington, Charles P., J., & Kilgore, Delbert L., J. (1973). Wind-induced ventilation of the burrow of the prairie-dog *Cynomys ludovicianus*. *Journal of comparative physiology*, 85(1), 1-14. <http://dx.doi.org/10.1007/BF00694136>

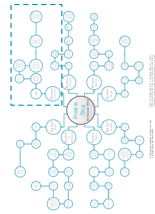
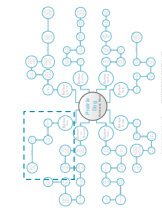
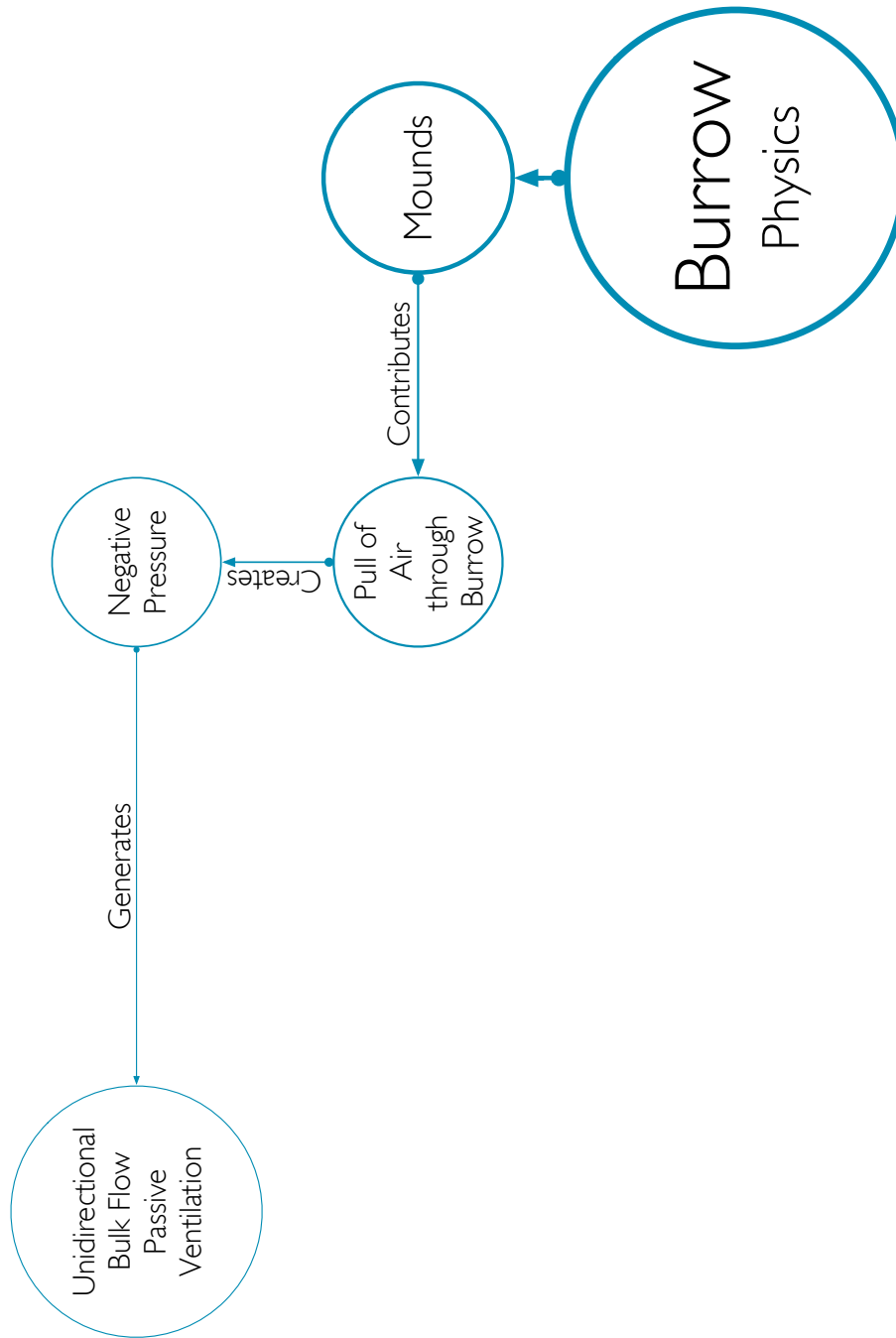


Figure 4.14. Prairie Dog Burrow Configuration Hierarchical Map



Wind-induced ventilation of the burrow of the prairie-dog

Vogel, S., Ellington, Charles P., J., & Kilgore, Delbert L., J. (1973). Wind-induced ventilation of the burrow of the prairie-dog *Cynomys ludovicianus*. *Journal of comparative physiology*, 85(1), 1-14. <http://dx.doi.org/10.1007/BF00694136>

Figure 4.15. Prairie Dog Burrow Physics Hierarchical Map

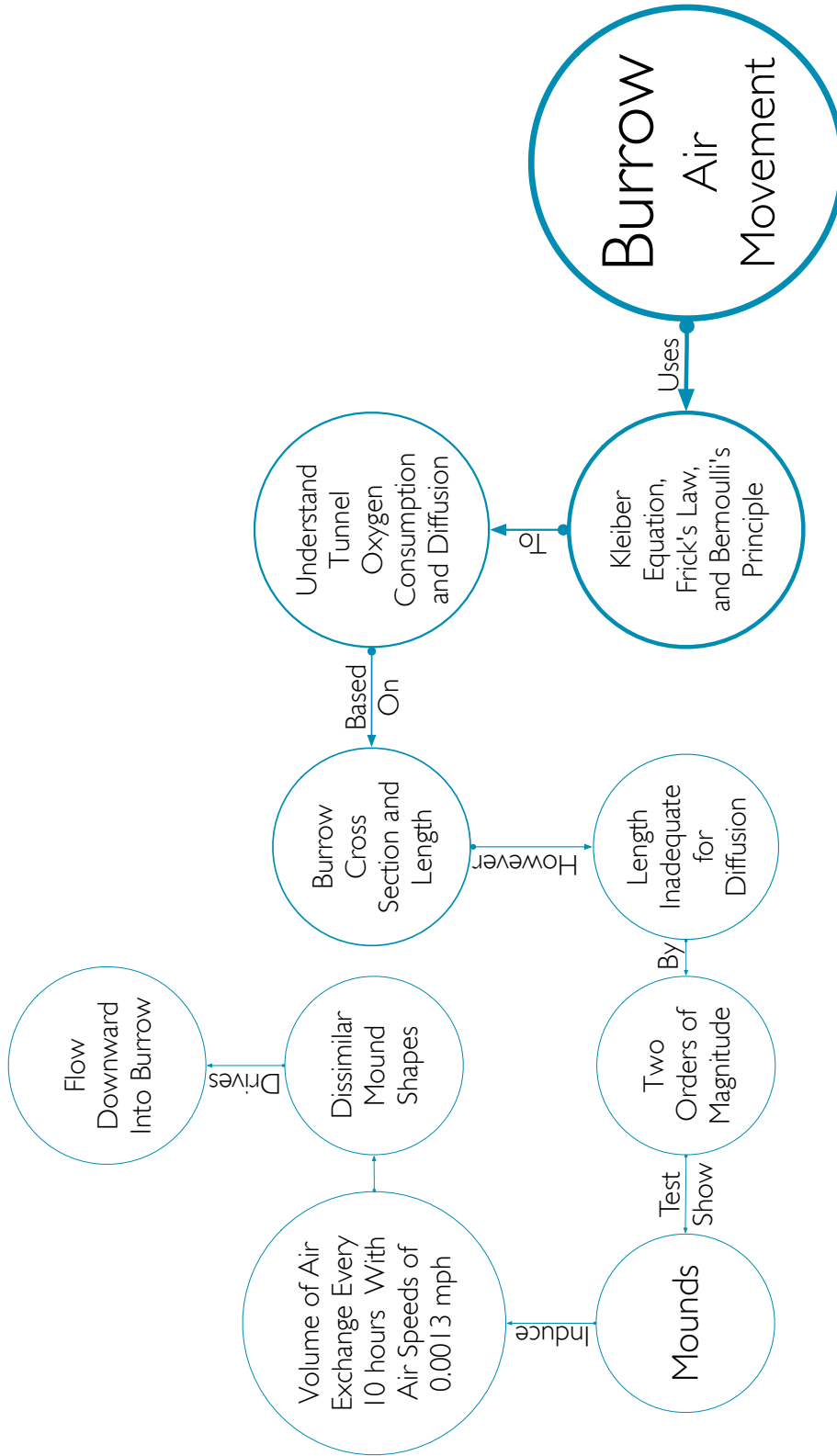
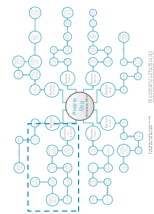


Figure 4.16. Prairie Dog Burrow Air Movement Hierarchical Map

Wind-induced ventilation of the burrow of the prairie-dog
 Vogel, S., Ellington, Charles P., J., & Kilgore, Delbert L., J. (1973). Wind-induced ventilation of the burrow of the prairie-dog *Cynomys ludovicianus*. *Journal of comparative physiology*, 85(1), 1-14. <http://dx.doi.org/10.1007/BF00694136>



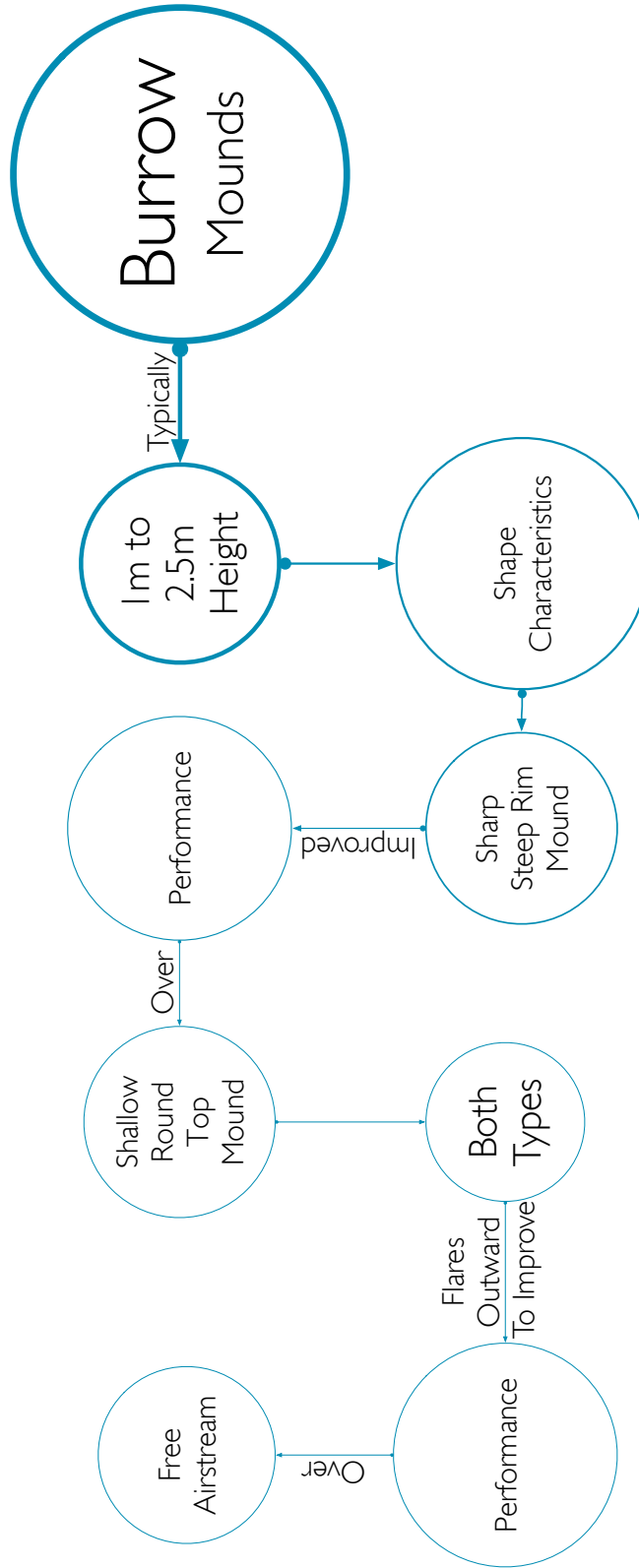
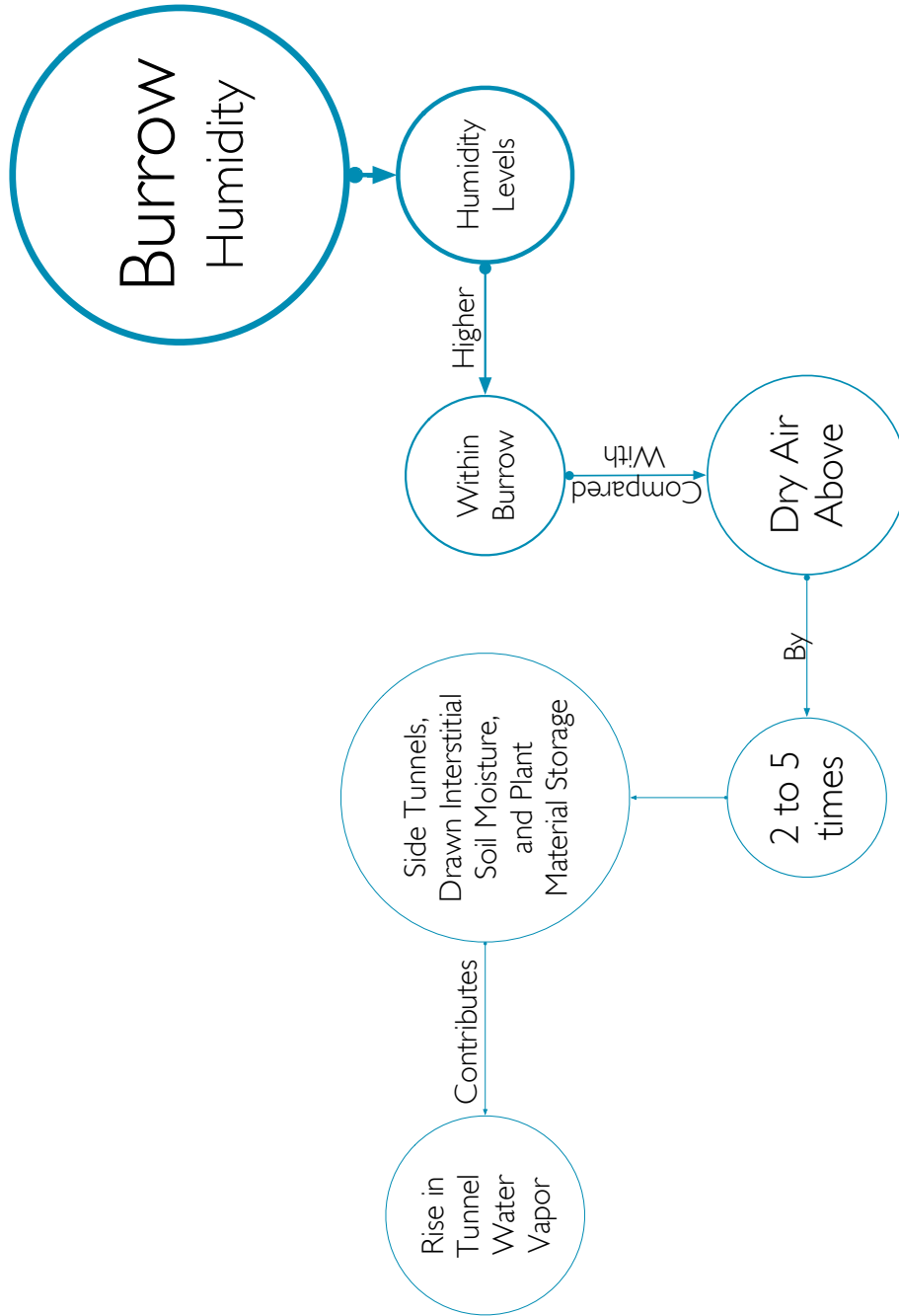
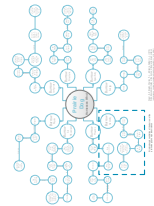


Figure 4.17. Prairie Dog Burrow Mounds Hierarchical Map

Wind-induced ventilation of the burrow of the prairie-dog
 Vogel, S., Ellington, Charles P., J., & Kilgore, Delbert L., J. (1973). Wind-induced ventilation of the burrow of the prairie-dog *Cynomys ludovicianus*. *Journal of comparative physiology*, 85(1), 1-14. <http://dx.doi.org/10.1007/BF00694136>



Wind-induced ventilation of the burrow of the prairie-dog



Vogel, S., Ellington, Charles P., J., & Kilgore, Delbert L., J. (1973). Wind-induced ventilation of the burrow of the prairie-dog *Cynomys ludovicianus*. *Journal of comparative physiology*, 85(1), 1-14. <http://dx.doi.org/10.1007/BF00694136>

Figure 4.18. Prairie Dog Burrow Humidity Hierarchical Map

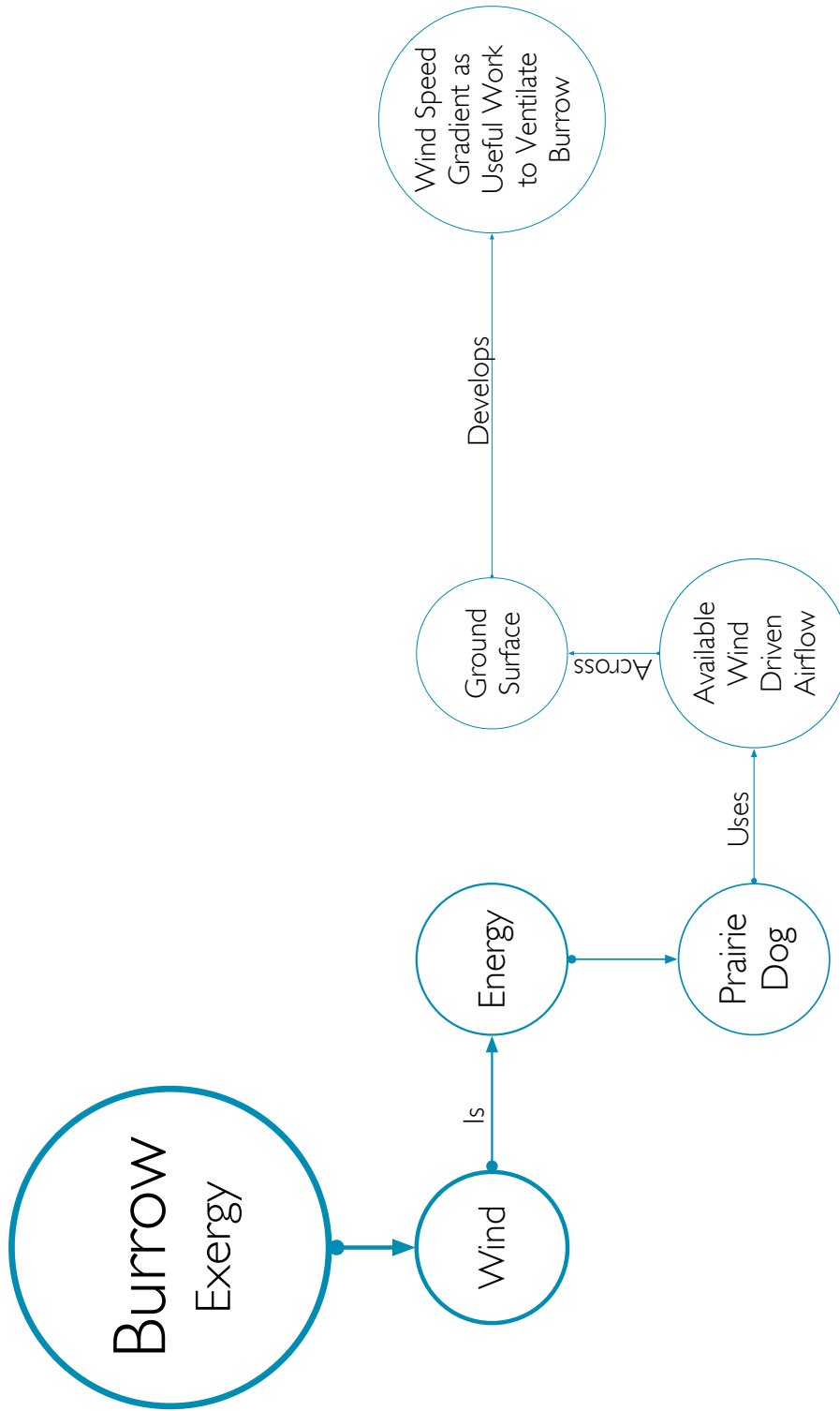
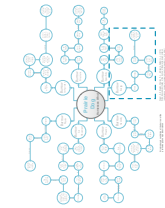


Figure 4.19. Prairie Dog Burrow Exergy Hierarchical Map



Wind-induced ventilation of the burrow of the prairie-dog

Vogel, S., Ellington, Charles P., J., & Kilgore, Delbert L., J. (1973). Wind-induced ventilation of the burrow of the prairie-dog *Cynomys ludovicianus*. *Journal of comparative physiology*, 85(1), 1-14. <http://dx.doi.org/10.1007/BF00694136>

4.2 Models for Decoupling Dehumidification from Air Conditioning

4.2.1 Liquid Desiccant Mass Transfer Physics

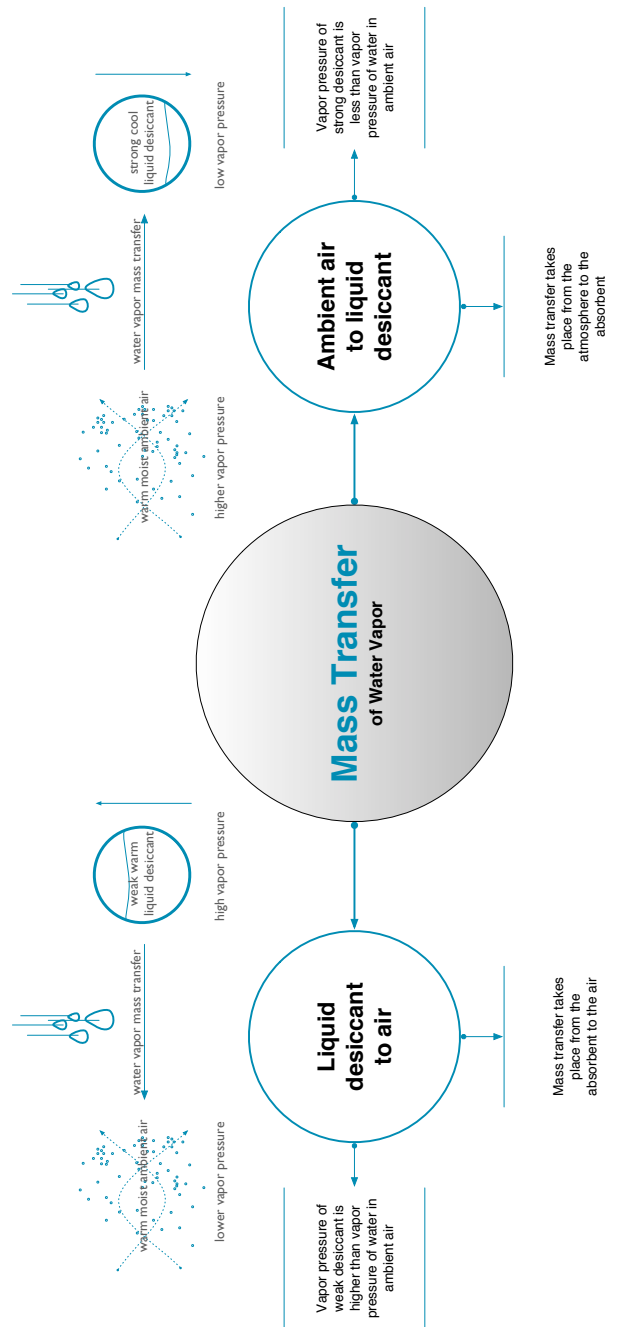
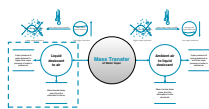
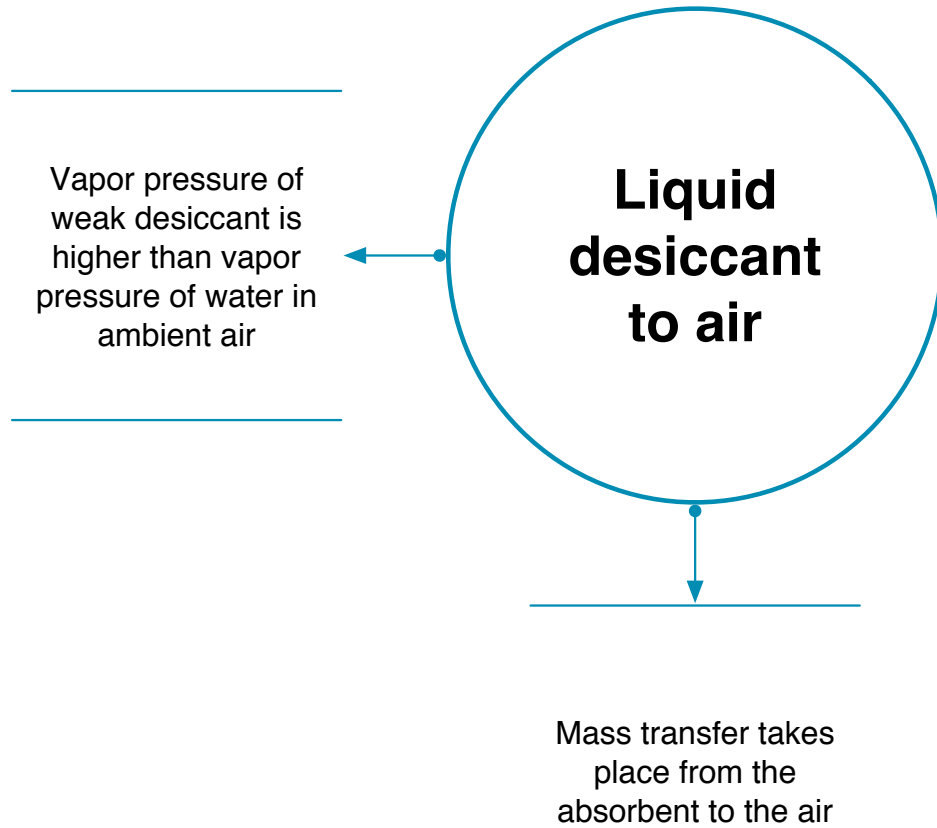


Figure 4.20. Liquid Desiccant Mass Transfer Physics Hierarchical Key Map

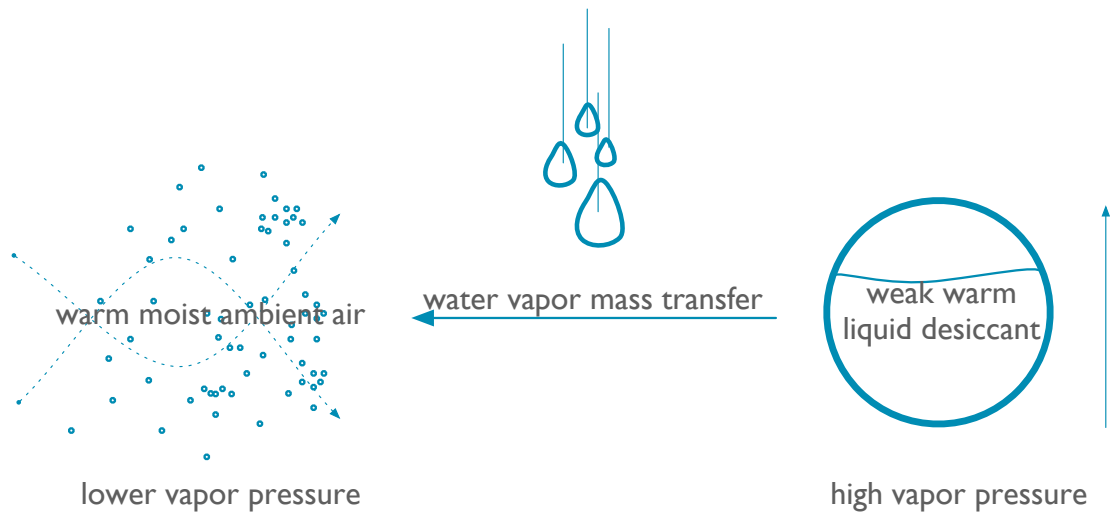
4.2.1.1 *Mass Transfer Water Vapor from Liquid Desiccant to Ambient Air*

Figure 4.20 shows the overall structure of the hierarchical key map for mass transfer of water vapor. Liquid desiccants show flexibility to scavenge water vapor from ambient air when cool and diluted. Heating liquid desiccants allow water to evaporate as water vapor when hot and concentrated. The evaporated water collects as condensation in a recovery vessel. Figure 4.21 shows the process for mass transfer of water vapor from absorbent to ambient air. Liquid desiccant surface vapor pressure is higher than the vapor pressure of water vapor in ambient air when cool and weak. A weak liquid desiccant is a solution with a high water to salt concentration. Figure 4.22 shows directional movement of water vapor from liquid desiccant to ambient air. The process shown in Figure 4.22 drives the liquid desiccant to a low water to salt concentration.



Mass Transfer of Water Vapor

Figure 4.21. Liquid Desiccant to Ambient Air Mass Transfer Physics Hierarchical Map

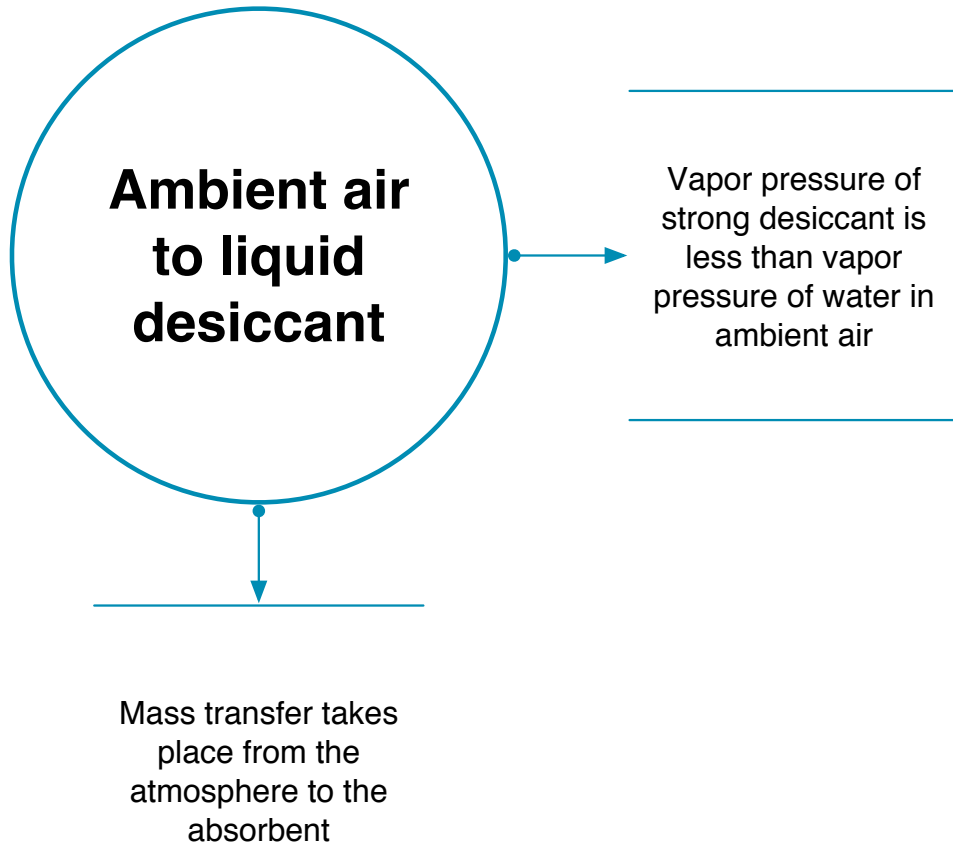


Mass Transfer of Water Vapor

Figure 4.22. Liquid Desiccant to Ambient Air Mass Transfer Physics Diagram

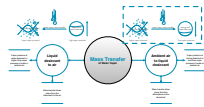
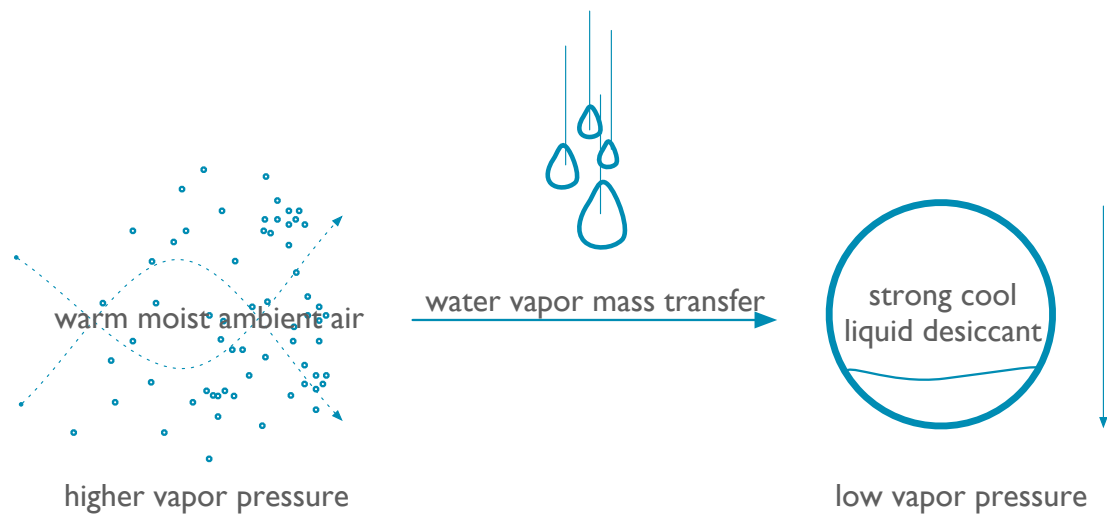
4.2.1.2 Mass Transfer Water Vapor From Ambient Air to Liquid Desiccant

Figure 4.23 shows process for mass transfer of water vapor from atmosphere to absorbent. Liquid desiccant surface vapor pressure is lower than the vapor of water vapor in ambient air when hot and strong. A strong liquid desiccant is a solution with a low water to salt concentration. Figure 4.24 shows the direction movement of water vapor from ambient air to liquid desiccant. The process shown in Figure 4.24 drives the liquid desiccant to a high water to salt concentration.



Mass Transfer of Water Vapor

Figure 4.23. Ambient Air to Liquid Desiccant Mass Transfer Physics Hierarchical Map



Mass Transfer of Water Vapor

Figure 4.24. Ambient Air to Liquid Desiccant Mass Transfer Physics Diagram

4.2.2 Solar Absorption Unit Characteristics

Gandhidasan provides the basic premise for the characteristics of an absorption solar unit [14]. Figure 4.25 shows the overall structure of the hierarchical key map for an absorption solar unit. The absorption solar unit makes use of solar energy to transfer water vapor in a unique system process. An absorption solar unit uses solar energy to evaporate water from a liquid desiccant. The evaporation drives mass transfer of water vapor from the liquid desiccant to scavenging dry ambient air source.

4.2.2.1 Absorption Solar Unit System Process

Figure 4.26 shows an enlargement of the system process of the absorption solar unit. The diagram shows the characteristics of an absorbent such as calcium chlorite[14]. The liquid desiccant scavenges water vapor from ambient moist air. The components of a liquid desiccant solution are water and salts. Water vapor is readily available in various phases. Some salt compounds are economical while others are expensive. Most salt compounds present low toxicity to humans[14]. The mixture of water and salt compounds has high thermal conductivity with lower properties for density, freezing point, corrosion risk, and viscosity[14]. Liquid desiccants readily absorb water vapor with low surface vapor pressure[14]. Liquid desiccants are stable with low thermal decomposition such that low-grade energy can desorb vapor moisture. The system process of the absorption solar unit make use of a liquid desiccant composed of readily available and low cost salt compounds and water:

4.2.2.2 Absorbent Performance

Figure 4.27 shows the process for an absorption solar unit that uses solar energy to produce fresh water from ambient air. The process is based on Gandhidasan's premise for an absorption solar unit[14]. The unit will generate water from water vapor in humid ambient air. The reclamation of absorbed water requires the use of solar energy[14]. The absorption solar unit dependencies on climatic factors limit its effectiveness as a dehumidification system. The absorption solar unit performance for scavenging water vapor depends on liquid desiccant concentration[14]. Low liquid desiccant surface vapor pressure scavenges water vapor from ambient air. The scavenging capacity is limited by temperature[14]. The absorption solar unit uses a liquid desiccant (absorbent) with higher temperature than ambient air. In humid climates, this can be a problem if the ambient air is moist and hot. The temperature difference between the absorbent and ambient air stream influences mass transfer of water vapor. Smaller temperature differences between absorbent and ambient air stream reduces absorbent surface vapor pressure. Ambient temperature drives ambient humidity. Higher ambient air temperatures hold more water vapor. A chemical process has better performance to drive the mass transfer of water vapor from high ambient air temperature. The absorbent concentration drives chemical process to scavenge water vapor from ambient air:

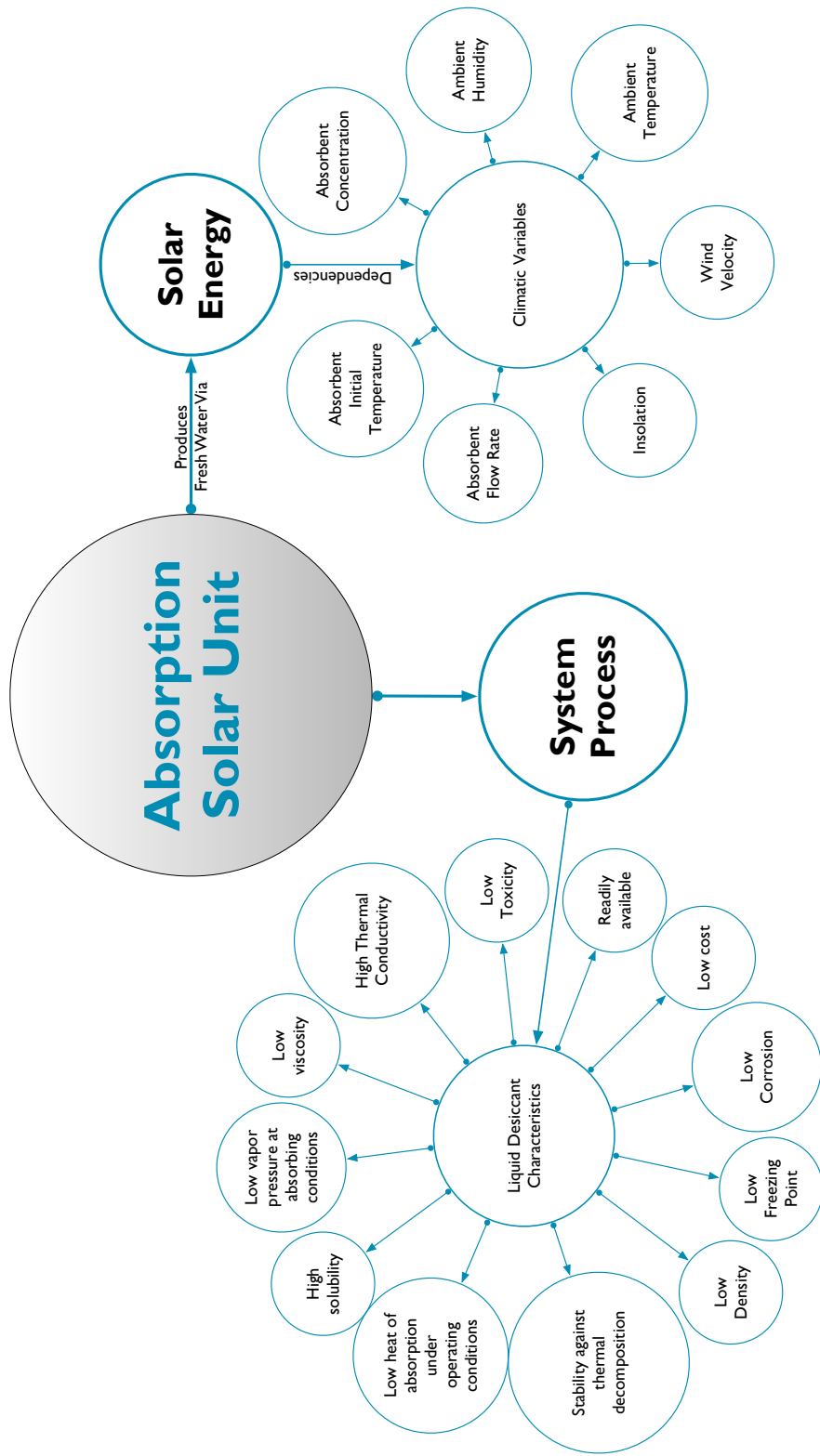


Figure 4.25. Absorption Solar Unit Hierarchical Key Map

Absorption Solar Unit

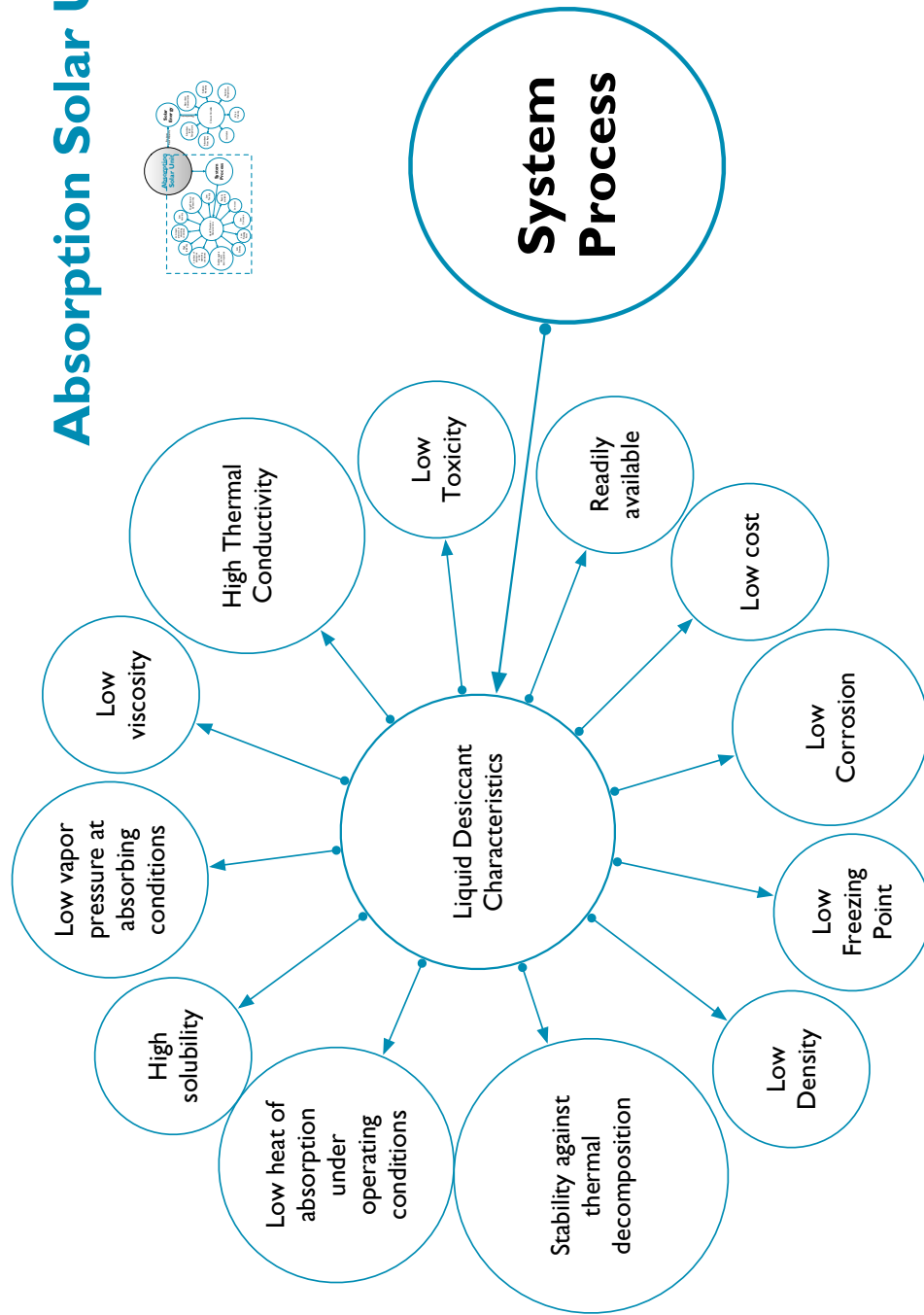


Figure 4.26. Absorption Solar Unit System Process Hierarchical Map

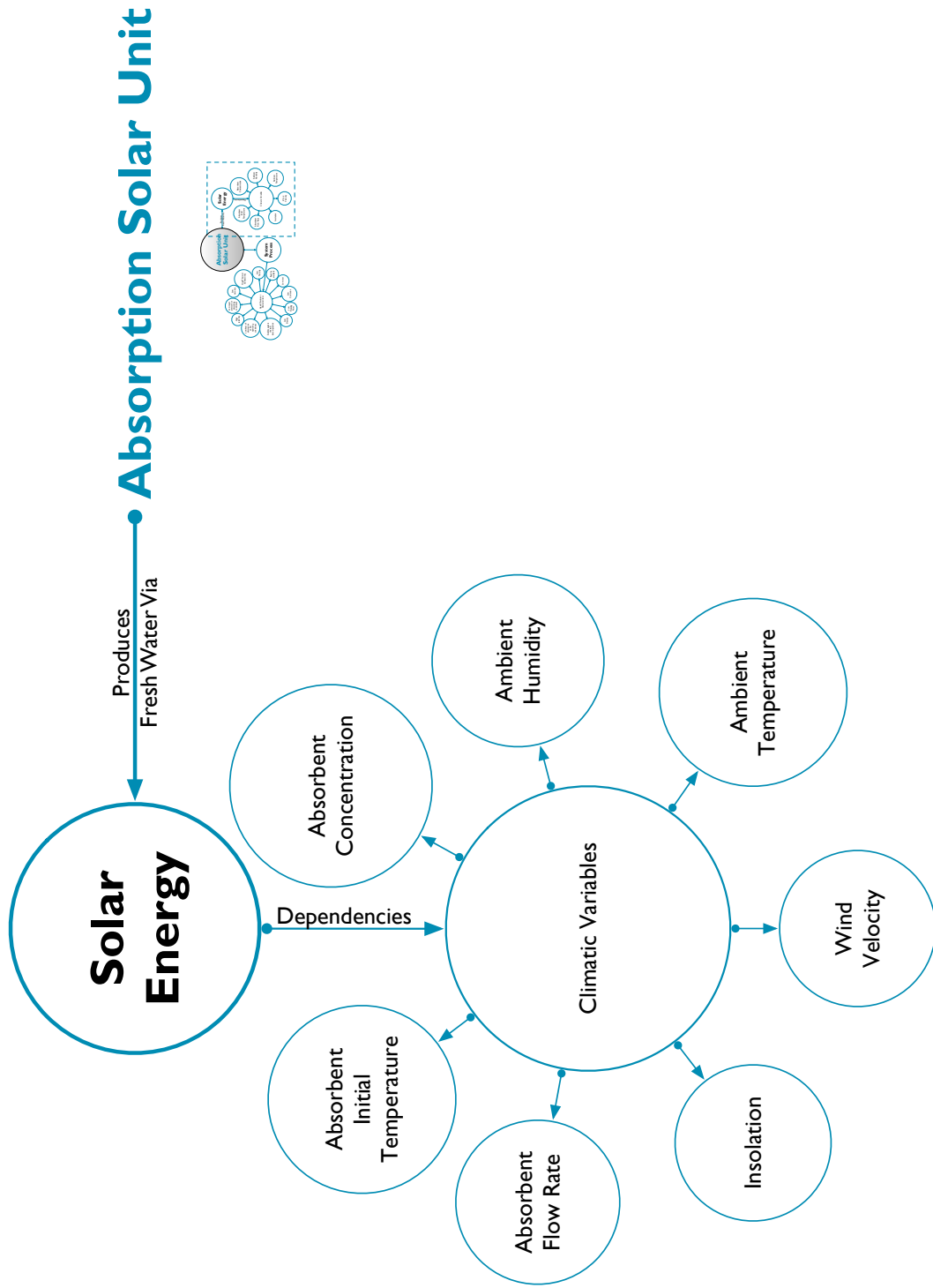


Figure 4.27. Absorption Solar Unit Energy Characteristics Hierarchical Map

4.2.3 Liquid Desiccant Solar Absorption Diurnal System

Absorberfig:diurnalcyclemap shows a hierarchical mapping of the diurnal cycle for an absorption solar unit. The diagram is inspired from Gandhidasan's work[14]. The diagram breaks down the day and night cycle of an absorbent with side-by-side conceptual representation of an absorption solar unit. The absorption solar unit consists of a sloped enclosure component with an absorber back surface and glass cover.

4.2.3.1 Absorption Solar Unit Day Function

Figure 4.29 shows the process for use of liquid desiccant in a simple absorption solar unit. In the context of the absorption solar unit, the liquid desiccant performs as a thin absorbent film. During the day cycle, the absorbent absorbs water from moist and warm ambient air. Weak diluted absorbent from the previous night flows up and over an absorber surface as a thin film[14]. During the day, the enclosure absorber surface receives solar radiation. The high temperature absorber surface heats the thin film absorbent[14]. The thin film requires low heat temperature to evaporate water from the desiccant solution. Rising sensible heat evaporates a small amount of water from the thin flowing absorbent film. The evaporating process removes heat from the absorbent film through the latent heat of vaporization. Water evaporates and rises towards sloping glass cover. The water vapor collects and condenses against the underside of the glass cover. A thin film of condensate water flows along the underside of the sloping glass cover to a recovery container[14]. The concentration of the absorbent is strong desiccant solution with low water to salt content.

4.2.3.2 Absorption Solar Unit Day System

Figure 4.32 shows the system diagram for a flat blackened tilted surface covered with single glazing for a daytime system[14]. The system exposes the liquid desiccant to solar radiation from the sun. The tilted flat blackened absorber surface has direct orientation with sun. A sloped transparent glass cover is forward of the blacked absorber surface. Liquid desiccant performs as a thin film absorbent. The absorbent flows as a thin film via a low energy pump up to the top of the tilted flat blackened absorber away from the sun. The absorbent heavily dilutes with water from previous cycle. It is a weak and cool liquid desiccant at the start of the day cycle. The flat blackened tilted surface at the start of the day cycle provides a plane for a falling film of weak cool liquid desiccant. The system diagram shows a heavy blue line for day cycle of liquid desiccant. Arrows point towards

the glass cover to represent the evaporation of water from the liquid desiccant. Solar radiation from sun strikes the sloped glass plane. Some of the solar radiation reflects back to ambient. A small amount of solar radiation convects away from the outer surface of the glass plane. A majority of the solar radiation conducts through the glass cover. Some of the conductive energy in the glass is absorbed into the glass cover. More of the conducted energy transmits through the glass cover. The inner surface of the glass cover is cooler than the outer surface. Heat convects away from the inner surface of the glass cover. More of the transmitted heat in the glass cover radiates to the flat tilted blackened surface. The falling film liquid desiccant conducts heat away from the tilted flat blackened surface. The water from the falling film liquid desiccant evaporates. The water vapor collides with the cooler glass cover and condenses. The sloping plane of the glass cover allows water to flow along the underside to a recovery container. The absorption solar unit during the day provides a source of strong warm liquid desiccant.

4.2.3.3 *Absorption Solar Unit Night Function*

Figure 4.31 shows hierarchical diagram for the absorption solar unit night function. Gandhidasan's system for the night uses strong warm liquid desiccant from heating and during the day cycle. The system changes the path of the falling film of liquid desiccant to flow on the outside glass cover with exposure to ambient air. The liquid desiccant has direct contact with ambient air in this configuration. The liquid desiccant absorbs water vapor from the ambient air. The mass transfer of water vapor during the day cools and dilutes the liquid desiccant during the night cycle.

4.2.3.4 *Absorption Solar Unit Night System*

Figure 4.32 shows the system diagram for a flat blackened tilted surface covered with a single glazing from the Gandhidasan's work for a nighttime system[14]. The night cycle works more like a regenerator. The system has similar components that were present during the day cycle. The flat blackened tilted surface no longer provides a path for the falling liquid desiccant film. The underside of the glass cover does not provide a path for water condensation. There is no water condensate for the recovery container to collect. The absorption solar unit provides a path for falling liquid desiccant film to flow on the outside glass cover. Moist ambient air contacts the falling liquid desiccant film. The surface vapor pressure of the falling liquid desiccant film is lower than ambient air vapor pressure. The difference in partial vapor pressure between ambient air and liquid desiccant drives

the mass transfer of water vapor. The falling liquid desiccant film absorbs water vapor. The liquid desiccant temporarily heats up from dehumidification but eventually cools down with higher water and low salt content. The cycle continues until solar radiation is available to drive the absorber day cycle.

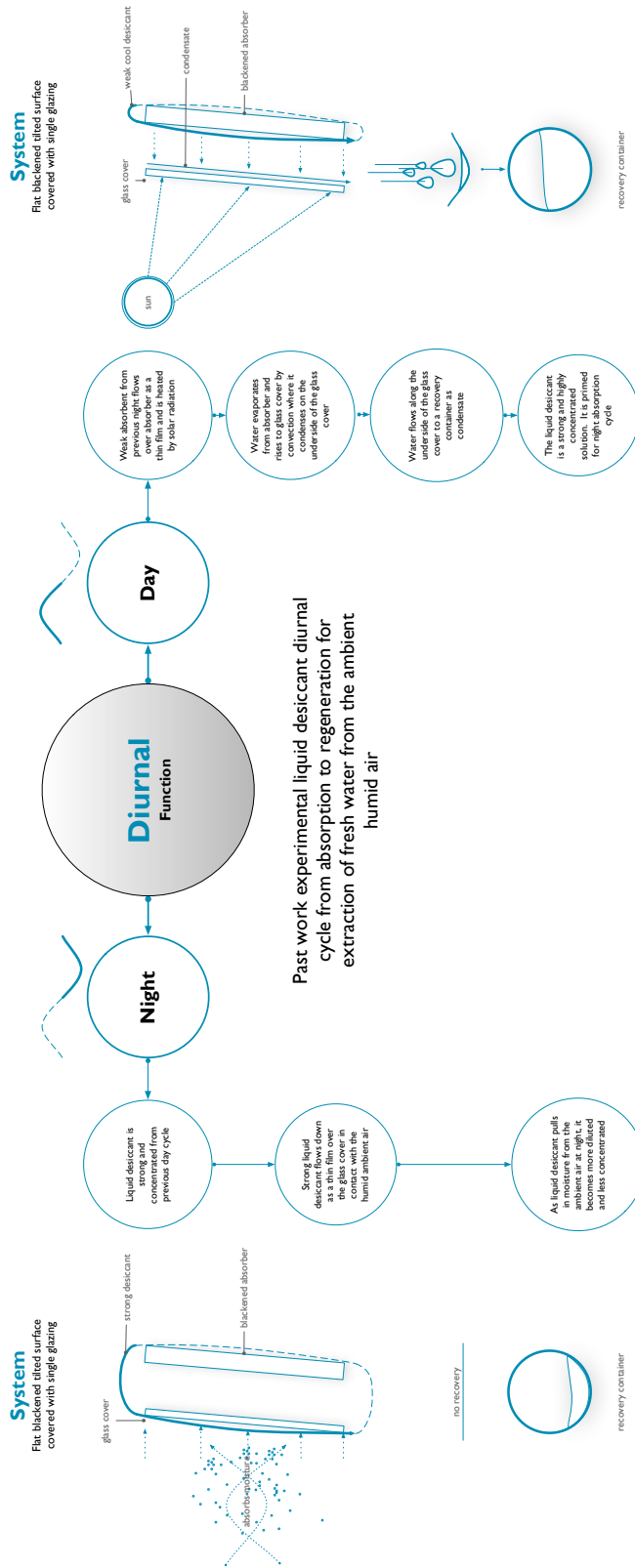


Figure 4.28. Absorption Solar Unit Diurnal Hierarchical Key Map

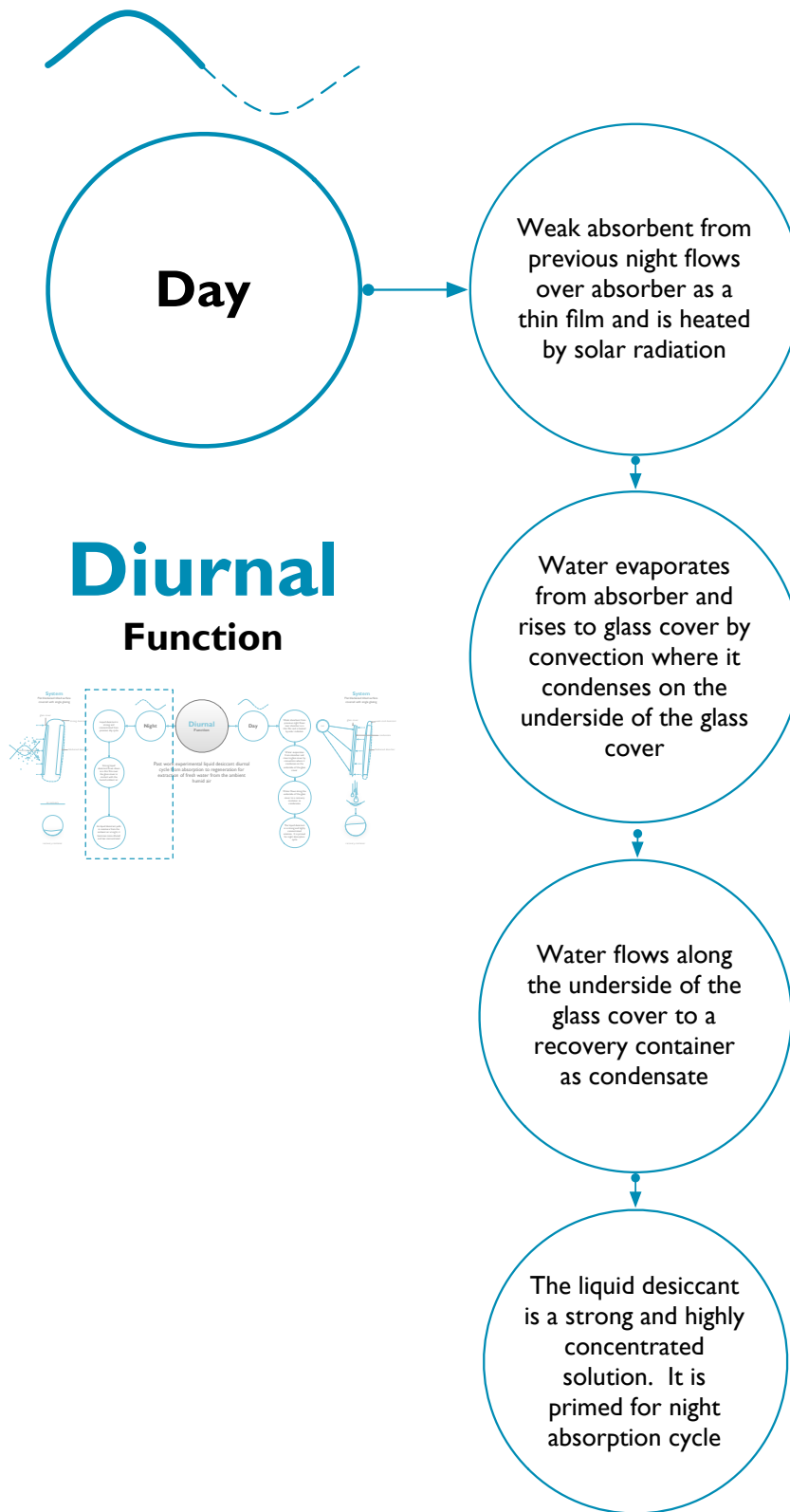
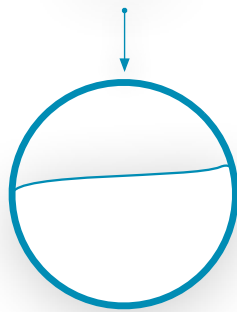
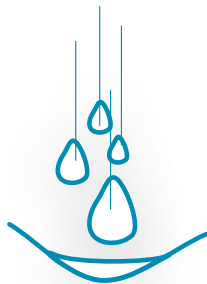
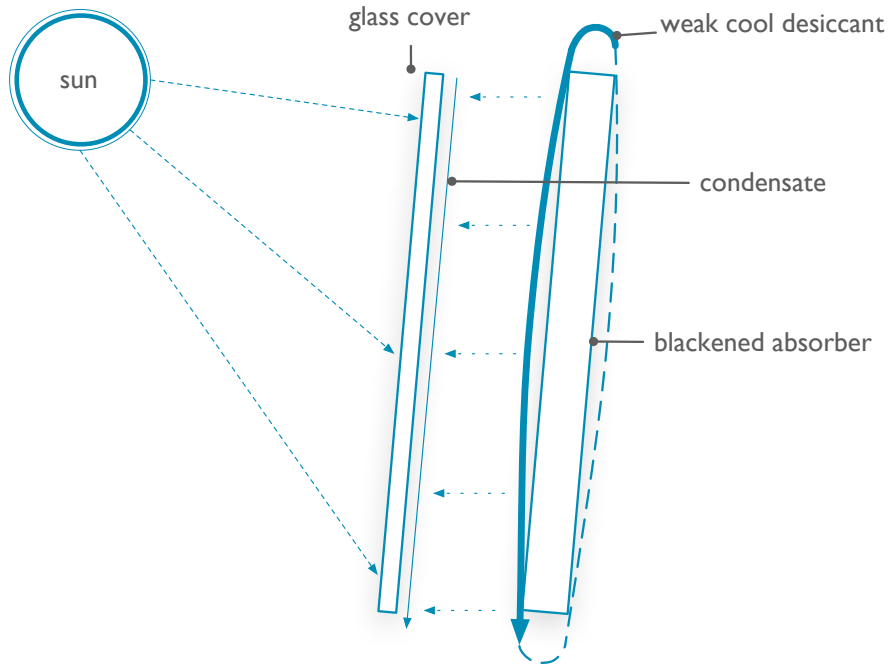


Figure 4.29. Absorption Solar Unit Day Function Hierarchical Map

System

Flat blackened tilted surface covered with single glazing



recovery container

Diurnal Function

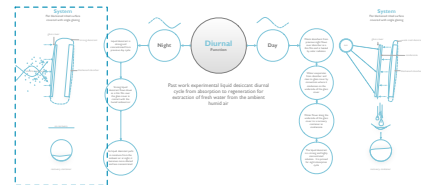


Figure 4.30. Absorption Solar Unit Day System Hierarchical Map

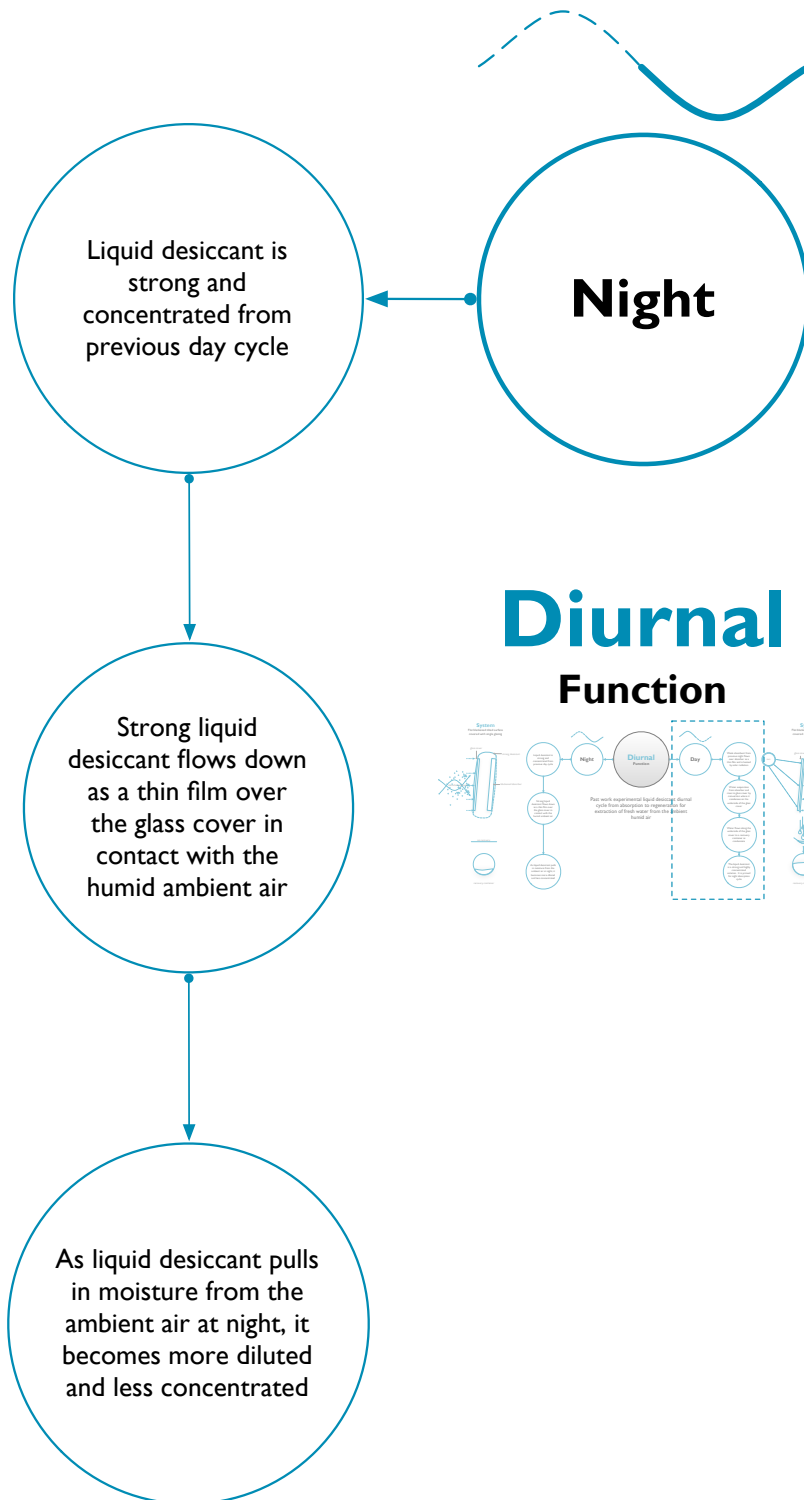
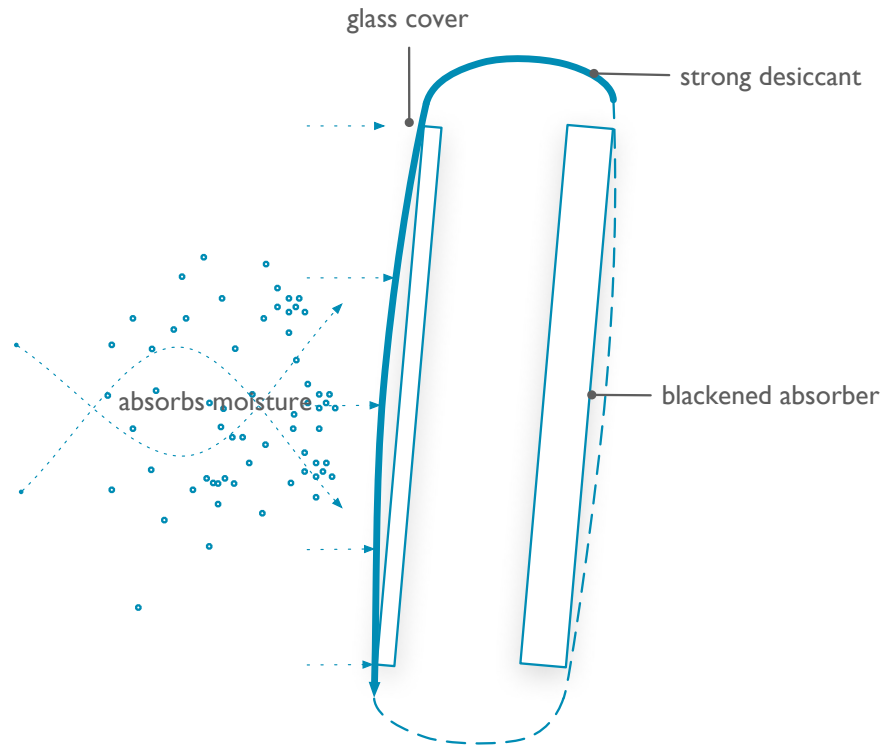


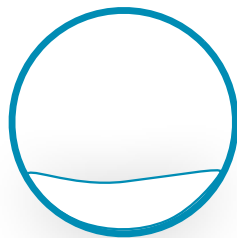
Figure 4.31. Absorption Solar Unit Night Function Hierarchical Map

System

Flat blackened tilted surface covered with single glazing



no recovery



recovery container

Diurnal Function

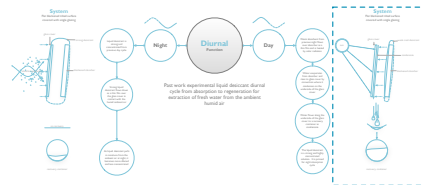


Figure 4.32. Absorption Solar Unit Night System Hierarchical Map

4.2.4 Liquid Desiccant Solar Absorption System Absorber and Regenerator

4.2.4.1 The Absorber

The absorption cycle in Gandhidasan's absorption solar unit dilutes the liquid desiccant. The absorber has two inlets: one for fresh humid air from the bottom, and a second for liquid desiccant from the top. Inside the absorber, liquid desiccant falls as a thin spray in direct contact with fresh air. The partial vapor pressure of the fresh air is higher than the surface vapor pressure of the liquid desiccant. The lower surface vapor pressure of the liquid desiccant absorbs vapor moisture from fresh air. The process condenses water and releases heat. Dry air leaves the top of the absorber while dilute liquid desiccant leaves the bottom. Low temperature and low water to salt concentration liquid desiccant improve system performance.

4.2.4.2 The Regenerator

The regenerator cycle in Gandhidasan's absorption solar unit concentrates the liquid desiccant. The regenerator receives weak liquid desiccant from the absorber. Heating the weak desiccant reverses the mass transfer of water vapor such that water evaporates from the liquid desiccant. The liquid desiccant cools from latent heat of evaporation. The liquid desiccant leaving the regenerator is cool and strong. Additional heat exchangers passing liquid desiccant over chilled water coils lowers the temperature further. The larger the temperature difference between liquid desiccant and fresh air entering the absorber increases the amount of moisture vapor transfer in the system.

4.2.5 Different Methods for Water Extraction from Humid Air

Figure 4.33 is a hierarchical mapping of different methods for extracting water from humid air. The diagram is an inspired spatial mapping with relevant detail to understand how the methods work. The 'blue' markings represent functions similar to a solar liquid desiccant system absorber and condenser. The 'red' markings represent functions similar to a solar liquid desiccant system regenerator. 'Orange' markings represent potential issues with particular water extraction system. The water extraction systems in this spatial arrangement represent potential models for dehumidification control.

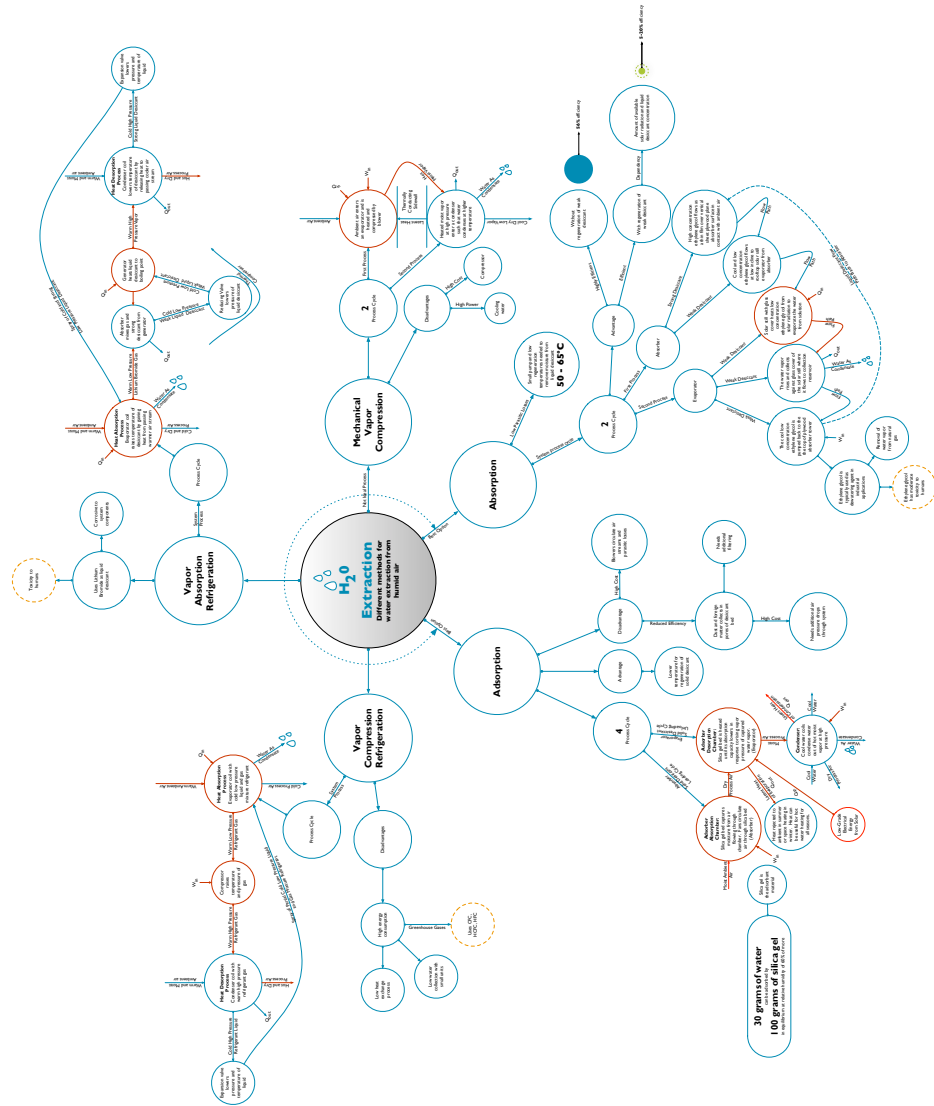


Figure 4.33. Models for Liquid Desiccant Air Conditioning Hierarchical Key Map

4.2.5.1 Vapor Absorption

Figure 4.34 shows the workings of a vapor absorption system. The use of a vapor absorption system for water extraction is problematic. The vapor absorption system uses lithium bromide as a liquid desiccant. Lithium bromide is highly toxic to humans and corrodes metal system components.

Figure 4.35 shows the evaporation and absorber process cycle of the vapor absorption system. The inputs to

the evaporator are heat, fresh air, and a spray of cold strong low-pressure liquid desiccant. The outputs from the evaporator are warm low-pressure lithium bromide gas, condensate, and cold dry process air. The evaporator is a heat absorption process. The passing stream of warm moist air raises the temperature of the evaporator coils by convective heat transfer. The evaporator coils transfer heat into the liquid desiccant by convective heat transfer. Warm low-pressure lithium bromide gas leaves the evaporator and enters the absorber. Water vapor from the warm moist air stream condenses on the evaporator coils. Water falls to the bottom of the evaporator and leaves as condensate to ambient. Cooler dry process air leaves the evaporator.

Figure 4.36 shows the absorber and generator of the vapor absorption system. The absorber is a mixing chamber for warm low-pressure lithium bromide gas and strong warm liquid desiccant from the generator. The input to the absorber is warm low-pressure lithium bromide gas, and strong hot liquid desiccant. The outputs from the absorber are cold and weak low-pressure liquid desiccant and heat. Warm low-pressure lithium bromide gas flows from the evaporator into the absorber. Hot strong liquid desiccant flows from the generator into the absorber. The lithium bromide gas condenses in the absorber. The latent heat of condensation cools the strong liquid desiccant from the generator. The reducing valve has cold low-pressure liquid desiccant as input and output. A reducing valve further reduces the pressure of the cold low-pressure weak liquid desiccant from the absorber. The input to the generator is heat and cold low-pressure weak liquid desiccant. The output from the generator is warm high-pressure vapor. Cold and lower pressure weak liquid desiccant enters the generator from the reducing valve. The generator heats the cold low-pressure weak desiccant. Warm high-pressure vapor leaves the generator and flows into a condenser. A heat desorption process in the condenser lowers the temperature of lithium bromide vapor flowing in the condenser coils. Cool air passes over and lowers the temperature of the condenser coils by convective heat transfer. The condenser coils condense lithium bromide vapor inside the coil by convective heat transfer. The condensing coils pass cool strong and low-pressure lithium bromide to the evaporator.

The lithium bromide works to transfer heat in the evaporator; absorber; generator; and condenser. The process of changing the temperature and pressure of the liquid desiccant in the evaporator, absorber, and generator is inefficient for the process of water extraction. Water extraction capacity is ideal for dehumidification. Vapor absorption as a process for water extraction from humid air is energy consumptive. The source of water generation in the process is the condensate that leaves the evaporator.

4.2.5.2 Vapor Compression

Figure 4.37 shows the workings of a vapor compression system. The use of vapor compression system for water extraction is problematic. The system uses CFCs, HCFCs, and HFCs as refrigerants. The refrigerants in the system contribute to ozone depletion and global warming potential. The low heat exchange process is high energy consumptive.

Figure 4.38 shows the evaporator, compressor, and expansion valve of the vapor compression system. The evaporator functions as a heat absorption process. The inputs to the evaporator are heat, warm ambient air, and cold low-pressure refrigerant. The outputs from the evaporator are condensate, cold process air, and warm low-pressure refrigerant gas. Warm humid air flows into the evaporator. Ambient air passes over evaporator coils. Cold low-pressure liquid and gas refrigerant mixture flows through the evaporator coils. The air stream raises the temperature of the evaporator coils by convective heat transfer. The evaporator coils transfer heat into the liquid and gas refrigerant mixture by convective heat transfer. Water vapor from the warm ambient air stream condenses on the evaporator coils. Water falls to the bottom of the evaporator and leaves in small amounts as condensate to ambient. Cooler dry process air leaves the evaporator. An expansion valve lowers the pressure and temperature of refrigerant passing into the evaporator coils. Warm low-pressure refrigerant gas leaves the evaporator and enters the compressor.

Figure 4.39 shows the evaporator, compressor, condenser, and expansion valve of the vapor compression refrigerant system. The condenser functions as a heat desorption process. The inputs to the compressor are warm low-pressure refrigerant gas from the evaporator and work. The output from the compressor is warm high-pressure refrigerant gas. The compressor is a pump that compresses the warm low-pressure refrigerant gas. The compressor raises the temperature and pressure of the gas. The inputs to the condenser are warm and moist ambient air and warm high-pressure refrigerant gas from the compressor. The outputs from the condenser are hot and dry process air, energy, and cold high-pressure liquid refrigerant. Warm and moist ambient air flows over condenser cooling coils. The warm high-pressure refrigerant gas transfers heat by convection to the condenser coils. The condenser coils transfer heat by convection to the ambient air stream passing over the coils. The air stream leaves the condenser as hot process air with higher moisture content. The refrigerant in the condenser coils leave the condenser as cold high-pressure liquid refrigerant. The input to the expansion valve is cold high-pressure liquid refrigerant. The expansion valve lowers pressure and temperature of the inward flowing refrigerant liquid.

The vapor compression system uses refrigerants that negatively affect the environment. The system consumes far more energy than the water it generates. The refrigerants are effective at heat transfer but at high-energy cost. The process of raising and lowering the pressure of the refrigerant is inefficient for purpose of low water generation in the evaporator.

4.2.5.3 Adsorption

Figure 4.40 shows advantages and disadvantages for adsorption system. The cycle features heating, pressurization, desorption, and condensation. The system requires maintenance to filter dust and foreign objects that collect in the pores of desiccant bed[14]. Blowers to circulate air streams may create parasitic system energy losses[14]. The system is one of the better models for water extraction.

Figure 4.41 shows a diagram of a simple heat driven cooling cycle for the adsorption system. Two chambers provide for the thermal operation of the adsorption system. The absorption and desorption chambers can switch operation characteristics. Figure 4.41 shows the cycle when the absorption chamber is loading the solid desiccant with moisture from mass transfer of water vapor. The adsorbent is a solid silica gel desiccant. Silica gel takes up water. The inputs to the adsorption chamber work from fan air blowers, and ambient air[14]. The output from the adsorber heating process is dry process air. The desiccant bed has capacity to adsorb 30 grams of water with 100 grams of silica gel at relative humidity of 60% or higher[14]. The absorption chamber continues taking up water from ambient air until its absorption capacity drives vapor pressure of the silica gel and water mixture greater than the ambient air. A second chamber that has undergone water take-up by silica gel until its surface vapor pressure feeds the dry process air from the absorption chamber. Fans circulate heat and air through the desorption chamber at $50\text{ to }90^{\circ}\text{C}$. Solar energy is sufficient to drive the high temperature desorption chamber. Pressure rises in the evaporator until it reaches equilibrium with condenser pressure. Desorption chamber inputs are heat, and dry air. The outputs from the desorption chamber is heat rejection from the evaporator process and moist air. Desorption drives mass transfer for water vapor from silica bed to dry process air stream. Heat rejection from the latent heat of evaporation in the desorber chamber can be useful in space heating in the winter and as hot water heat, otherwise it rejects to ambient. The absorption chamber can become a desorption chamber and vice versa.

The condenser connects to both chambers and provides condensation of moist air stream from desorption chamber process, the inputs to the condenser are condensing coil water, work from fan air blowers, and moist

process air. The outputs from the condenser are heat, condensate, and condensing coil water. The moist process air stream flows into the condenser from the adsorber desorption chamber. Cool water flows into the condenser coils. The moist process air stream transfers heat by convection to condenser coils. Water condenses on the condenser coils and it falls to the bottom of the condenser as condensate. The condensate drains to ambient.

The adsorption system drives moisture from ambient air stream through an adsorber, desorber, and condenser. The system uses expensive silica desiccant beds, high-grade electrical energy blowers to heat the silica bed and move process air. The parasitic losses from the blowers drive energy consumption and system inefficiencies. The potential for high mass transfer of water moisture through the silica gel beds is possible but at high-energy cost.

4.2.5.4 Absorption

Figure 4.42 shows the characteristics of an absorption system. The system uses smaller pumps with lower parasitic losses[14]. The system requires lower temperatures to regenerate liquid desiccant[14]. The system uses an absorber and an evaporator configuration. Liquid desiccant works as a mass transfer of water vapor medium. Regeneration of liquid desiccant requires low-grade electrical energy source. Solar radiation from the sun may provide low-grade electrical energy. The bias for low-grade electrical energy for liquid desiccant regeneration improves efficiency for the system.

Figure 4.43 shows the absorber and evaporator of the absorption system. Ethylene glycol is the liquid desiccant in an absorption system. The compound has moderate toxicity to humans. The inputs to the absorber are strong liquid desiccant, and ambient air. The output from the absorber is weak liquid desiccant. The open system allows for contact between ambient air and strong liquid desiccant. Strong liquid desiccant flows as thin falling film over vertical absorber surface. Liquid desiccant at the bottom of the absorber is cool and diluted. The cool and diluted desiccant flows along an incline to solar heated evaporator. The input to the solar heated evaporator is cool weak liquid desiccant. The solar heated evaporator is similar to the flat tilted black absorber proposed by Gandhidasan. The evaporator has a glass cover. Solar radiation from the sun strikes the glass cover. The glass cover heats the liquid desiccant by convection heat transfer. Water evaporates from the liquid desiccant. The water condenses on the glass cover. The water collects against the glass cover and flows to a collection reservoir. The liquid desiccant pumps back to the absorber to repeat the cycle.

4.3 Issues Present in Current Models

Five models for water extraction have potential as dehumidification system for indoor air. The mechanical vapor compression model provides water extraction and generates water from a condenser. The mechanical vapor compression system has high costs associated with compression cycle and energy consumption for water-cooling. Vapor absorption water extraction generates water as condensate, but has high-energy consumption in the generator and uses corrosive refrigerant. The vapor absorption system provides better operation as a cycle to cool another fluid rather than primarily dehumidification of air. Vapor compression water extraction uses refrigerants that contribute to production of greenhouse gases. Most of the other water extractions models exhaust condensate to ambient or are of very low water take up volume. High water extraction is necessary to provide proper dehumidification performance. Dehumidification performance measures the desiccant capacity to take up water and release it. Direct contact between desiccant and water provide the best capacity for absorption. The adsorber and absorption systems provide thermal performance by direct contact between desiccant and humid air. The adsorber evaporator requires energy to heat and compress dry process air. The refrigerant in the absorption system has toxicity to humans and it is an open-air system. The issues of using an open-air system in a building envelope and better refrigerants toxicity is a matter for the thesis proposal for component configuration.

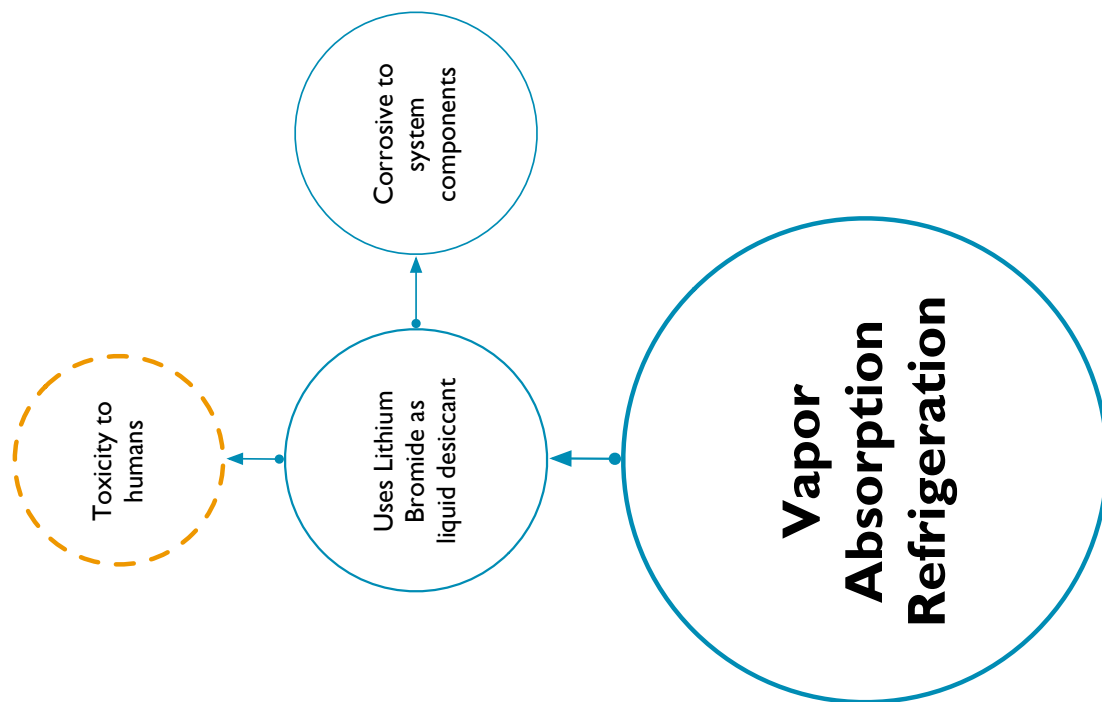


Figure 4.34. Vapor Absorption Hierarchical Map

Vapor Absorption Refrigeration

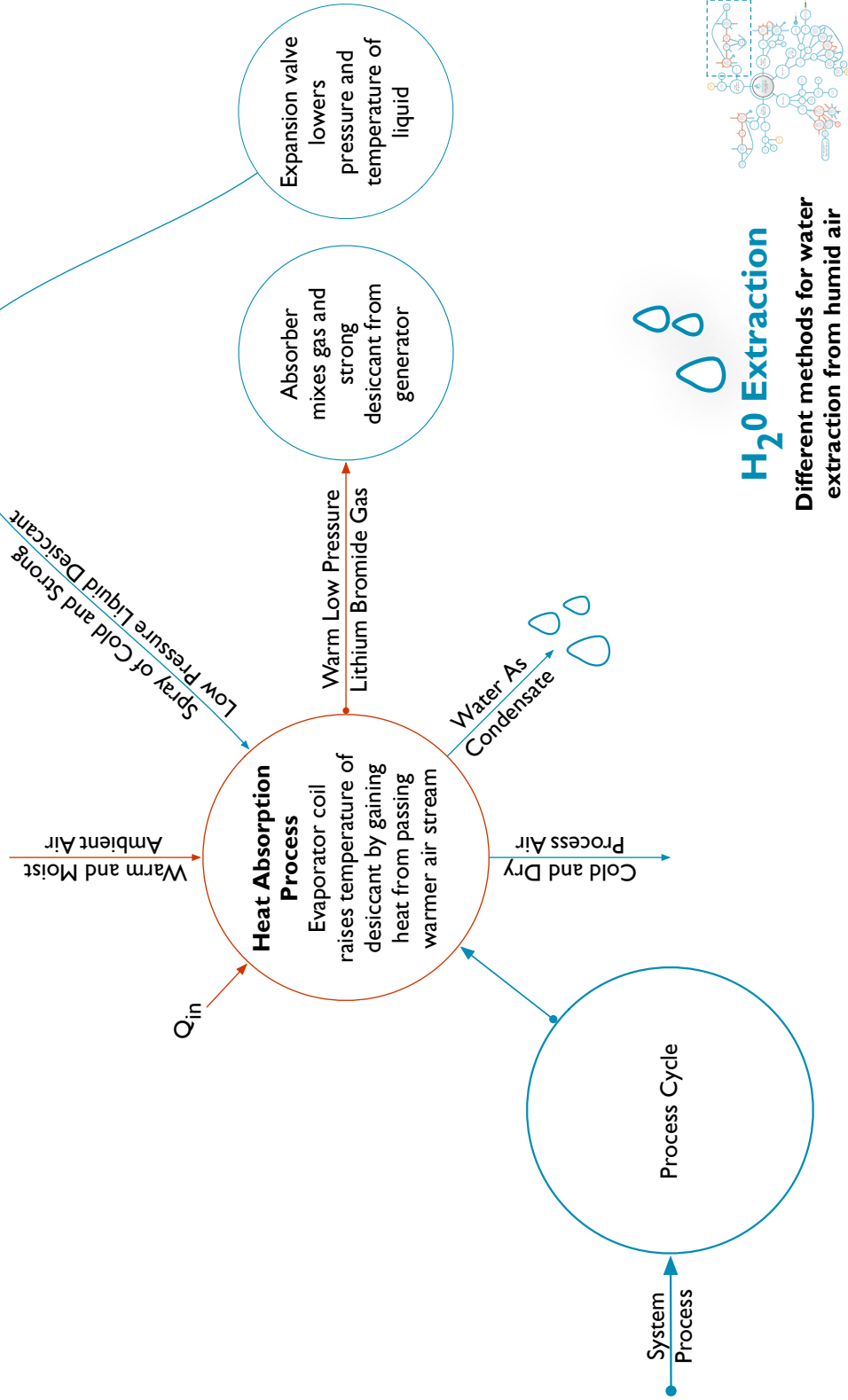


Figure 4.35. Vapor Absorption Hierarchical Map

Vapor Absorption Refrigeration

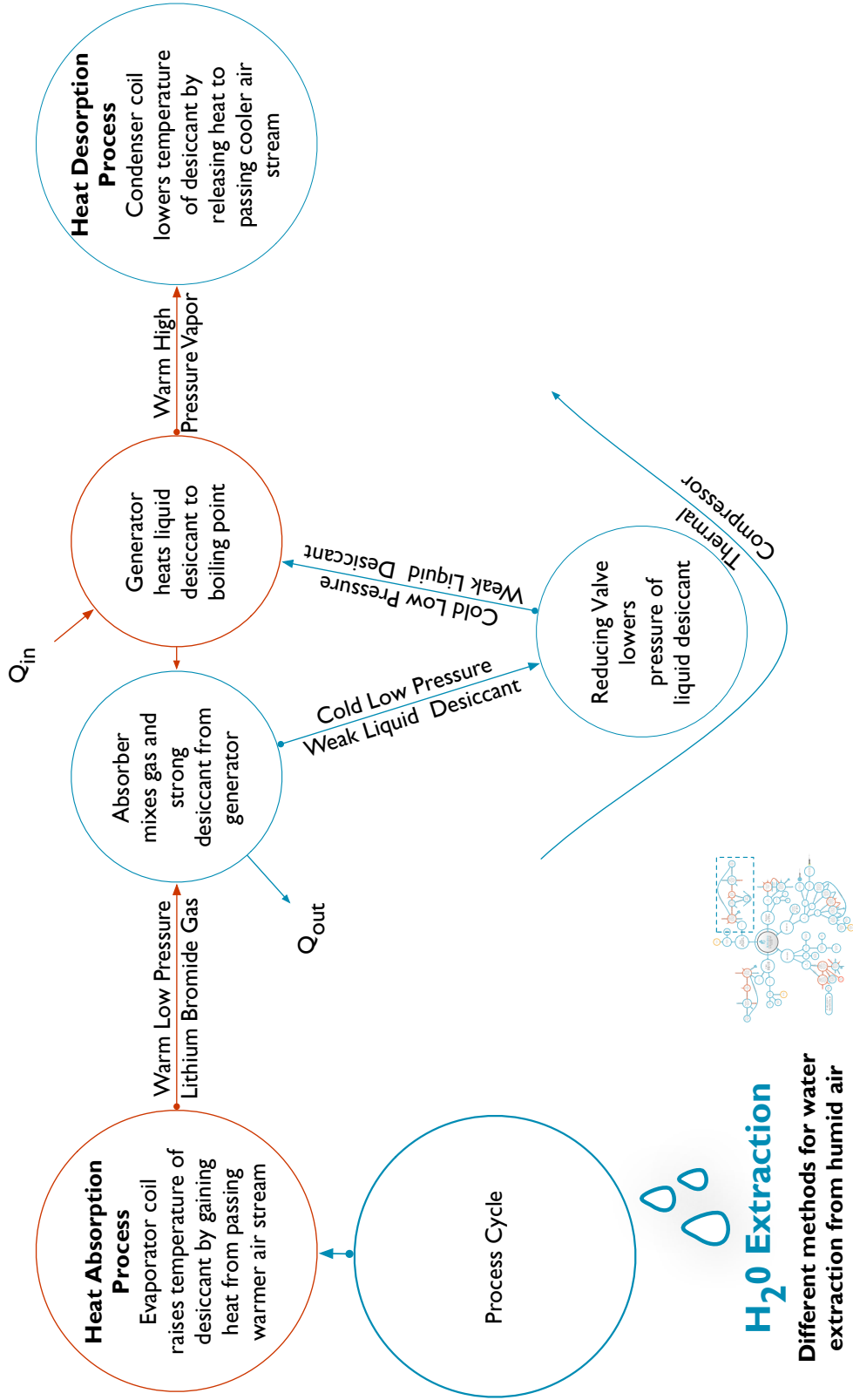
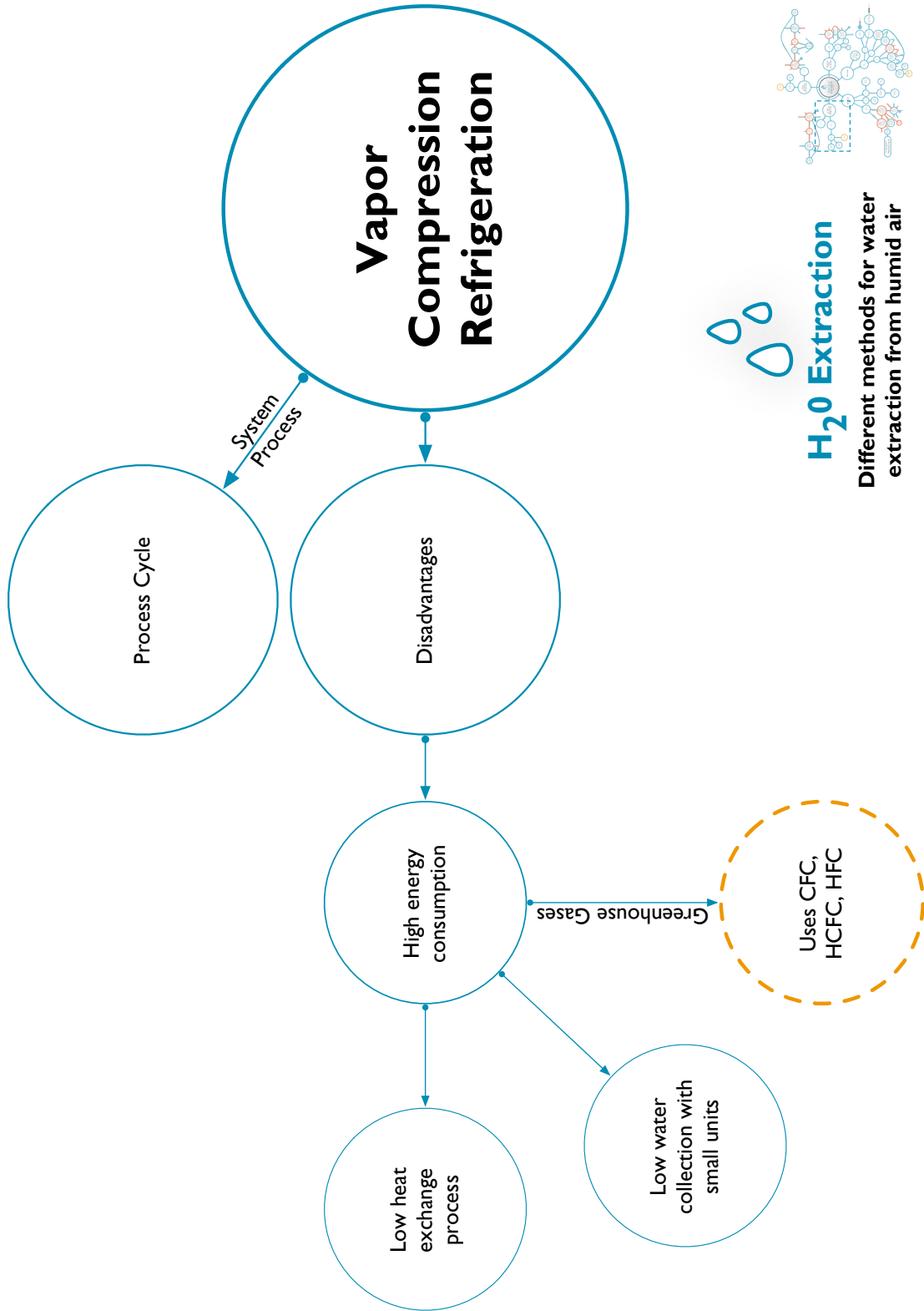


Figure 4.36. Vapor Absorption Hierarchical Map



H₂O Extraction

Different methods for water extraction from humid air



Figure 4.37. Vapor Compression Hierarchical Map

Vapor Compression Refrigeration



H₂O Extraction

Different methods for water extraction from humid air

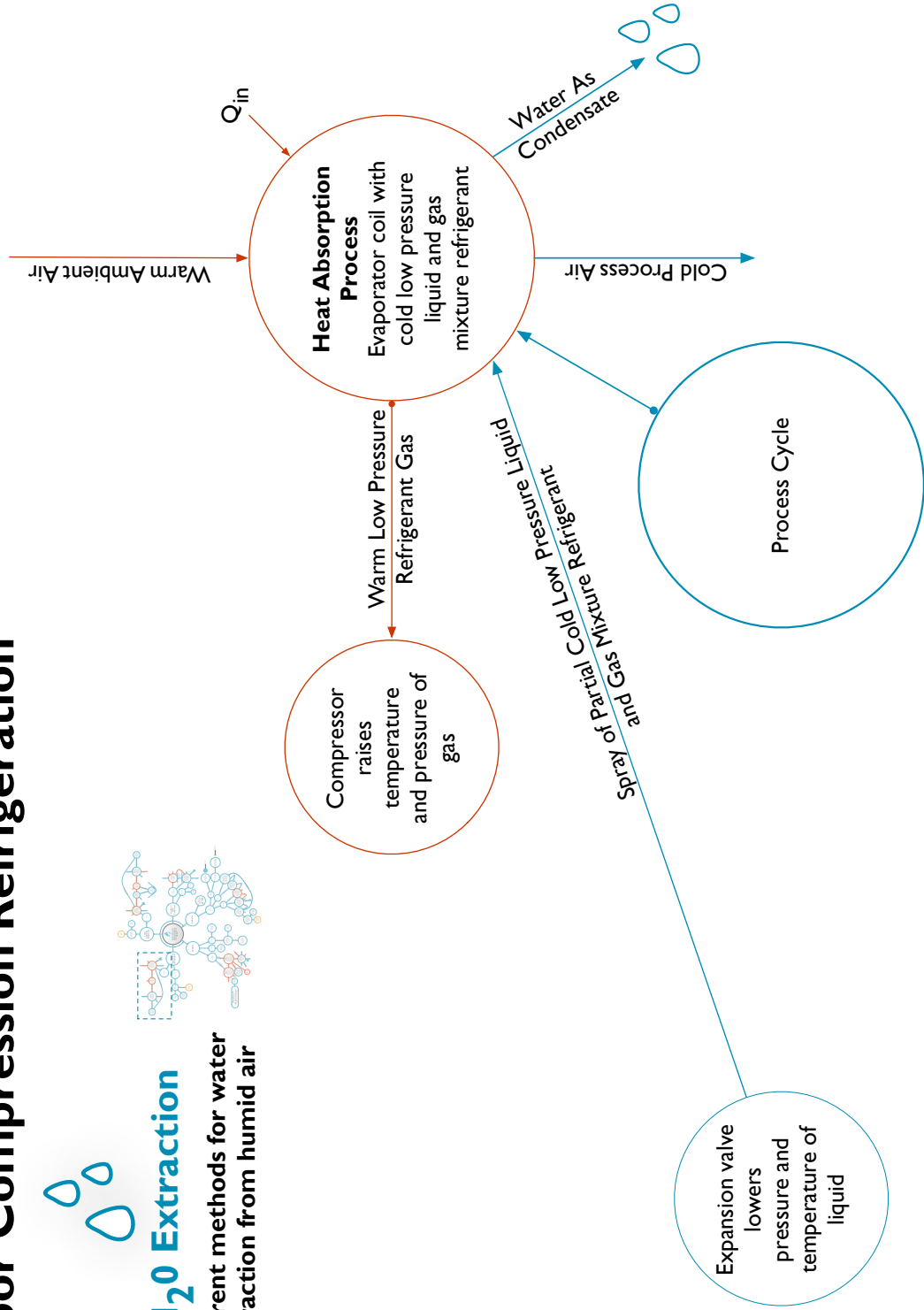


Figure 4.38. Vapor Compression Hierarchical Map

Vapor Compression Refrigeration



H₂O Extraction



Different methods for water extraction from humid air

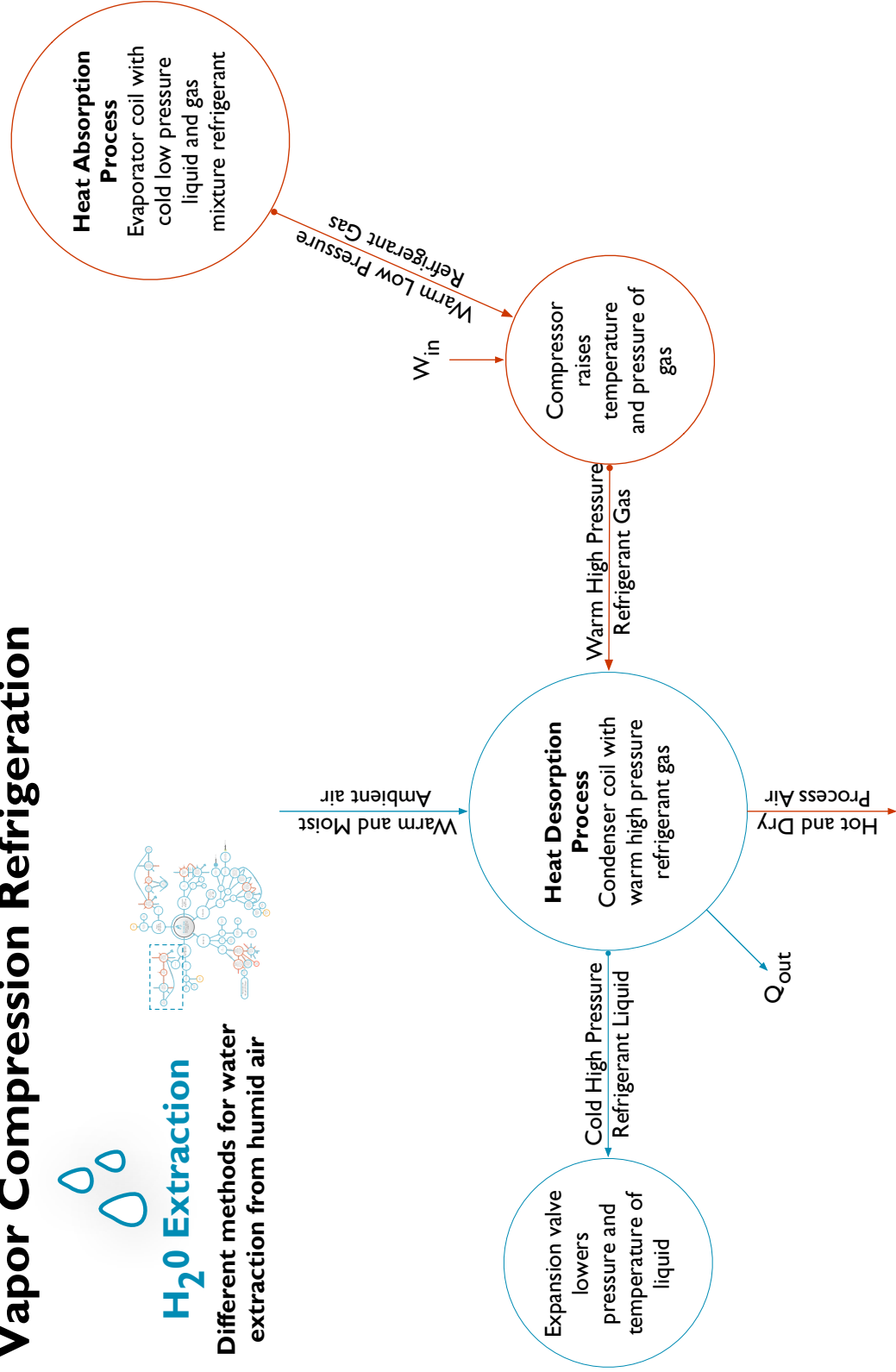


Figure 4.39. Vapor Compression Hierarchical Map

H₂O Extraction

Different methods for water extraction from humid air



Adsorption

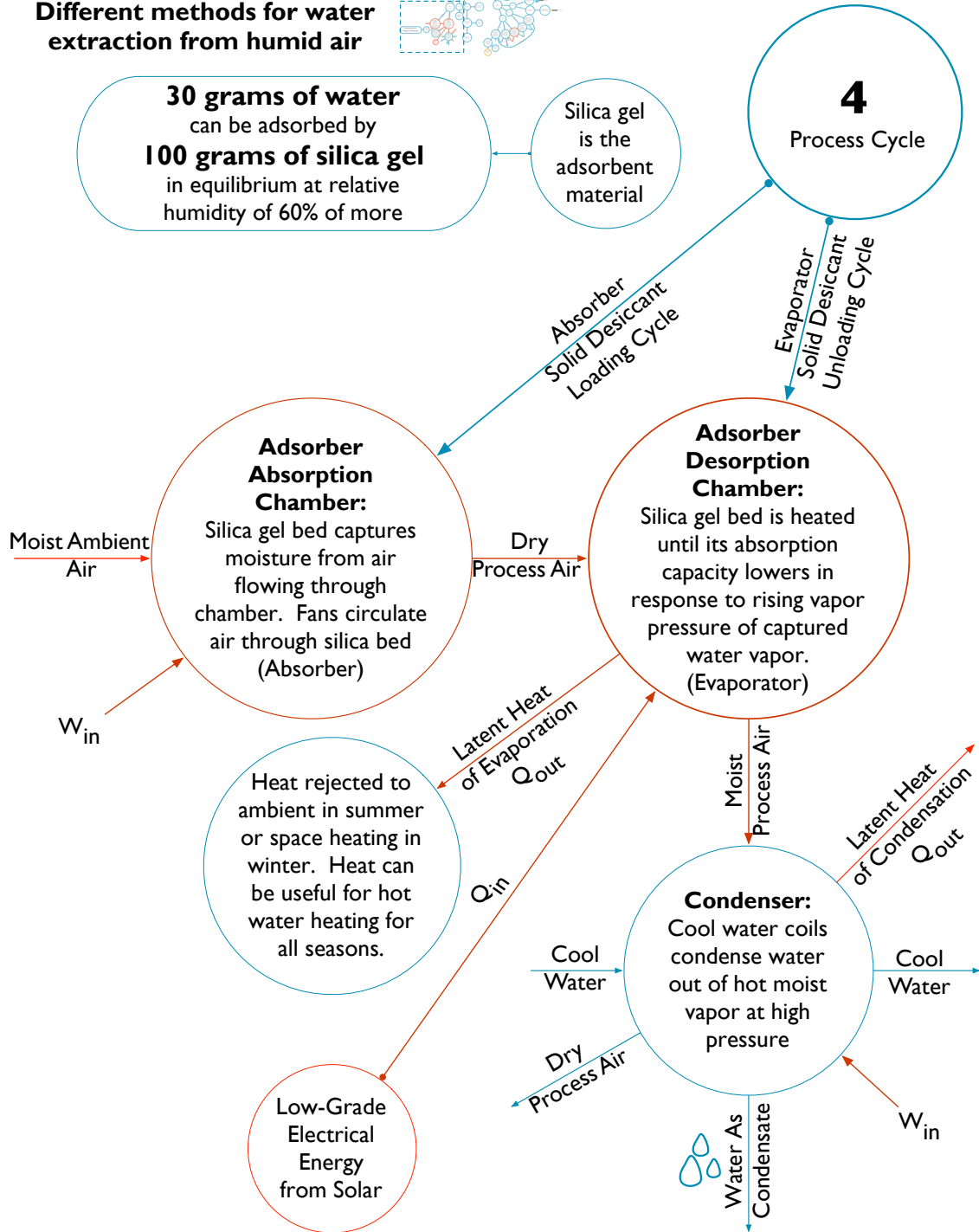


Figure 4.41. Adsorption Hierarchical Map

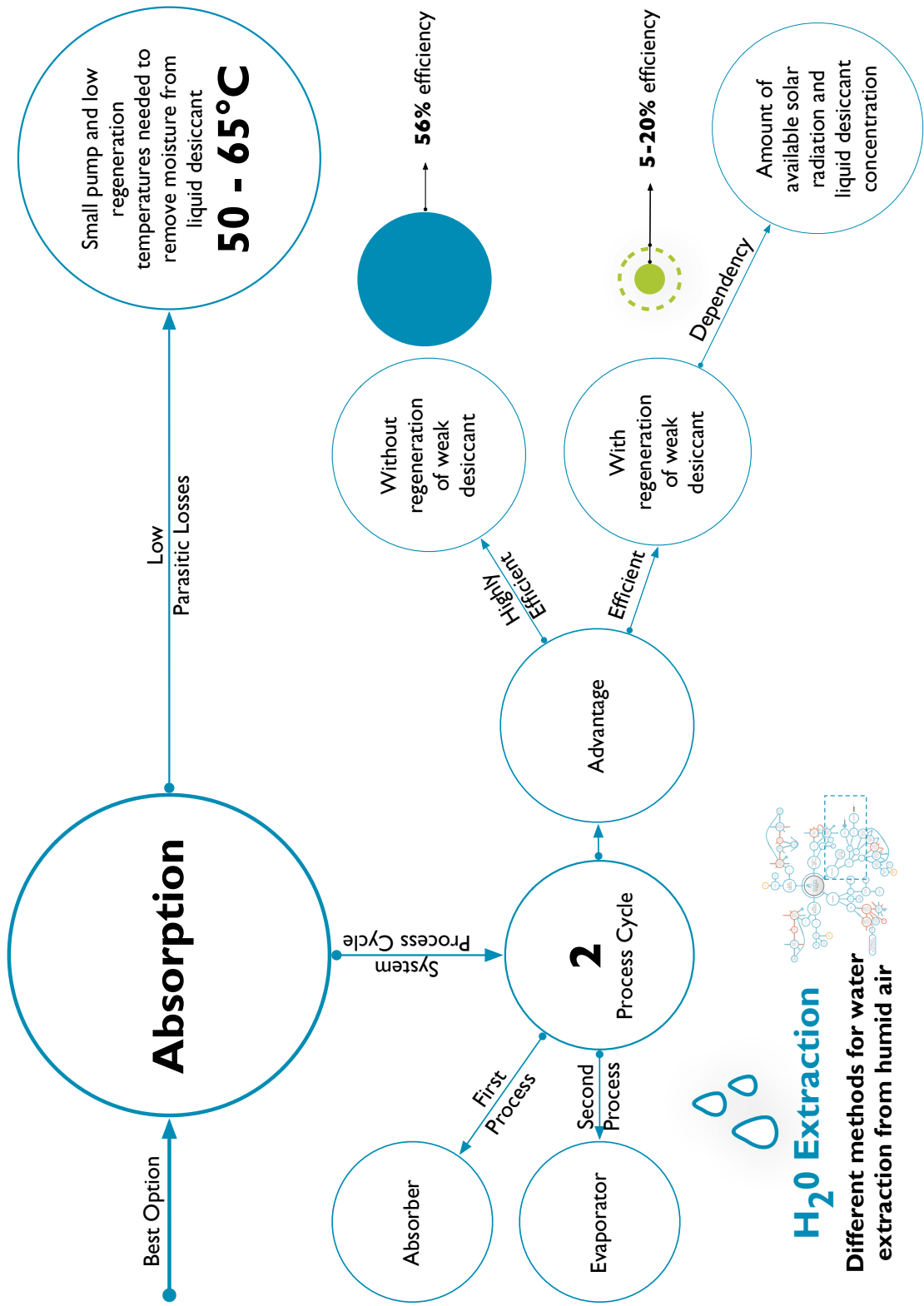


Figure 4.42. Absorption Hierarchical Map

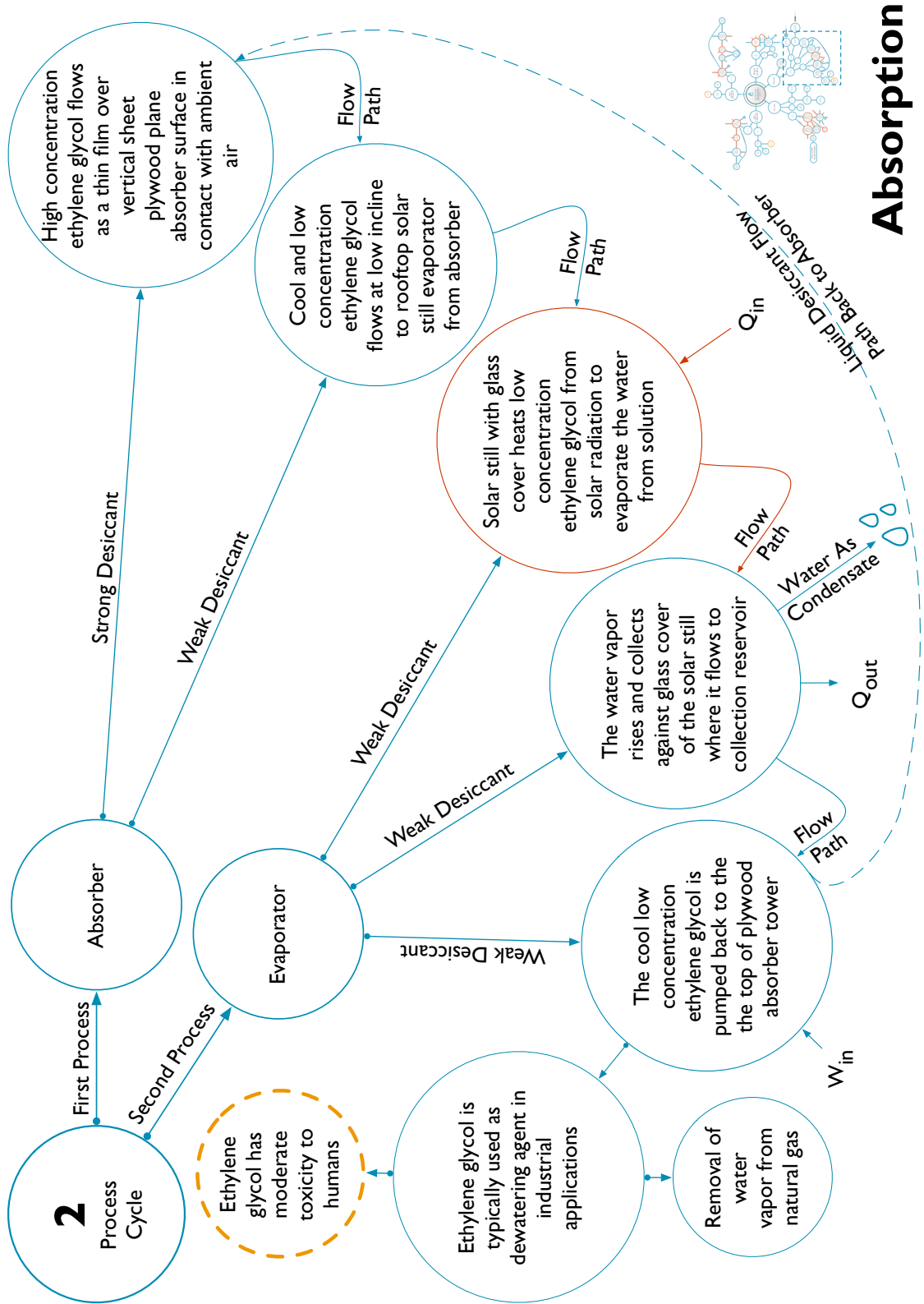


Figure 4.43. Absorption Hierarchical Map

CHAPTER 5: PROGRAM AND SYSTEM

5.1 Architectural Program

The program for the project serves technology driven entrepreneurial demand for co-working spaces. The ground floor allocates space for private conference, additional offices, or contemplation areas. The socially connective collaborative spaces feature shared reception, restroom, compact kitchen, and meeting area in an open plan configuration on the second floor. Shared workplace cafés allow for casual serendipitous interactions on the ground floor. The open office level is the primary focus of work in this thesis. The configuration with partition less work surfaces allows for knowledge sharing that builds collaboration to intensify innovation and community[19]. In lieu of private conference and office areas, the compact space features whiteboard wall surfaces for graphical expression of ideas and discussion. The combination of open plan configuration, partition less work areas and whiteboard walls foster modern collaborative office incubator.

5.2 Project Specifics

The project tests the case of a two-story office-building prototype. The energy modeling for the project is a simple one-zone model with only one floor shown for simulation. The configuration of the floor plan is 32'-0" x 32'-0" with offset external stair and elevator core to either the east or west. The project objective for design is to provide a comfortable daylight micro-office footprint. The primary workspace includes eight work desks with each measuring 2' - 7 1/2" x 6' -0", storage, and 12-seat open conference space. Figure 5.1 shows a sketch of the primary workspace with dashed lines for location of offset elevator and stair core on west elevation. The objective for energy is to strike a balance between low window to wall ratio to minimize energy loss in the winter and excessive solar heat gains in the summer. The model contains glazing and components for solar liquid desiccant system on south and north facades with radiant ceiling panels as part of integrated building envelope on east, and west facades for the best trade-off between daylighting and energy design objectives. The building envelope and structure benefits from integral components of cross-laminated timber and rain screen exterior phenolic wood resin panels.

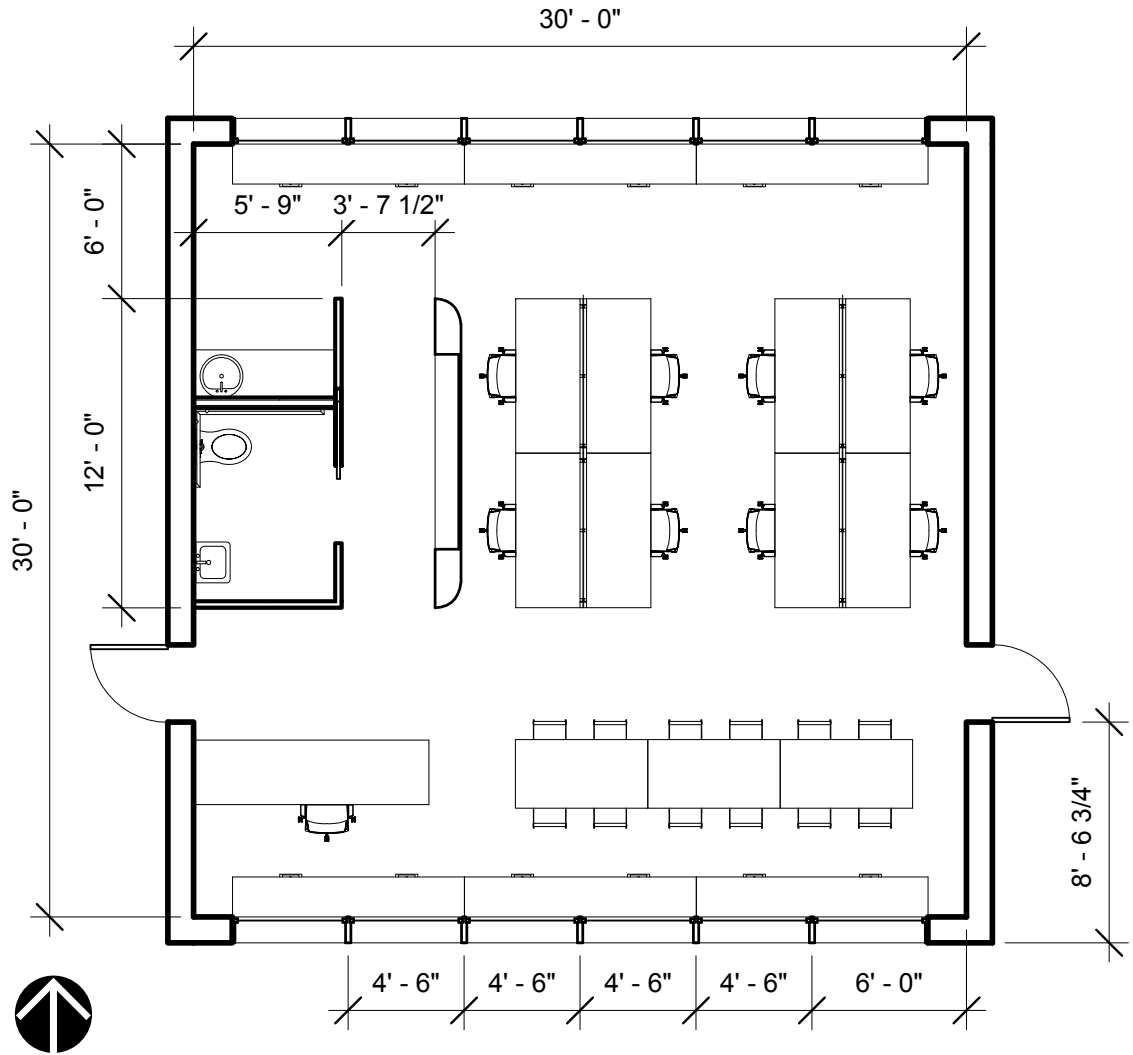


Figure 5.1. Proto|Model Primary Workspace Floor Plan Sketch

5.3 Cross Laminated Timber Panel Exterior Wall, Interior Wall, Floor, Ceiling, and Roof Construction

Cross-laminated timber provides a number of benefits for the design and energy model. The benefits that pertain to design and energy for cross laminated timber are its energy-efficient construction for air-tightness from low air permeance affords less building envelope heat losses in the winter and less building envelope heat gains in the summer. This of course assumes that the construction includes necessary thermal insulation and air barrier and water-resistive barrier to the exterior of the cross-laminated timber panels and vapor permeable interior finish[20]. The hygroscopic effects from exposed cross-laminated timber surfaces may offer beneficial mass transfer of water vapor to and from operational air flowing through indoor spaces. Analysis of moisture

storage and release in exposed cross-laminated timber in interior spaces requires confirmation for any benefits. Cross-laminated panels are by nature low weight and low mass due to their fabrication as engineered timber products. The low weight and low mass cross-laminated panels with exterior insulation has limited thermal mass storage within the building[21]. The use of cross-laminated timber provides good benefits for design and energy model with other advantageous such as carbon sequestration, avoidance of thermal bridges, and simple fast onsite construction process[21].

5.4 Reversible Hygroscopic Envelope Wall Operation

The north and south facade features a theoretical reversible solar liquid desiccant air conditioning with dedicated outdoor air system to provide decoupling of air conditioning from dehumidification. The floor level is equipped with its own independent system. Each facade can provide dehumidification of fresh air while the opposite facade provides dehumidification or humidification of operational process air. The system may use biologically inspired articulated flaps to control aperture sizes of air inlet areas. The flaps use an energy management system respond to relative humidity levels within the interior office space. The control of air admittance, shaping of flap apertures, and height offsite follow bio-inspiration from the Great Plains Prairie dog harness of wind. Vertical height displacement of sets of flaps admits air into absorber section of hygroscopic building envelope and allows air to mix with indoor air as dehumidified process air. The height displacement follows bio-inspiration from the leaf-cutting ant's use of mound openings to allow air inflow of air into the mound and outflow of air through the top mound openings.

5.5 Desiccant Characteristics

The driving force for dehumidification relies on a difference in vapor pressure between bulk air and the surface vapor pressure of a liquid desiccant at the interface between the air and the desiccant liquid[22]. Fresh air dehumidification requires direct contact with liquid desiccant in the dehumidifier[23]. Liquid desiccant leaving the dehumidifier regenerates by addition of solar energy or waste heat[23]. Most liquid desiccant systems use lithium chloride or lithium bromide. Lithium chloride and lithium bromide are expensive desiccant salts while calcium chloride and zinc chloride are low cost salts[24]. Table 5.1 shows list of desiccants with respect to stability, cost, and performance and concentration effectiveness. Table 5.2 shows calcium chloride and calcium nitrate mixture performance. The system in this thesis will use one of the desiccant salts shown in Table 5.3 for

its low toxicity.

In terms of stability the following is a list of most stable to least stable including cost:

- Lithium chloride most stable with large dehydration concentration of 30 to 40% and high cost at \$8.00 per 16.00 kg
- Lithium chloride can reduce relative humidity by up to 60%[24].
- Calcium chloride is the least stable and cheapest hygroscopic salt at about 40 cents per kilogram with high availability
 - Dependent on air inlet conditions and salt concentration in the Hygroscopic Brine Solution.
 - Calcium chloride has high vapor pressure[24].

The follow list shows performance and cost benefit of mixing hygroscopic salts in a solution of water to produce a maximum depression of surface vapor pressure:

- Performance indicates that it is possible to arrive at lower surface vapor pressures from a mixture of hygroscopic salts in solution than separately[24].
- Calcium chloride hygroscopic salt can be more stable if mixed with a higher performing stable hygroscopic salt in specific mixtures that balance cost and performance

Table 5.1. Desiccant Characteristics, Portion Of Data Derived from [22]

Desiccant	Stability	Cost	Performance	Effectiveness
Lithium Bromide	—	—	—	—
Tri Ethylene Glycol	—	—	—	—
Lithium Chloride	Highly Stable	Expensive	Relative Humidity Reduction of 15%	30-45%
Calcium Nitrate	—	Expensive	—	20%
Calcium Chloride	Highly Unstable	Inexpensive	—	—
Sodium Chloride	—	—	—	—

Table 5.2. Calcium Chloride and Calcium Nitrate Concentration Performance, Data Derived from [22]

Characteristics	Calcium Chloride and Calcium Nitrate Mixture
Mixture Concentration	50% Calcium Chloride with 20% Calcium Nitrate
Temperature Conditions	28 °C or 82.4 °F
Vapor Pressure Response	Low Vapor Pressure At Different Temperatures And Limited by Solubility Limits

Table 5.3. Best Neutral Salt Mixtures for Hygroscopic Brine Solution

Hygroscopic Salt Mixture	Mixture Characteristics
LiCl and CaCl	High toxicity, high performance, high heat, and not benign
NaCl and CaCl	Low low toxicity, lower performance, high heat, and benign

5.6 Hygroscopic Building Envelope

A hygroscopic building envelope is a dedicated outdoor air system. Hygroscopic building envelopes like the one proposed for the south and north facades have limited dry duct systems. Dry duct systems afford less vapor moisture air and dust-free environment to prevent dust collection and fungus, mold and bacterial growth. Dust, fungus, mold, and bacterial growth lower indoor air quality. High levels of vapor moisture introduction within indoor air environments increase operational maintenance to remediate mold, mildew, corrosion, and replacement of wall and window coverings and carpet. Outdoor air systems like the liquid desiccant system remove latent heat energy and improve dehumidification management when compared with other mechanical ventilation systems[8]. They remove moisture without cooling air supply temperatures to the point of condensation. Relative humidity levels below 70 percent keeps surfaces dry and free of mold and bacterial growth[8]. The hygroscopic solution in these systems has superior scavenging action to remove airborne contaminants and increase fresh air volumes[8][1]. Decoupled air conditioning systems are not necessarily new inventions, but when these systems are part of the latent energy removal process there is value in its capacity to scavenge vapor moisture, and particulates to improve indoor air quality.

It is worth noting that the model differs from other dedicated outdoor air systems. The thesis considers a south façade only thermo-hygroscopic liquid desiccant system. The potential for a north and south façade system with bi-directional operation is possible to remove vapor moisture from outside air or indoor air. Bi-directional

operation affords the system particulate removal from outside air and in the reverse direction from indoor air[1].

A hygroscopic building envelope uses radiant ceiling panels for sensible energy removal. The system is a variant of the dedicated outdoor air system. It runs as an all air system without return air and ductwork. This design eliminates crossing of indoor air with indoor particulate sources. Typical dedicated outdoor air systems provide lower energy use from radiant ceiling panels with higher heat exchanger efficiencies over conventional air conditioning systems[25]. These systems can provide electrical energy savings of 42 percent over conventional variable air volume systems[25].

The south façade of the prototype office model uses solar energy to drive the regeneration of the liquid desiccant. Typical flat-plate solar thermal collectors in a liquid desiccant system would have an installed cost of \$25/ft.² to \$40/ft.² (\$270/m² - \$430/m²) [8]. In a single effect system where the liquid desiccant cycles through the system only once there is a much lower peak thermal coefficient of performance of 0.44 and installation cost of \$2,650 per peak ton (\$9,320/kW) of cooling capacity[8]. This is much more than the cost of commercial unitary 10-ton system that cost \$1,000 per ton(\$3,500/kW)[8]. The use of east and west solar thermal liquid desiccant units may allow for higher efficiencies and better coefficient of performance to improve installation costs for flat-plate panel installation. Typical solar liquid desiccant systems coupled with solar hot water systems with wider adoption may provide better cost benefit over traditional air conditioning installation. Bi-directional hygroscopic building envelope driven by solar energy for liquid desiccant regeneration improves system efficiency and cost benefit analysis but further work requires simulation verification.

CHAPTER 6: DATA

6.1 Site Specific Data for Atlanta, Georgia Near Auburn Ave and Jackson Street

The project site situates itself in an urban neighborhood supportive of light rail, bus, biking, and pedestrian oriented transit. The site consists of two parcels at the intersection of Auburn Avenue and Jackson Street in Atlanta, Georgia is nearby. The concept for the northern parcel is compact terraced and zero energy home based business residences over a retail podium along Jackson and Old Wheat Street. The smaller southern parcel is where a smaller series of low energy compact terraced innovation incubator offices and retail along Auburn Avenue.

6.2 Cross-laminated Timber

The office prototype predilection for carbon neutral construction materials uses cross-laminated timber primarily in the building envelope as an alternative to concrete and steel. Cross-laminated timber (CLT) design supports open plan configurations[26]. CLT engineered solid wood panels wood achieves strength through laminations of perpendicular oriented layers. The panel thickness varies from a few inches up to 16 inches(Green). Panel dimensions may span up to 64 by 8 feet[26]. Walls, floor, and roof of the project use CLT construction. Steel beams and braces provide ductility for lateral stability. Insulated concrete form panels provide below grade construction for walls and floors, and foundation. CLT requires minimal assembly at construction site due to its prefabrication of wall and floor panels. Tables 6.1, 6.2, and 6.3 show the construction of CLT and phenolic resin wood panel rain screen envelope. The thermal resistance of the wall and the integration of liquid desiccant components require adaptation from thin wall to thick wall.

6.3 Fire Protection Performance of Cross-Laminated Timber Panel

CLT solid panels resist fire without additional protective membrane barriers. Fire testing in Europe and Canada demonstrate that the solid panels can withstand 2-hour fire-resistance rating[26]. CLT panels often receive classification as mass timber because it forms a protective char layer during combustion[26].

Table 6.1. CLT and Phenolic Resin Wood Rainscreen Wall Thermal and Physical Properties

	Exterior Walls	(k)	Btu·ft/h·ft ² ·F
<i>–Interior Side</i>			
5 Perm Low VOC Matte Clear 2 Coats Vapor Retarder		–	Btu·ft/h·ft ² ·F
<i>–Structural Core Boundary</i>			
6 7/8" (180 mm) CLT Panel 5-Ply	0.0636		Btu·ft/h·ft ² ·F
<i>–Structural Core Boundary</i>			
25mm Phenolic Insulation Board (RSI 1.19M ² K/W)	0.0121		Btu·ft/h·ft ² ·F
10 Perm Vapor Retarder EPS 1/8"	0.0202		Btu·ft/h·ft ² ·F
1" Air Space	0.0144		Btu·ft/h·ft ² ·F
1/2" Phenolic Resin Vented Façade Panels	0.1624		Btu·ft/h·ft ² ·F
<i>–Exterior Side</i>			
<i>Totals</i>			

Table 6.2. CLT and Phenolic Resin Wood Rainscreen Wall Thermal and Physical Properties

	Exterior Walls	Dim (L)	ft	(L/k)	ft ² ·f·hr/Btu
<i>–Interior Side</i>					
5 Perm Low VOC Matte Clear 2 Coats Vapor Retarder		–	ft	–	ft ² ·f·hr/Btu
<i>–Structural Core Boundary</i>					
6 7/8" (180 mm) CLT Panel 5-Ply	0.5708	ft	8.9754	ft ² ·f·hr/Btu	
<i>–Structural Core Boundary</i>					
25mm Phenolic Insulation Board (RSI 1.19M ² K/W)	0.0820	ft	6.7785	ft ² ·f·hr/Btu	
10 Perm Vapor Retarder EPS 1/8"	0.0104	ft	0.5157	ft ² ·f·hr/Btu	
1" Air Space	0.0833	ft	5.7870	ft ² ·f·hr/Btu	
1/2" Phenolic Resin Vented Façade Panels	0.5000	ft	3.0788	ft ² ·f·hr/Btu	
<i>–Exterior Side</i>					
<i>Totals</i>					

6.4 Lower Embodied Energy of Cross Laminated Timber Panel

Harvested wood, a rapidly renewable resource, reduces greenhouse gas emissions and provides carbon sequestration. Concrete production and steel manufacturing have a large carbon footprint. These materials require high-energy intensive processes to produce and manufacture. Concrete production process represents 5 percent of world carbon dioxide emissions (Canadian Wood Council 2004). Producing and transporting concrete represents more than 5 times the carbon footprint of the airline industry (Canadian Wood Council 2004). Emissions from steel manufacture and concrete production embody 26% and 57% more energy relative to wood harvesting (Canadian Wood Council 2004). Steel and concrete emit 34% and 81% more greenhouse gases. Steel and concrete release 24% and 47% more pollutants into the air. Steel and concrete discharge 400% and 350% more water and pollution (Canadian Wood Council 2004). The building envelope dominant prototype model for office in this thesis is mostly CLT with the exception of beams, bracing, and below grade construction. The construction typology for the prototype model reduces embodied carbon as low as reasonably possible.

Table 6.3. CLT and Phenolic Resin Wood Rainscreen Wall Thermal and Physical Properties

Exterior Walls (EPC)	Density	lbm/ft ³	(c)	Btu/lbm·F
<i>–Interior Side</i>				
5 Perm Low VOC Matte Clear 2 Coat	–	lbm/ft ³	–	Btu/lbm·F
<i>–Structural Core Boundary</i>				
6 7/8”(180 mm) CLT Panel 5-Ply	33.9618	lbm/ft ³	0.3821	Btu/lbm·F
<i>–Structural Core Boundary</i>				
4” Fiberglass Mesh Faced Polyisocyanurate Foam Board	2.8093	lbm/ft ³	–	Btu/lbm·F
10 Perm Vapor Retarder	1.5607	lbm/ft ³	0.3344	Btu/lbm·F
1” Air Space	0.0718	lbm/ft ³	0.2539	Btu/lbm·F
1/2” Phenolic Resin Vented Façade Panels	84.2802	lbm/ft ³	0.2221	Btu/lbm·F
<i>–Exterior Side</i>				

6.5 Phenolic Resin Wood Panels Exterior Rain Screen Panels

Phenolic resin wood panel exterior rain screen construction provides decorative cladding with many benefits. The panels install as ventilated facade with vertical air chamber between panels and insulation. The ventilated facade lowers solar radiation thermal energy storage to CLT. Metal battens and adjusting base anchor rainscreen panels to CLT. The panel construction diffuses moisture vapor to prevent condensation formation on the back of the panels. Insulation on the exterior side of CLT prevents thermal bridging from CLT to exterior rain screen panel.

CHAPTER 7: DAYLIGHTING

7.1 Daylighting

The design of the prototype model considers the impact of waste heat that electric lighting generates and its consequent removal by the mechanical system. A Daylighting design provision for the prototype model lowers electric lighting and conserves energy. The design incorporates visual and top daylighting glazing to control the admission of natural light, sunlight, and diffuse skylight into the interior. Exterior visual glazing shading device reduces glare and excess contrast into the workspace. Consideration to window glazing selection, reflective interior finishes, and partition work areas enhance the daylighting design. Strong daylighting strategies enhance the goal of providing a collaborative incubator co-sharing office model.

7.2 Proto|Model Assumptions

The prototype model assumes the workspaces have illuminate tasks requiring category 'D' for high contrast[27]. Figure shows the graphical site description of total daylight factor calculation with influences from sky component (SC), externally reflected component (ERC), internally reflectance for interior, and ground components. The site faces a parking lot to the south. Externally reflectance from buildings to the south is minimal.

7.3 Metrics for Simulation Work

Using table from [27] and Millet and Bedrick 1980 reference, the desired ranges for daylight factor is 1.5 to 2.5 percent for general office work. Daylight calculation for the model uses Equation 7.1. Table 7.1 shows the results of the calculation based on model dimensions.

$$DF_{average} = 0.2 \cdot \frac{\text{Window Area}}{\text{Floor Area}} \quad (7.1)$$

Table 7.1. Proto|Model Average Daylight Factor Calculations, See section 7.1 for equation

Model	Window Area	Floor Area	Avg Daylight Factor ¹	DF Calculated	DF Desired
Iteration Model I	289.44	900.00	0.06	6.43%	2.50%

7.3.1 2.5 H Guideline Daylight Calculation

Table 7.2 and Figure 7.2 shows the 2.5H guideline calculation and graphical section drawing for sufficient workspace luminance at desk plane height. The method delivers adequate daylighting into the space at a depth of 2.5 times the height of window glazing above the desk plane.

Table 7.2. Proto|Model 2.5 H Daylight Guideline Calculations

Model	Visual Window Height (ft)	2H Guideline (2.5 · H)
Iteration Model I	6.08	15.21

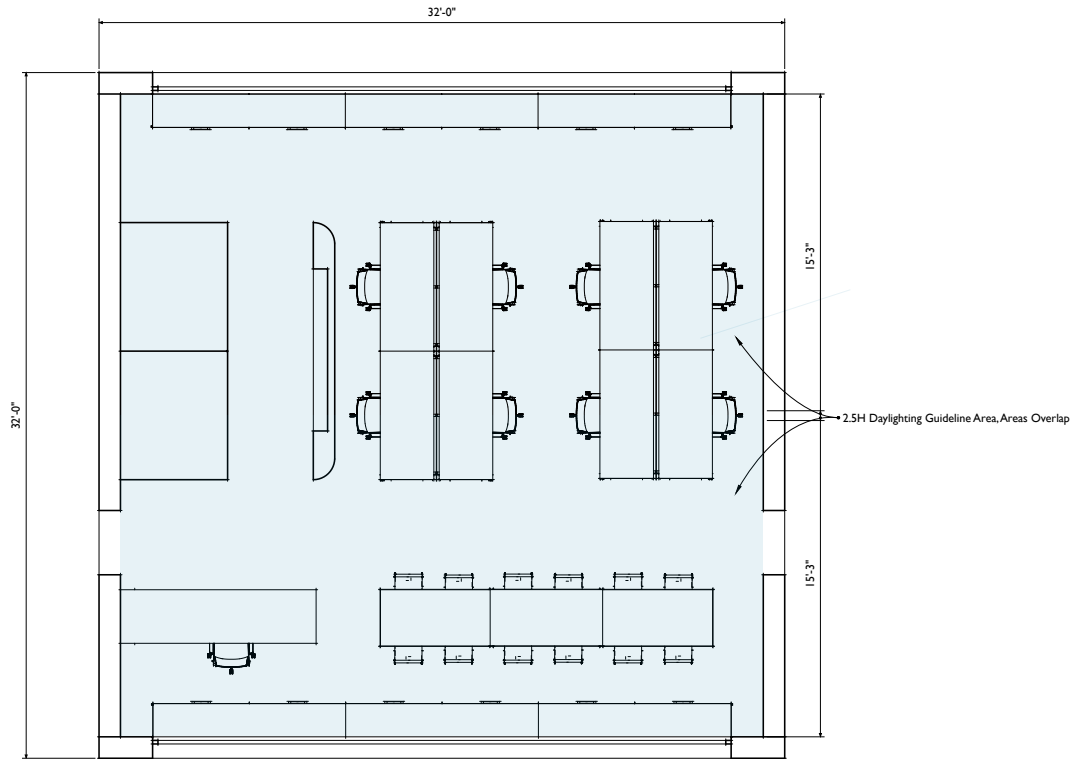


Figure 7.1. Section 2.5H Guideline for Daylighting of Proto|Model

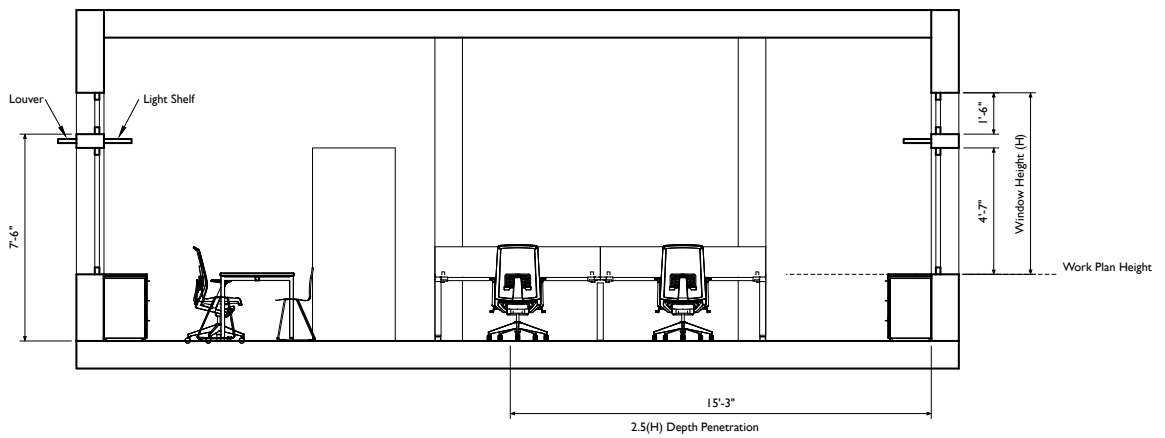


Figure 7.2. Section 2.5H Guideline for Daylighting of Proto|Model

7.3.2 15/30 Guideline for Daylighting Calculation

The 15/30 guideline for daylighting measures daylighting performance from window wall to work surface at three different zones. Distances up to 15 ft. (4.8 m) from window wall provides sufficient daylighting to work surface without supplemental or primary electric lighting. The intermediate zone from 15 ft. to 30 ft. (4.8 to 9.0 m) requires supplementary electric lighting. Lastly, the 30 ft. (9m) and beyond zone receives insufficient daylighting and requires primary electric lighting. Table 7.3 and Figure 7.3 shows calculation and graphical confirmation of guideline for sufficient daylighting without supplemental or primary electrical lighting.

Table 7.3. Proto|Model 15/30 Guideline Daylight Factor Calculations

Model	First 15' Satisfied	15' to 30' Supplemental EL	30' Beyond Primary EL
Iteration Model I	Yes	NA	NA

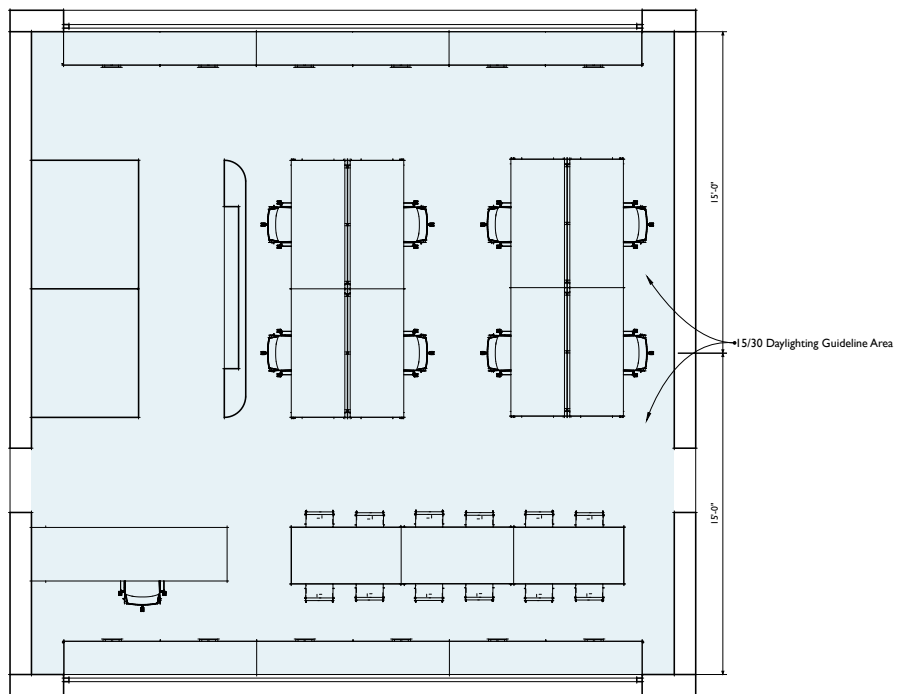


Figure 7.3. Floor Plan of 15/30 Guideline for Daylighting of Proto|Model

Table 7.4 shows assumptions for simulation luminance values for the prototype model. Table 7.5 shows assumptions for surface reflectance for walls, ceilings, and work surfaces. Table 7.6 shows calculations for summer, fall, and winter illumination for solar maximum altitude in Atlanta. Table 7.7 show summer, fall, and winter minimum and maximum daylight factor calculations in Atlanta. Table 7.8 shows minimum and maximum indoor luminance level calculations for summer, fall, and winter in Atlanta. The tables use Equations 7.2, 7.3, and 7.4 to calculate the data shown. The calculations confirm availability of sufficient daylighting luminance levels during summer, winter, and fall for Atlanta as shown in Table 7.8.

Table 7.4. Proto|Model Assumptions for Desired Daylighting Simulation

Luminous Flux	Units	Luminous Flux	Units
300-500	Lux	20-50	Foot-candles

Table 7.5. Proto|Model Detail Interior Assumptions for Desired Daylighting Simulation

Preferred Luminance	Candela/m ²	Lumen/m ²
Walls	25-250	2.323-23.226
Ceilings	50-250	4.645-23.226
Task surfaces	100-500	9.290-46.451

Table 7.6. Daylighting Illuminance Calculations for Atlanta 33.63° N Latitude

Time Period	Solar Maximum Altitude in (°)	Exterior Illumination(E_H) in (lux) ^{4,2}
21-Jun	79.87	20,972.64
21-Mar	56.37	17,785.26
21-Dec	32.87	11,697.43

Table 7.7. Daylighting Illuminance Calculations for Atlanta 33.63° N Latitude

Time Period	Min Daylight Factor (DF) in % ³	Max Daylight Factor (DF) in % ³
21-Jun	1.50%	2.50%
21-Mar	1.50%	2.50%
21-Dec	1.50%	2.50%

Table 7.8. Daylighting Illuminance Calculations for Atlanta 33.63° N Latitude

Time Period	Min Indoor Illumination (E_i) in (lux) ^{5,2}	Max Interior Illumination (E_i) in (lux) ^{5,2}
21-Jun	314.59	524.32
21-Mar	266.78	444.63
21-Dec	175.46	292.44

Table 7.9. Daylighting Preferred Illuminance Values for Atlanta 33.63° N Latitude

Time Period	Recommended Illuminance in (lux)
21-Jun	300-500
21-Mar	300-500
21-Dec	300-500

Notes for Tables 7.6, 7.7, 7.8, and 7.9

¹ Maximum Solar Altitudes Derived from [27],

$$\text{Summer Solstice Solar Max Altitude} = 90^\circ - \text{Latitude} + \text{Declination}(23.5) \quad (7.2)$$

$$\text{Spring/Fall Equinox Solar Max Altitude} = 90^\circ - \text{Latitude} + \text{Declination}(0) \quad (7.3)$$

$$\text{Winter Solstice Solar Max Altitude} = 90^\circ - \text{Latitude} - \text{Declination} \quad (23.5) \quad (7.4)$$

² Derived from Reference [28]

³ See reference [27]

⁴ Krochman Formula, where A is solar altitude in, see reference [27],

$$E_H = 300 + 21,000 \cdot \sin A \quad (7.5)$$

⁵ Daylight Factor; see reference [27],

$$DF = \frac{E_i(\text{Indoor Illuminance})}{E_H(\text{Outdoor Illuminance})} \quad (7.6)$$

7.4 High Performance Building Design Strategy

7.4.1 Daylight Optimized Building Footprint and Climate Responsive Window to Wall Area Ratio

The Proto|Model optimizes building footprint to leverage daylighting into interior office space for improved energy conservation. The floor plate uses a 30 ft. 0 in. x 30 ft. 0 in. structural plan with maximum north and south exposure for daylighting and view lighting concepts.

South and north facing facades provides easiest controllable daylight fenestration in the model. The east and west facades are opaque facades.[29]. Table 7.10 shows calculations for window to wall area ratio for the prototype model. Glazing percentage for one floor level is less than 25 percent.

Table 7.10. Daylight Window to Wall Ratio Percentages for Proto|Model

Designation	Window Area (sf)	Wall Area (sf)	Window/Wall Ratio in %
North	144.72	227.66	63.57%
East	-	360.00	
South	144.72	227.66	63.57%
West	-	360.00	
Total	289.44	1,175.31	24.63%

7.4.2 Daylighting Optimized Fenestration Design

Daylighting and glazing configuration influences heat transmission that affects mechanical system performance. The upper and lower glass areas use triple glazing with spectrally selective film. Figure 7.2 shows the daylighting glass windowsill at 7 ft. 6 in. above the finished floor. The upper daylighting glass area uses higher visible transmittance than the lower visual lighting glass. Daylighting glass projects light deep into floor plate with its high head height. The upper daylighting glass allows for more light emission with less heat transmission. The lower visual lighting glass reduces glare with less heat transmission. Table 7.11 shows the visible light transmittance values applied to glass for simulation model.

Table 7.11. Proto|Model Daylighting and Visual lighting Glass

Simulation Visible Light Transmittance Glazing	Transmittance Value
Visual Glazing Low Tvis Model Simulation	0.42
Daylighting Glazing High Tvis Model Simulation	0.78

7.4.3 Daylight Redirection Devices, Solar Shading Devices, and Exterior Overhand Louver

The model uses daylight redirection devices to deliver direct beam sunlight onto ceilings. Figure 7.2 shows light shelf on north and south interior facing façade. The light shelves reduce glare and sunlight away from occupants and deliver daylight deep into floor plate than possible without these devices[29]. Exterior overhang louver is shown in Figure 7.2 to control solar gains and glare from view lighting glass transmitted into interior[29]. Figure ?? shows graphical depiction of redirection device strategies response to incident solar radiation in summer, spring, and winter:

7.4.4 Daylight Responsive Electric Lighting Controls and Optimized Interior Design

The model features daylight response electric lighting controls to save energy by continuous dimmers, stepped ballast light fixtures, and power off photocells for when luminance from daylighting is sufficient. The co-share collaborative workplace design considers furniture, placement, and room surface finishes to enhance daylight performance[29]. The workspace is partition less and features open office plan without enclosed or private offices. Table 7.12 shows surface properties modeled for the simulation.

Table 7.12. Proto|Model Simulation Surface Properties

Surface	Property	Value
Walls Ext	Reflectance	0.84
	Roughness	0.03
	Specularity	0
Walls Int	Reflectance	0.84
	Roughness	0.03
	Specularity	0
Ceilings	Reflectance	0.84
	Roughness	0.03
	Specularity	0
Floor	Reflectance	0.35
	Roughness	0.05
	Specularity	0
Roof	Reflectance	0.84
	Roughness	0.03
	Specularity	0

7.5 Proto|Model Basis and Simulation

Figures 7.4 through 7.39 show the simulation of the 3D model with daylighting performance strategies. The method of simulation uses CIE standard for overcast sky conditions. The simple method provides minimal conditions to simulate daylight performance. The images show clear indication of lowest light levels during normal working hours over the summer, winter, and spring seasons in Atlanta. The results show that the middle range of values such as 250-lux works for the design, confirms, and validates the initial assumptions and calculations.

7.5.1 Daylighting Simulation Proto|Model Iteration 1

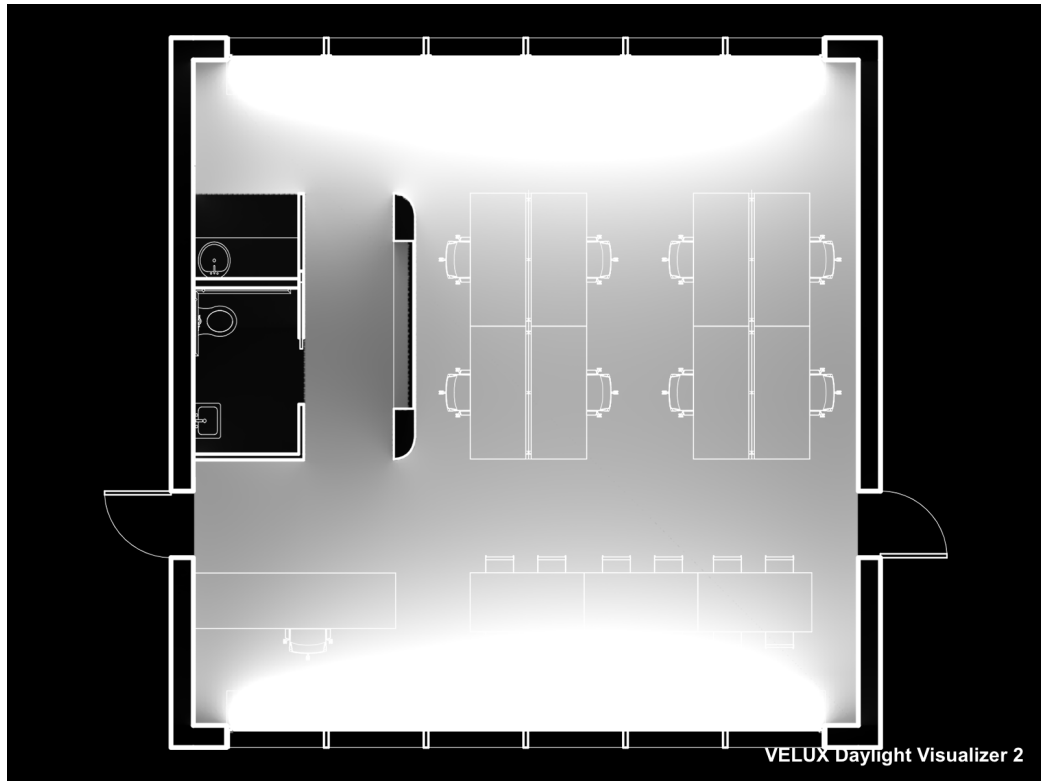


Figure 7.4. Daylighting for Atlanta Summer Noon Overcast Sky Plan View in VELUX

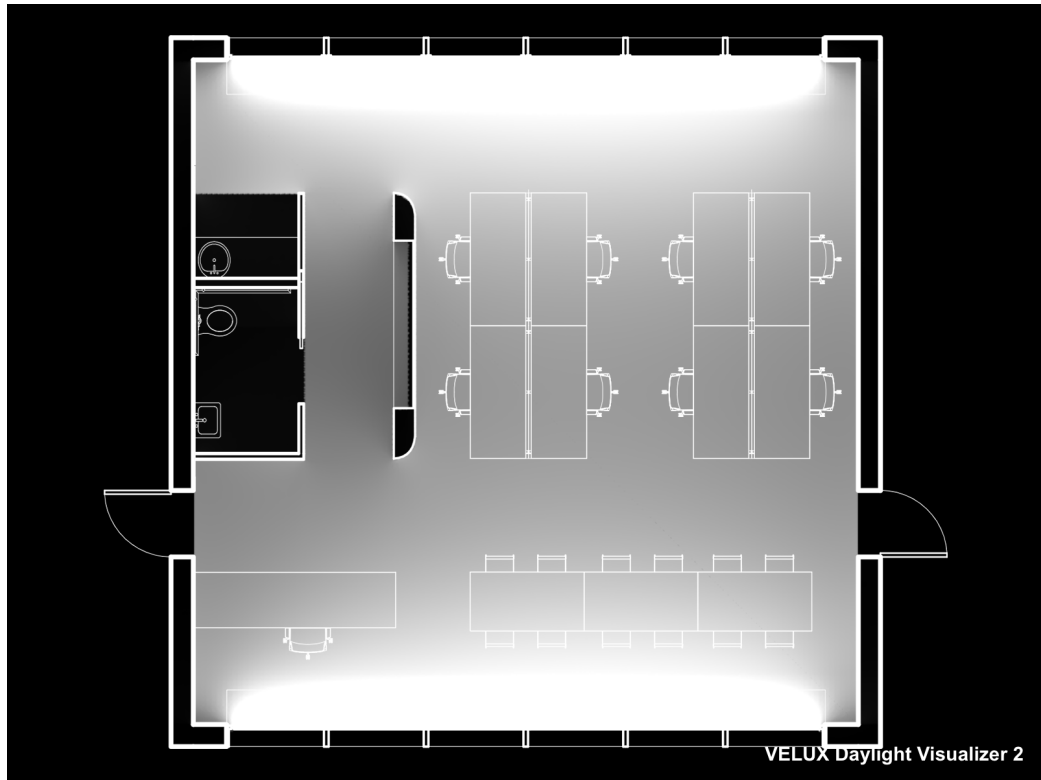


Figure 7.5. Daylighting for Atlanta Spring Noon Overcast Sky Plan View in VELUX

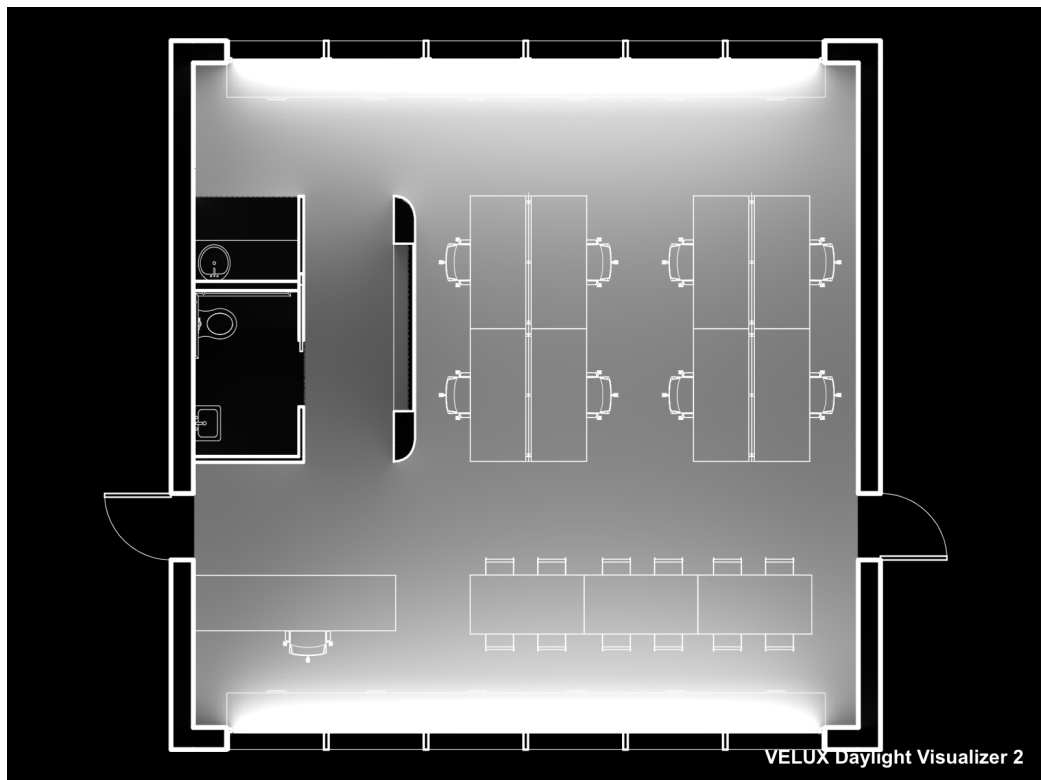


Figure 7.6. Daylighting for Atlanta Winter Noon Overcast Sky Plan View in VELUX

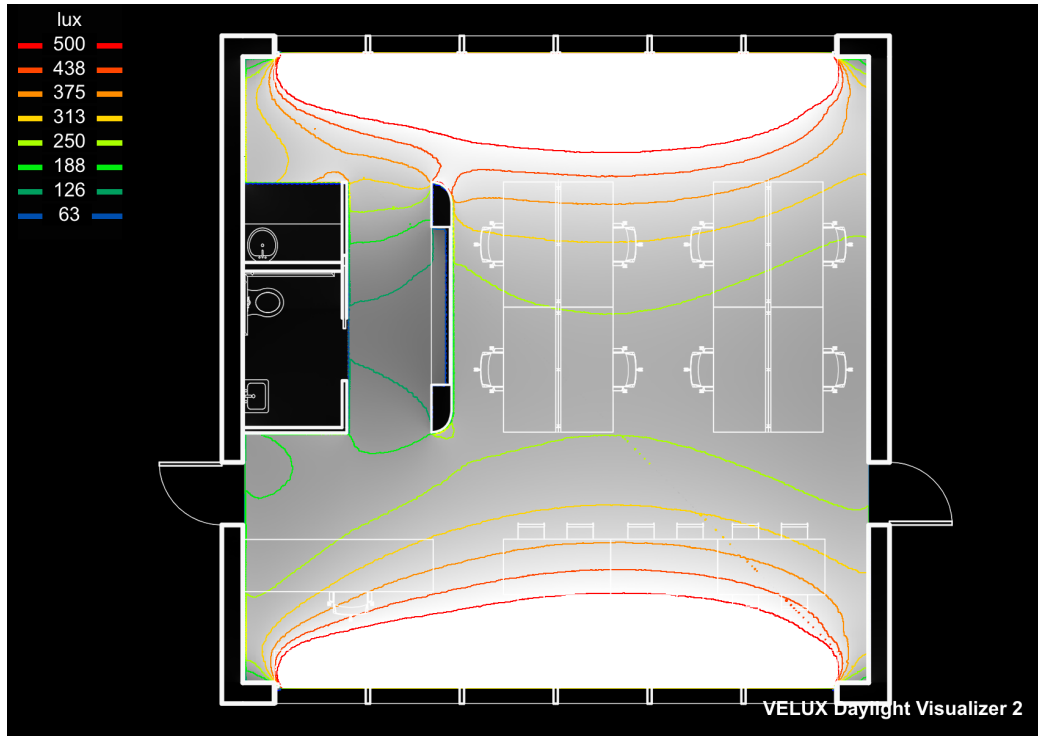


Figure 7.7. Daylighting for Atlanta Summer Noon Overcast Sky Iso Contour Plan View in VELUX

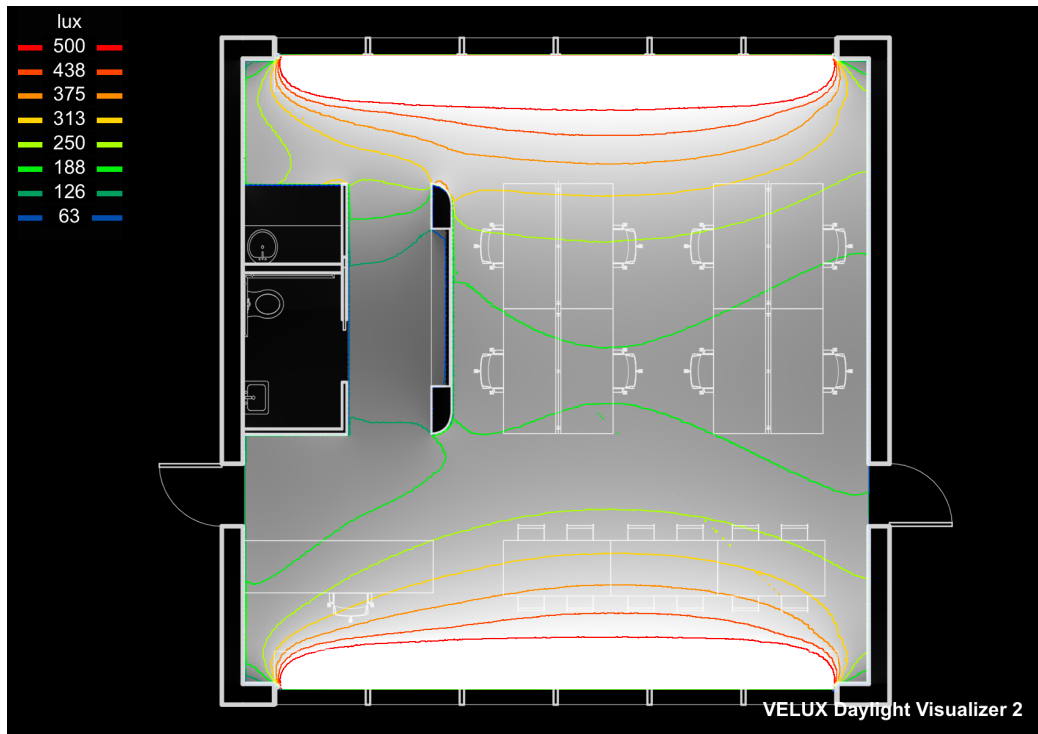


Figure 7.8. Daylighting for Atlanta Spring Noon Overcast Sky Iso Contour Plan View in VELUX

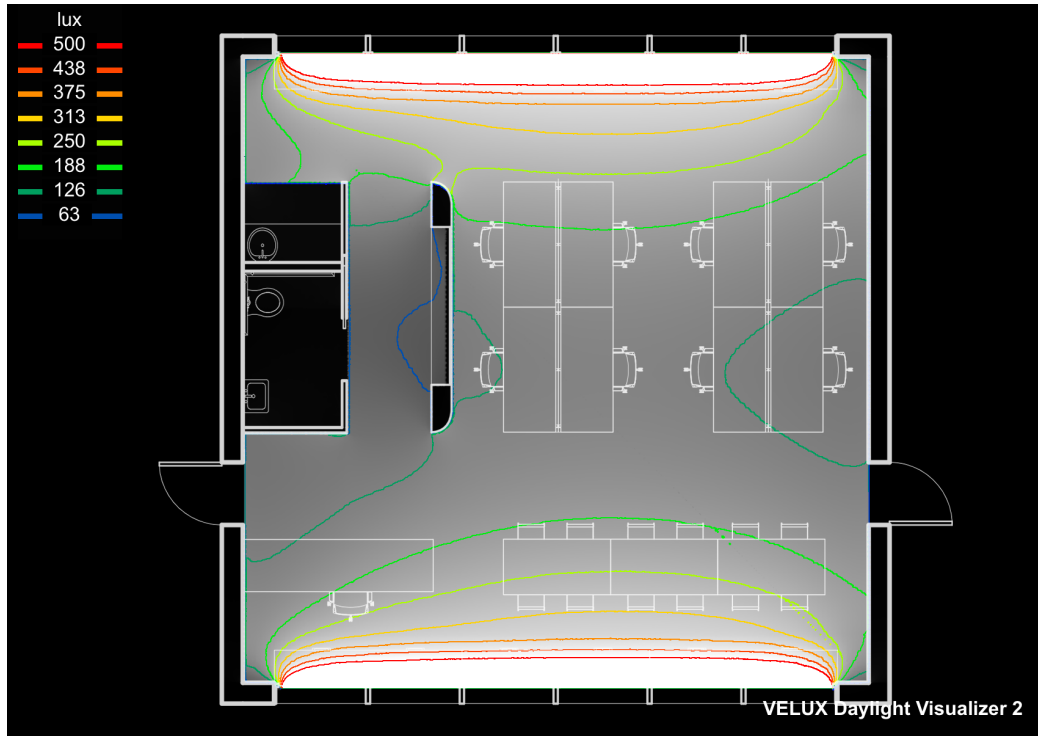


Figure 7.9. Daylighting for Atlanta Winter Noon Overcast Sky Iso Contour Plan View in VELUX

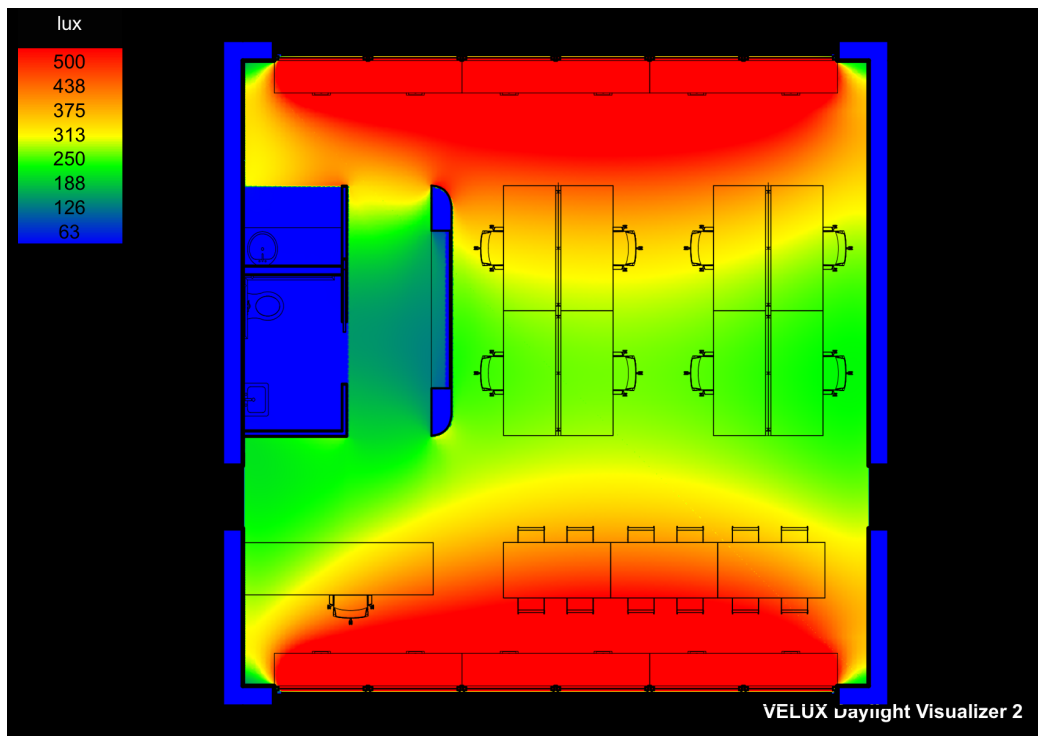


Figure 7.10. Daylighting for Atlanta Summer Noon Overcast Sky False Color Plan View in VELUX

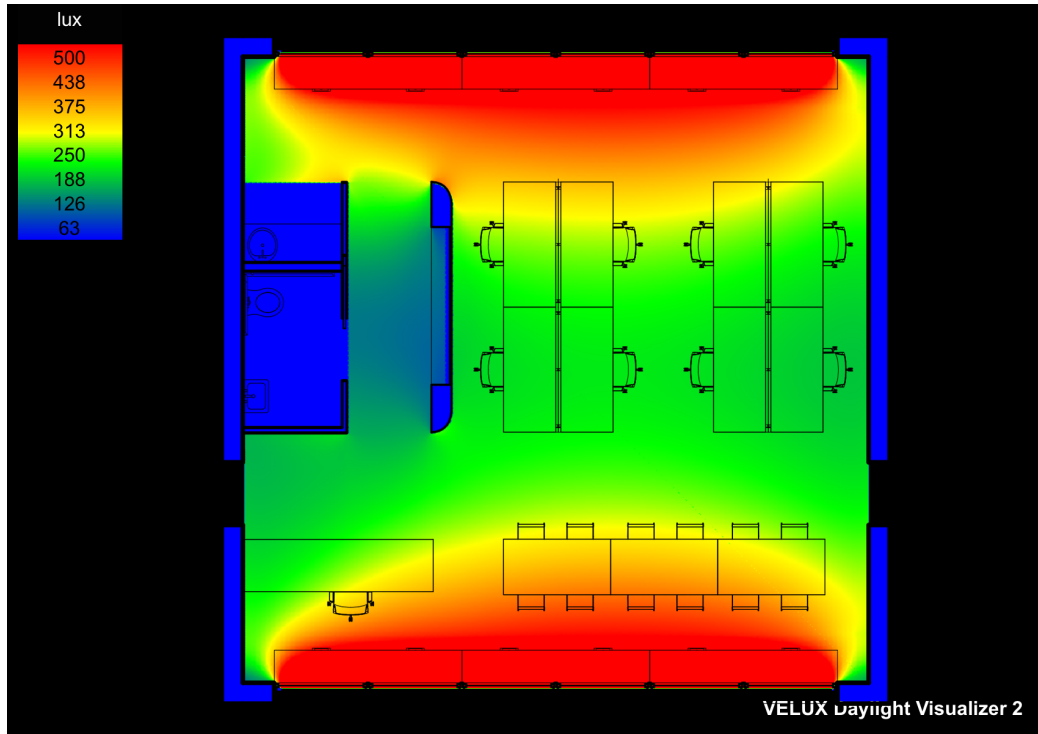


Figure 7.11. Daylighting for Atlanta Spring Noon Overcast Sky False Color Plan View in VELUX

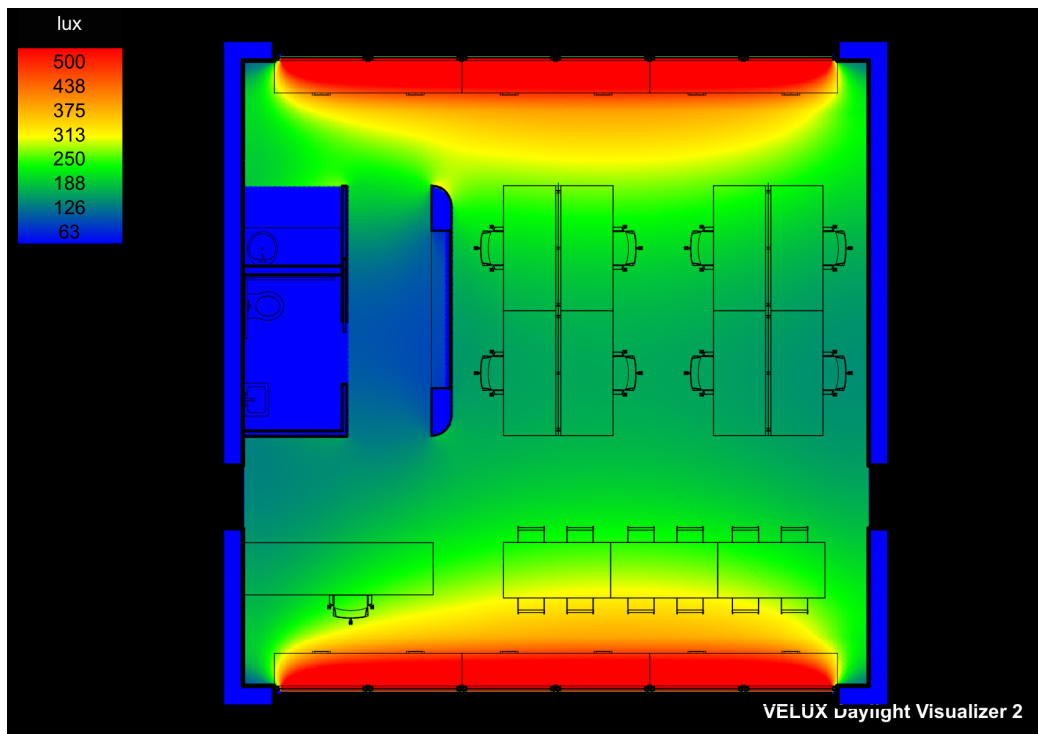


Figure 7.12. Daylighting for Atlanta Winter Noon Overcast Sky False Color Plan View in VELUX



Figure 7.13. Daylighting for Atlanta Summer Noon Overcast Sky North South Section View in VELUX



Figure 7.14. Daylighting for Atlanta Spring Noon Overcast Sky North South Section View in VELUX



Figure 7.15. Daylighting for Atlanta Winter Noon Overcast Sky North South Section View in VELUX

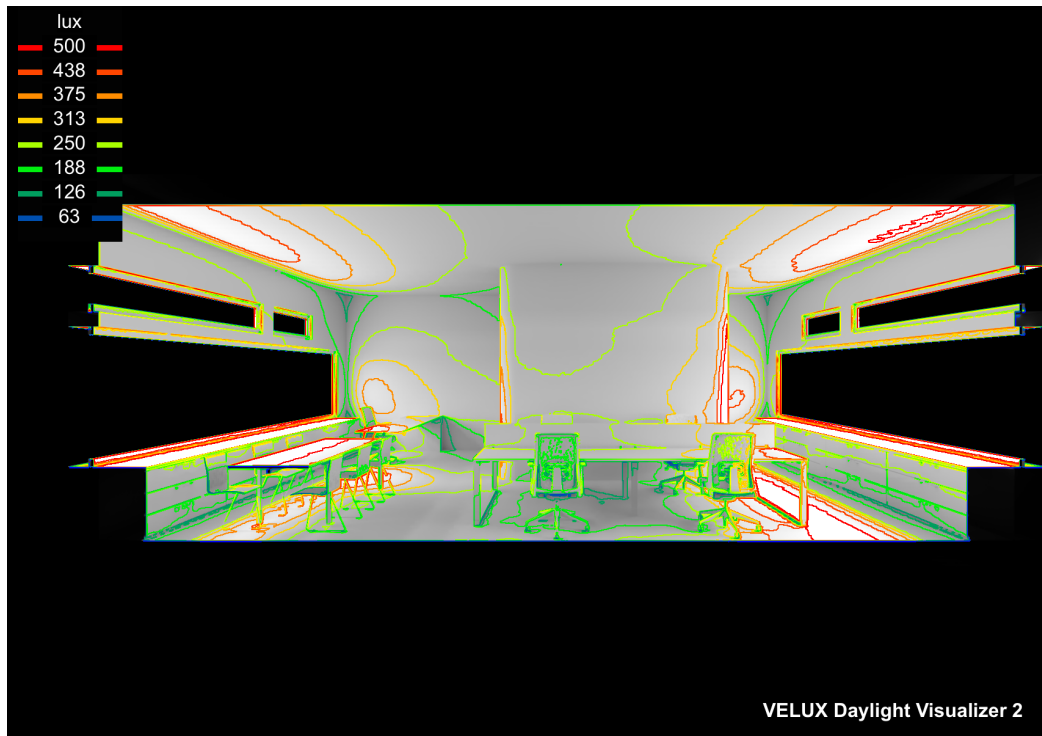


Figure 7.16. Daylighting for Atlanta Summer Noon Overcast Sky Iso Contour North South Section View in VELUX

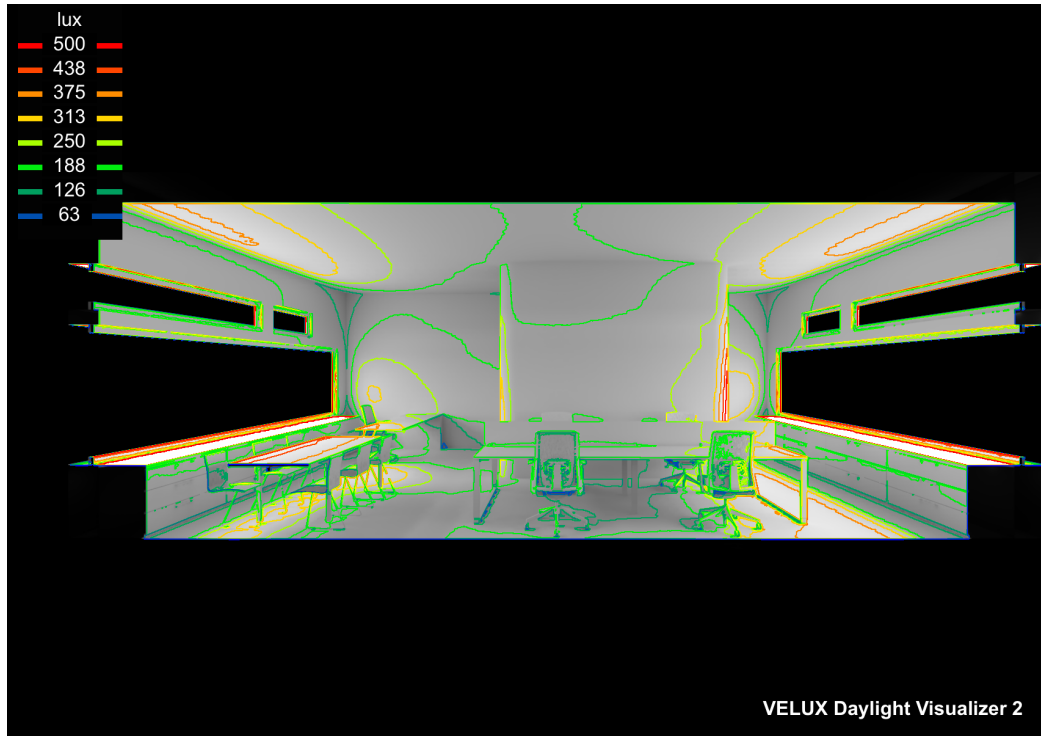


Figure 7.17. Daylighting for Atlanta Spring Noon Overcast Sky Iso Contour North South Section View in VELUX

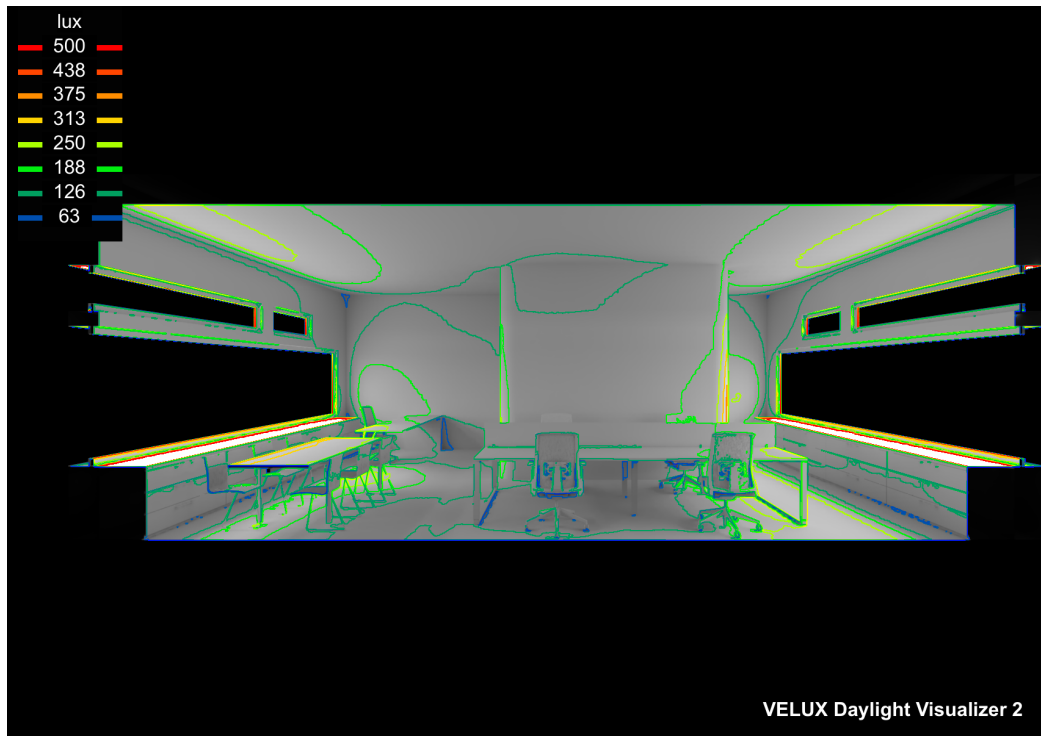


Figure 7.18. Daylighting for Atlanta Winter Noon Overcast Sky Iso Contour North South Section View in VELUX

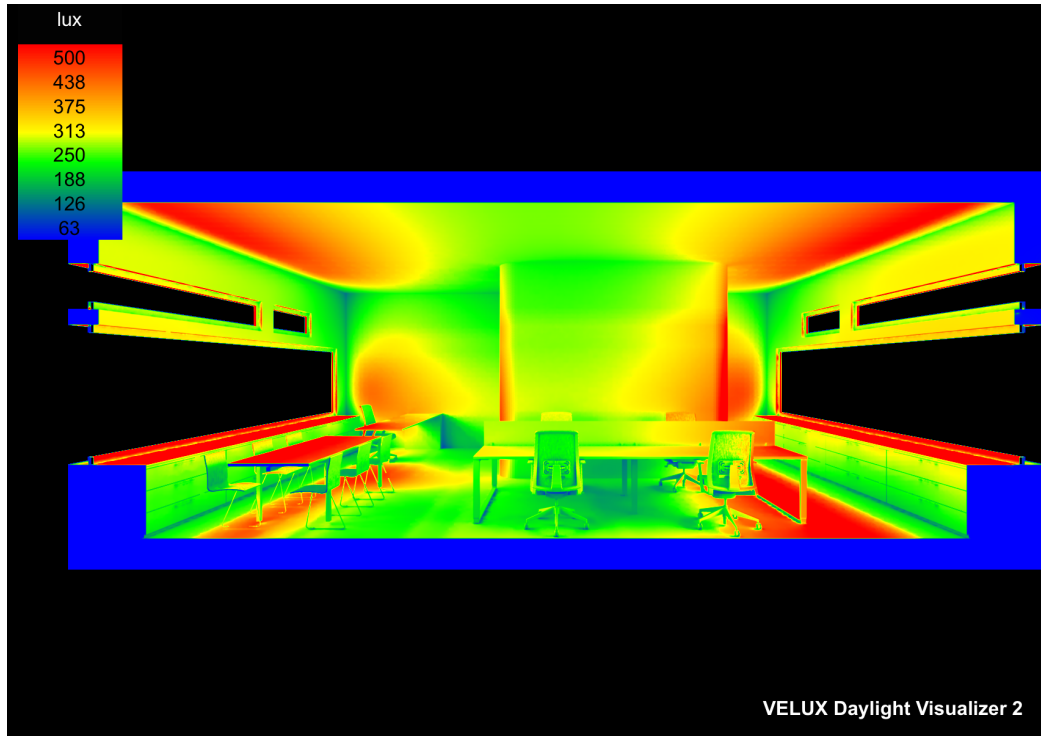


Figure 7.19. Daylighting for Atlanta Summer Noon Overcast Sky False Color North South Section View in VELUX

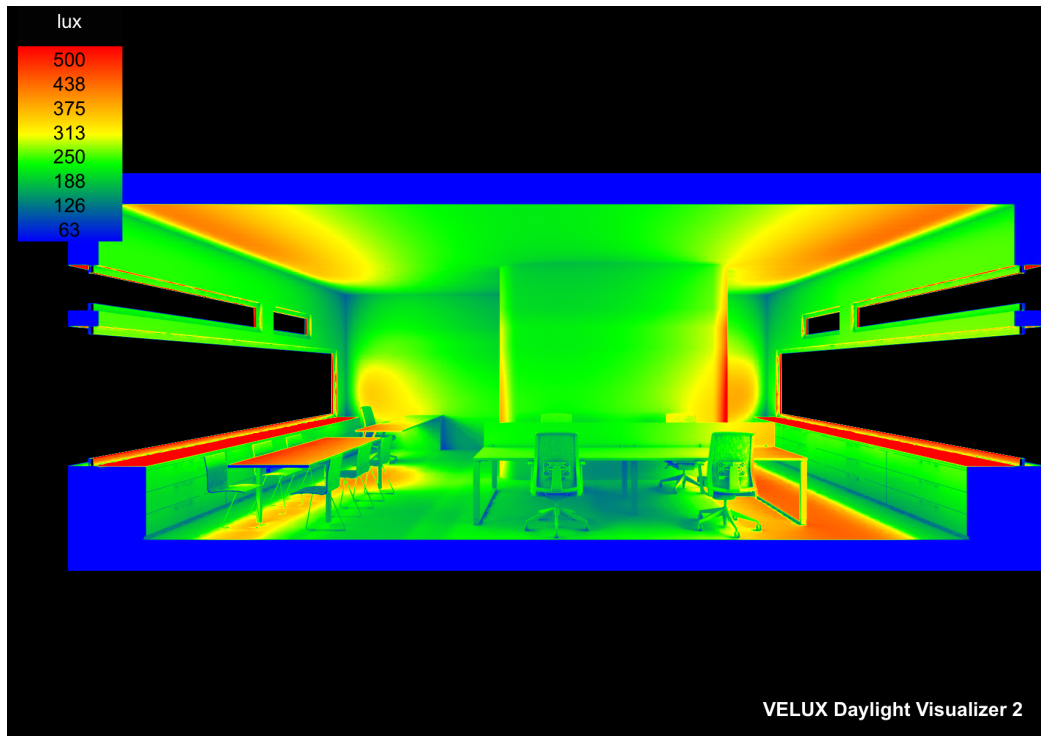


Figure 7.20. Daylighting for Atlanta Spring Noon Overcast Sky False Color North South Section View in VELUX

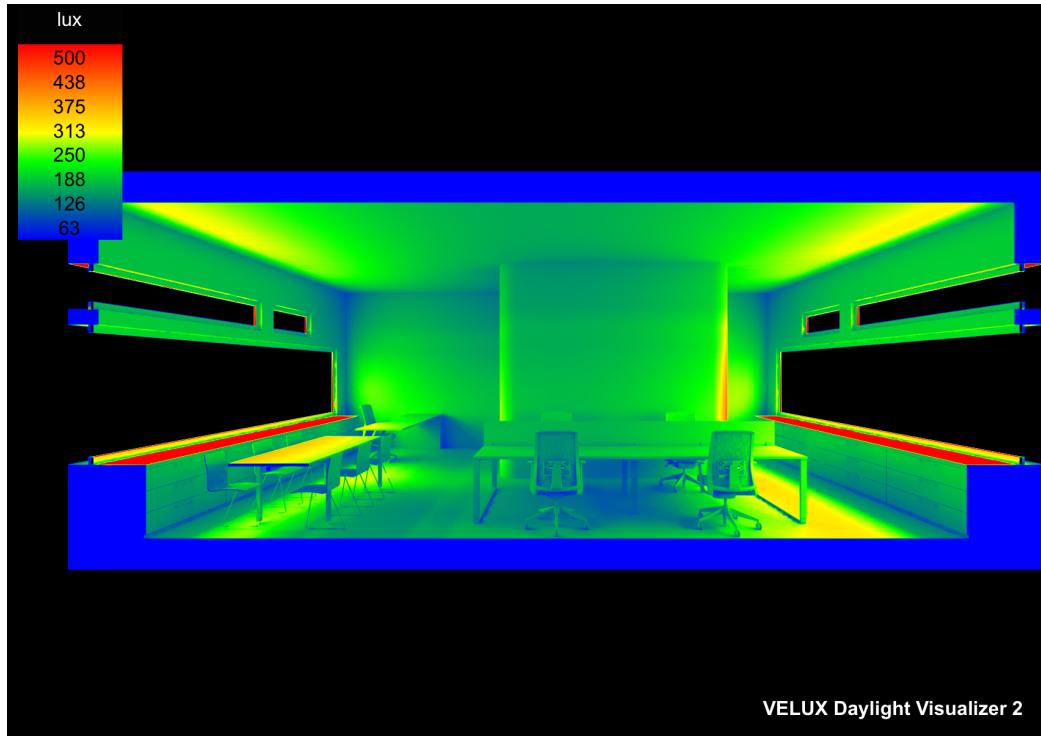


Figure 7.21. Daylighting for Atlanta Winter Noon Overcast Sky False Color North South Section View in VELUX



Figure 7.22. Daylighting for Atlanta Summer Noon Overcast Sky East West Section View in VELUX



Figure 7.23. Daylighting for Atlanta Spring Noon Overcast Sky East West Section View in VELUX



Figure 7.24. Daylighting for Atlanta Winter Noon Overcast Sky East West Section View in VELUX

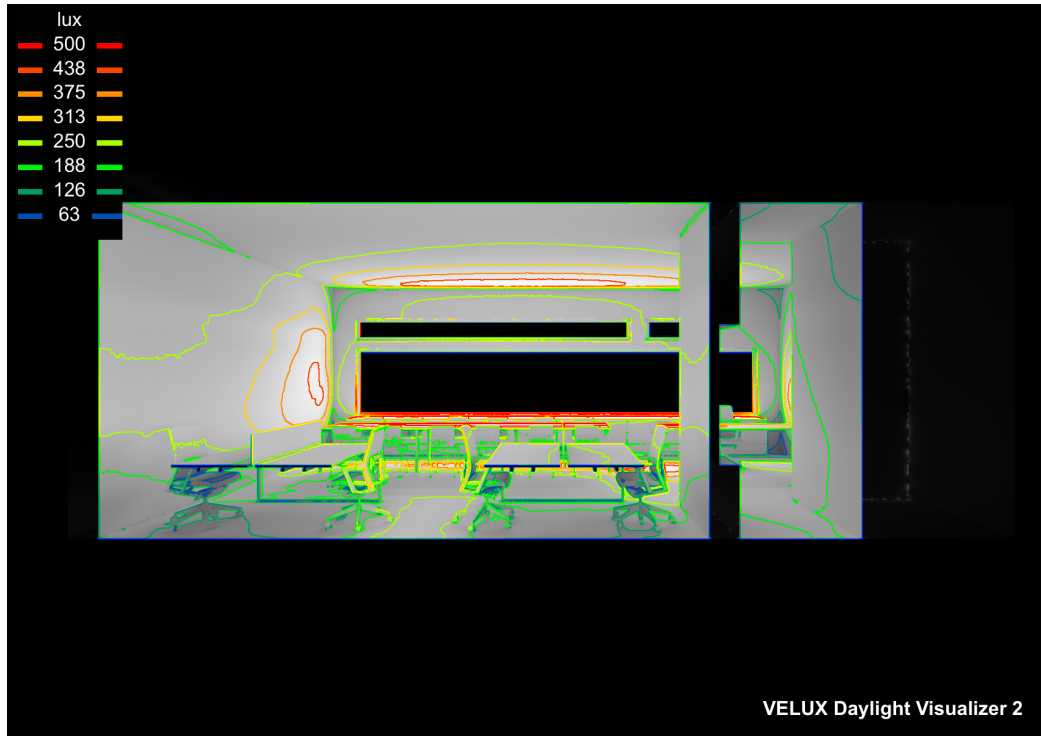


Figure 7.25. Daylighting for Atlanta Summer Noon Overcast Sky Iso Contour East West Section View in VELUX

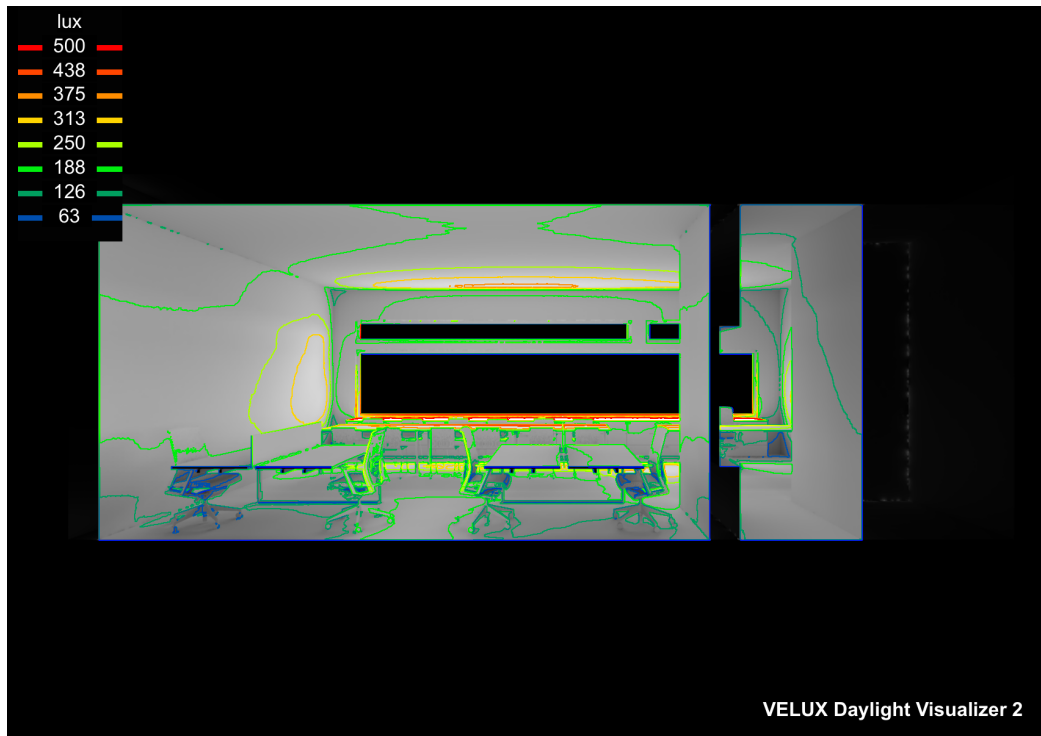


Figure 7.26. Daylighting for Atlanta Spring Noon Overcast Sky Iso Contour East West Section View in VELUX

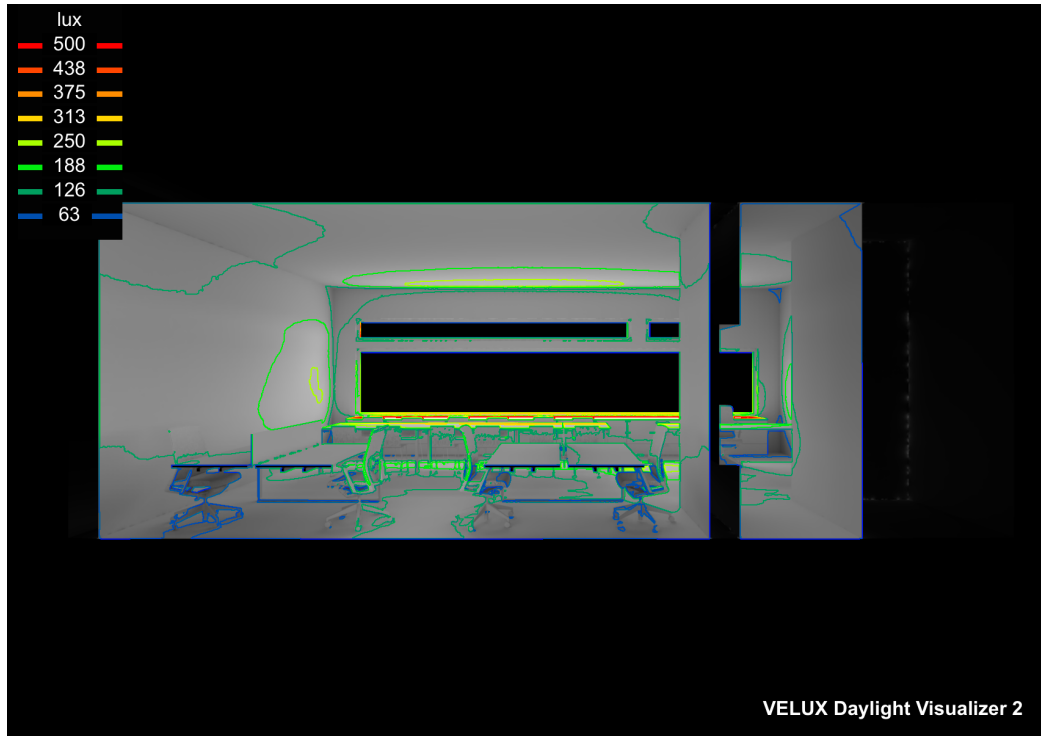


Figure 7.27. Daylighting for Atlanta Winter Noon Overcast Sky Iso Contour East West Section View in VELUX

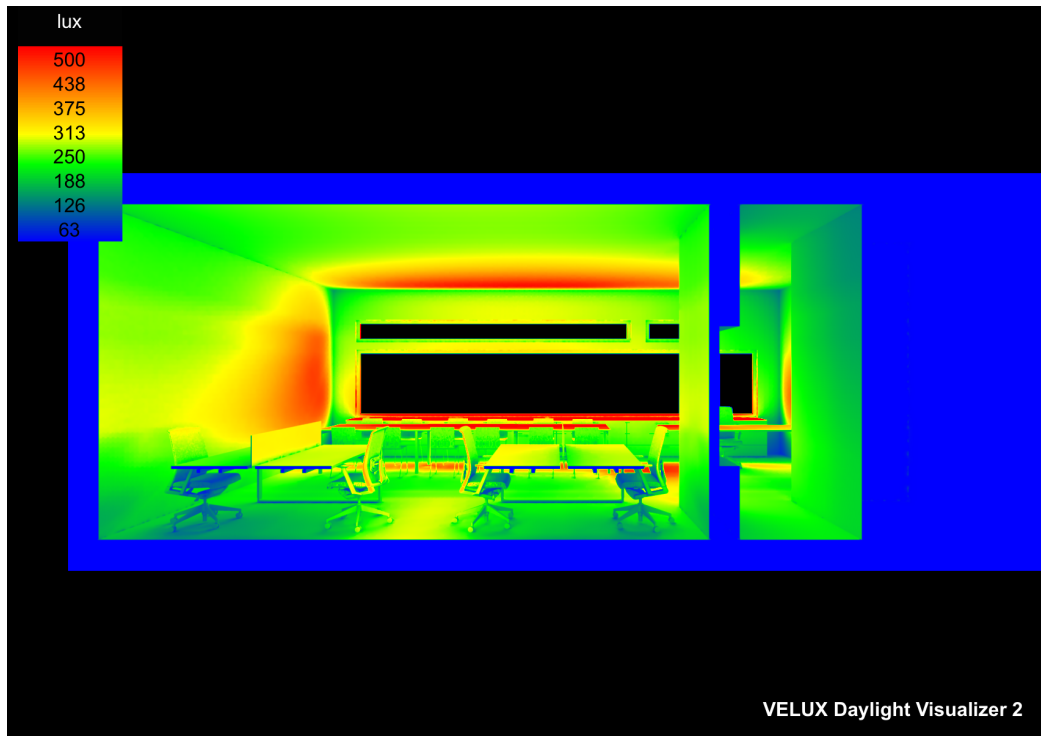


Figure 7.28. Daylighting for Atlanta Summer Noon Overcast Sky False Color East West Section View in VELUX

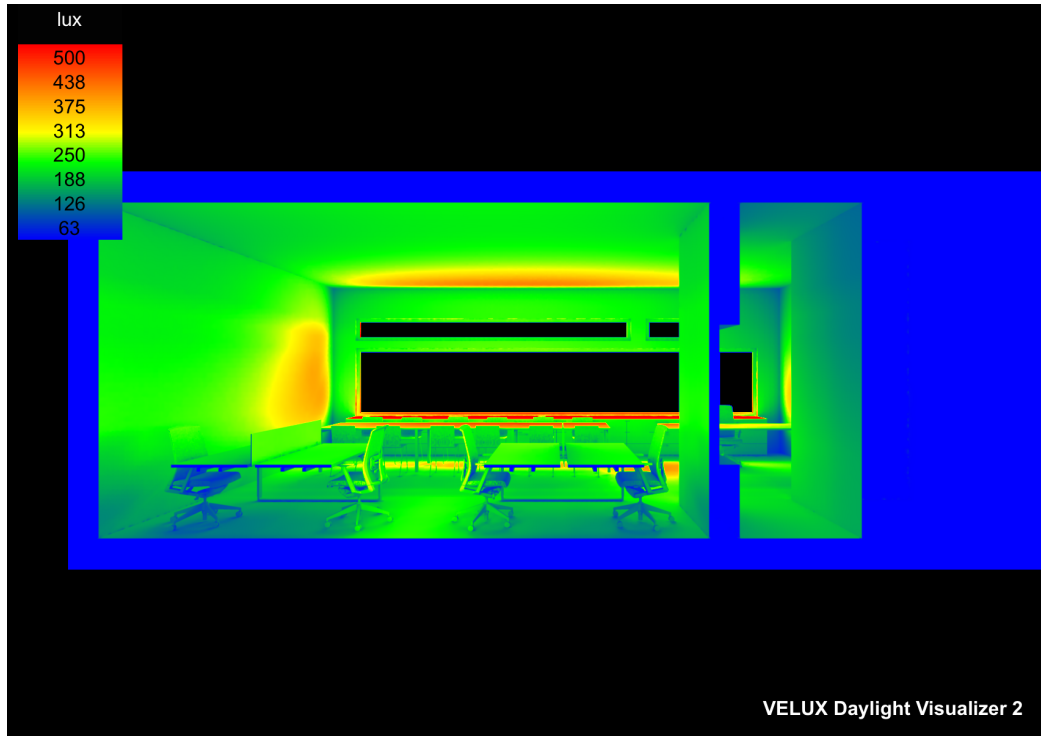


Figure 7.29. Daylighting for Atlanta Spring Noon Overcast Sky False Color East West Section View in VELUX

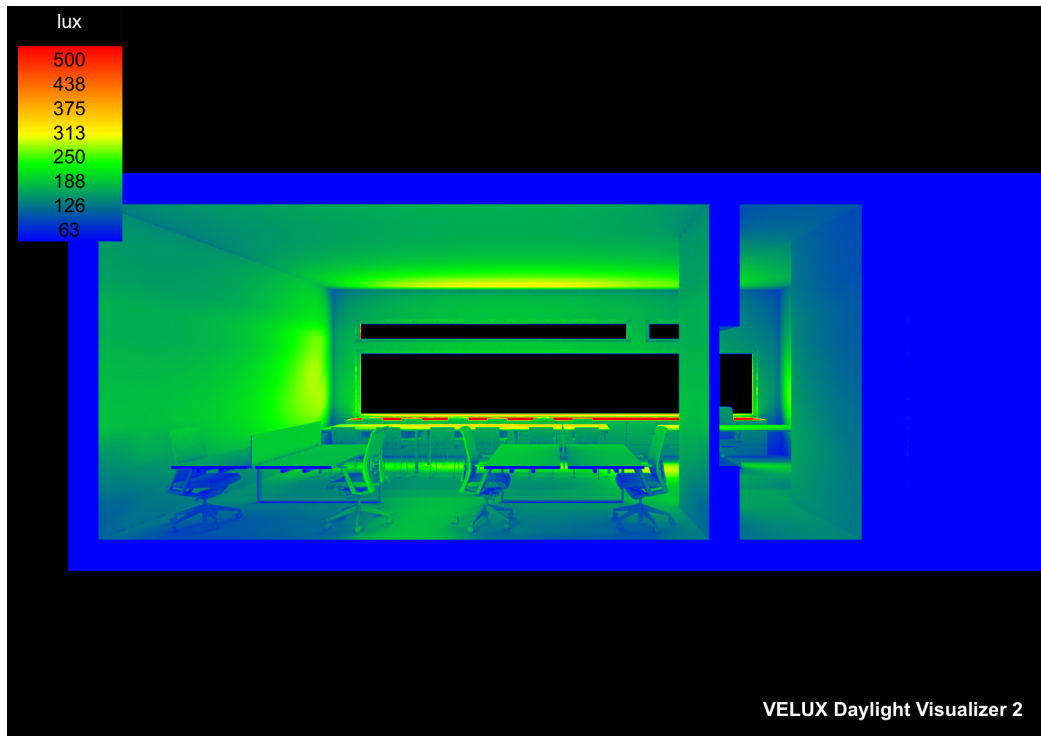


Figure 7.30. Daylighting for Atlanta Winter Noon Overcast Sky False Color East West Section View in VELUX



Figure 7.31. Daylighting for Atlanta Summer Noon Overcast Sky Perspective View in VELUX



Figure 7.32. Daylighting for Atlanta Spring Noon Overcast Sky Perspective View in VELUX



Figure 7.33. Daylighting for Atlanta Winter Noon Overcast Sky Perspective View in VELUX

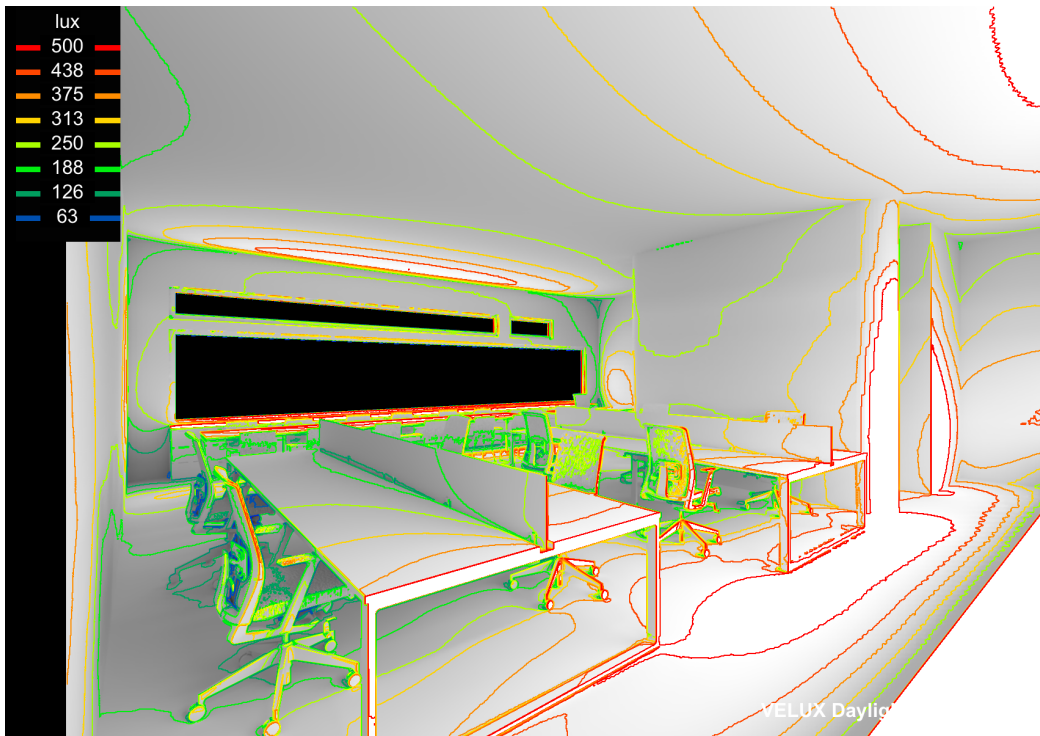


Figure 7.34. Daylighting for Atlanta Summer Noon Overcast Sky Iso Contour Perspective View in VELUX

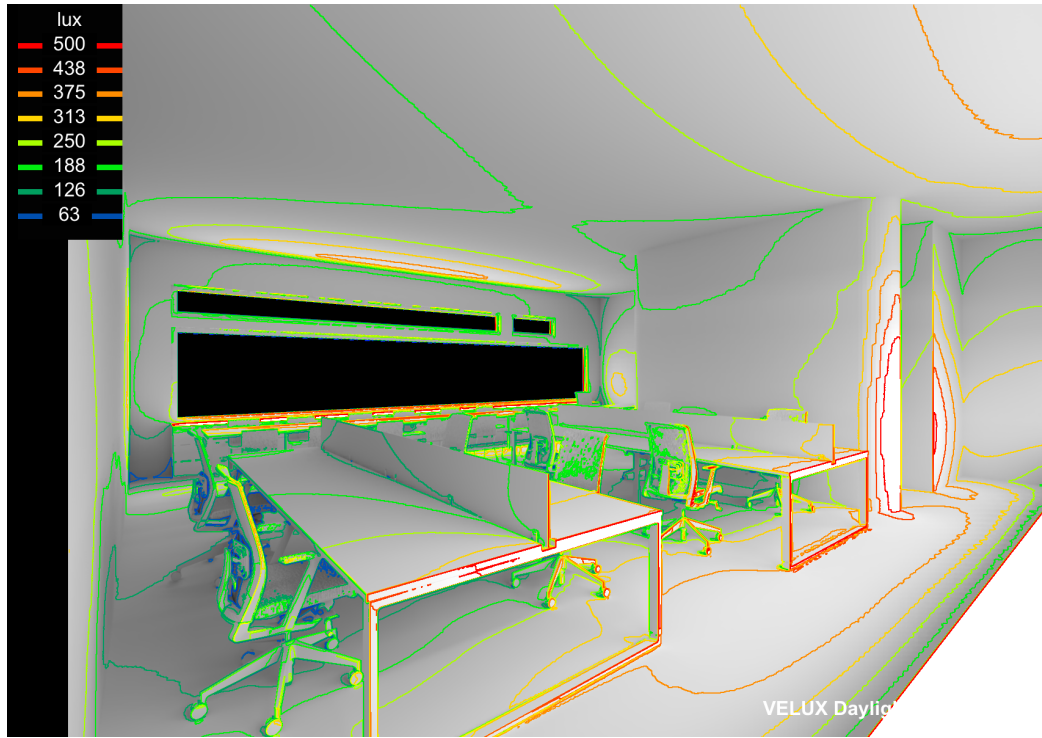


Figure 7.35. Daylighting for Atlanta Spring Noon Overcast Sky Iso Contour Perspective View in VELUX

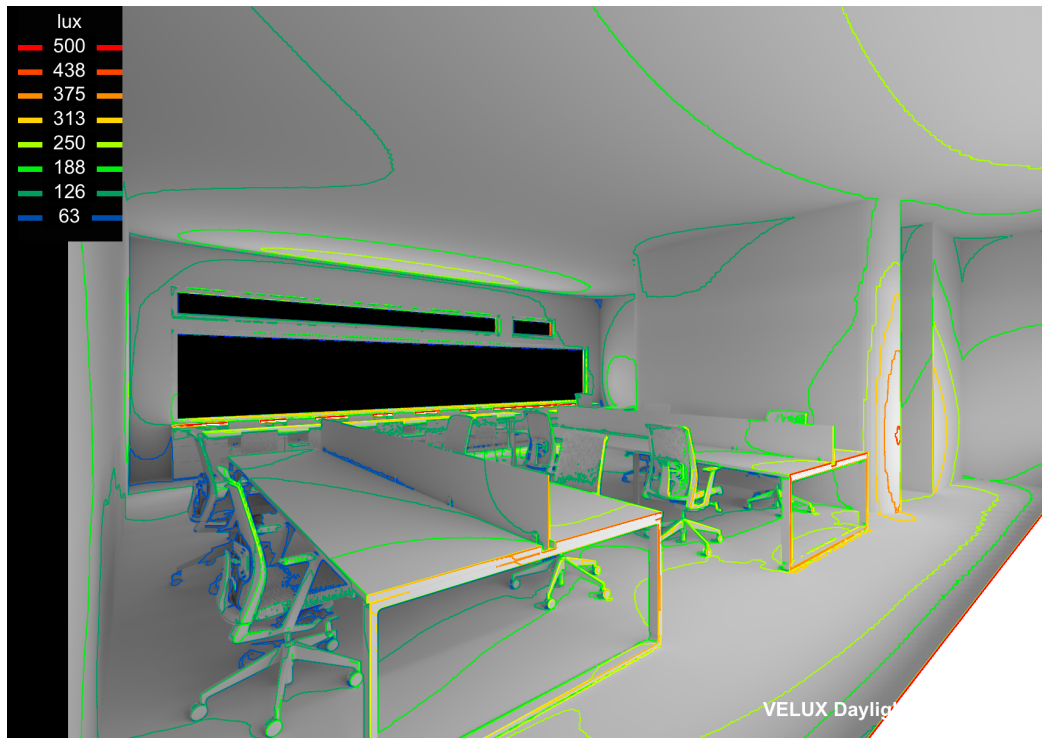


Figure 7.36. Daylighting for Atlanta Winter Noon Overcast Sky Iso Contour Perspective View in VELUX

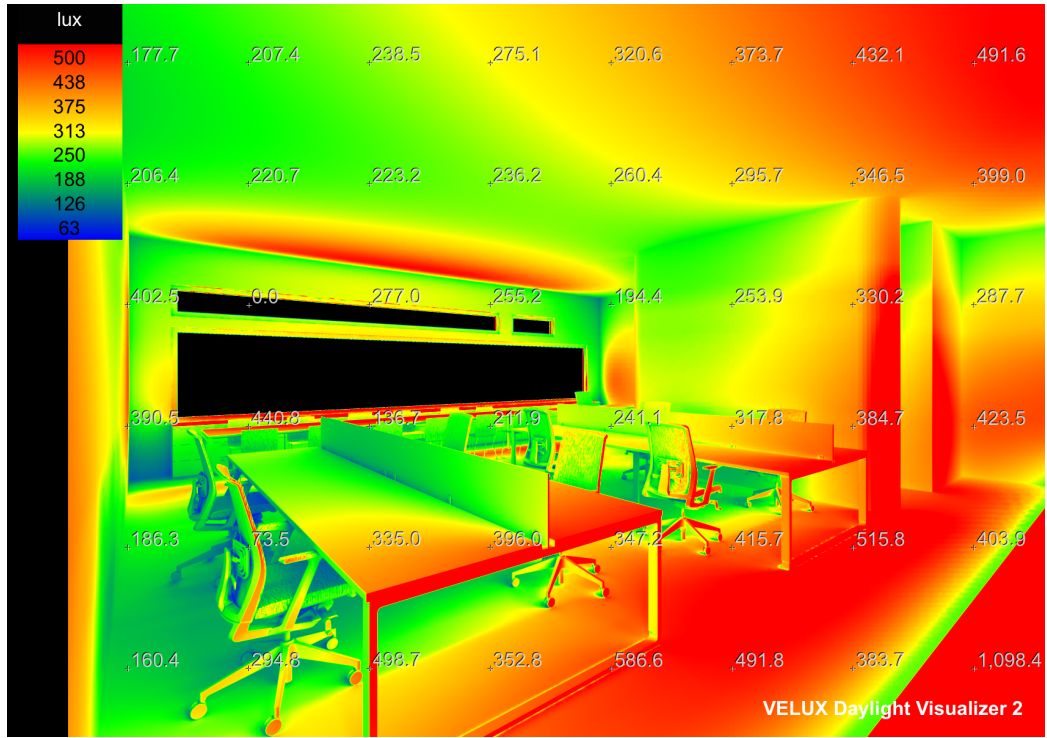


Figure 7.37. Daylighting for Atlanta Summer Noon Overcast Sky False Color Perspective View in VELUX

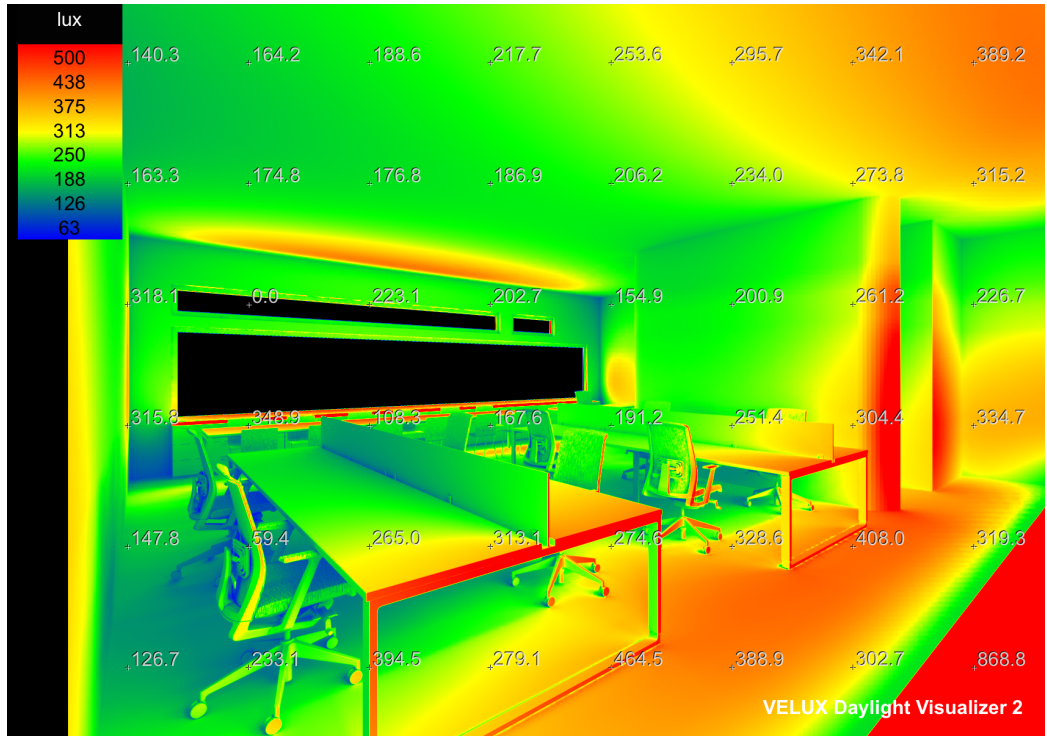


Figure 7.38. Daylighting for Atlanta Spring Noon Overcast Sky False Color Perspective View in VELUX

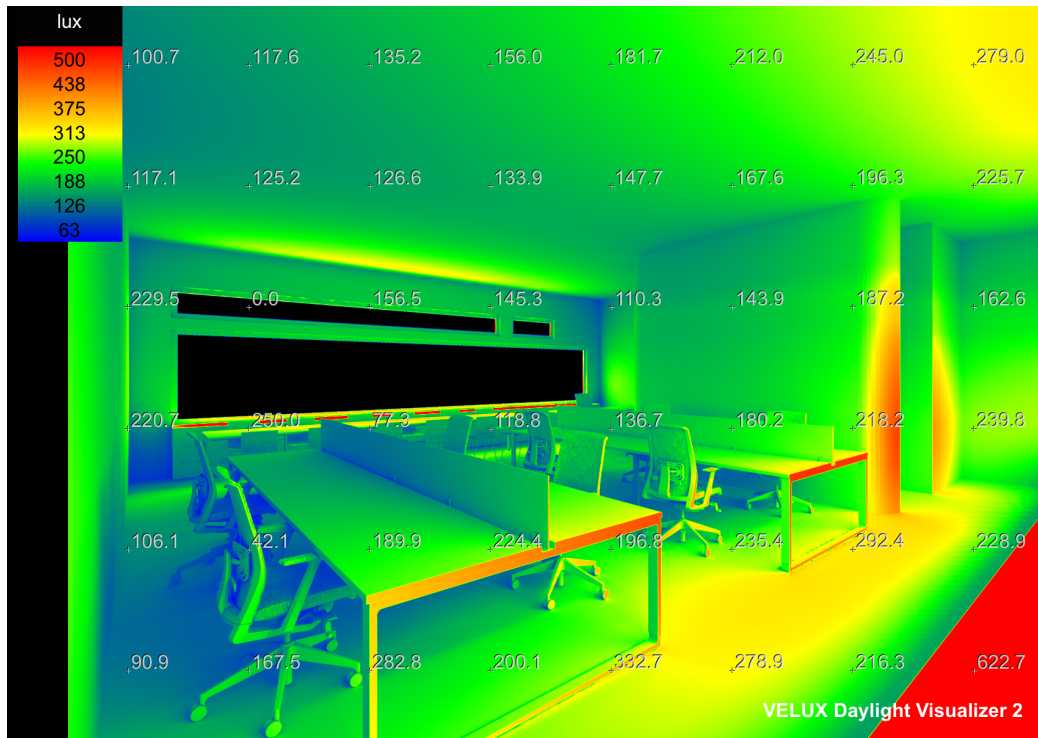


Figure 7.39. Daylighting for Atlanta Winter Noon Overcast Sky False Color Perspective View in VELUX

CHAPTER 8: SYSTEM

8.1 Direct Expansion Vapor Compression Refrigeration Air Conditioning System

Figure 8.1 shows layout and components of the direct expansion vapor compression system. The system moves refrigerant around a closed loop removing heat from outside air and feeding cool air into a space. The sketch describes the thermodynamic state of refrigerant as it cools and dehumidifies the warm outside air. Figure 8.2 and 8.3 show the thermodynamic state of the air stream in the vapor-compression refrigeration system. Numbers in 'RED' color show relationship between the diagrams. Outside air at state 0 mixes with return air at state 4. The mixed air stream enters the evaporator coil at state 5. The supply air is in direct contact with the evaporator. The cool dry air stream leaves evaporator at 55 °F and 50% relative humidity at state 1. The mechanical system warms and slightly humidifies the air temperature to 74 °F with near constant relative humidity coinciding with state 2 or the conditioned space. The supply air and recirculation air mixes, warms, and humidifies in the conditioned space as represented by line segment from state 3 to 4 in Figure 8.3. A fan draws air from the conditioned space to state 4. The process repeats with outside air at state 0 entering the mixing box. The system here provides a simpler case for heat transfer by refrigerant from fresh air than more complex systems that where air flows over intermediate fluid; the fluid or chilled water then flows over the evaporator of a chiller.

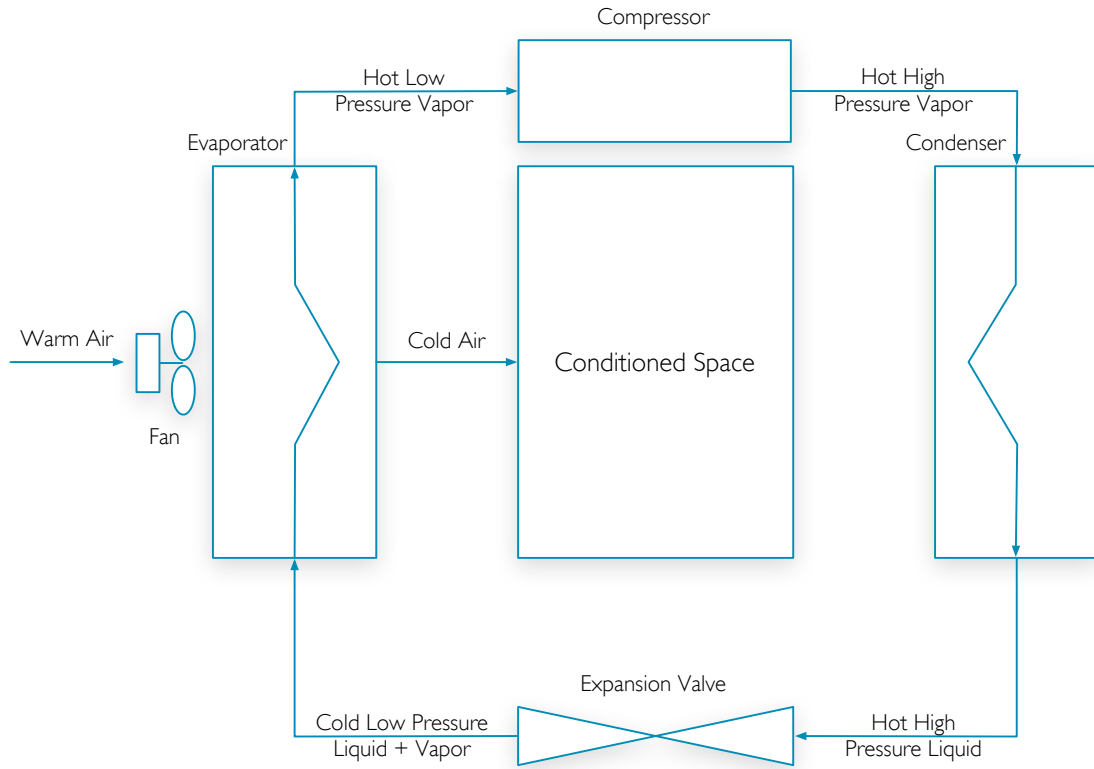


Figure 8.1. Direct Expansion Vapor Compression Refrigeration System Sketch, Derived from[30]

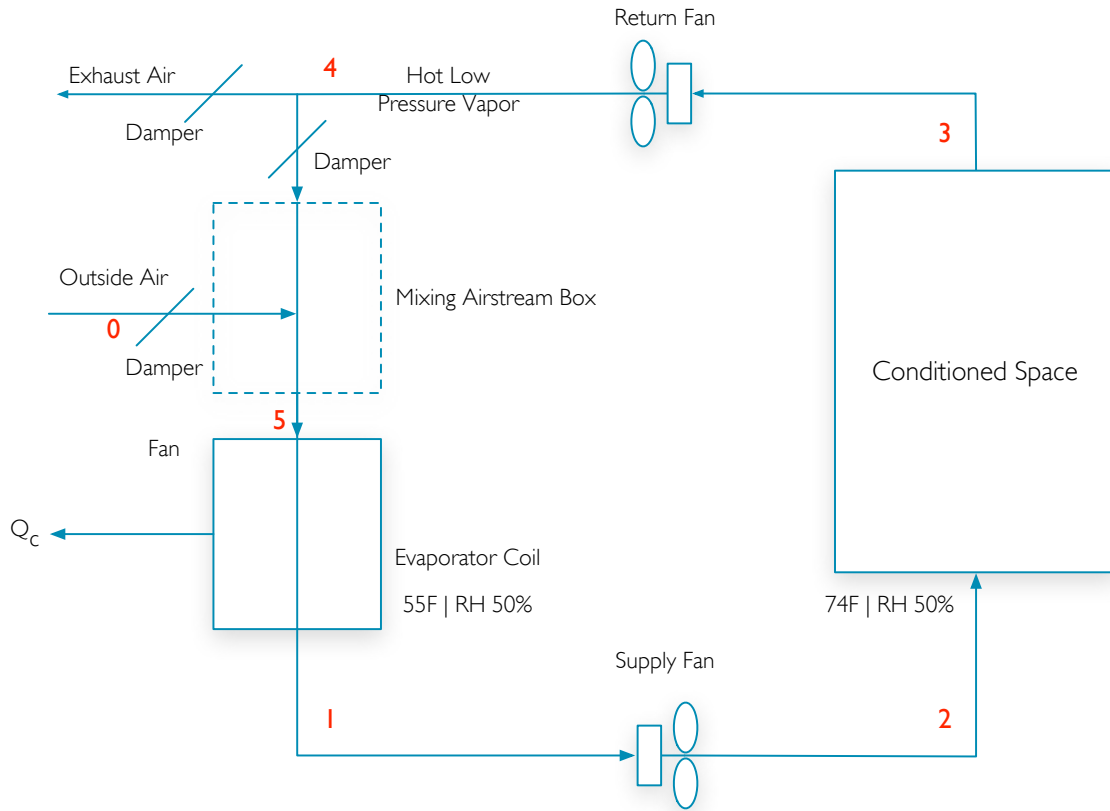


Figure 8.2. Building Air Conditioning Process Sketch, Derived from [30]

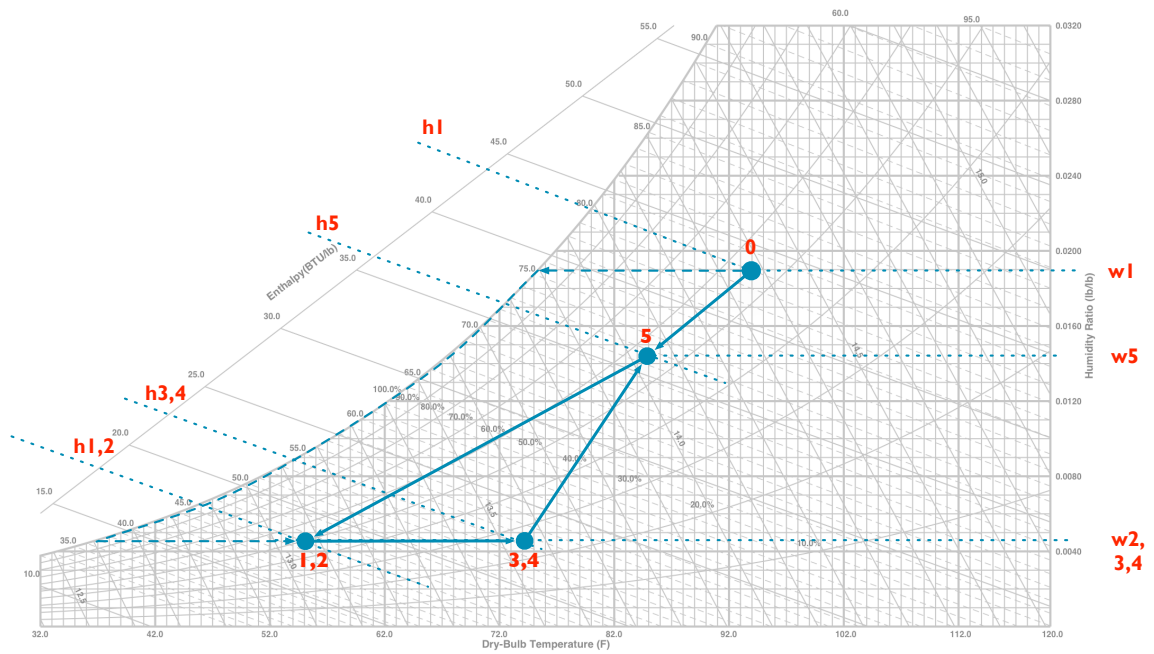


Figure 8.3. Direct Expansion Vapor Compression Refrigeration Process Psychrometric Chart

8.2 Thermo-hygroscopic Solar Liquid Desiccant Air Conditioning System

The thesis explores a design space for different plan configuration and facade orientation for the thermo-hygroscopic building envelope. A dashed line represents the location for the thermo-hygroscopic building envelope. Figure 8.4 and 8.4 show plan sketches of different arrangements of length and width for different stair and elevator core arrangements. For design option 'A,' the plan shows the thermo-hygroscopic envelope on the south facade. Design option 'B' shows the thermo-hygroscopic envelope on north and south facade. Figure 8.6, 8.7, and 8.8 show section sketches of the plan configurations and solar access for liquid desiccant solar regenerator. The $X = Y$ plan configuration refer to length and width dimensions for external core on either the west or east side offers improvement for daylighting and views. Solar liquid desiccant regenerators use incline to direct flow downward by gravity to desiccant dehumidifier. The regenerator panel requires an appropriate tilt angle and orientation as close to true south with least amount of shading from site elements or self-shading by building. Figure 8.6 shows single sided options for thermo-hygroscopic envelope facing south with unobstructed access to sun improves liquid desiccant regeneration. Figure 8.7 shows dual sided options for thermo-hygroscopic envelope facing north and south. North facing envelopes do not align with true south. A different configuration to regenerator liquid desiccant moves the regenerator further away from dehumidifier components to overcome building self-shading on north facade. Figure 8.8 shows dual sided option for thermo-hygroscopic envelope facing east and west. The configuration in this option allows building self-shading to affect fixed solar regenerators units from changing sun path. The design space study informs the development of the thesis.

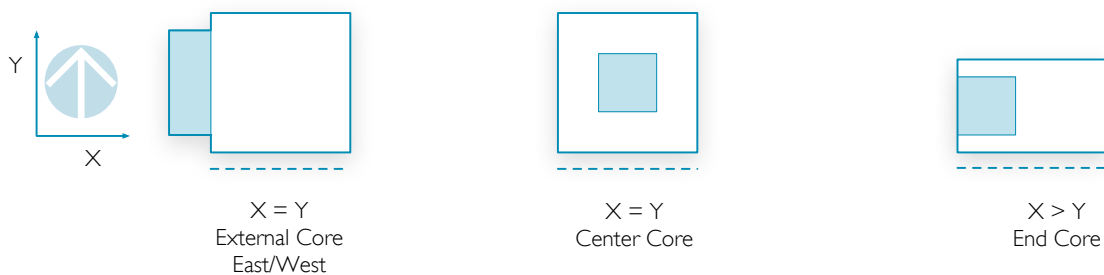


Figure 8.4. Plan Sketch of South Thermal-hygroscopic Envelope Design Option A

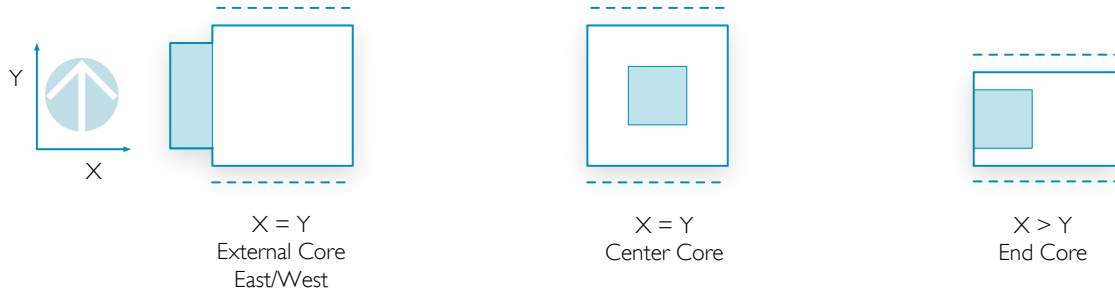


Figure 8.5. Plan Sketch of North and South Thermal-hygroscopic Envelope Design Option B

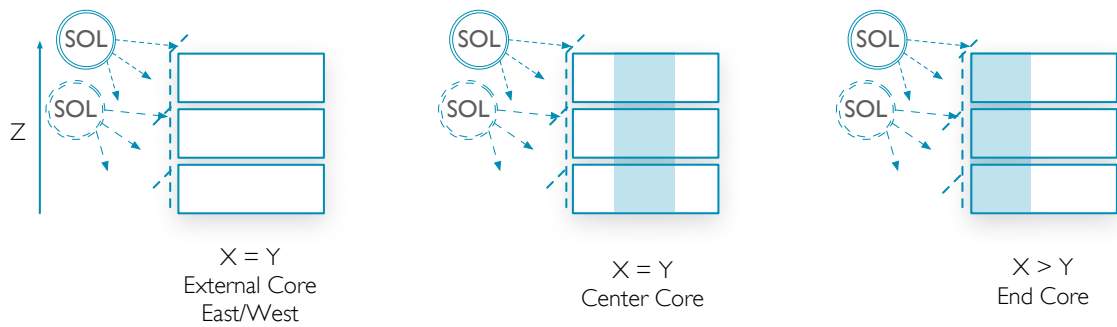


Figure 8.6. Section Sketch of South Thermal-hygroscopic Envelope Design Option A

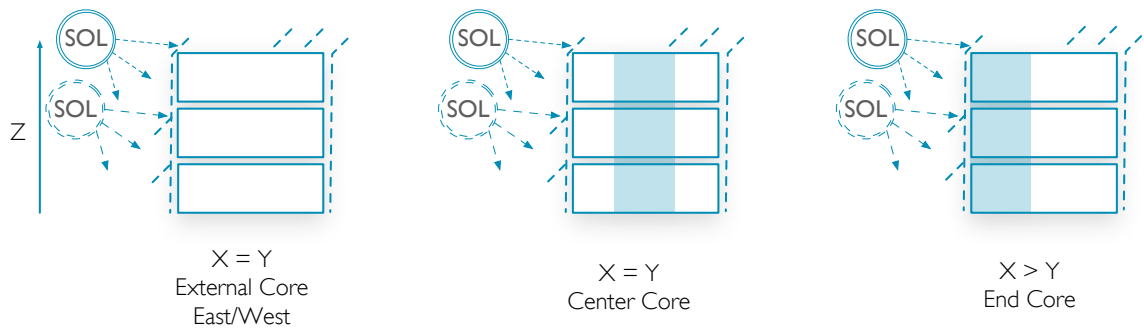


Figure 8.7. Section Sketch of North and South Thermal-hygroscopic Envelope Design Option B

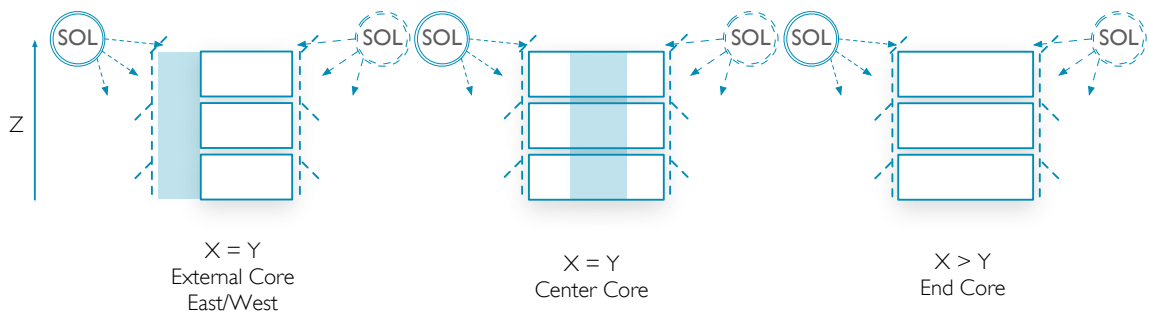


Figure 8.8. Section Sketch of East and West Thermal-hygroscopic Envelope Design Option

The thermo-hygroscopic building envelope decouples sensible and latent heat energy removal through an all airside ventilation system and water side cooling and heating system. The system uses hydronic cooling, heating radiant ceiling panels for sensible energy loads, and solar liquid desiccant air conditioning system for latent energy loads. Radiant ceiling panels use chilled water to transfer heat by radiation and convection. The work is similar to a system proposed by Yin et al for their liquid desiccant dehumidification radiant cooling system[31][32]. The system uses similar components including solar regenerator, dehumidifier, direct evaporative cooler, and radiant cooling dehumidifier ventilation units. However, the thesis system differs by an additional dehumidifier and configuration of these components within the building envelope. Figures 8.9, 8.10, and 8.12 shows a re-imagining of the system within the building envelope.

Radiant ceiling panels circulate chilled water through small tubing to remove sensible heat energy. To prevent condensation issues chilled water must be above ambient dew point usually between 55°F and 60°F. The higher chilled water and room temperature reduces temperature differential to 19°F and 14°F. Radiant ceiling panels take dehumidified air from liquid desiccant system through separate diffuser from ceiling mounted units for further cooling. The design requires less than one air changes per hour, which is within capacity of radiant ceiling system. Higher chilled water operating temperature reduces pump size and parasitic energy. Chapter 1 of the thesis discusses issues with CFC and HCFC refrigerants. Direct expansion vapor compression refrigeration systems use a refrigerant with global warming and ozone depletion potential and energy to chill water[32]. The thesis system inspired by Yin et al chills supply water to radiant ceiling panels with a direct evaporative cooler to minimize reliance on refrigerants.

The spatial configuration purposely incorporates a small single thermal zone with ductless air volume. Bio-inspired articulated torrent flaps on the building envelope controls airflow rate by opening and closing. The flaps articulation is an inspired concept from the leaf cutting ants nest openings and prairie dogs burrow mounds. Outside air flows through articulated flaps into liquid desiccant dehumidifier. The Liquid desiccant flows from top to bottom of the dehumidifier perpendicular to air flows from bottom to top. The thermodynamic state of air drives the ventilation rate with supplemental fans. Air temperature varies throughout the system to remove sensible heat energy.

The solar liquid desiccant system removes latent heat energy. The hygroscopic building envelope is an integrated building solar liquid desiccant air conditioning system. The solar liquid desiccant air conditioning system delivers dry conditioned air to the compact office space. The separation of dehumidification or outdoor and recirculation

air is done to limit issues with air infiltration from crossing air streams and condensation issues through the building envelope. The system uses dry air to reduce the amount of supply air volume needed for ventilation from lower humidity ratio when compared with all-air single-stage vapor compression refrigeration[32]. Fan and flaps control amount air volume based on latent thermal loads. Less air volume and movement of dry air reduces fan size and parasitic energy. A gas heater regenerates the liquid desiccant in the solar regenerator for conditions that inhibit solar radiation.

The two systems do not remove sensible or latent energy loads primarily through convection. Lower air volumes from radiant ceilings and solar liquid desiccant dehumidification minimize air velocities within the same to minimize drafts.

The thesis organizes the primary components within the building envelope. Comparison of latent and sensible load of dehumidifying air for single stage vapor compression and solar liquid desiccant system is possible. The relative size of the units shown in Figures 8.9, 8.10, and 8.12 have the potential to work in thick building envelope.

Figure 8.11 shows a sketch of the psychrometric chart of the process for dehumidifying outside air for the system. The psychrometric chart corresponds to the system sketch. An inlet at the facade draws in outdoor air at state 0. Outdoor air temperature is **93.92 °F**. The fresh air indirectly cools by weak liquid desiccant from state 0 to 1. Fresh air at state 1 enters a mixing box. Fresh air at state 1 mixes with return air from direct evaporator at state 2 and cools in the mixing box. The supply air enters the liquid desiccant dehumidifier and leaves with lower enthalpy. The dehumidifier heats and dries the air from state 2 to 3 with constant enthalpy. The hot dry air leaving the dehumidifier cools with chiller water from state 3 to 4. The dry air-cools again indirectly from air leaving direct evaporative cooler cooler at state 2. A second dehumidifier heats and dries return air from state 5. The dry air leaving the second dehumidifier cools to state 6. A portion of the cool and dry air enters the conditioned space leaving state 6 while another enters the direct evaporator. The cool and dry air entering the direct evaporator passes over coils that deliver cooling water to radiant ceiling panels. The air leaves the direct evaporator at state 2 to mix with air at state 1. The process repeats with fresh air drawn into articulated flaps by differential air pressure to the mixing box at state 1.

The liquid desiccant system works as dehumidifier in the summer and as a humidifier in the winter. The process previously discussed in Chapter 7.5.1 discusses summer operation of the system. In the winter, the system runs in reverse to cool and humidify the fresh air shown in Figure 8.9 at state 4. The cool conditioned air indirectly

heats from water heat changer at state 5.

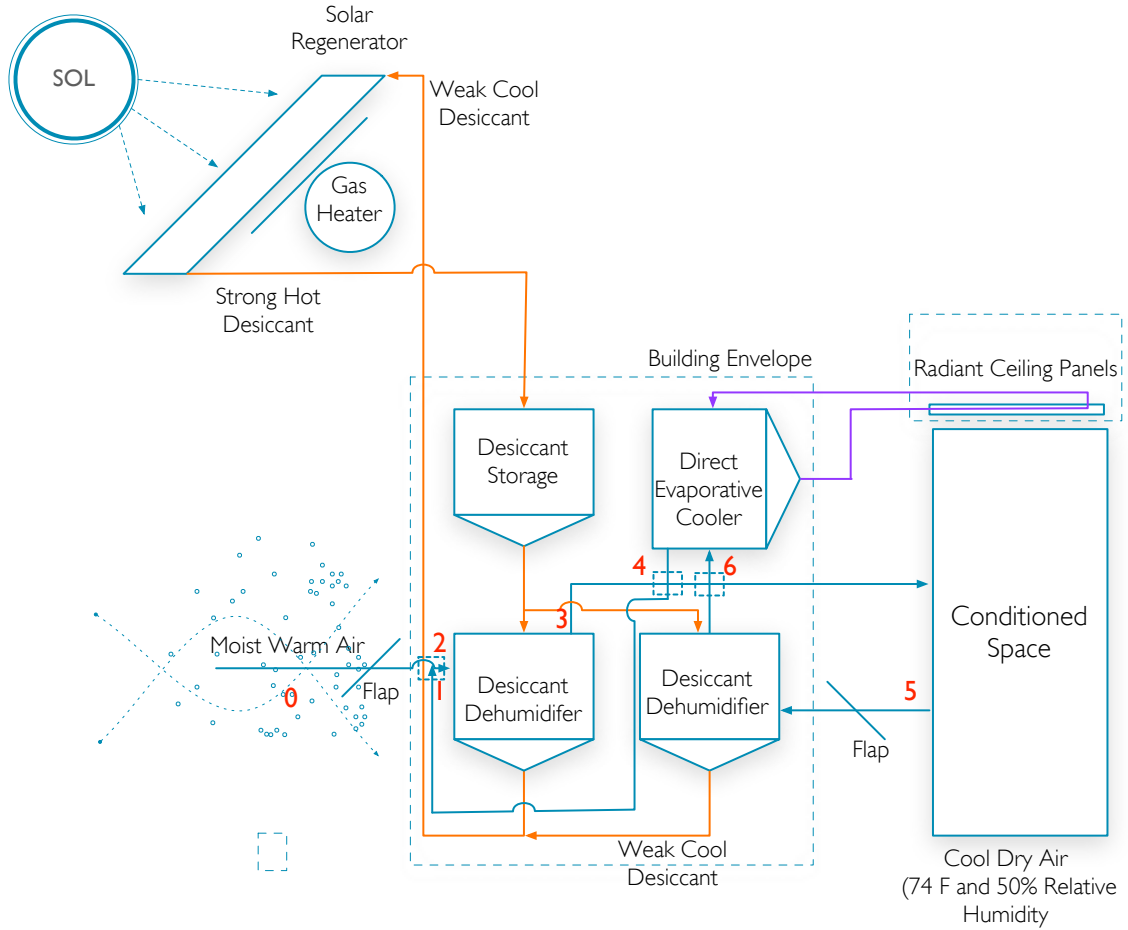


Figure 8.9. Solar Liquid Desiccant Air Conditioning Building Envelope System Sketch

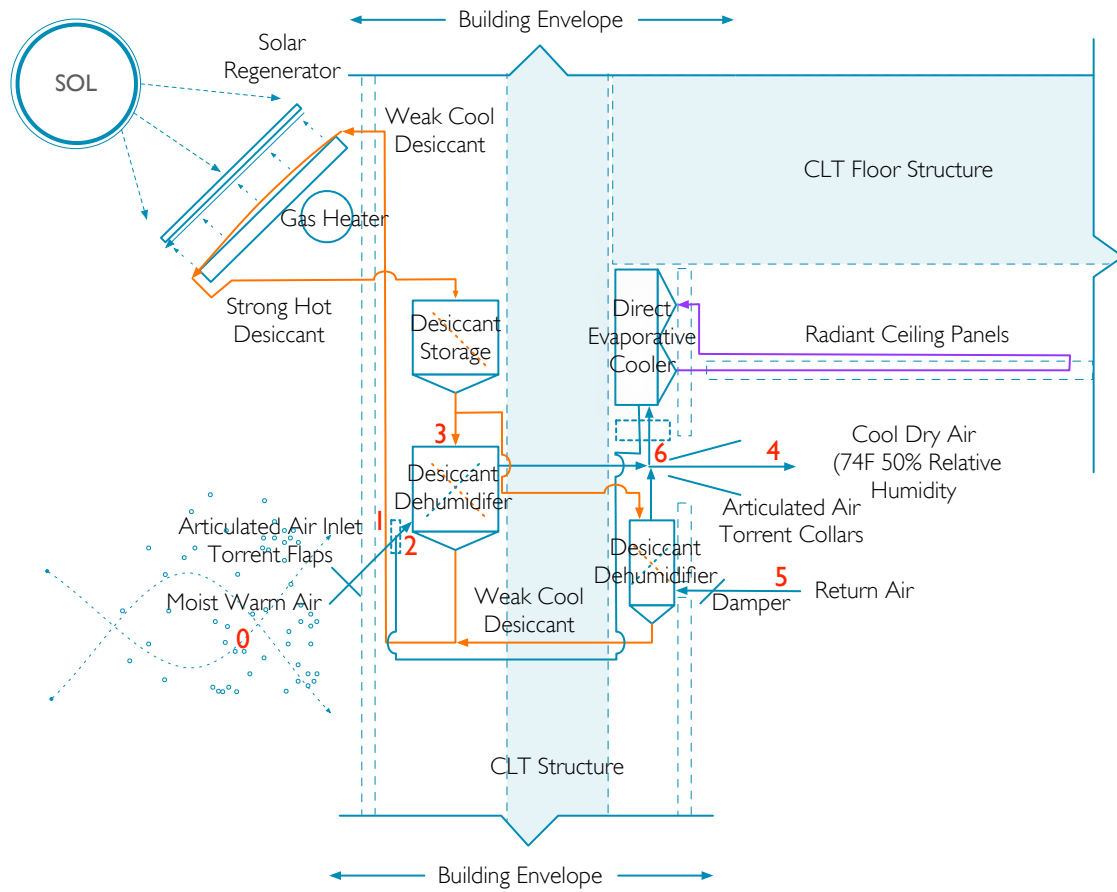


Figure 8.10. Solar Liquid Desiccant Air Conditioning Building Envelope System Sketch Detail

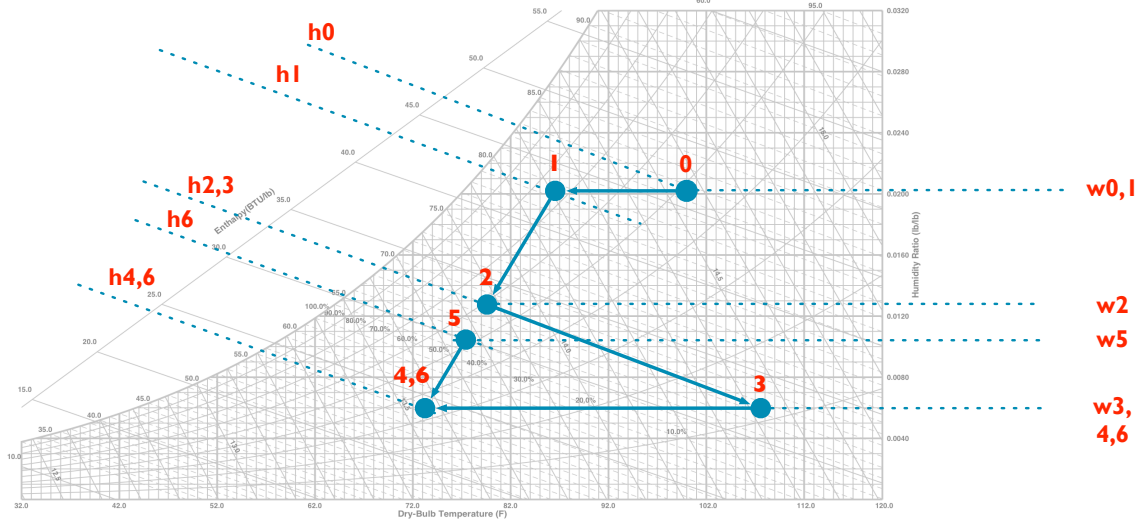


Figure 8.11. Air Conditioning Dehumidification Process in Psychrometric Chart for Thesis Liquid Desiccant System

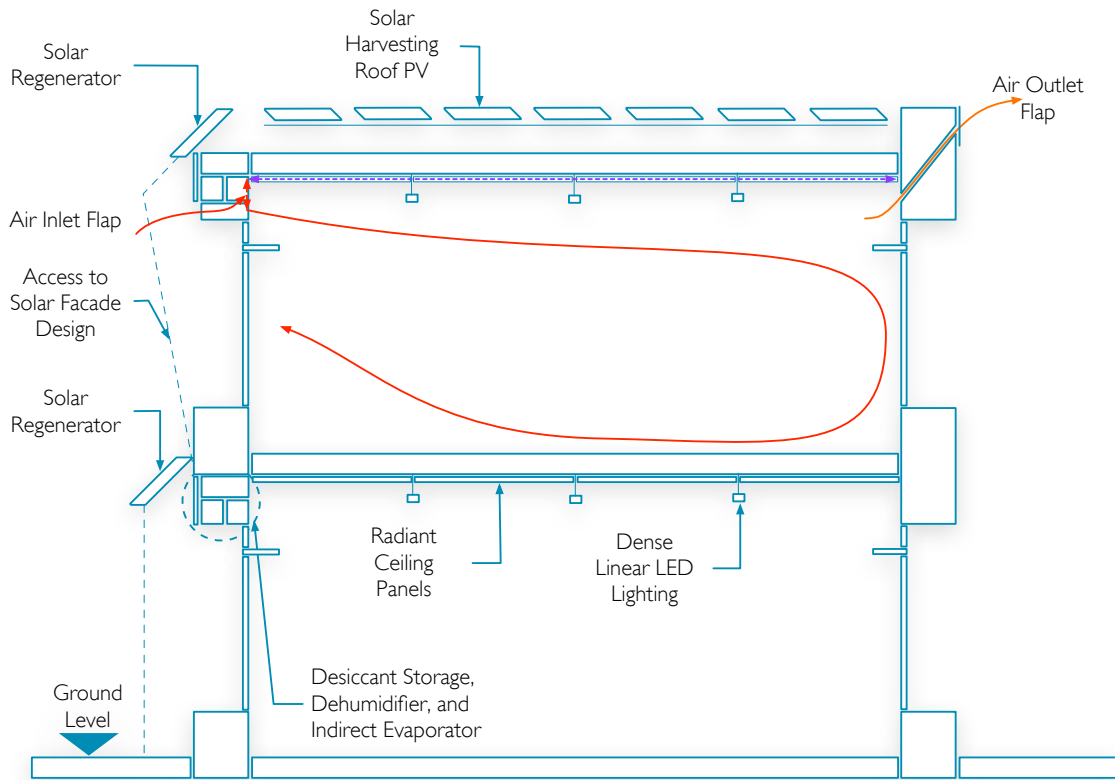


Figure 8.12. Solar Liquid Desiccant Air Conditioning Building Envelope Multi-Level Section Sketch

Table 8.1, 8.1, 8.1, 8.5, and Figure 8.13 show calculation of total heat removal for the thesis in the summer.

Assumptions for occupant load, ventilation requirement per person allow for calculation of a number of model data points. The heat transmission and solar gain from internal loads allows for computation of sensible and latent loads. Temperature states for outdoor air, conditioning of supply air; and office space air allow for plot on a psychrometric chart. The amount of supply ventilation, room ventilation is calculated. The total heat load allows for sizing of equipment to cool the space.

Table 8.1. Thermo-hygroscopic Model Data and Conditions for Summer Heat Load

Model Data	Value	Units
Prototype Floor Area	1,014.82	ft ²
Floor Area Per Person	50.00	ft ²
Number of Occupants	20.30	Persons
Ventilation Per Occupant	17.00	cubic feet minute/Person
Supply Air Temperature	55.00	°F
Room Dry Bulb Temperature	74.12	°F
Room Relative Humidity	50.00	%
Outdoor Temperature	93.92	°F
Delta T	19.12	°F
Window Area	317.85	ft ²
Wall Area	1,536.15	ft ²
Roof Area	1,024.00	ft ²

Table 8.2. Heat and Solar Gain Transmission from People, Lights, Equipment, Walls, Windows, and Roof

Space Gains	Value	Units
Sensible Load, Derived From	250.00	Btu/h
Latent Load, Derived From	200.00	Btu/h
Sensible Load for Office Equipment, Derived from[27]	0.80	Btu/hr · ft ²
Sensible Load Lights, Derived From[27]	2	Btu/hr · ft ²
Window Gains (Design Temp 100F °F), Derived From[27]	21.00	Btu/hr · ft ²
Wall Gains (Design Temp 100F °F, Derived From[27]	25.00	Btu/hr · ft ²
Roof Gain(Design Temp 100F °F, Derived From[27]	45.00	Btu/hr · ft ²

Table 8.3. Calculation of Amount of Cooling Needed for Prototype Model

Load Calculation		Loads	
Sensible	Sensible Heat · Number of Occupants	5,074.10	Btu/h
Latent	Latent Load · Number of Occupants	4,059.28	Btu/h
Sensible	Lights · Floor Area	2,029.64	Btu/h
Sensible	Equipment · Floor Area	811.856	Btu/h
Sensible	Heat Gains Window (Window/Floor Area) · Gain	6.58	Btu/h
Sensible	Heat Gains Walls(Walls/Floor Area) · Gain	37.84	Btu/h
Sensible	Heat Gains Roof (Roof/Floor Area) · Roof Gain	45.41	Btu/h
Sensible Total	Total Summer People and Internal Gains (Room Sensible Heat)	8,005.42	Btu/h
Latent Total	Total Summer People and Internal Gains (Room Latent Heat)	4,059.28	Btu/h
Calculation	Portion of Load Sensible Heat Factor (RSH/RSH+RLH)	0.66	
Calculation	Quantity of Air (RSH/1.1 Delta T) Needed to Cool Prototype	380.63	cfm
Calculation	Supply Air Volume (Occupants · cfm per Person)	345.04	cfm
Calculation	Outdoor Portion of Supply Air (Needed Air/Supply Air Volume)	91%	

Table 8.4. Heating Load on Cooling Equipment, Tons of Cooling Required Calculation

Notes	Total Heat Be Removed By Cooling Equipment	Value	Units
Psychrometric	h_2	20.4	Btu/lb
	h_4	41.7	Btu/lb
Calculation	$Q_t = 4.5 \cdot \text{cfm} \cdot (h_4 - h_2)$	33,071.97	Btu/h
	Tons of Cooling (1 ton = 12,000 Btu/h)	2.76	tons

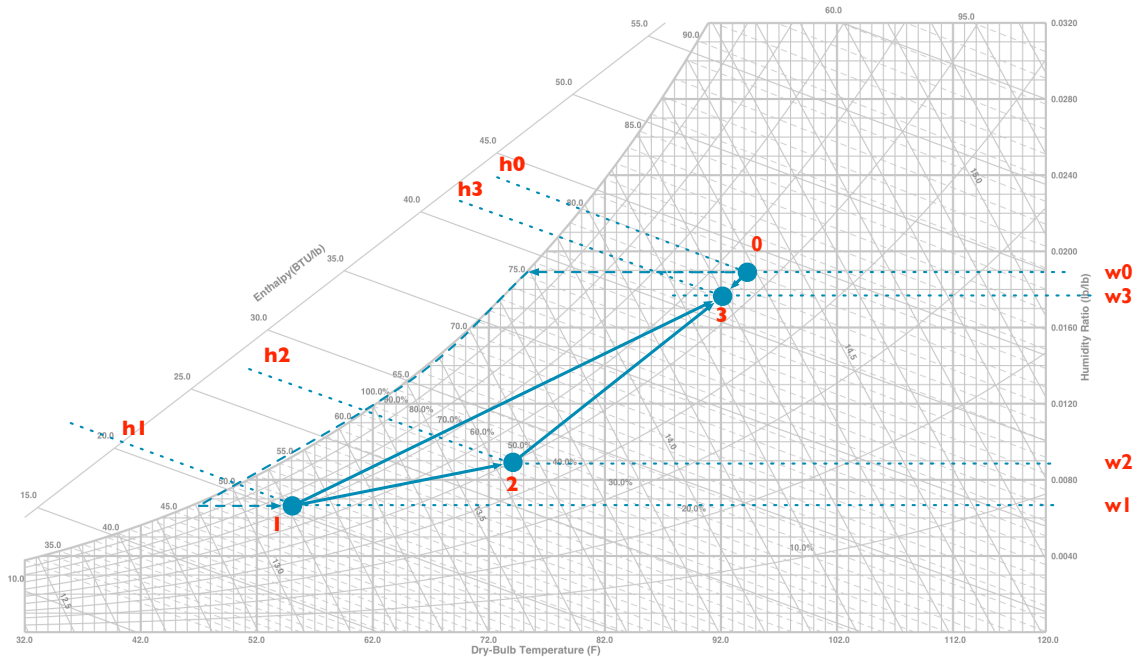


Figure 8.13. Psychrometric Chart for Plot of Tables 8.1, 8.2, 8.3, and 8.4 Calculations

Table 8.5. Psychrometric Data for Plot of Table 8.1, 8.2, 8.3, and 8.4

Point	Description
0	Room Dry Bulb Temperature
1	Supply Air Temperature
2	Outdoor Temperature
3	Calculated From Outdoor Portion Supply Air and Psychrometric Chart

CHAPTER 9: SYNTHESIS

9.1 Historical Implications

The historical implications for the thesis provide a working platform for further work that transfers characteristics to improve the speculative thermo-hygroscopic building envelope. Table 9.1 shows comparable performance criteria between the thermo-hygroscopic 'thick wall' and the earlier discussion of dewponds in Chapter 2.1.5. The list shows characteristics that are the same, similar, and different. The differences provide opportunity for making a change in an existing system to improve it in some way. The dewpond structurally decouples from the ground. The thermo-hygroscopic envelope decouples heat loads. Two seemingly divergent methods for water desorption provide application transfer. The strategy to decouple one of the components in the solar liquid desiccant system such as the regenerator from the dehumidifier at first may not make sense. Fresh air heats up as it dehumidifies in the dehumidifier. Chilled water coils remove the sensible heat from the supply air leaving the dehumidifier. The sensible heat from the air in the dehumidifier temperature can regenerate cold weak liquid desiccant. The energy savings, component reduction, and reduction of space in the 'thick' thermo-hygroscopic envelope improve the simplification of the system. Figure 9.2 provides similar opportunities for transfer applications to improve the feasibility of the thermo-hygroscopic envelope. Comparisons between the thermo-hygroscopic envelope and air well show differences in the mechanism for water generation. The air wells require low thermal lag response to maintain the condenser surface cool enough to work. Applying this characteristic to solar thermal liquid desiccant air conditioning systems could quicken the regeneration cycle from hot strong concentration to cool weak concentration. A faster regeneration cycle improves dehumidification performance without added energy input. The two examples for list as a tool can drive the decision making process for transferable performance criteria to improve the thesis thermo-hygroscopic envelope.

9.2 Biological Inspiration Implications

Bio-inspired analysis follows similar process the thesis takes for comparing historical implications. The process requires knowledge of analogues and systems for comparison. The thesis work involves research, diagram making, and development of the comparative analysis. There are mechanisms in the historical references and biological references that delineate obvious improvements to those that differ too greatly for incorporation. Figures 9.3 and 9.4 show a range of divergence and convergence mechanisms between thermo-hygroscopic

Table 9.1. Thermo-hygroscopic Envelope and Dewponds

Performance Criteria	Thermo-hygroscopic Envelope	Comparison	Dewponds
Condensing Mechanism	Contact with Ambient Air	Same	Contact with Ambient Air
Regenerative Function	Regeneration	Same	Regeneration
Regeneration Mechanism	Heating	Same	Drying
Condensing Constraints	Short Time	Different	Long Time
Condensing Surface Area	Large /Thin Falling Film	Same	Large and Thin Surface Area
Regeneration Shape	Angle of Incline	Different	Depression
Regeneration Orientation	Vertical	Different	Horizontal
Condensing Material	Liquid Desiccant	Different	Solid Desiccant
Water Desorption	Differential Surface Vapor Pressure	Different	Decoupled from ground
Water Generation	Solar and Water Harvesting	Different	Stable Insulation Layer
Exergy	Solar and Wind Harvesting	Different	Water and Dry Air Harvesting

Table 9.2. Thermo-hygroscopic Envelope and Air wells

Performance Criteria	Thermo-hygroscopic Envelope	Comparison	Air wells
Condensing Mechanism	Contact with Ambient Air	Same	Contact with Ambient Air
Regenerative Function	Regeneration	Same	Regeneration
Regeneration Mechanism	Heating	Same	Drying
Condensing Constraints	Short Time	Different	Long Time
Condensing Surface Area	Large /Thin Falling Film	Same	Large and Thin Surface Area
Regeneration Shape	Angle of Incline	Different	Depression
Orientation	Vertical	Different	Horizontal
Condensing Material	Liquid Desiccant	Different	Porous Desiccant
Water Desorption	Desorbs Water Vapor	Different	Decoupled from ground
Water Generation	Surface Vapor Pressure	Different	Low thermal lag response
Exergy	Solar and Water Harvesting	Different	Water and Dry Air Harvesting

envelope to prairie dog burrow and leaf-cutting ant nest. The prairie dog and leaf-cutting ants orient their nest and burrow openings to parallel orientation with the wind. Orienting the liquid desiccant solar regenerator to the wind does not improve the system. Orienting the thermo-hygroscopic intake flaps is beneficial to improve the system. The orientation of the system to the sun moves the system out of alignment with the wind direction for Atlanta, which is mostly northwest and northeast. Articulation of the ventilation flaps with torrents and collars offers improvement to wind-induced ventilation. The thermo-hygroscopic envelope benefits passive ventilation of fresh air through the dehumidifier. Better airflow improves the coefficient of performance of the falling film of liquid desiccant. Faster moving airflow over the liquid desiccant lowers the requirement for power to run pumps and pump parasitic losses. The thesis compares conventional air conditioning systems to the prairie dog and leaf-cutting ant. Figure 9.5 and 9.6 show criteria for selective performance and functional mechanisms to improve conventional air conditioning systems. The articulation of vents offer improvements to intake and exhaust performance. The biological analogue comparison can offer benefits to conventional as well as speculative air conditioning systems. The data from this process delivers rich untapped resource for further

work to improve the design and integration of the thermo-hygroscopic building envelope.

Table 9.3. Thermo-hygroscopic Envelope and Leaf-Cutting Ant Nest

Performance Criteria	Thermo-hygroscopic Envelope	Comparison	Leaf-Cutting Ant Nest
Seasonal Adaptation	Flap Orient to Wind Direction	Similar	Wind Orientated
Adaptation Mechanism	Articulated Flaps Open/Close	Similar	Open/Close Nest Openings
Structure	More Parallel Flows	Similar	Parallel Connecting Tunnels
Humidity Control	Liquid Desiccant	Different	Nest Cultivation of Fungus
Thermal Convection	Passive Assist to Convection	Different	Convective/Diffusive
Airflow Movement	Passive Assist to Convection	Different	Convective/Diffusive
Airflow Mechanism	Offset Inlet and Outlet	Same	Offset Inlet and Outlet
Airflow Performance	Pressure Drop	Different	Pressure Drop
Airflow Penetrations	Large Number	Same	Large Number
Airflow Adaptation	Torrent Definition	Same	Torrent Articulation
Directional Adaptation	Orient Intakes	Similar	Openings Parallel to Wind
Exergy Adaptation	Solar and Wind Harvesting	Similar	Wind Harvesting

Table 9.4. Thermo-hygroscopic Envelope and Prairie Dog Burrow

Performance Criteria	Thermo-hygroscopic Envelope	Comparison	Great Plains Prairie Dog Burrow
Seasonal Adaptation	Flaps Oriented to Wind	Same	Wind Orientated
Adaptation Mechanism	Articulated Flaps Open/Close	Different	No specific Adaptation
Structure	More Parallel Flows	Same	Parallel Connecting Tunnels
Humidity Control	Liquid Desiccant	Different	Side Passages Balance Humidity
Thermal Convection	Passive Assist to Convection	Different	Induced Wind Airflow
Airflow Movement	Passive Assist to Convection	Different	Induced Wind Airflow
Airflow Mechanism	Offset Inlet and Outlet	Different	Offset Inlet and Outlet
Airflow Performance	Pressure Drop	Different	Pressure Drop
Airflow Penetrations	Large Number	Same	Small Number
Airflow Adaptation	Torrent Definition	Same	Torrent Articulation
Directional Adaptation	Orient Intakes	Similar	Openings Parallel to Wind
Exergy Adaptation	Solar and Wind Harvesting	Similar	Wind Harvesting

9.3 Implications for Energy Reductions, Consumption, and Cost

Yu et al decoupled liquid desiccant system consists of a single regenerator and desiccant storage tank serving individual building level desiccant dehumidifiers [1]. The performance of their system shows energy, consumption, and cost reductions for summer and winter. With latent loads between 10% and 50%, the system energy consumption and operational costs are 80% and 75% of conventional air conditioning systems [1]. The reductions and savings can be much less in their model with solar energy to regenerate liquid desiccant and ground water for radiant ceiling panel cooling water with latent loads between 10% and 50%. Other studies show that liquid desiccant systems use solar energy to regenerate liquid desiccant. Alteration in the system sketch shown in Figure 8.9 and 8.10 of an air to water radiant ceiling panel system can use ground water to offer potential simplification of the system. The solar regenerator can be of simple construction wood and glass unit, however, an integrated

Table 9.5. Conventional Air Conditioning Equipment Systems and Leaf-Cutting Ant Nest

Performance Criteria	Air Conditioning Systems	Comparison	Leaf-Cutting Ant Nest
Seasonal Adaptation	Fixed	Different	Wind Orientated
Adaptation Mechanism	Variable Air Volume	Similar	Open/Close Nest Openings
Structure	Parallel Connecting Ductwork	Similar	Parallel Connecting Tunnels
Humidity Control	Evaporative Condenser	Different	Nest Cultivation of Fungus
Thermal Convection	Forced Convection	Different	Convective/Diffusive
Airflow Movement	Forced Convection	Different	Convective/Diffusive
Airflow Mechanism	Offset Inlet and Outlet	Same	Offset Inlet and Outlet
Airflow Performance	Pressure Drop	Similar	Pressure Drop
Airflow Penetrations	Small Number	Different	Large Number
Airflow Adaptation	Vents	Different	Torrent Articulation
Directional Adaptation	No Specific Adaptation	Different	Openings Parallel to Wind
Exergy Adaptation	No Specific Adaptation	Different	Wind Harvesting

Table 9.6. Conventional Air Conditioning Equipment Systems and Prairie Dog Burrow

Performance Criteria	Air Conditioning Systems	Comparison	Great Plains Prairie Dog Burrow
Seasonal Adaptation	Fixed	Different	Wind Orientated
Adaptation Mechanism	Variable Air Volume	Different	No specific Adaptation
Structure	Parallel Connecting Ductwork	Similar	Parallel Connecting Tunnels
Humidity Control	Evaporative Condenser	Different	Side Passages Balance Humidity
Thermal Convection	Forced Convection	Different	Induced Wind Airflow
Airflow Movement	Forced Convection	Different	Induced Wind Airflow
Airflow Mechanism	Offset Inlet and Outlet	Similar	Offset Inlet and Outlet
Airflow Performance	Pressure Drop	Similar	Pressure Drop
Airflow Penetrations	Small Number	Same	Small Number
Airflow Adaptation	Vents	Different	Torrent Articulation
Directional Adaptation	No Specific Adaptation	Different	Openings Parallel to Wind
Exergy Adaptation	No Specific Adaptation	Different	Wind Harvesting

unit with the building envelope requires higher level of fabrication. The cost associated with uncertainty with the integration of solar liquid desiccant components within the building envelope requires further investigation.

Adoption of liquid desiccant systems remains an issue for commercial buildings due to their higher energy costs, first costs, and liquid desiccant moisture carryover. Liquid desiccant corrosion of metal components leads to more expensive components and design modifications in equipment. Further development to test liquid desiccant concentrations with sodium chloride and calcium chloride improves consideration for solutions with less corrosion and toxicity issues. Use of low-cost waste heat and solar energy for liquid desiccant offer benefits to driving cost of these systems lower. Research on micro-porous membranes that allow water to migrate to air but impervious to desiccant in desiccant dehumidifiers avoids carry over and corrosion issues[8]. Special surfaces that form thin desiccant film flows offer improvements in minimizing carryover and corrosion issues[8]. Thinner film flows of liquid desiccant offer improvements to solar regenerator with more surface area contact

with liquid desiccant and absorber surface.

9.3.1 *Proto|Model System for Stacking Humidity and Temperature Control*

There is uncertainty in independent stacking of decoupled latent components performance as discrete units or as joined-configurable levels. Further work on a single floor performance using all primary and secondary components of the solar liquid regenerator is required. The case of co-joined configurable levels allows for redundancy, load sharing, and switching off latent thermal loads for floor levels. Tenant-less floors offer the capacity to completely disable the system or use its solar liquid desiccant regeneration capacity for levels with higher than peak thermal loads.

9.4 Building Systems Including Decoupled Mechanical and Fabrication Implications

The floor level redundancy of regenerator, dehumidifier, and direct evaporative cooler components improves integration of services for independent control of latent and sensible heat loads for each floor. The primary and secondary components require tight tolerance and spatial configuration in context to CLT structure. Fabrication, installation, assembly, and cost of these components require off-site manufacturing for improvements to site delivery and assembly. Thermo-hygroscopic components include off-site factory installation of mass customization of radiant ceiling panels, solar liquid desiccant regenerator components, secondary components, and services. On-site work hard connects factory assembled components to site services. CLT modular construction allows for whole walls, floors, elevator and stair cores, and ceilings to crane into position with factory installed windows, doors, weather resistant barriers, kitchen, restroom, electrical chases and conduits, and lighting fixtures and controls. The design of the compact office stacks vertically to increase footprint up to limits of CLT construction or 12 floors without a concrete core. Final work investigates necessary commissioning assessments for the system operation after construction work.

9.4.1 *Systems Packages*

There is a lack of experimental work to locate components such as solar regenerator and dehumidifier in alternative locations. Placement of these components on the roof of the project or on mechanical level for multiple stories is the obvious choice. With that solution, the uncertainty of building simulation in determining how best

to size and deploy regenerator and dehumidifiers remains an issue future work. However, roof placement of the equipment competes with an already crowded space taken up by photovoltaics. Direct placement of these components within the building envelope allows immediate action to dehumidify and cool fresh air with minimal ductwork to reach conditioned space. Further improvements to organization of regenerators, dehumidifiers, and direct evaporative coolers on the north and south façade can enhance bi-directional benefits. Bi-directional operation reduces by half conditioned space volume, air rates, and ventilation rates for each facade unit. Further work to understand system component size and airflow through various components and thermodynamic states of air improves building simulation of the model.

9.4.2 Interior Packages

The thesis proposes interior packages follow suit with mass customization and fabrication off-site for compact secondary spaces within the thesis project for restrooms, kitchen, built in furnishings and workspaces. The interior packages follow assembly of CLT frames, and hygroscopic envelope system components. The impact of packaging factory installed mass customization packages with exterior CLT frame, and services improves reduction of first cost, assembly, and construction of project.

9.5 Potential mechanical assembly testing issues

The tolerance and spatial configuration of solar liquid desiccant regenerator within the building envelope requires tighter accuracy and placement of components. Off-site fabrication of envelope and services improves fitting and installation for faster on-site arrival of these packages.

9.6 Conclusion

The thesis considers the environmental, historical, bio-inspired design, past systems, and materials and components for a hygroscopic building envelope. The feasibility of the system limits itself to thermodynamic understanding of liquid desiccant performance and fresh air in this system. The mechanism transfer from beneficial performance criteria in the historical and biological examples provide an array of improvements to the system. Integration of the primary components at a schematic level provides enhanced understanding of the difficulties of the thesis proposition. The building envelope at best offers limited space for additional components. The op-

portunity to deal directly with fresh air to reduce ductwork requirements and air conditioning refrigerants allows an opportunity to rethink the integration of building and thermal design. Bio-inspired design requires future work to advance and incorporate improvements in thermal components for thermo-hygroscopic envelope assembly. Bidirectional solar liquid desiccant units on the north and south elevation offer higher level of system functioning. The system uses flaps to control air volume of fresh air into the two-dehumidifier units. The opening and closing of the system provides inspiration from the leaf-cutting ants' strategy for mound ventilation. The prairie dog offset and shaping of borrow mounds entrances improves the location and shaping of fresh air inlet and return air outlets on the exterior and interior side of building envelope. The solar regenerator uses solar radiation in the regenerator of the liquid desiccant as a case for system exergy. Future work can improve understanding of liquid desiccant energy storage by varying concentration levels. Direct evaporative cooler transfers waste heat from fresh air to exhaust air and conserves energy. The use of other low-grade heat source exchanges provides dry air ventilation and chiller water for radiant ceilings[32]. Water condenses on the underside of the solar regenerator glass and flows downward to collection reservoir. Water use and water use intensity per square meter improves future work for water harvesting from the solar regenerator. Future work in calculating building envelope latent energy air mass and vapor conversions improves latent energy transformations for condensation and evaporation mass balance, and evaluation of the integrated components. The thesis explores the initial groundwork to intensify integration of bio-inspiration, architectural, and thermodynamic design. The introduction to complex nature of all three areas of design requires a delicate balance of constraints. The long lead-time in developing improvements system design shortens with strategic bio-inspired design process but this requires an integrative approach with engagement with agents from other areas of design, engineering, structure, building science, and biology. In light of these constraints, multiple areas for improvement gives rise to breaks in barriers for re-think of alternative decoupling air-conditioning systems that can be responsive to ecological and thermal issues.

REFERENCES

- [1] B.F. Yu, Z.B. Hu, M. Liu, H.L. Yang, Q.X. Kong, and Y.H. Liu. Review of research on air-conditioning systems and indoor air quality control for human health. *International Journal of Refrigeration*, 32(1):3 – 20, 2009. ISSN 0140-7007. doi: <http://dx.doi.org/10.1016/j.ijrefrig.2008.05.004>. URL <http://www.sciencedirect.com/science/article/pii/S0140700708000984>.
- [2] P. Gandhidasan and M.A. Mohandes. Artificial neural network analysis of liquid desiccant dehumidification system. *Energy*, 36(2):1180 – 1186, 2011. ISSN 0360-5442. doi: <http://dx.doi.org/10.1016/j.energy.2010.11.030>. URL <http://www.sciencedirect.com/science/article/pii/S0360544210006754>.
- [3] Ozone layer protection regulatory programs: Hcfc phaseout schedule, February 2012. URL <http://www.epa.gov/ozone/title6/phaseout/hcfc.html>.
- [4] U.S. Department of Energy (DOE). 2011 buildings energy data book, March 2012. URL http://buildingsdatabook.eren.doe.gov/docs/DataBooks/2011_BEDB.pdf. Buildings Technologies Program Energy Efficiency and Renewable Energy.
- [5] Marionyt Tyrone Marshall. Hygroscopic climatic modulated boundaries: a strategy for differentiated performance using a natural circulative and energy captive building envelope in hot and moisture rich laden air environments. *Perkins+Will Research Journal*, 02(01):41–54, 2010. URL http://perkinswill.com/sites/default/files/PWRJ_Vol0201.pdf.
- [6] Yonggao Yin, Junfei Qian, and Xiaosong Zhang. Recent advancements in liquid desiccant dehumidification technology. *Renewable and Sustainable Energy Reviews*, 31(0):38 – 52, 2014. ISSN 1364-0321. doi: <http://dx.doi.org/10.1016/j.rser.2013.11.021>. URL <http://www.sciencedirect.com/science/article/pii/S1364032113007703>.
- [7] Kyoto protocol, 1997. URL <http://www.unfccc.int>.
- [8] John Dieckmann, Kurt Roth, and James Brodrick. Liquid desiccant air conditioners. *ASHRAE Journal*, 50(10): 90–95, October 2008.
- [9] Arthur J. Hubbard and George Hubbard. *Neolithic dew-ponds and cattle-ways*. Longmans, Green and Co., London, United Kingdom, third edition, 1916. URL <https://archive.org/details/neolithicdewponds00hubb>.
- [10] V.S. Nikolayev, D. Beysens, A. Gioda, I. Milimouka, E. Katiushin, and J.-P. Morel. Water recovery from dew. *Journal of Hydrology*, 182(1–4):19 – 35, 1996. ISSN 0022-1694. doi: [http://dx.doi.org/10.1016/0022-1694\(95\)02939-7](http://dx.doi.org/10.1016/0022-1694(95)02939-7). URL <http://www.sciencedirect.com/science/article/pii/0022169495029397>.
- [11] G. Nebbia. The problem of obtaining water from the air. In A.G. Spanides, editor, *Proceedings of the International Seminar on Solar and Aeolian Energy*, pages 33–46, New York, 1961. Plenum Press.
- [12] C.S. Khalid Ahmed, P. Gandhidasan, and A.A. Al-Farayedhi. Simulation of a hybrid liquid desiccant based air-conditioning system. *Applied Thermal Engineering*, 17(2):125 – 134, 1997. ISSN 1359-4311. doi:

[http://dx.doi.org/10.1016/S1359-4311\(96\)00025-7](http://dx.doi.org/10.1016/S1359-4311(96)00025-7). URL <http://www.sciencedirect.com/science/article/pii/S1359431196000257>.

- [13] P. Gandhidasan and A.A. Al-Farayedhi. Solar regeneration of liquid desiccants suitable for humid climates. *Energy*, 19(8):831 – 836, 1994. ISSN 0360-5442. doi: [http://dx.doi.org/10.1016/0360-5442\(94\)90035-3](http://dx.doi.org/10.1016/0360-5442(94)90035-3). URL <http://www.sciencedirect.com/science/article/pii/S0360544294900353>.
- [14] H.I. Abualhamayel and P. Gandhidasan. A method of obtaining fresh water from the humid atmosphere. *Desalination*, 113(1):51 – 63, 1997. ISSN 0011-9164. doi: [http://dx.doi.org/10.1016/S0011-9164\(97\)00114-8](http://dx.doi.org/10.1016/S0011-9164(97)00114-8). URL <http://www.sciencedirect.com/science/article/pii/S0011916497001148>.
- [15] Michael Pawlyn. *Biomimicry in architecture*. Riba Publishing, 15 Bonhill Street, London, 2011.
- [16] M. Bollazzi, L.C. Forti, and F. Roces. Ventilation of the giant nests of atta leaf-cutting ants: does underground circulating air enter the fungus chambers? *Insectes Sociaux*, 59(4):487–498, 2012. doi: 10.1007/s00040-012-0243-9. URL <http://dx.doi.org/10.1007/s00040-012-0243-9>.
- [17] Christoph Kleineidam, Roman Ernst, and Flavio Roces. Wind-induced ventilation of the giant nests of the leaf-cutting ant atta vollenweideri. *Naturwissenschaften*, 88(7):301–305, 2001. ISSN 0028-1042. doi: 10.1007/s001140100235. URL <http://dx.doi.org/10.1007/s001140100235>.
- [18] Steven Vogel, Jr. Ellington, Charles P., and Jr. Kilgore, Delbert L. Wind-induced ventilation of the burrow of the prairie-dog, *Cynomys ludovicianus*. *Journal of comparative physiology*, 85(1):1–14, 1973. doi: 10.1007/BF00694136. URL <http://dx.doi.org/10.1007/BF00694136>.
- [19] John Sullivan. The death of the cubicle and the killers are collaboration and innovation., 2012. URL <http://www.ere.net/2012/05/21/the-death-of-the-cubicle-and-the-killers-are-collaboration-and-innovation/>.
- [20] Karacabeyli, E. and Douglas, B. (Eds.). *CLT handbook: cross laminated timber*. FP Innovations and Binational Softwood Lumber Council, Pointe-Claire, Quebec, Canada, u.s. edition, 2013. URL <http://steveeasley.com/images/CLTHandbook-2013-Chpt10-BldgEnclosureDesignXLaminatedTimber.pdf>.
- [21] Andy Sutton, Daniel Black, and Pete Walker. Cross-laminated timber: an introduction to low-impact building materials, 2011. URL http://www.bre.co.uk/filelibrary/pdf/projects/low_impact_materials/ip17_11.pdf.
- [22] A.A.M. Hassan and M. Salah Hassan. Dehumidification of air with a newly suggested liquid desiccant. *Renewable Energy*, 33(9):1989 – 1997, 2008. ISSN 0960-1481. doi: <http://dx.doi.org/10.1016/j.renene.2007.12.002>. URL <http://www.sciencedirect.com/science/article/pii/S0960148107003837>.
- [23] X.H. Liu, X.M. Chang, J.J. Xia, and Y. Jiang. Performance analysis on the internally cooled dehumidifier using liquid desiccant. *Building and Environment*, 44(2):299 – 308, 2009. ISSN 0360-1323. doi: <http://dx.doi.org/10.1016/j.buildenv.2008.03.009>. URL <http://www.sciencedirect.com/science/article/pii/S0360132308000437>.
- [24] S. Younus Ahmed, P. Gandhidasan, and A.A. Al-Farayedhi. Thermodynamic analysis of liquid desiccants. *Solar Energy*, 62(1):11 – 18, 1998. ISSN 0038-092X. doi: [http://dx.doi.org/10.1016/S0038-092X\(97\)00087-X](http://dx.doi.org/10.1016/S0038-092X(97)00087-X).

URL <http://www.sciencedirect.com/science/article/pii/S0038092X9700087X>.

- [25] Jae-Weon Jeong, Stanley A. Mumma, and William P. Bahnfleth. Energy conservation benefits of a dedicated outdoor air system with parallel sensible cooling by ceiling radiant panels. *ASHRAE Transactions: Symposia*, 109(2):627–636, 2003.
- [26] Michael Green. The case for tall wood buildings, February 2012. URL <http://mg-architecture.ca/tallwood/>.
- [27] Walter T Grondzik, Alison G. Kwok, John S. Reynolds, and Benjamin Stein. *Mechanical and Electrical Equipment for Buildings*. John Wiley and Sons, Hoboken, New Jersey, USA, 2006.
- [28] Climate Consultant 5.5 BETA Build 3. *Computer Software*. UCLA Department of Architecture and Urban Design, Los Angeles, CA, USA, 3 2014.
- [29] Gregg D. Ander. Daylighting, 2012. URL http://www.wbdg.org/resources/daylighting.php?r=minimize_consumption.
- [30] Jan F. Kreider and Ari Rabl. *Heating and cooling of buildings: design for efficiency*. McGraw-Hill, Inc., New York, 1994. Editors: Corrigan, John J. and Bradley, James W.
- [31] Yonggao Yin, Xiaosong Zhang, and Zhenqian Chen. Experimental study on dehumidifier and regenerator of liquid desiccant cooling air conditioning system. *Building and Environment*, 42(7):2505 – 2511, 2007. ISSN 0360-1323. doi: <http://dx.doi.org/10.1016/j.buildenv.2006.07.009>. URL <http://www.sciencedirect.com/science/article/pii/S0360132306001879>.
- [32] Yonggao Yin, Xiaosong Zhang, and Qingyan Chen. A new liquid desiccant system for air-conditioned spaces with high latent and cooling load. In *A new liquid desiccant system for air-conditioned spaces with high latent and cooling load*, page 8. International Refrigeration and Air Conditioning Conference, 2008. URL <http://docs.lib.purdue.edu/iracc/861>. Paper 861.